ISSN: 3059-9865 (Print)

ISSN: 3059-9873 (Online)

JoTSE

Journal on Transportation System and Engineering

A Peer Reviewed Journal

Special Edition

Volume 1 Issue 2 December 2025

Published by

SOCIETY OF TRANSPORT ENGINEERS NEPAL
Lalitpur, Nepal

Journal on Transportation System and Engineering (JoTSE)

Volume-1, Issue-2 (December , 2025)

MAILING ADDRESS

Journal of Transportation System and Engineering (JoTSE)

Society of Transport Engineers Nepal (SOTEN)

Lalitpur, Nepal

contact: +977- 9741660286

Mail: info@soten.org.np

website: www.soten.org.np

Journal on Transportation System and Engineering (JoTSE)

ISSN: 3059-9873(Online), 3059-9865(Print)
Volume-1, Special Edition (December 2025)

Advisory Board

Editorial Board

EDITORIAL

It is with great pride and enthusiasm that we present the second edition of the *Journal on Transportation System and Engineering*. This publication remains a dedicated platform for sharing high-quality research and innovations in transportation systems, infrastructure, planning, and technology. Moreover, it stands as a reflection of the identity and commitment of transportation professionals working under and beyond the banner of the Society of Transport Engineers Nepal (SOTEN).

As transportation remains a cornerstone of economic development, urban growth, and social connectivity, the need for innovative solutions and sustainable practices has never been more critical. In this issue, we bring together scholarly contributions that address a wide range of topics from intelligent transport systems and traffic engineering to sustainable mobility and infrastructure resilience. These papers reflect the dynamic challenges faced by transportation professionals and offer practical insights and forward-thinking solutions.

Each submission has undergone a comprehensive peer-review process to ensure academic rigor, technical depth, and relevance to the evolving needs of the field of transportation. I am confident that the research and discussions featured in this volume will inspire further innovation, support policy development, and contribute to the advancement of transportation science and engineering.

I would like to extend my sincere appreciation to our editorial board members, advisors, reviewers, and authors, whose time, expertise, and commitment to excellence have made this issue possible. Your contributions uphold the journal's mission to be a credible and impactful source of knowledge.

We hope this edition will be both informative and inspiring for researchers, practitioners, policymakers, and students alike.

Thank you for your continued support.

Prof. Dr. Thusitha Chandani Shahi, PEng
Editor in Chief
Journal of Transportation System and Engineering
Society of Transport Engineers Nepal

Table of Content

Journal on Transportation System and Engineering
ISSN: 3059 9865(Print) 3059-9873(Online)
Vol. 1. Issue 2, 2025(December): 1-10
DOI: https://doi.org/10.3126/jotse.v1i2.87727

Research Articles
Received Date: March 29, 2025
Revised Date: September 28, 2025
Accepted Date: November 20, 2025
Published Date: December 21, 2025

Assessment of Air Traffic Noise level: A Case Study of Chiang Mai International Airport

Patcharida Sungtrisearn[1], Chaiwat Sangsrichan[1], Preda Pichayapan[2*]

[1] *Doctor of Philosophy Program in Civil Engineering, Faculty of Engineering, Chiang Mai University, Chiang Mai, Thailand*
[2] *Department of Civil Engineering, Faculty of Engineering, Chiang Mai University, Chiang Mai, Thailand*

Abstract

This study aims to analyze the aircraft noise levels at Chiang Mai International Airport and assess the impact of noise pollution on the surrounding areas. The Weighted Equivalent Continuous Perceived Noise Level (WECPNL) index was used as the primary indicator. Noise level measurements were conducted at 6 noise measuring point following the guidelines of the International Civil Aviation Organization (ICAO, 2018) and the Pollution Control Department (2021). The results indicated that the majority of the surrounding areas had noise levels within the standard limits, except for the northern runway end, where the WECPNL value was 70.7, slightly exceeding the standard. This area requires land-use control measures to prevent impacts on the nearby communities. The study also found a correlation between noise levels and factors such as distance from the runway, aircraft takeoff and landing directions, and flight frequency.

Spatial data analysis using the Inverse Distance Weighting (IDW) method clearly presented the noise level distribution and can be effectively applied in planning noise management strategies for airport areas. The findings propose various measures to mitigate aircraft noise impacts, such as designing appropriate flight paths, adjusting land-use zones, developing noise-reducing aircraft technologies, and adhering to ICAO guidelines and noise standards set by relevant authorities in Thailand. These measures aim to align with international standards and minimize noise pollution impacts on surrounding communities.

Keywords: *Aircraft Noise, Noise Level Airport, Noise Contour WECPNL Method, Chiang Mai International Airport*

1. Introduction

Airports serve as gateways connecting economic centers, tourist destinations, and government hubs. Air transportation has seen significant advancement, particularly at large and popular airports. Chiang Mai International Airport, serving as the aviation hub of Northern Thailand, has gained considerable popularity as a tourist destination. Statistical data from 2019 to 2023 ranks it as the fourth busiest airport in Thailand (State of Thai Aviation Industry [CAAT], 2023). This rapid economic growth has led to increased air traffic density. In 2022, the airport served 10 scheduled airlines with a total of 33,185 flights, representing a 51.57% increase (Airports of Thailand [AOT], 2023). The rise in flight frequency correspondingly increases aircraft noise exposure.

Frequent exposure to aircraft noise in the surrounding communities of Chiang Mai International Airport can lead to significant health impacts. If the noise level exceeds 70 decibels, it may cause anxiety, discomfort, hearing issues, and vascular problems. If noise exceeds 80 decibels, it can severely affect overall health and, if prolonged, may cause temporary or permanent hearing loss (Suma'mur, 2013; Correia et al., 2013). Prolonged exposure to high noise levels may also impair work performance. These conditions lead to distress among residents, reducing their quality of life and potentially causing damage to the community (Thongsun, 2007), which results in complaints to the airport authority.

Given the significance of these issues, the researcher is interested in studying the noise levels from air traffic at Chiang Mai International Airport. The study aims to measure noise levels at the airport in Chiang Mai and calculate the noise index using the Weighted Equivalent Continuous Perceived Noise Level (WECPNL) method, following the guidelines of the International Civil Aviation Organization (ICAO).

Previous studies have highlighted similar concerns at other airports. Research by Nofriandi et al. (2018) at Raja Haji Fisabilillah airport in Tanjung Pinang found significant noise impacts, with levels reaching 95.24 dB(A) near takeoff points.

Corresponding author. *E-mail address: preda.p@cmu.ac.th*

Their study revealed that points closest to aircraft takeoff positions recorded the highest noise intensities, with WECPNL values exceeding 75.30 in some areas. These findings emphasize the importance of comprehensive noise monitoring and management, particularly in areas directly under flight paths and near takeoff points. Their methodology, which followed ICAO guidelines for measurement points at various distances from the runway (300-4000 meters), provides a valuable framework for similar studies at other airports. The correlation they found between noise levels and factors such as distance from the runway, aircraft operations, and flight frequency aligns with the objectives of this current study at Chiang Mai International Airport.

Other related studies have also examined various aspects of airport noise impacts. Research by Thongsun (2007) at Suvarnabhumi Airport assessed noise effects on surrounding communities, while Riyangga et al. (2014) analyzed noise pollution's impact on worker health and safety in airport ground handling areas. Additionally, Correia et al. (2013) found significant associations between aircraft noise exposure and cardiovascular-related hospital admissions in their multi-airport study. These studies collectively demonstrate the wide-ranging impacts of airport noise on both community health and operational safety, further supporting the need for comprehensive noise assessment and management strategies.

2. Methodology

2.1 Scope of the study

2.1.1 Scope of the Area

The study utilized aircraft noise level measurement data from 6 noise measuring point in Chiang Mai Province (Airports of Thailand Public Company Limited, 2023). These measuring points were located along the runway and in surrounding communities, as shown in Figure 1.

Figure 1. Noise measuring point at Chiang Mai International Airport (*Airports of Thailand Public Company Limited, 2023)*

2.1.2 Scope of Time

The data collection was conducted from November 15-21, 2023.

2.2 Data collection

2.2.1 Air Traffic Volume Statistics

The primary data collected from field measurements include aircraft noise level measuring at 6 points location in Chiang Mai Province. The data collection focused on noise levels during aircraft take-off and landing. The secondary data consist of aircraft movement frequency, aircraft types, airport layout, and total passenger data for Chiang Mai International Airport in 2023.

2.2.2 Noise measuring point

The measurement points were established according to International Civil Aviation Organization recommendations (ICAO, 2018), with measurements taken at distances of 300 and 600 meters parallel to the runway, as well as 1,000 and 2,000 meters from both runway ends. These locations align with the noise certification reference measurement positions described in Annex 16, Volume 1. The detailed positions of the measurement points

Table 1. Noise measuring point

No.	Points Location	Distance from Runway (m)	Coordinate
1	Northern Runway End (Faculty of Agriculture, Chiang Mai University)	1,000	X = 495902 Y = 2077938
2	Passenger Terminal Front Parking Area (Eastern side of Chiang Mai International Airport)	600	X = 496579 Y = 2075538
3	Southern Runway Area in front of Fire Station (Airside Zone)	300	X = 496516 Y = 2074575
4	Ton Kuk Community, Moo 7, Suthep Sub-district, Mueang District, Chiang Mai Province (Western side of Chiang Mai International Airport)	300	X = 495701 Y = 2074098
5	Mae-Hia Community near Mae-Hia Municipality, Mueang District, Chiang Mai Province (Southeastern side of Chiang Mai International Airport)	2,000	X = 496184 Y = 2071900
6	Ban Umong Community, Suthep Sub-district, Mueang District, Chiang Mai Province (Northwestern side of Chiang Mai International Airport)	600	X = 495535 Y = 2076865

2.3 Data Analysis

2.3.1 Noise measurement method

The noise levels at the airport were measured using both permanent and mobile Sound Level Meters. Data was collected during aircraft movements, specifically during landing and take-off. The equipment used for these measurements is shown in Figure 2.

(A) Fixed-Station Sound Level Meter (B) Mobile Sound Level Meter

Figure 2. Sound Level Meter

Mobile level meters are precision instruments designed for portable noise monitoring applications with measurement capabilities ranging from 30-140 dB(A) and 35-140 dB(C) across a frequency response of 20 Hz to 20 kHz. These devices comply with IEC 61672-1 Class 1 or Class 2 standards, providing measurement accuracy within ±1.4 dB for Class 1 and ±2.0 dB for Class 2 instruments. The meters feature 0.1 dB resolution with selectable time weighting options including Fast (125 ms), Slow (1 s), and Impulse (35 ms) responses. Technical specifications include 32-128 GB internal data storage capacity, 12-24 hours of continuous battery operation, and operational temperature range from -10°C to +50°C. Connectivity options encompass USB 2.0, Bluetooth 4.0, and Wi-Fi 802.11b/g/n interfaces, with total instrument weight typically ranging from 300-800 g including battery.

Fixed-station sound level meters represent permanent installations designed for continuous environmental noise surveillance, featuring extended measurement ranges of 25-140 dB(A) with enhanced dynamic range capabilities. These systems operate reliably across extreme temperature conditions from -40°C to +70°C while maintaining IP65/IP67 weather protection ratings. Power management incorporates solar panel systems ranging from 20-100W capacity coupled with battery backup systems providing 7-14 days of autonomous operation without solar charging. Data management capabilities include GSM/4G/LTE, LoRaWAN, or Ethernet connectivity options for real-time data transmission, with local storage capacity sufficient for 1-5 years of continuous monitoring data. Remote access functionality provides web-based interfaces for real-time monitoring, configurable threshold-based alert systems via SMS/email notifications, and remote calibration verification capabilities with annual on-site calibration requirements. Installation specifications require mounting heights of 3-4 meters above ground level, minimum distances exceeding 1 meter from reflective surfaces, mandatory wind screen protection for outdoor applications, and concrete foundation systems with proper grounding for lightning protection.

2.3.2 Method of calculating the noise index at the airport

The calculation of aircraft noise levels using the Weighted Equivalent Continuous Perceived Noise Level (WECPNL) method is a standard approach for assessing the impact of aircraft noise. This metric follows the guidelines of the International Civil Aviation Organization (ICAO) and accounts for variations in noise perception during different times of the day by applying different weighting factors (Ministry of the Environment Japan, 2023). The general formula used is:

$$dB(A) = 10log\ [\frac{10^{\frac{L1}{10}} + 10^{\frac{L2}{10}} + 10^{\frac{L3}{10}} + \ldots\ldots + 10^{\frac{Ln}{10}}}{n}] \quad (1)$$

Where,
$dB(A)$: Average Noise level
L: The Noise Value at the Time of plane activities
N: Number of Aircraft

The calculation of aircraft noise levels using the Weighted Equivalent Continuous Perceived Noise Level (WECPNL) method is a standard approach for assessing the impact of aircraft noise under formula (1) using the following equation (ICAO, 2018; Ministry of the Environment Japan, 2023) and accounts for variations in noise perception during different times of the day by applying different weighting factors. The general formula used is:

$$WECPNL = dB(A) + 10logN - 27 \quad (2)$$

where,
$dB(A)$: Average Noise level
N: Number of arrivals and departures in 24 hours

2.3.3 Spatial Estimation Using the Inverse Distance Weighting (IDW) Method

Watson & Philip (1985) described spatial estimation using the Inverse Distance Weighting (IDW) method as an interpolation technique that estimates values at unknown locations based on sampled points. The influence of each sample point decreases as the distance from the estimated cell increases. Consequently, points closer to the target cell are assigned higher weights than those farther away. The number of points used for interpolation can be specified, or all points within a predefined radius can be included in the estimation process, as shown in Figure 3.

The IDW method is particularly suitable for variables that are distance-dependent, where each sample point influences the estimation based on its proximity. This approach is effective for mapping variables that vary smoothly over space, such as noise levels.

A key parameter in IDW interpolation is the power value of the equation. A higher power value places more emphasis on nearby points, leading to a less smooth surface. Conversely, a lower power value distributes influence more evenly across the points, resulting in a smoother interpolated surface, as shown in Figure 4.

For this study, IDW was applied to analyze noise level distribution patterns, using spatial interpolation based on noise measurements. A buffer of 3 kilometers around Chiang Mai International Airport was defined as the boundary for environmental settings to ensure a focused analysis of aircraft noise impacts.

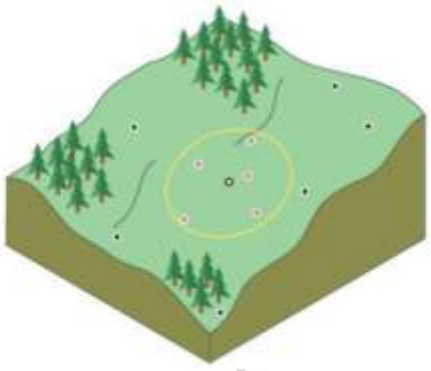

Figure 3. Concept of Spatial Estimation Using the IDW Process (ESRI, 2023)

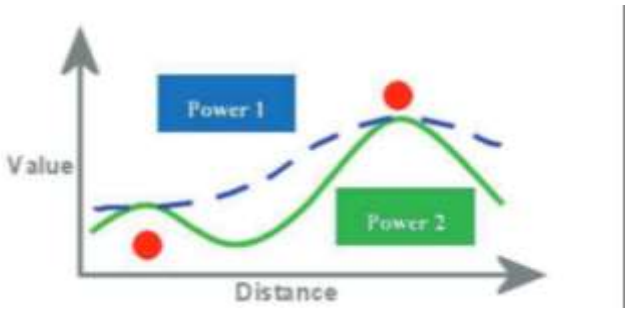

Figure 4. Comparison of Surfaces Estimated with Different Power Values (ESRI, 2023)

3. Results and Discussion

3.1 Results of Noise Measurements

3.1.1 Noise Level Measurements

The noise level measurements were conducted at 6 points location around Chiang Mai International Airport, located in both the runway area and surrounding communities. The results for each points location are as follows:

Points Location 1, located at the northern end of the runway near the Faculty of Agriculture at Chiang Mai University, recorded a 24-hour average noise level ($L_{eq24\ hr}$) between 65.9-66.5 dBA, a maximum noise level (L_{max}) between 92.4-95.0 dBA, and a day-night average noise level (L_{dn}) between 69.8-70.8 dBA.

Points Location 2, located at the parking lot in front of the passenger terminal on the east side of the airport, recorded a 24-hour average noise level ($L_{eq24\ hr}$) between 61.9-65.2 dBA, a maximum noise level (L_{max}) between 79.5-92.6 dBA, and a day-night average noise level (L_{dn}) between 66.0-69.2 dBA.

Points Location 3, located near the south runway by the fire station in the Airside area, recorded a 24-hour average noise level ($L_{eq24\ hr}$) between 63.2-66.2 dBA, a maximum noise level (L_{max}) between 86.9-97.3 dBA, and a day-night average noise level (L_{dn}) between 67.5-70.9 dBA.

Points Location 4, located in the Ton Kuk community in Moo 7, Suthep Subdistrict, Mueang District, on the west side of the airport, recorded a 24-hour average noise level ($L_{eq24\ hr}$) between 58.3-60.3 dBA, a maximum noise level (L_{max}) between 85.3-87.3 dBA, and a day-night average noise level (L_{dn}) between 62.2-63.7 dBA.

Points Location 5, located in the Mae Tia community near the Mae Hia Subdistrict Office in Mueang District, southeast of the airport, recorded a 24-hour average noise level ($L_{eq24\ hr}$) between 60.5-62.6 dBA, a maximum noise level (L_{max}) between 88.2-92.1 dBA, and a day-night average noise level (L_{dn})between 63.4-65.9 dBA.

Points Location 6, located in the Umong Village in Suthep Subdistrict, Mueang District, northwest of the airport, recorded a 24-hour average noise level ($L_{eq24\ hr}$) between 59.5-60.2 dBA, a maximum noise level (L_{max}) between 82.6-90.2 dBA, and a day-night average noise level (L_{dn}) between 63.4-64.6 dBA.

The details of the measurement results are summarized in Table 2.

Table 2. Maximum and minimum noise measurement results

No.	Points Location	Distance from Runway (m)	Noise Level dB(A)	
			Min	Max
1	Northern Runway End (Faculty of Agriculture, Chiang Mai University)	1,000	65.9	66.5
2	Passenger Terminal Front Parking Area (Eastern side of Chiang Mai International Airport)	600	61.9	65.2
3	Southern Runway Area in front of Fire Station (Airside Zone)	300	63.2	66.2
4	Ton Kuk Community, Moo 7, Suthep Sub-district, Mueang District, Chiang Mai Province (Western side of Chiang Mai International Airport)	300	58.3	60.3
5	Mae-Hia Community near Mae-Hia Municipality, Mueang District, Chiang Mai Province (Southeastern side of Chiang Mai International Airport)	2,000	60.5	62.6
6	Ban Umong Community, Suthep Sub-district, Mueang District, Chiang Mai Province (Northwestern side of Chiang Mai International Airport)	600	59.5	60.2

3.1.2 Noise Average Level Measurements

Chiang Mai International Airport operates approximately 200 flights daily, serving both incoming and outgoing passengers. The study on noise intensity caused by aircraft involved measurements at six stations, with each station recording the average noise intensity from all aircraft types, as shown in Table 3. It was found that the highest average noise intensity occurred at Points Location 1 (66.2 dB(A)), located at the northern end of the runway near the Faculty of Agriculture at Chiang Mai University. This station recorded the highest levels because it is located close to the flight path, where aircraft require maximum engine power during take-off.

From the data collected at all six stations, the researcher chose to use the 24-hour average noise level ($L_{eq24\ hr}$), as it provides the most comprehensive data. In a week (seven days), this data reflects a complete round of aircraft take-off and landings. The highest noise levels were not selected because their values are less reliable, as the highest noise events could be caused by only a few aircraft during a single hour. The results of the 24-hour average noise measurements from all 6 points location show that the noise level is closely related to the distance from the runway and the aircraft's take-off and landing paths. Points location closer to the runway and within the flight path experience higher noise impacts, as do areas with higher frequencies of runway usage. This is demonstrated in Table 3 and can be used to create a noise level contour map around Chiang Mai International Airport, showing the distribution pattern of the noise levels as shown in Figure 5.

Table 3. Average noise level.

No.	Points Location	Distance from Runway (m)	Noise Level dB(A)
1	Northern Runway End (Faculty of Agriculture, Chiang Mai University)	1,000	66.2
2	Passenger Terminal Front Parking Area (Eastern side of Chiang Mai International Airport)	600	62.7
3	Southern Runway Area in front of Fire Station (Airside Zone)	300	64.5
4	Ton Kuk Community, Moo 7, Suthep Sub-district, Mueang District, Chiang Mai Province (Western side of Chiang Mai International Airport)	300	59.1
5	Mae-Hia Community near Mae-Hia Municipality, Mueang District, Chiang Mai Province (Southeastern side of Chiang Mai International Airport)	2,000	60.9
6	Ban Umong Community, Suthep Sub-district, Mueang District, Chiang Mai Province (Northwestern side of Chiang Mai International Airport)	600	59.8

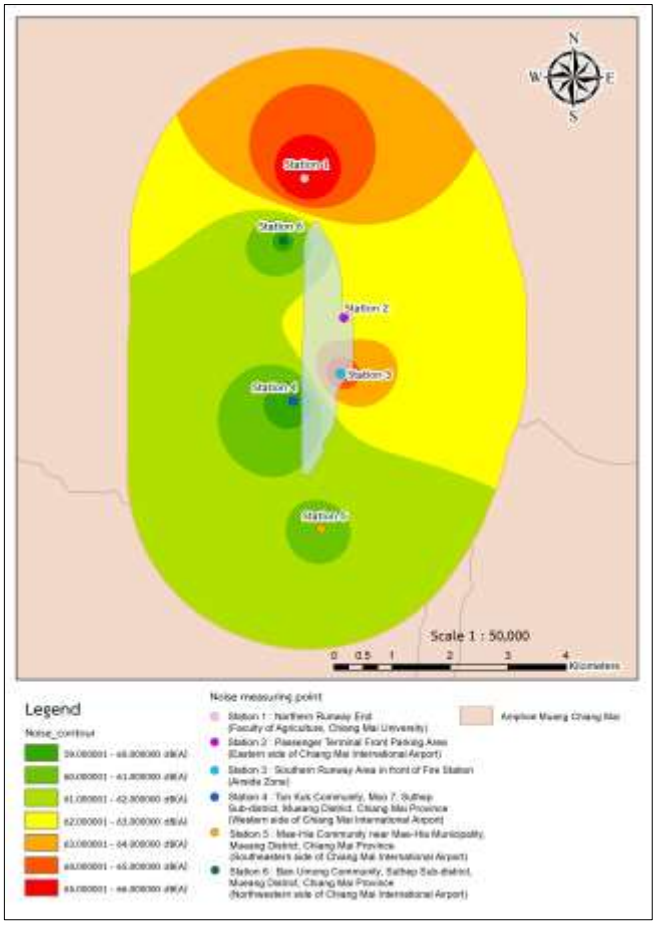

Figure 5. Average Noise Level Contours Around Chiang Mai International Airport

3.2 Results of The Weighted Equivalent Continuous Perceived Noise Level index (ICAO)

Flight frequency during the day was measured from 07:00 to 07:00 the following day. During the study period, the total aircraft movements (N) using the runway amounted to 200 flights per day, including both commercial and cargo aircraft (ICAO, 2016; FAA, 2021). It was assumed that each aircraft movement generated noise for a duration of 60 seconds. The highest calculated WECPNL index of 70.7 was recorded at the northern runway threshold (Faculty of Agriculture, Chiang Mai University), despite being 1,000 meters away from the runway. This high reading was due to its location directly under the aircraft takeoff-landing path and being a point where aircraft require maximum engine power during takeoff (Airports Authority of Thailand, 2020). The second highest readings were recorded at the southern runway area near the fire station (69.0 WECPNL) and the passenger terminal parking area (67.2 WECPNL). Meanwhile, surrounding communities exhibited lower WECPNL index values, particularly the Ton Kuk community, which recorded the lowest value (63.6 WECPNL) despite being only

300 meters from the runway. This lower reading was attributed to its location alongside the runway rather than directly under the aircraft takeoff-landing path (Pollution Control Department, 2020; Office of Natural Resources and Environmental Policy and Planning, 2021), as shown in Table 4.

Table 4. WECPNL index (ICAO) at each location.

No.	Points Location	Noise Level dB(A)			WECPNL
		Min	Max	Average	
1	Northern Runway End (Faculty of Agriculture, Chiang Mai University)	65.9	66.5	66.2	70.7
2	Passenger Terminal Front Parking Area (Eastern side of Chiang Mai International Airport)	61.9	65.2	62.7	67.2
3	Southern Runway Area in front of Fire Station (Airside Zone)	63.2	66.2	64.5	69.0
4	Ton Kuk Community, Moo 7, Suthep Sub-district, Mueang District, Chiang Mai Province (Western side of Chiang Mai International Airport)	58.3	60.3	59.1	63.6
5	Mae-Hia Community near Mae-Hia Municipality, Mueang District, Chiang Mai Province (Southeastern side of Chiang Mai International Airport)	60.5	62.6	60.9	65.4
6	Ban Umong Community, Suthep Sub-district, Mueang District, Chiang Mai Province (Northwestern side of Chiang Mai International Airport)	59.5	60.2	59.8	64.3

3.3 Environmental Noise Status Assessment

The environmental noise assessment from aircraft operations at Chiang Mai Airport in this research utilized the WECPNL (Weighted Equivalent Continuous Perceived Noise Level) index, comparing measured noise levels against established standards. According to the International Civil Aviation Organization standards (ICAO, 2018), areas with WECPNL $\leq$ 70 are considered suitable for residential use, while areas with WECPNL 70-75 may experience moderate noise impacts and require mitigation measures. Areas with WECPNL > 75 are considered heavily impacted and unsuitable for residential use. Similarly, the Pollution Control Department (2021) sets comparable standards, where areas with WECPNL $\leq$ 70 are suitable for residential properties, educational institutions, and religious establishments, areas with WECPNL 70-75 require land use controls, and areas with WECPNL > 75 are deemed unsuitable for residential use.

The noise level measurements from all 6 points location around Chiang Mai Airport revealed that Points Location 1 (Northern Runway End (Faculty of Agriculture, Chiang Mai University)) recorded a WECPNL value of 70.7, slightly exceeding the standard and falling within the range requiring land use control measures. The other noise measuring point (Points Location 2-6) recorded WECPNL values between 63.6-69.0, which are within standard limits and suitable for residential use.

Overall, most areas surrounding Chiang Mai Airport maintain noise levels within standard limits, except for the northern runway threshold area, which slightly exceeds the standard. This area should be subject to land use control measures and noise impact mitigation to protect nearby communities (Office of Natural Resources and Environmental Policy and Planning, 2021). Since exceeding noise standards directly influences zoning decisions, urban planners should adopt tiered zoning restrictions based on noise contour maps, ensuring land-use compatibility. Specifically, areas within the 70+ WECPNL zone should be allocated for industrial or commercial purposes rather than residential development, while buffer zones should be designated to prevent the encroachment of noise-sensitive uses.

In addition, corridor-based planning approaches that account for flight path orientations are recommended, directing urban growth away from primary flight corridors and encouraging noise-compatible developments along these paths. Furthermore, the observed correlation between noise levels and distance from runways supports the use of graduated development density controls, whereby building heights and population densities decrease progressively with closer proximity to the airport.

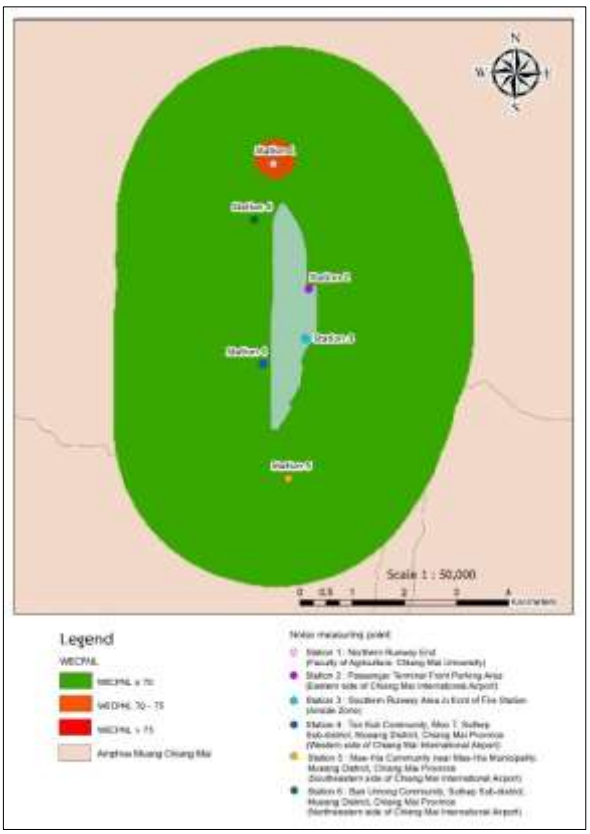

Figure 6. the WECPNL Noise Level Map Around Chiang Mai International Airport

3.4 Airport Development Policy Recommendations

The study's findings necessitate comprehensive policy frameworks that integrate noise management into airport expansion planning. Current airport development policies should incorporate mandatory noise impact assessments for any runway extensions, terminal expansions, or changes in flight operations. The WECPNL methodology demonstrated in this study should be standardized as a requirement for all major airport development projects in Thailand, ensuring consistent assessment criteria across different airports.

Policy frameworks should also address the economic implications of noise-induced land use restrictions. Compensation mechanisms for affected communities and incentive programs for noise-compatible development should be established. This includes tax incentives for businesses willing to locate in higher noise zones and community benefit programs funded through airport revenue sharing.

4. Conclusion

This study analyzed aircraft noise impacts at Chiang Mai International Airport using the WECPNL (Weighted Equivalent Continuous Perceived Noise Level) index as the primary indicator for noise level assessment. The findings revealed that most areas surrounding the airport-maintained noise levels within the standards established by the International Civil Aviation Organization and Thailand's Pollution Control Department. However, Points Location 1 at the Northern Runway End (Faculty of Agriculture, Chiang Mai University) or northern runway threshold recorded a WECPNL value of 70.7, slightly exceeding the standard limit. This area falls into a zone requiring land use control measures and noise impact mitigation to prevent health issues and protect the well-being of nearby residents.

Furthermore, the spatial analysis approach using Inverse Distance Weight (IDW) effectively enabled the creation of noise distribution maps around the airport area. This study's results provide insights into noise distribution patterns and can serve as guidelines for future airport noise management policies, including the implementation of noise mitigation measures such as flight path modification, land use zoning, and aircraft

noise reduction technology development. These measures aim to comply with international standards while minimizing impacts on the quality of life of communities surrounding the airport.

5. Acknowledgements

The researchers would like to express their gratitude to their corresponding author for their guidance, as well as the Department of Civil Engineering, Faculty of Engineering, Chiang Mai University, for their support in successfully completing this research.

6. References

Airports Authority of Thailand. (2020). Environmental impact assessment report: Chiang Mai International Airport development project.

Airports of Thailand. (2023). Annual air traffic statistics report. Airports of Thailand Public Co., Ltd.

Civil Aviation Authority of Thailand. (2023). State of Thai aviation industry report 2023. Ministry of Transport.

Correia, A. W., Peters, J. L., Levy, J. I., Melly, S., & Dominici, F. (2013). Residential exposure to aircraft noise and hospital admissions for cardiovascular diseases: Multi-airport retrospective study. BMJ, 347, f5561. https://doi.org/10.1136/bmj.f5561

ESRI. (2023). Esri Thailand ArcG/S. Retried 5 December 2023. Retrieved from https:/www.esrith.com/?gad_source=1&gclid=EAlalQobChMI2OyE2KH2ggMVXSCDAxOseACLEAAYASAAEgKxK_D_BWE. [In Thai].

Federal Aviation Administration. (2021). Airport noise and access restrictions (Advisory Circular 150/5020-1A). U.S. Department of Transportation.

International Civil Aviation Organization. (2016). Environmental protection (Annex 16 to the Convention on International Civil Aviation, Vol. 1: Aircraft Noise). ICAO.

International Civil Aviation Organization. (2018). Airport planning manual, Part 2: Land use and environmental control. ICAO.

International Civil Aviation Organization. (2018). Environmental protection (Annex 16 to the Convention on International Civil Aviation, Vol. 1: Aircraft Noise, 8th ed.). ICAO.

Ministry of the Environment, Government of Japan. (2023, April 1). Environmental quality standards for aircraft noise. https://www.env.go.jp/en/air/noise/aircraft.html

Nofriandi, H., Wijayanti, A., & Fachrul, M. F. (2018). Study of noise level at Raja Haji Fisabilillah airport in Tanjung Pinang, Riau Islands. IOP Conference Series: Earth and Environmental Science, 106(1), 012024. https://doi.org/10.1088/1755-1315/106/1/012024

Office of Natural Resources and Environmental Policy and Planning. (2021). Guidelines for environmental impact assessment of noise from airport development. Ministry of Natural Resources and Environment, Thailand.

Pollution Control Department. (2020). Manual for aircraft noise measurement. Ministry of Natural Resources and Environment, Thailand.

Pollution Control Department. (2021). Aircraft noise level criteria. Ministry of Natural Resources and Environment, Thailand.

Riyangga K., Purwaningsih R., & Rumita R. R. (2014). Analisis Kebisingan Untuk Peningkatan Kesehatan dan Keselamatan Pekerja pada Area Kerja Apron Ground Handling (Studi Kasus di Bandar Udara Ahmad Yani, Semarang). Industrial Engineering Online Journal, 3(1).

Suma'mur, P. K. (2013). Industrial hygiene and occupational health (HIPERKES) (2nd ed.). Sagung Seto.

Thongsun, P. (2007). Assessment of airport noise impact on communities surrounding Suvarnabhumi Airport [Doctoral dissertation]. King Mongkut's University of Technology Thonburi.

Watson, D. F., & Philip, G. M. (1985). A refinement of inverse distance weighted interpolation. Geoprocessing, 2(4), 315-327.

Journal on Transportation System and Engineering
ISSN: 3059 9865(Print) 3059-9873(Online)
Vol. 1. Issue 2, 2025(December): 11-26
DOI: https://doi.org/10.3126/jotse.v1i2.87728

Research Articles
Received Date: April 10, 2025
Revised Date: October 12, 2025
Accepted Date: November 10, 2025
Published Date: December 21, 2025

Artificial Neural Networks and Multiple Linear Regression in Pavement Deterioration Forecasting

Krishna Singh Basnet[1], Jagat Kumar Shrestha[2], Rabindranath Shrestha[3]

[1]*Institute of Engineering, Tribhuvan University, krishnasinghbasnet@gmail.com*
[2]*Institute of Engineering, Tribhuvan University, jagatshrestha@ioe.edu.np*
[3]*Institute of Engineering, Tribhuvan University, rabindra@ioe.edu.np*

Abstract

Assessing pavement conditions in Nepal is costly and time-consuming, with rising traffic and aging infrastructure making maintenance increasingly challenging. This study developed and compared pavement deterioration models to predict the Surface Distress Index (SDI) without manual assessment, using historical road data. SDI was modeled as a function of five key factors: International Roughness Index (IRI), pavement age, total annual rainfall, annual temperature range, and commercial vehicle traffic. Data were collected from relevant government sources, covering 157 road sections with a combined length of 15,783 km, for the period from 2012 to 2022. Multiple Linear Regression (MLR) and Artificial Neural Network (ANN) models were developed for SDI prediction. MLR analysis, conducted in Microsoft Excel, assessed statistical significance through ANOVA, R^2 values, and regression coefficients. In contrast, ANN modeling utilized a Multi-Layer Perceptron (MLP) architecture implemented in TensorFlow and Keras. The ANN model was optimized through iterative experimentation with varied architectures, employing ReLU activation and the Adam optimizer for adaptive learning. The study evaluated a range of architectures, beginning with simple single-layer networks and extending to Deep Neural Networks (DNNs) with up to four hidden layers. Results showed that, during model development, MLR achieved an R^2 of 0.735, whereas the ANN model, with a 5-232-1 structure and 104 epochs, outperformed MLR with an R^2 of 0.809. Validation of both models indicated strong alignment between observed and predicted values, with ANN demonstrating superior predictive accuracy (R^2 = 0.816) compared to MLR (R^2 = 0.74). The error histogram further confirmed ANN's better performance, which confirms its improved reliability. The study highlights the effectiveness of both models while emphasizing ANN's advantage in capturing complex nonlinear relationships. These findings suggest that integrating ANN into Nepal's pavement management framework can enhance predictive accuracy, reduce assessment costs, and support more efficient maintenance planning.

Keywords: Pavement, Surface Distress Index, International Roughness Index, Multiple Linear Regression, Artificial Neural Network

1. Introduction

Efficient pavement management is essential for sustaining transport networks that promote economic and social development. Pavement Management Systems (PMS) offer a structured approach to plan maintenance, repair, and rehabilitation (M&R), optimizing limited resources and enhancing safety (Abaza et al., 2004; Ferreira et al., 1999; Kulkarni & Miller, 2003; Mathavan et al., 2015; Zakeri et al., 2017). A well-implemented PMS maintains serviceability, structural integrity, and cost-effectiveness while minimizing environmental and social impacts (Fwa et al., 2000). Core PMS components include a road database, condition assessment, cost and performance models, and a Maintenance Optimization System (MOS). The MOS guides M&R strategies using prioritization (Kulkarni et al., 2004; Wong et al., 2003) or optimization models (Abaza, 2006; Durango-Cohen & Tadepalli, 2006; Meneses et al., 2013; Picado-Santos et al., 2004). Understanding pavement deterioration enables better timing of interventions, reducing costs and preserving condition. Performance prediction models are key to determining optimal intervention times (Kerali et al., 2000).

In Nepal, the Department of Roads (DoR) is responsible for the management of 11,179 km of National Highways (NH) (DoR, 2022). The Nepalese government allocates an approximate budget of NRs 7 billion for maintenance. The DoR uses the Annual Road Maintenance Plan (ARMP) as a part of its PMS (DoR, 2007). The DoR collects IRI, SDI, and traffic data to develop the integrated ARMP using a 1995 empirical method

Corresponding Author's Email Address Krishnasinghbasnet@gmail.com

(Department of Roads & Maintenance Branch, 2005). Presently, IRI is measured on-site, while SDI requires time-consuming videography analysis, leading to higher costs. In 2022, 73% of NHs were in fair to good condition (SDI: 0-3) (Highway Management Information System-Information & Communication Technology (HMIS-ICT) Unit, 2022), but aging infrastructure and rising traffic make it challenging to maintain over 95% of the network in good condition. To address these challenges, a pavement deterioration model is required to simplify data collection, optimize budget allocation, and enhance long-term maintenance planning. Nepal's PMS lacks a performance prediction model, relying instead on annual IRI and SDI assessments, which are labor-intensive, costly, and time-consuming. This reactive approach delays maintenance decisions and reduces efficiency. Manual prioritization, combined with a limited annual maintenance budget of NRs 7 billion, further constrains effective planning. Research on pavement deterioration in Nepal is scarce and often omits key variables. A study in 2021 analyzed relationships between IRI, Pavement Condition Index (PCI), and SDI using regression, but their study had a small sample size and excluded critical factors such as pavement age, traffic, and environmental conditions (S. Shrestha & Khadka, 2021). Sigdel & Pradhananga (2021) developed an IRI model using data from 1,745 road sections, incorporating variables like rainfall and commercial vehicles. However, traffic data were sourced from only 160 stations, raising concerns about accuracy and representativeness. Pavement age, a crucial factor, was also omitted. Although Sigdel et al. (2024) later applied an ANN model, issues with traffic data and age remained unresolved. Similarly, Shakya et al. (2023) used a Markov hazard model but excluded factors such as axle loads, traffic, and climate variables.

This study developed pavement deterioration models to forecast SDI without manual assessment, using a road condition dataset from 2012 to 2022, which uses readily available data to estimate pavement lifespan, support life-cycle cost analysis, and enhance performance prediction. The study employs both MLR and ANN to build the model and compares their effectiveness in predicting SDI.

2. Literature Review

Performance prediction models/Deterioration models are used to forecast the future condition, functionality, or service level of an asset. Prediction models are classified into three sub-categories: deterministic, probabilistic, and machine learning. Deterministic models use fixed mathematical equations to predict outcomes, while probabilistic models rely on probability distributions to estimate the likelihood or range of possible future conditions (Anyala et al., 2014; Sanabria et al., 2017; Wang et al., 2017). The empirical method is one of the deterministic models that apply statistical analysis to key deterioration factors like pavement age and traffic load, often using linear or nonlinear regression techniques (Anyala et al., 2014). Univariable regression analyses a single factor, whereas multivariable regression considers multiple variables. Given the complexity of asset deterioration, univariable models often lack accuracy compared to multivariable approaches. The regression modelling process starts with data collection and quality checks, followed by diagnostics to explore variable relationships and interactions. If issues are found, remedial measures like data transformation are applied. Relevant explanatory variables are selected, and interaction or non-linear effects are further analysed. Residuals and diagnostics help assess model fit, with additional corrections if needed. A tentative model is then chosen and validated. If it meets assumptions and performs well, it becomes the final regression model. This iterative process ensures accuracy and reliability (Neter et al., 1996). Regression models are flexible and easy to use, allowing for various functional forms to analyze data. Their performance is typically evaluated using statistical metrics that measure fit quality. While the coefficient of determination (R^2) is commonly used, some researchers advocate for error-based metrics, such as percentage errors, to better assess model accuracy (Arhin & Noel, 2014; Ashrafian et al., 2020; Gong et al., 2019).

ANNs are one of the machine learning models, which are AI-based computational models capable of solving complex, nonlinear engineering problems like pavement condition assessment and prediction (Adeli, 2001). Inspired by the human brain, ANNs process data through interconnected artificial neurons (mathematical analogs of biological neurons) using weighted connections to learn and make decisions (Georgiou et al., 2018; Mosa, 2017). ANNs are increasingly used in pavement performance forecasting, leveraging condition indicators to predict deterioration such as cracking, rutting, or roughness (Bosurgi & Trifirò, 2005; Domitrović et al., 2018). Building an ANN involves defining three core components: (1) the number of layers—a minimum of three: input,

hidden, and output; (2) the number of neurons per layer; and (3) the activation functions and training parameters (Elshamy et al., 2020). Feed-Forward Neural Networks (FFNNs), a common ANN type, operate in one direction without feedback loops. They consist of input, hidden, and output layers, where each neuron computes outputs by applying an activation function to the weighted sum of inputs. FFNNs may be single-layer or multi-layer; the latter includes hidden layers that enable the extraction of complex features (Sazlı, 2006). Fully connected networks link every neuron in one layer to all neurons in the next layer (Haykin, 1998). The Multi-Layer Perceptron Neural Network (MLPNN) is a typical FFNN structure comprising at least one hidden layer. When it includes multiple hidden layers, it is referred to as a Deep Neural Network (DNN). Training adjusts weights via algorithms like gradient descent or Levenberg-Marquardt to minimize prediction error (A. Shrestha & Mahmood, 2019). Rectified Linear Unit (ReLU) is a widely used activation function that mimics the brain's sparse neuron activation—only a small fraction of neurons fire at a time, reducing computational load and overfitting risks. ReLU outputs zero for negative inputs and scales linearly for positives, mirroring biological neuron responses (Glorot et al., 2011; LeCun et al., 2015).

3. Methodology

3.1 Variables

The study defined SDI as a function of five independent variables: IRI, pavement age (Age), total annual rainfall (RF), annual temperature range (TD), and Commercial Vehicles per day (CV), with reference to the literature review of several past studies, as shown in the equation 1. The variable Age refers to the number of full years elapsed since the most recent major structural intervention that effectively reset the pavement's deterioration lifecycle. The variable RF represents the cumulative depth of precipitation that occurred during the twelve months preceding the year of prediction. The TD variable denotes the annual temperature range experienced at the road section, calculated as the difference between the average daily maximum and minimum temperatures over a continuous twelve-month period. Lastly, CV indicates the average number of commercial vehicles, specifically trucks (light, heavy, and multi-axle) and buses (large, mini, and micro), passing a road section per day.

$$SDI=f\ [IRI, Age, RF, TD, CV] \ldots\ldots\ldots (1)$$

3.2 Study Area and Data Collection

This study focused on the national highways of Nepal, which connects major urban centres, trade corridors, and border points. Data were collected from the HMIS of the DoR, the RBN, and the Department of Hydrology and Meteorology (DHM) for the period 2012-2022.

Though SDI/IRI measurements in Nepal began in 1995, a systematic online database was only established in 2012, limiting the study to data from that year onward. Moreover, though there are a greater number of road sections within the SRN, reliable traffic data exist only for 160 sections in the HMIS, as traffic count stations are located on or near these sections (DoR, 2023). Assigning traffic volumes from distant stations could produce misleading estimates because of location variations in access patterns, land use, and traffic composition. Among them, three lacked corresponding roughness data; hence, 157 sections were used for modelling. These sections, averaging 15.7 km in length and totalling 15,783 km (from 2012 to 2022). Therefore, only sections with both direct traffic and surface-condition data were retained to maintain reliability. The road sections and traffic count stations taken for the study are shown in Figure 1. All selected road sections were flexible pavements as listed in the DoR inventory. Although the SRN includes other surface types, sub-type data for flexible pavements have not been consistently recorded since 2012. Therefore, the study treated flexible pavements as a general category representative of Nepal's SRN.

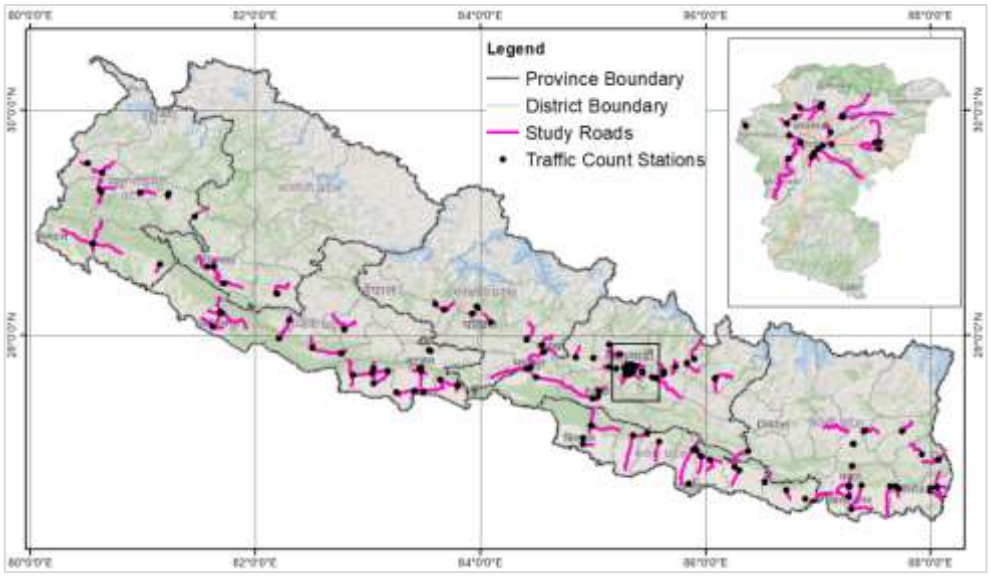

Figure 1 Study Area

Data on SDI, IRI, and traffic were collected from the HMIS (DoR, 2023) as discussed earlier. Climatic variables were obtained from the nearest DHM meteorological stations (Figure 2), which provide the only official long-term climatic records in Nepal. Average annual rainfall and temperature difference were computed for each road section. Despite potential micro-climatic variations, these datasets offer the best available representation of regional climatic influences on pavement deterioration. Due to the unavailability of direct records on pavement age, it was estimated indirectly by identifying abrupt reductions in SDI or IRI values, which typically indicate overlays or major rehabilitation works. These deduced ages were then cross-validated with maintenance and rehabilitation records from the RBN. Pavement age was assigned as zero for years in which major structural improvements were detected.

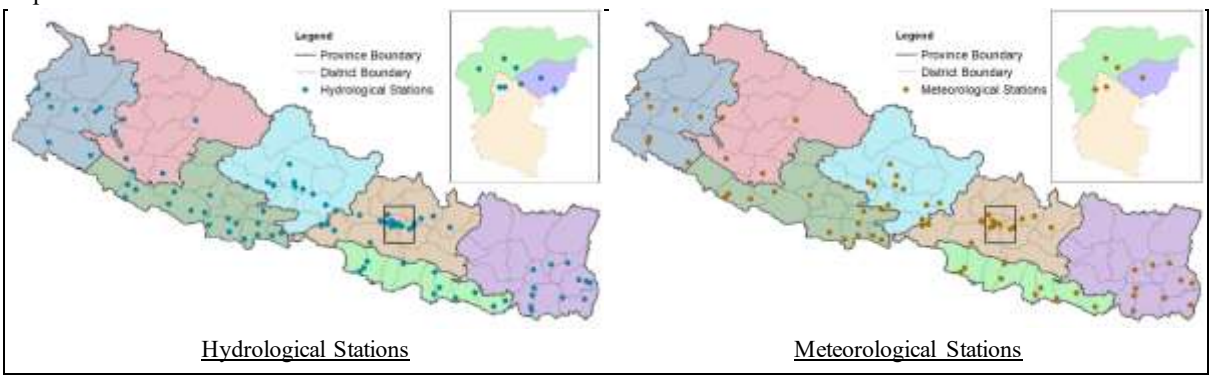

Figure 2 Climate Stations used for the study

3.3 Data preprocessing

Before model development, the data were organized and cleaned to remove inconsistencies and outliers. This involved using imputation to fill missing values, allowing incomplete records to be retained, and capping to limit extreme values by replacing them with defined thresholds. These techniques helped maintain the integrity of the dataset. Furthermore, Pearson's correlation coefficients were computed using Microsoft Excel to assess multicollinearity among independent variables.

3.4 Multi-linear Regression (MLR)

Multiple linear regression analysis was conducted using Microsoft Excel to establish the relationship between SDI and the specified five independent variables. The dataset was split into two parts: 80% for model development and 20% for validation. The MLR model was built using the development dataset and evaluated on the validation dataset using key performance metrics. The regression aimed to predict the dependent variable (SDI) based on multiple independent variables, using the general model as presented by the equation 2.

$$y = b_0 + b_1x_1 + b_2x_2 + ... + b_nx_n \quad \ldots\ldots\ldots (2)$$

where, y is the dependent variable, x_1 to x_n are predictors, and b_0 to b_n are regression coefficients. The model's statistical significance and explanatory power were evaluated using ANOVA and the coefficient of determination (R^2). ANOVA tested whether the model significantly explained variance in the dependent variable, while R^2 measured the proportion of SDI variance accounted for by the independent variables, indicating goodness-of-fit. Model reliability was verified using the validation dataset, comparing predicted SDI values against observed values to assess predictive performance. Furthermore, k-fold cross-validation was conducted in 5-folds to check the statistical robustness of the model.

3.5 Artificial Neural Network (ANN)

In this study, an ANN model was developed using a supervised learning approach to predict the SDI. The full dataset was divided into two subsets: 80% for model development (training and testing) and 20% for validation. Furthermore, k-fold cross-validation in 5-folds was conducted to check the statistical robustness of the model.

The model was developed in Python using TensorFlow, with Keras providing a high-level interface for streamlined construction and training. A MLP was employed to capture complex data relationships through multiple interconnected layers. The model iteratively calculated weight and bias matrices using a feed-forward architecture with backpropagation. During the feed-forward phase, input data passes through hidden layers, where weighted sums are computed and processed via the ReLU activation function, f(x)=max(x,0), introducing non-linearity. The output is compared with actual values to compute error, which is then propagated back to adjust weights. The Adam optimizer was used to adaptively update learning rates, enhancing training efficiency, especially with sparse gradients or noisy data. The iteration process is illustrated in Figure 3.

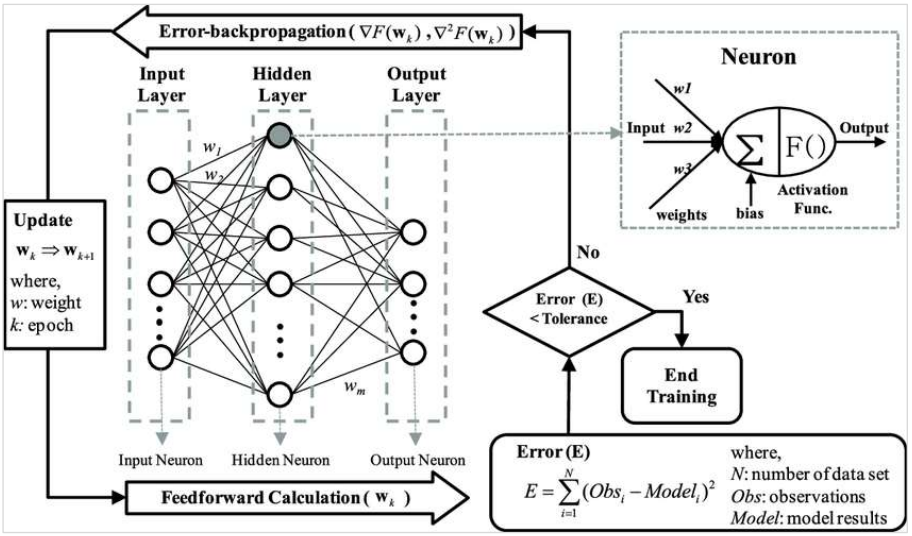

Figure 3 Iteration Process (Kim & Seo, 2015)

The architecture consisted of an input layer with five nodes corresponding to the selected features. Hidden layer configurations were determined through iterative experimentation, testing different combinations of layers and neurons. The optimal architecture was selected based on performance metrics, including R^2 and mean squared error (MSE), with training iterations (epochs) run until the highest R^2 and lowest MSE were achieved. The study explored the performance of ANN with up to two hidden layers and further investigated DNN with up to four hidden layers. The framework for ANN model development is shown in Figure 4.

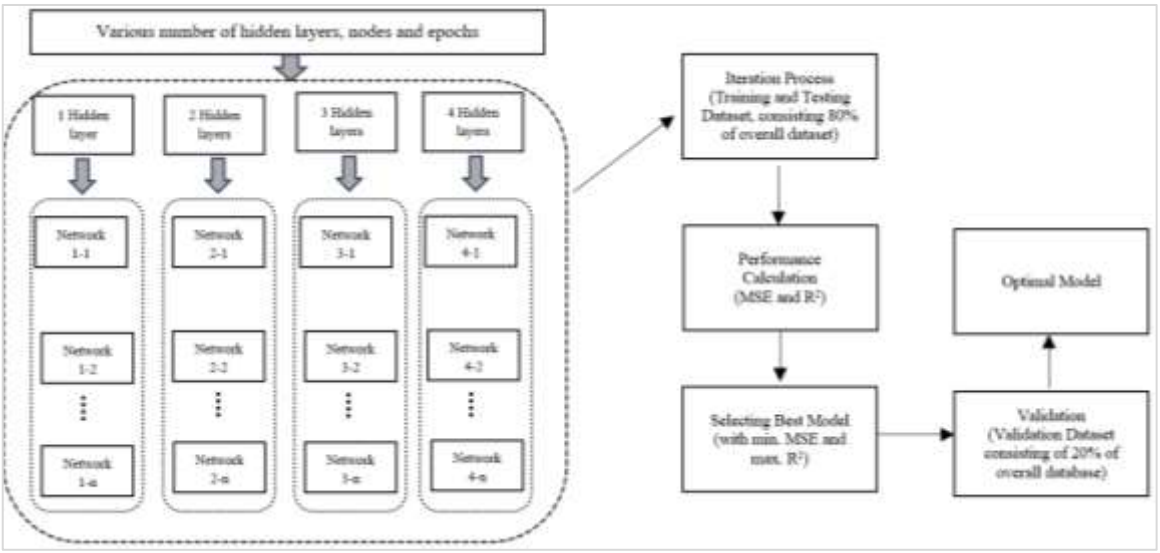

Figure 4 ANN Model Development Framework

Model training involved minimizing the error between predicted and actual SDI values, quantified using the squared error function as presented in the equation 3 while weight updates during backpropagation, following the equation 4.

$$E = \sum_{i=1}^{N} (Obs_i - Model_i)^2 \quad \ldots\ldots\ldots (3)$$

$$W_{new} = W_{old} + \alpha * (Obs - Model) * x \quad \ldots\ldots\ldots (4)$$

Where, E: Error; Obs: Observed Value; Model: Model Predicted Value; α: Learning rate; x: Input Value; W_{new}: New Weightage; W_{old}: Old Weightage.

After training the MLPNN, the model output can be expressed using a specific mathematical formulation. For instance, an MLPNN with a single hidden layer and a single output neuron can be represented as shown in the equation 5 (Yang et al., 2021).

$$Output = f_0[B_O + \sum_K W_K f_H(B_{HK} + \sum_i W_i Input_i)] \quad \ldots\ldots\ldots (5)$$

Where, f_o and f_H are activation functions used in the output layer and hidden layer; B_O and B_H are biases for the output layer and hidden layer; W is the weight between the nodes; K is the number of nodes in the hidden layer; and i is the number of the input variables.

3.6 Sensitivity Analysis

A sensitivity analysis was conducted on the developed prediction models to identify the most and least influential parameters in predicting SDI. The study employed the equation 6 to compute the sensitivity index (Chang & Liao, 2012).

$$S = \left\{ \left(\frac{O2 - O1}{I2 - I1} \right) * \left(\frac{Iavg}{Oavg} \right) \right\} \quad \ldots\ldots\ldots (6)$$

where, S: Sensitivity Index; I_1,I_2: Minimum and Maximum Input values respectively; O_1,O_2: Output values corresponding to I_1 and I_2 respectively; I_{avg},O_{avg}: Average I_1, I_2 and Average O_1,O_2 respectively.

4. Results and Discussion

4.1 Multi-Collinearity

Figure 5 illustrates the Pearson correlation heatmap, which revealed coefficients ranging from 0.01 to 0.58, indicating weak to moderate correlations and no significant multicollinearity. Therefore, all five variables were included in the pavement performance prediction model. The correlation between IRI and Age was highest (r = 0.58), followed by IRI and Rainfall (r = 0.25), both indicating weak relationships.

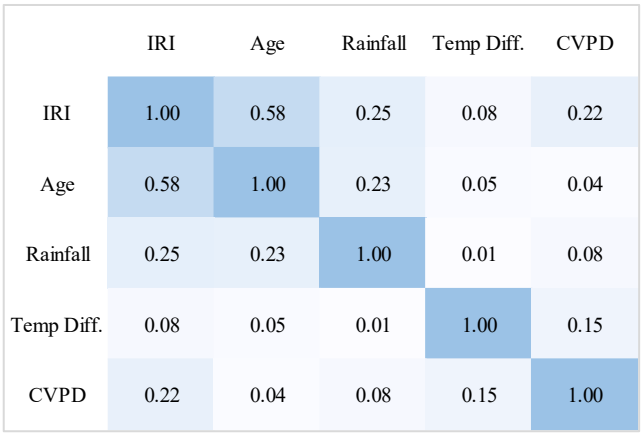

Figure 5 Pearson Correlation Coefficient Heatmap

4.2 MLR

ANOVA test results as presented in Table 1 show an F-statistic of 429.224 with a p-value below 0.05, indicating a statistically significant relationship between SDI and the independent variables. This leads to the rejection of the null hypothesis, confirming the presence of correlations. The degrees of freedom were 5 (regression) and 784 (residual), reflecting five estimated parameters and 784 unexplained data points. The Regression Mean Square (83.5) and Residual Mean Square (0.19) indicate that most variability is explained by the model. Similarly, the Regression Sum of Squares (SSR = 417.6) exceeds the Residual Sum of Squares (SSE = 152.5), suggesting the model captures a substantial portion of the total variance in the dependent variable.

Table 1 ANOVA Results

	Degree of freedom (df)	Sum of Squares (SS)	Mean of Squares (MS)	F Statistics	Significance F (p - value)
Regression	5	417.677	83.535	429.224	1.3153E-221
Residual	784	152.582	0.195		
Total	789	570.259			

Regression statistics, as presented in Table 2, show model quality and accuracy. A Multiple R of 0.856 indicates a strong positive linear relationship between independent and dependent variables. The R-Square value of 0.732 shows that 73.2% of the variation in SDI is explained by the model, while the Adjusted R-Square of 0.731 accounts for the number of predictors. The Standard Error of 0.441 reflects the average deviation of observed values from predicted values, confirming the model's strong fit using the five selected independent variables.

Table 2 Regression Statistics

Regression Statistics	
Multiple R	0.856
R Square	0.732
Adjusted R Square	0.731
Standard Error	0.441
Observations	790

Table 3 presents the coefficients and test statistics from the multiple linear regression analysis. All five predictors: IRI (0.146), Pavement Age (0.167), Rainfall (0.058), Temperature Difference (0.018), and CV (0.052), show positive relationships with SDI. IRI and Age are the most influential, while CV has a moderate impact, likely due to maintenance in high-traffic areas. All predictors are statistically significant ($p < 0.05$), with high t-values and narrow confidence intervals confirming estimate reliability.

Table 3 Test Statistics and Coefficients

	Coefficients	Standard Error	t Stat	P-value	Lower 95%	Upper 95%
Intercept	0.310	0.113	2.749	0.006	0.089	0.531
IRI	0.146	0.009	17.094	0.000	0.129	0.163
Age	0.167	0.007	22.427	0.000	0.152	0.181
RF (in m)	0.058	0.025	2.302	0.022	0.009	0.108
TD (in °C)	0.018	0.082	2.175	0.030	0.017	0.341
CV (in '000 veh)	0.054	0.010	5.197	0.000	0.034	0.074

Based on the outcomes of the multiple linear regression analysis, the model for SDI concerning Nepal's national highway pavements is formulated as the equation 7.

$$SDI = 0.31 + 0.146\ IRI + 0.167\ Age + 0.058\ RF + 0.018\ TD + 0.054\ CV \quad \ldots\ldots\ldots (7)$$

Where, SDI: Surface Distress Index; IRI: International Roughness Index / Performance function (m/Km); Age: Pavement Age in years; RF: Total Rainfall in m; TD: Annual Max and Min Temperature Difference in °C; CV: Number of Commercial Vehicles per Day in thousands (thousand veh.)

For validation, the model was tested on a separate dataset of 189 observations (20% of the total). The R^2 value for validation was 0.7404, slightly higher than the model's training R^2, indicating that 74.04% of the SDI variance was accurately predicted.

Figure 4.4 shows scatter plots comparing observed and predicted SDI for the model development, validation, and combined datasets. The model performed well in both phases, showing strong correlations and good generalization. The MLR model explains about 73% of the variance in the overall SDI dataset.

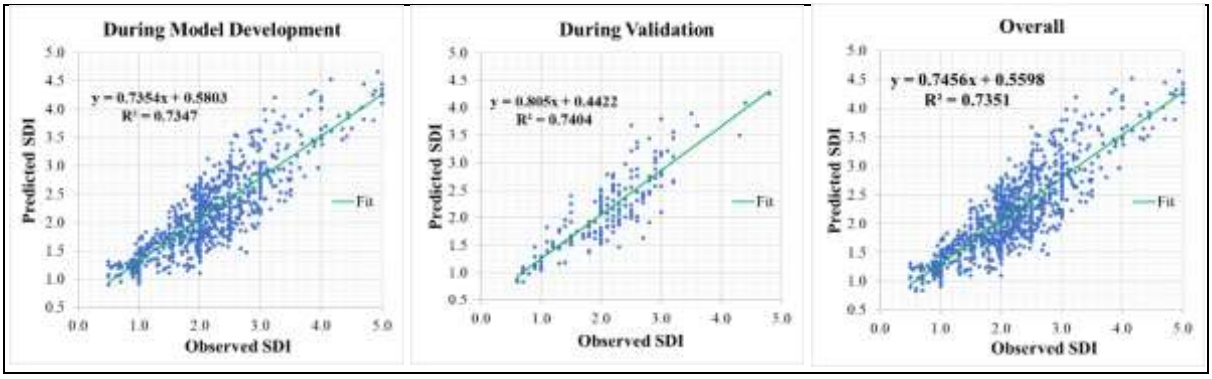

Figure 6 Predicted SDI Vs measured SDI under MLR

The results of the 5-fold cross-validation presented in Table 4 demonstrate the robustness and consistency of the MLR model. The R^2 values range from 0.724 to 0.742, with an average of 0.733, indicating that the model explains approximately 73% of the variation in the SDI. The low variation across folds and the relatively small MSE (0.194) and MAE (0.362) confirm the model's stability.

Table 4 k-fold Cross-validation for MLR

Fold	R^2	MSE	MAE
1	0.724	0.202	0.374
2	0.736	0.197	0.36
3	0.729	0.19	0.358
4	0.742	0.186	0.35
5	0.733	0.193	0.365
Mean	**0.733**	**0.194**	**0.362**

4.3 ANN

The study began with a simple ANN architecture using one hidden layer, testing node counts from 32 to 256 and epochs from 32 to 112 (in steps of 8), totalling 319 iterations. This was followed by testing two hidden layers (275 iterations), then three (187 iterations), and finally four (11 iterations), each time recording R^2 and

MSE. As the number of layers and nodes increased, so did the computational demand. Figure 7 summarizes results for one and two hidden layer networks. For one hidden layer, the 5-232-1 architecture achieved the best performance with a minimum MSE of 0.138 and a maximum R^2 of 0.808 at epoch 104. For two hidden layers, the 5-224-32-1 architecture achieved a minimum MSE of 0.139 and R^2 of 0.80 at epoch 72.

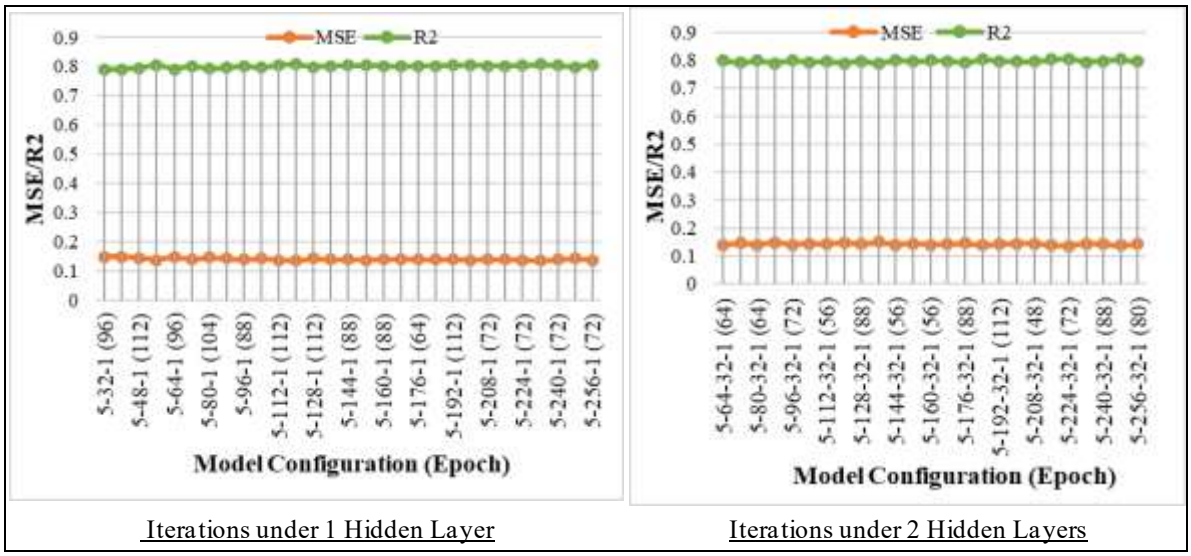

Figure 7 Iterations for Optimum Network Model under ANN

Similarly, Figure 8 illustrates the iterations conducted using a DNN with 3 to 4 hidden layers. For the network with three hidden layers, the architecture 5-208-64-32-1 yielded a minimum MSE of 0.143 and a maximum R^2 of 0.79 at epoch 72. The latter, with the architecture 5-256-128-64-32-1, yielded a minimum MSE of 0.153 and a maximum R^2 of 0.78 at epoch 40.

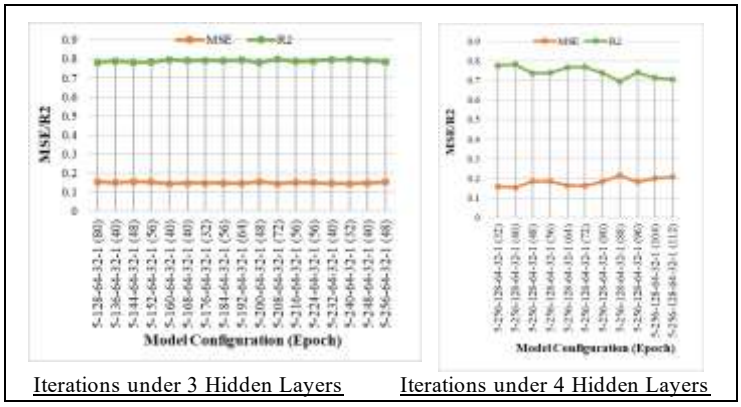

Figure 8 Iterations for Optimum Network Model under DNN

The optimal ANN model was identified as 5-232-1 with 104 epochs, as shown in Figure 9. In the figure, blue dots represent inputs, reddish denotes hidden layers, and green indicates the output. This model demonstrated high computational efficiency, requiring just 2.2 seconds to train on an AMD Ryzen 7 6800H (3.20 GHz) with 16 GB RAM. Given that the dataset spans 10 years and is unlikely to grow significantly, training time remains minimal, making frequent model updates practical.

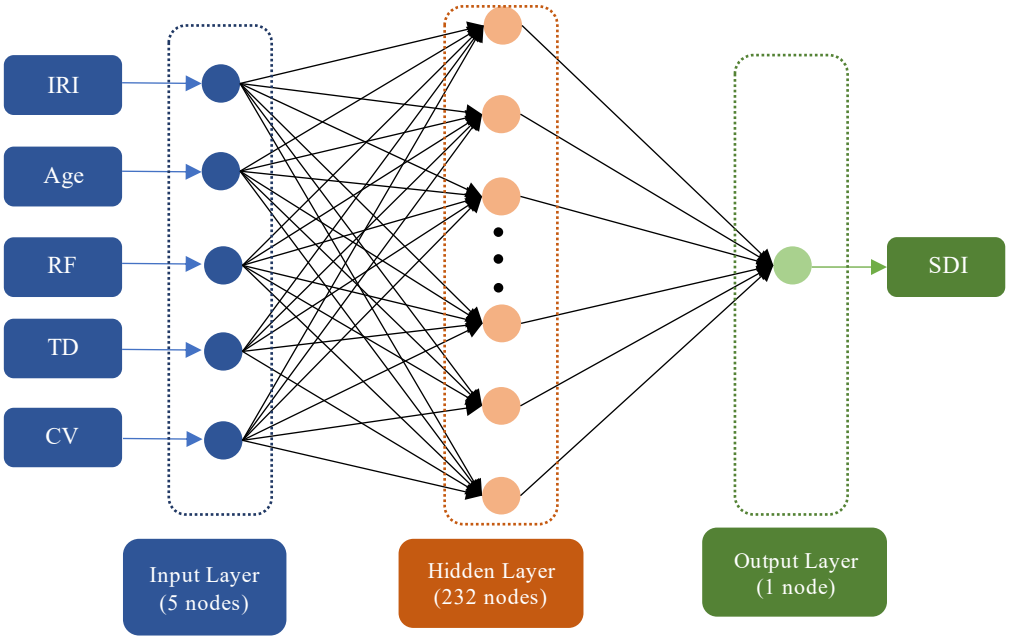

Figure 9 The 5-232-1 NN Model Architecture

The equations for transformations in the hidden layer can be written as the equation 8. The output layer applies a weighted sum of the hidden layer outputs to produce the final output, which can be written as the equation 9. Finally, when combining the transformations in all the layers, the complete equation for the output y can as written as the equation 10. The model for predicting SDI can be written as the equation 11.

$$h_j = \text{ReLU}\left(\sum_{i=1}^{5} W_{1ji} X_i + b_{1j}\right) \ldots\ldots\ldots (8)$$

For j = 1, 2, …, 232 nodes in the hidden layer.

$$y = \sum_{l=1}^{232} W_{2j} h_j + b_2 \ldots\ldots\ldots (9)$$

$$y = \sum_{j=1}^{232} W_{2j}\ \text{ReLu}\left(\sum_{i=1}^{5} W_{1ji}\ X_i\ + b_{1j}\right) + b_2 \ldots\ldots\ldots (10)$$

$$SDI_{Predicted} = W_O * [W_i * I + B_1] + B_2 \ldots\ldots\ldots (11)$$

where, W_O = Output Weight Matrix; W_i = Input Weight Matrix; B_1,B_2 = Bias Matrix for hidden and Output Layers; X_i = i-th input feature (where i=1,2,3,4,5 for IRI, PA, RF, TD, CV respectively); W_{1ji} = weight from the i-th input node to the j-th hidden node; b_{1j} = bias for the j-th hidden node; h_j = output of the j-th hidden node after applying the ReLU activation function; W_{2j} = weight from the j-th hidden node to the output node; b_2 = bias for the output node; y = predicted SDI

The ANN model was validated using 189 observations (20% of the dataset), achieving an R^2 of 0.816, slightly higher than during training, indicating that 81.6% of the SDI variance was accurately predicted. Figure 10 compares observed and predicted SDI for the training, validation, and overall datasets. The model shows strong correlations and consistent performance across all phases, with minor prediction errors. The ANN model explains about 80% of SDI variability in the overall dataset.

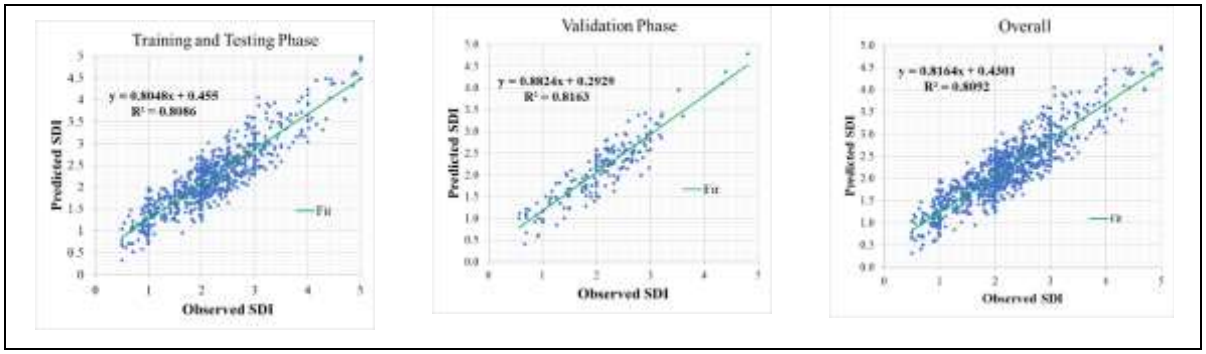

Figure 10 Predicted SDI Vs observed SDI using ANN

The 5-fold cross-validation results in Table 5 confirm the superior performance and reliability of the ANN model. The R^2 values range from 0.799 to 0.817, with an average of 0.809, indicating that the ANN model explains about 81% of the variation in the SDI (a notable improvement over the MLR model). The mean values of MSE (0.134) and MAE (0.292) are consistently lower across all folds, suggesting higher predictive accuracy and better generalization.

Table 5 k-fold Cross-validation for ANN

Fold	R^2	MSE	MAE
1	0.799	0.141	0.304
2	0.812	0.134	0.289
3	0.808	0.131	0.295
4	0.817	0.128	0.283
5	0.810	0.136	0.291
Mean	**0.809**	**0.134**	**0.292**

4.4 Comparison

Table 6 and Figure 11 summarize model performance across development, validation, and overall datasets. The MLR model showed decent accuracy with an R^2 of 0.735, MSE of 0.191, and MAE of 0.367 during development. Validation slightly improved with R^2 of 0.740, MSE of 0.141, and MAE of 0.307. In comparison, the ANN model outperformed MLR in all phases. It achieved an R^2 of 0.809, MSE of 0.138, and MAE of 0.301 during development, and improved further in validation (R^2 = 0.816, MSE = 0.102, MAE = 0.263). ANN showed stronger accuracy and generalization in predicting SDI.

Table 6 Summary of performance evaluation parameters

Model	Eqn. (No.)	Phase/Data Set	No. of Data Set	MSE	MAE	MAPE	MAD	R2	RMSE
MLR	7	Model Development	790	0.191	0.367	19.758	0.192	0.735	0.437
		Validation	189	0.141	0.307	16.573	0.166	0.740	0.375
		Overall	979	0.191	0.367	19.758	0.192	0.735	0.437
ANN	11	Training and Testing (Model Development)	790	0.138	0.301	16.414	0.182	0.809	0.372
		Validation	189	0.102	0.263	15.290	0.150	0.816	0.319
		Overall	979	0.131	0.294	16.197	0.176	0.809	0.363

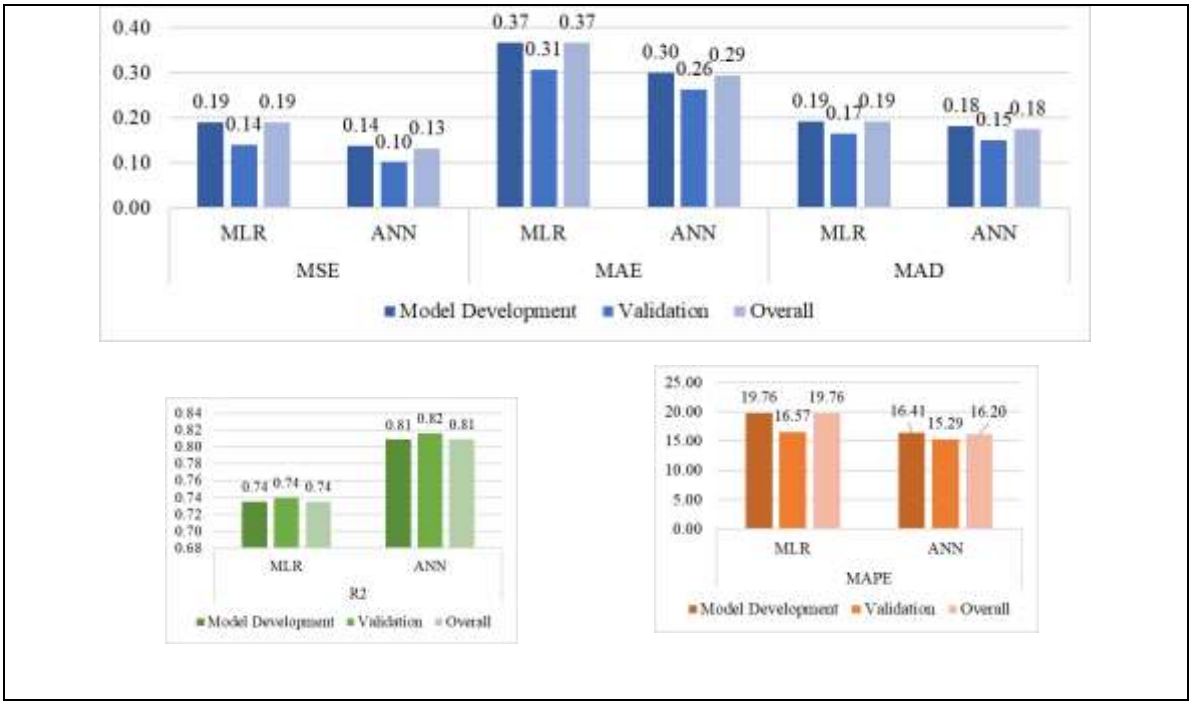

Figure 11 Comparison of evaluation parameters of developed models

Figure 12 compares error distributions of the developed models, highlighting differences in predictive accuracy. The MLR model shows a wider error spread, indicating higher variance and moderate accuracy. In contrast, the ANN model exhibits a tighter distribution centred around zero, reflecting greater accuracy and consistency.

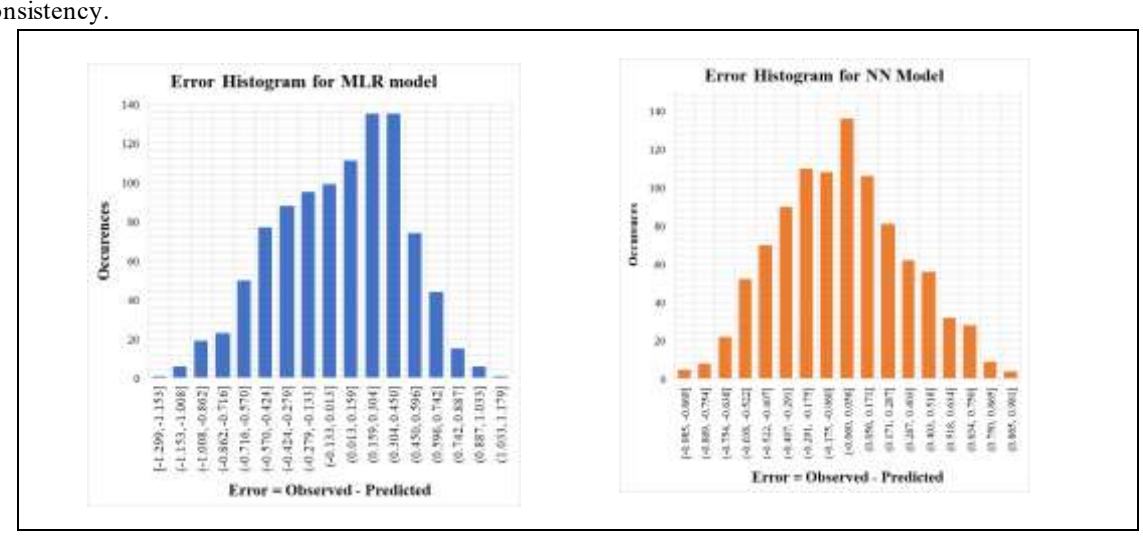

Figure 12 Error Histogram

Figure 13 compares the predicted and observed SDI values for MLR and ANN models. The MLR model shows greater deviation and variability, especially during validation, indicating moderate accuracy. In contrast, the ANN model closely follows observed values across both phases, capturing trends and fluctuations more effectively.

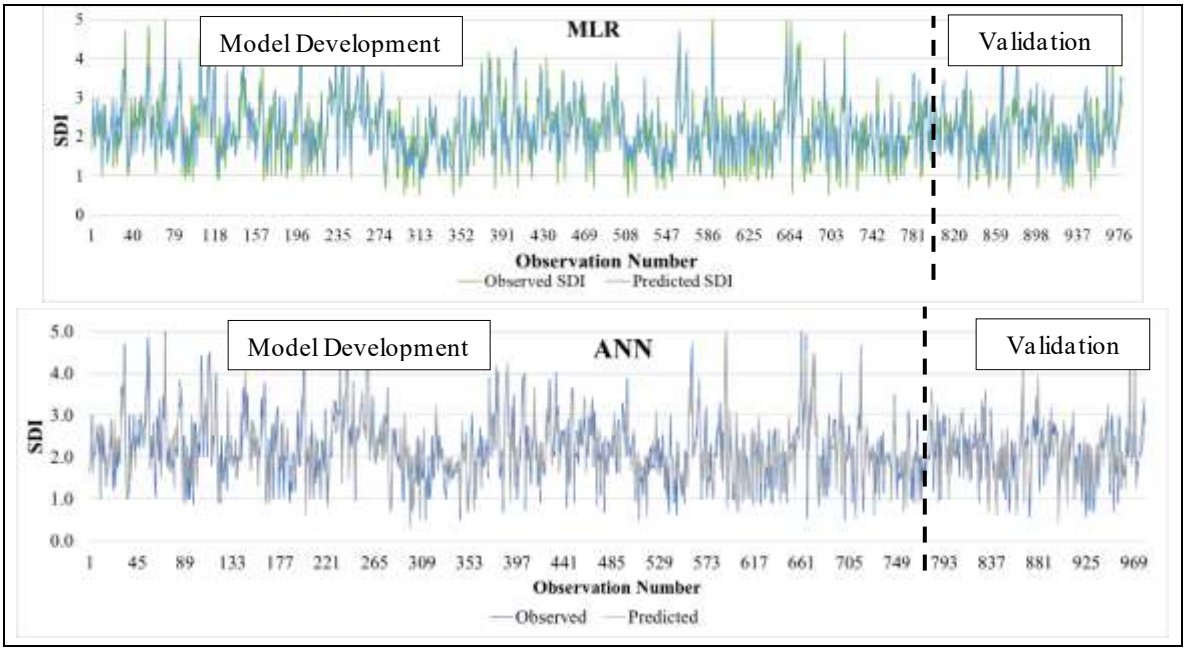

Figure 13 Comparison between predicted and observed SDI under MLR and ANN

4.5 Sensitivity Analysis

Table 7 presents the sensitivity index for each variable in the developed models. IRI is the most influential predictor, with the highest sensitivity in both MLR (0.78) and ANN (0.76). Age and Rainfall show similar influence across models, though MLR gives Age more weight (0.38 vs. 0.34) and less to Rainfall (0.21 vs. 0.24) than ANN. Temperature has a moderate impact (MLR: 0.37, ANN: 0.36), while CV shows the least sensitivity (MLR: 0.09, ANN: 0.13), likely due to maintenance interventions in high-traffic sections.

Table 7 Sensitivity Index in Variables

	IRI	Age	Rainfall	Temp. Diff.	CV
MLR	0.78	0.38	0.21	0.37	0.09
ANN	0.76	0.34	0.24	0.36	0.13

4.6. Discussion

The study developed prediction models using all available and verified data from the national database. However, the findings are constrained by the limited availability and completeness of reliable datasets in Nepal. The absence of detailed pavement classification records restricted the analysis to a generalized category of flexible pavements. Further disaggregation by surface type would have significantly reduced the dataset and compromised the statistical robustness of the models. Similarly, the limited number of permanent traffic count stations constrained the study to road sections with verified traffic and roughness data, despite the presence of a larger number of road sections in the SRN. The use of climatic data from the nearest DHM stations introduces another potential source of uncertainty, as Nepal's complex topography causes substantial variation in rainfall and temperature over short distances. Nevertheless, the DHM remains the only institution maintaining continuous and standardized climatic datasets, and using the nearest available stations ensured methodological consistency and reliability under current data constraints.

Despite these limitations, the selected road sections span diverse physiographic and climatic regions, including the Terai, mid-hill, and mountain zones, capturing a broad range of environmental and traffic conditions. Therefore, the developed models are considered reasonably representative of Nepal's flexible pavement performance at a national scale within the bounds of existing data.

5. Conclusion

The study developed and evaluated two predictive models: MLR and ANN, to forecast the SDI of Nepal's national highway pavement network using five key variables: IRI, pavement age, annual rainfall, annual temperature difference, and commercial vehicle traffic. Using a comprehensive dataset covering 157 road sections over ten years (2012–2022), the models were trained and validated to assess their performance and predictive capabilities. The correlation analysis showed no signs of multicollinearity, validating the inclusion of all variables. MLR analysis was conducted in Microsoft Excel, which assessed statistical significance through ANOVA, R^2 values, and regression coefficients. The MLR model demonstrated a dependable predictive performance with an R^2 of 0.735 during development and 0.740 in validation, explaining approximately 73% of the variance in SDI. All five predictors were statistically significant, with IRI and pavement age having the most substantial impact. Despite its interpretability and simplicity, MLR showed limitations in capturing non-linear interactions between variables. ANN modeling used a MLP architecture implemented in TensorFlow and the Keras library of Python programming, which involved a number of iterations throughout varied network architectures to achieve the optimal architecture with the least MSE and highest R^2 employing ReLU activation and the Adam optimizer. The research evaluated multiple Neural Network architectures, starting with simple single-layer networks and progressing to DNNs with up to four hidden layers. The optimal ANN model, the 5-232-1 model with 104 epochs, significantly outperformed MLR across all evaluation metrics. It achieved an R^2 of 0.809 during training and 0.816 during validation, indicating stronger predictive accuracy and generalization. The ANN's capacity to model complex, non-linear relationships between pavement distress and influencing factors resulted in improved estimation accuracy, reduced MSE, and narrower prediction error distributions. Sensitivity analysis revealed that IRI is the most influential predictor in both models, followed by pavement age and rainfall. Commercial vehicle traffic showed the least sensitivity, likely due to offsetting effects of maintenance on high-traffic routes.

The findings of this study offer actionable insights for the DoR in Nepal. By integrating ANN-based predictive models into the existing PMS, the DoR can improve maintenance planning, optimize budget allocation, and reduce reliance on labor-intensive condition assessments. The enhanced predictive accuracy allows for proactive intervention. Moreover, routine incorporation of variables such as IRI, rainfall, temperature range, and commercial vehicle traffic can support data-driven decision-making and reduce maintenance costs. Policymakers could also consider expanding traffic count stations and improving climatic monitoring to further strengthen model reliability and facilitate long-term infrastructure planning. Future studies could explore incorporating additional variables such as subgrade strength, construction quality, or socio-economic factors, and test deep learning architectures for further performance gains.

6. References

Abaza, K. A. (2006). Iterative linear approach for non-linear non-homogenous stochastic pavement management models. *Journal of Transportation Engineering*, *132*(3), 244–256.

Abaza, K. A., Ashur, S. A., & Al-Khatib, I. A. (2004). Integrated pavement management system with a Markovian prediction model. *Journal of Transportation Engineering*, *130*(1), 24–33. https://doi.org/10.1061/(ASCE)0733-947X(2004)130:1(24)

Adeli, H. (2001). Neural networks in civil engineering: 1989–2000. *Computer-Aided Civil and Infrastructure Engineering*, *16*(2), 126–142.

Anyala, M., Odoki, J. B., & Baker, C. J. (2014). Hierarchical asphalt pavement deterioration model for climate impact studies. *International Journal of Pavement Engineering*, *15*(3), 251–266. https://doi.org/10.1080/10298436.2012.687105

Arhin, S. A., & Noel, E. C. (2014). *Predicting pavement condition index from international roughness index in Washington, DC*.

Ashrafian, A., Taheri Amiri, M. J., Masoumi, P., Asadi-shiadeh, M., Yaghoubi-chenari, M., Mosavi, A., & Nabipour, N. (2020). Classification-based regression models for prediction of the mechanical properties of roller-compacted concrete pavement. *Applied Sciences*, *10*(11), 3707. https://doi.org/10.3390/app10113707

Bosurgi, G., & Trifirò, F. (2005). A model based on artificial neural networks and genetic algorithms for pavement maintenance management. *International Journal of Pavement Engineering*, *6*(3), 201–209.

Chang, C.-L., & Liao, C.-S. (2012). Parameter sensitivity analysis of artificial neural network for predicting water turbidity. *International Journal of Geological and Environmental Engineering*, *6*(10), 657–660.

Department of Road. (2023). *Highway Management Information System – ICT Unit*. https://www.dor.gov.np/home/page/hims-and-ict-unit

Department of Roads. (2022). *Statistics of National Highway*. https://ssrn.dor.gov.np/road_network/getNationCategoryAndPavement/

Department of Roads (DoR). (2007, April). HMIS Newsletter Vol. 22. *Highway Management Information System*.

Department of Roads, & Maintenance Branch. (2005). *Standard Procedure for Periodic Maintenance Planning*.

Domitrović, J., Dragovan, H., Rukavina, T., & Dimter, S. (2018). Application of an artificial neural network in pavement management system. *Tehnički Vjesnik*, *25*(Supplement 2), 466–473.

Durango-Cohen, P. L., & Tadepalli, N. (2006). Using advanced inspection technologies to support investments in maintenance and repair of transportation infrastructure facilities. *Journal of Transportation Engineering*, *132*(1), 60–68.

Elshamy, M. M. M., Tiraturyan, A. N., Uglova, E. V, & Zakari, M. (2020). Development of the non-destructive monitoring methods of the pavement conditions via artificial neural networks. *Journal of Physics: Conference Series*, *1614*(1), 012099.

Ferreira, A., Picado-Santos, L., & Antunes, A. (1999). Pavement performance modelling: State of the art. *Proceedings of Seventh International Conference on Civil and Structural Engineering Computing*, 157–264.

Fwa, T. F., Chan, W. T., & Hoque, K. Z. (2000). Multi-objective optimization for pavement maintenance programming. *Journal of Transportation Engineering*, *126*(5), 367–374.

Georgiou, P., Plati, C., & Loizos, A. (2018). Soft Computing Models to Predict Pavement Roughness: A Comparative Study. *Advances in Civil Engineering*, *2018*, 1–8. https://doi.org/10.1155/2018/5939806

Glorot, X., Bordes, A., & Bengio, Y. (2011). Deep sparse rectifier neural networks. *Proceedings of the Fourteenth International Conference on Artificial Intelligence and Statistics*, 315–323.

Gong, H., Sun, Y., Hu, W., Polaczyk, P. A., & Huang, B. (2019). Investigating impacts of asphalt mixture properties on pavement performance using LTPP data through random forests. *Construction and Building Materials*, *204*, 203–212. https://doi.org/10.1016/j.conbuildmat.2019.01.198

Haykin, S. (1998). *Neural networks: a comprehensive foundation*. Prentice Hall PTR.

Highway Management Information System-Information & Communication Technology (HMIS-ICT) Unit. (2022). *Traffic, Surface Distress and Road Roughness Surveys on Strategic Road Network*.

Kerali, H. G. R., Odoki, J. B., & Stannard, E. E. (2000). Overview of HDM-4. *The Highway Development and Management Series, Volume One, World Road Association, PIARC. World Bank, Washington DC, USA*.

Kulkarni, R. B., Miller, D., Ingram, R. M., Wong, C.-W., & Lorenz, J. (2004). Need-based project prioritization: alternative to cost-benefit analysis. *Journal of Transportation Engineering*, *130*(2), 150–158.

Kulkarni, R. B., & Miller, R. W. (2003). Pavement management systems: Past, present, and future. *Transportation Research Record*, *1853*(1), 65–71.

LeCun, Y., Bengio, Y., & Hinton, G. (2015). Deep learning. *Nature*, *521*(7553), 436–444.

Mathavan, S., Kamal, K., & Rahman, M. (2015). A review of three-dimensional imaging technologies for pavement distress detection and measurements. *IEEE Transactions on Intelligent Transportation Systems*, *16*(5), 2353–2362. https://doi.org/10.1109/TITS.2015.2428655

Meneses, S., Ferreira, A., & Collop, A. (2013). Multi-objective decision-aid tool for pavement management. *Proceedings of the Institution of Civil Engineers-Transport*, *166*(2), 79–94.

Mosa, A. M. (2017). Neural network for flexible pavement maintenance and rehabilitation. *Applied Research Journal*, *3*(4), 114–129.

Neter, J., Kutner, M. H., Nachtsheim, C. J., & Wasserman, W. (1996). *Applied linear statistical models*.

Picado-Santos, L., Ferreira, A., Antunes, A., Carvalheira, C., Santos, B., Bicho, M., Quadrado, I., & Silvestre, S. (2004). Pavement management system for Lisbon. *Proceedings of the Institution of Civil Engineers-Municipal Engineer*, *157*(3), 157–165.

Sanabria, N., Valentin, V., Bogus, S., Zhang, G., & Kalhor, E. (2017). *Comparing neural networks and ordered probit models for forecasting pavement condition in New Mexico*.

Sazlı, M. H. (2006). A brief review of feed-forward neural networks. *Communications Faculty of Sciences University of Ankara Series A2-A3 Physical Sciences and Engineering*, *50*(01).

Shakya, M., Sasai, K., & Kaito, K. (2023). Application of Markov Deterioration Hazard Model for Pavement Deterioration Forecasting of Strategic Road Networks in Nepal. *2 Nd International Conference on Integrated Transport for Sustainable Mobility*, 59–70.

Shrestha, A., & Mahmood, A. (2019). Review of deep learning algorithms and architectures. *IEEE Access*, *7*, 53040–53065.

Shrestha, S., & Khadka, R. (2021). Assessment Of Relationship Between Road Roughness and Pavement Surface Condition. *Journal of Advanced College of Engineering and Management*, *6*, 2021. https://doi.org/10.3126/jacem.v6i0.38357

Sigdel, T., & Pradhananga, R. (2021). *Development of IRI Prediction Model for National Highways of Nepal*. *10*, 2350–8906.

Sigdel, T., Pradhananga, R., & Shrestha, S. (2024). Artificial Neural Network-based model to predict the International Roughness Index of national highways in Nepal. *Transportation Research Interdisciplinary Perspectives*, *25*, 101128.

Wang, W., Qin, Y., Li, X., Wang, D., & Chen, H. (2017). Comparisons of Faulting-Based Pavement Performance Prediction Models. *Advances in Materials Science and Engineering*, *2017*, 1–9. https://doi.org/10.1155/2017/6845215

Wong, W. G., He, G. P., & Luk, S. T. (2003). Development of road management systems in China. *Proceedings of the Institution of Civil Engineers-Transport*, *156*(4), 179–188.

Yang, X., Guan, J., Ding, L., You, Z., Lee, V. C. S., Hasan, M. R. M., & Cheng, X. (2021). Research and applications of artificial neural network in pavement engineering: a state-of-the-art review. *Journal of Traffic and Transportation Engineering (English Edition)*, *8*(6), 1000–1021.

Zakeri, H., Nejad, F. M., & Fahimifar, A. (2017). Image based techniques for crack detection, classification and quantification in asphalt pavement: a review. *Archives of Computational Methods in Engineering*, *24*, 935–977. https://doi.org/10.1007/s11831-016-9194-z

Journal on Transportation System and Engineering
ISSN: 3059-9865(Print) 3059-9873(Online)
Vol. 1. Issue 2 (December) 2025: 27-36
DOI: https://doi.org/10.3126/jotse.v1i2.87741

Research Article
Received Date: March 29, 2025
Revised Date: September 11, 2025
Accepted Date: November 9, 2025
Published Date: December 21,2025

Enhancing at Crosswalks and Sidewalks: A Case Study of Kathmandu Metropolitan City

Divya Shahi[a], Thusitha Chandani Shahi[b]

[a] *Postgraduate Student, Nepal Engineering College- Center for Postgraduate Studies, Kathmandu, Nepal*
[b] *Professor Nepal Engineering College - Center for Postgraduate Studies, Kathmandu, Nepal*

Abstract

This study evaluates pedestrian safety and walkability in Kathmandu Metropolitan City by developing and applying two indices: the Sidewalk Condition Index (SCI) and the Crosswalk Condition Index (CCI). Through a comprehensive literature review, 16 sidewalk and 11 crosswalk attributes were identified. Expert consultations using the Analytical Hierarchy Process (AHP) provided relative weights for each attribute, while a user perception survey (n = 420) captured the experiences of pedestrians. This combined approach ensured both technical priorities and community perspectives were reflected in the assessment. Six urban road sections with the highest pedestrian fatality records were analyzed. Results show that effective signal control (weight = 0.50), zebra crossings (0.47), and sidewalk lighting (0.38) are the most influential factors. SCI values ranged from –0.04 to 1.10, and CCI values from –0.08 to 0.62, identifying S4 (Gongabu – Sarkaridhara) as the least safe section and S6 (Narayan Gopal Chowk – T.U. Teaching Hospital) as the most walkable. The study recommends prioritizing improvements such as enhanced signal timing with pedestrian phases, installation of zebra crossings and refuge islands at high-risk intersections, and regular sidewalk maintenance to ensure continuity and safety. These findings offer a transferable framework for enhancing pedestrian infrastructure in Kathmandu and other similar South Asian urban contexts.

Keywords: *Pedestrian Safety; Walkability; Sidewalks; Crosswalks; Condition index*

1. Introduction

Kathmandu Metropolitan City (KMC) faces significant challenges regarding pedestrian safety and walkability, issues that are exacerbated by rapid urbanization and increasing motorization. More than 70% of urban roads lack essential pedestrian amenities such as continuous sidewalks and marked crosswalks, forcing pedestrians to share road space with vehicles and thereby increasing exposure to crashes (Kathmandu Valley Traffic Police Office [KVTPO], 2024). National statistics also highlight the vulnerability of pedestrians: in Nepal, pedestrians account for approximately 23% of road traffic fatalities, a proportion consistent with South Asian trends where vulnerable road users constitute more than half of total crash victims (WHO, 2023).

Sidewalks and crosswalks are vital elements of an urban transport system that directly influence pedestrian safety and comfort (Sisiopiku & Akin, 2003). In KMC, however, sidewalks are often narrow, discontinuous, encroached upon, or poorly maintained, while over 80% of roads lack designated pedestrian crossings (KVTPO, 2024). These deficiencies not only discourage walking but also increase the risk of crashes for pedestrians. Despite such pressing issues, no standardized framework currently exists in Nepal to systematically evaluate sidewalk and crosswalk conditions.

This study addresses this gap by introducing two indices, the Sidewalk Condition Index (SCI) and Crosswalk Condition Index (CCI), to provide a quantitative, data-driven assessment of pedestrian facilities. The indices are derived through the Analytical Hierarchy Process (AHP), which assigns weights to key attributes based on expert judgment, combined with large-scale user perception surveys to capture public experience. By integrating expert and user perspectives, SCI and CCI go beyond merely identifying the lack of infrastructure; they allow policymakers to compare, rank, and prioritize pedestrian facilities, thereby providing a structured framework to inform targeted improvements.

Corresponding Author's Email Address shahidivya53@gmail.com

Six urban road sections with the highest pedestrian crash histories over the last three years were selected for detailed analysis ≥5 pedestrian fatalities each, as recorded by KVTPO, 2024). Field surveys, traffic and pedestrian counts, and structured questionnaires were conducted to calculate SCI and CCI values. For instance, low CCI scores in sections S2 and S4 reflect inadequate visibility and the absence of safe crossings, directly supporting the recommendation for installing zebra crossings and refuge islands at those locations.

By linking crash data, infrastructure conditions, and user perceptions into a single evaluation framework, this sstudy not only identifies critical deficiencies but also demonstrates how evidence-based interventions, such as improved signal phasing, enhanced lighting, and the introduction of pedestrian-specific crossings, can improve safety and walkability. The findings provide valuable guidance for urban planners and policymakers in KMC and offer a replicable approach for other South Asian cities facing similar challenges.

2. Literature Review

Pedestrian safety and walkability have emerged as critical concerns in rapidly urbanizing cities, particularly in South Asia, where vulnerable road users account for more than half of crash-related fatalities (WHO, 2023). In Nepal, pedestrians represent nearly one-quarter of road traffic deaths, underscoring the urgent need for systematic evaluation of pedestrian facilities (KVTPO, 2024). International studies consistently demonstrate that well-designed sidewalks, crosswalks, and curb ramps reduce pedestrian-vehicle conflicts and improve safety (Mukherjee & Mitra, 2020; Kadi et al., 2021). Conversely, inadequate pedestrian infrastructure in developing cities has been strongly linked to higher crash risks, particularly at intersections and mid-block crossings where vehicle speed and volume are significant factors (Eluru et al., 2008; Marisamynathan & Vedagiri, 2018).

Walkability, defined as the extent to which the built environment supports safe and comfortable pedestrian movement (Southworth, 2005), directly affects public health, accessibility, and sustainable urban development. The "complete streets" approach emphasizes multimodal design, while urban design scholars highlight safety, comfort, and connectivity as key elements for encouraging walking (Deb, 2005; Speck, 2018). Empirical studies confirm that features such as continuous sidewalks, effective crossings, pedestrian lighting, and traffic calming are essential for creating walkable spaces (Sisiopiku & Akin, 2003; Nag et al., 2020).

Several methodological approaches have been developed to evaluate pedestrian facilities. Level of Service (LOS) frameworks provide subjective measures of comfort and capacity (Mori & Tsukaguchi, 1987), while more recent studies have advanced condition indices to incorporate both safety and serviceability. For example, Bari et al. (2018) applied an SCI in Dhaka, while Patil et al. (2021) developed an SCI and CCI for Indian cities, using expert-derived weights for crash-prone locations. Majumdar et al. (2021) emphasized satisfaction-based prioritization, showing the value of user perceptions in identifying critical attributes. Similarly, Rashidi et al. (2016) and Muhammad et al. (2022) demonstrated that composite indices effectively highlight deficiencies and support targeted interventions.

The AHP has frequently been employed to derive attribute weights in transport studies due to its ability to structure complex decisions (Saaty, 1980; Piantanakulchai & Saengkhao, 2003). Prior research primarily relied on expert input for weighting, but critics have noted that excluding pedestrian perspectives may overlook contextual challenges (Oswald Beiler & Phillips, 2016). This study addresses that gap by combining expert-assigned AHP weights with user perception surveys, thereby bridging technical evaluation with community experience.

3. Study Area

The research was conducted in KMC, Nepal's largest urban center, located at 27°42′14″N and 85°18′32″E. KMC has experienced rapid urbanization and motorization in recent decades, yet more than 70% of its roads lack essential pedestrian amenities, resulting in elevated pedestrian crash risks (KVTPO, 2024).

For this study, six road sections were selected from an initial pool of fourteen based on two criteria: (i) high pedestrian activity, and (ii) a minimum of five pedestrian fatalities recorded between 2021 and 2024, as reported by

the KVTPO. This ensured that the analysis focused on crash-prone corridors with significant exposure, thereby maximizing the relevance of the findings for pedestrian safety improvements.

The selected sections represent diverse urban contexts within KMC, including mixed land-use neighborhoods, institutional areas, and commercial corridors connected to the ring road and central business districts. Fatality records and exposure data for these corridors were obtained from KVTPO (2021–2024), supplemented by field observations and survey data collected during this study. Table 1 summarizes the characteristics of the six study sections.

Table 1. Selected study sections in KMC

Section	Location (from–to)	Length (m)	Key land use	Fatalities (last 3 years)	Notes on pedestrian environment
S1	Balaju Chowk – Naya Bazar	847	Mixed land-use	9	Discontinuous sidewalks, poor crosswalk visibility
S2	Balkhu Chowk – Kuleshwor Ganeshthan Temple	580	Commercial	10	Narrow sidewalks, limited amenities
S3	Gaushala Chowk – Old Baneshwor Chowk	730	Institutional/market	7	Maintained sidewalks, inadequate street furniture
S4	Gongabu Chowk – Sarkaridhara Chowk	815	Mixed commercial	13	Poorly maintained sidewalks, frequent waterlogging
S5	Jadibuti Chowk – Ward Office 32	743	Residential/commercial	11	Wide sidewalks, affected by waterlogging
S6	Narayan Gopal Chowk – T.U. Teaching Hospital	774	Institutional/healthcare	6	Well-marked crosswalks, tactile tiles, adequate lighting

4. Methodology

This study adopted a mixed-methods approach, combining both primary and secondary data, to evaluate the safety and walkability of pedestrian infrastructure in KMC. The methodology was designed to integrate expert judgment, user perceptions, and field-based assessments, ensuring a comprehensive analysis of sidewalk and crosswalk conditions.

4.1 Research Design

The research design followed sequential steps: identification of key attributes through literature review, collection of expert and user perceptions, field-based inventory surveys, and analytical modeling using the AHP and weighted sum methods. This enabled the systematic formulation of the SCI and CCI.

4.2 Data Collection

4.2.1 *Primary Data*

Primary data were obtained through expert surveys, user perception surveys, field observations, and key informant interviews. Twenty-five professionals in transportation engineering, urban planning, and road safety completed AHP-based pairwise comparison questionnaires, with reliability confirmed using a consistency ratio ($CR < 0.10$; Sinha & Labi, 2011). A structured user survey, designed with Cochran's formula (Cochran, 1977), gathered 420 valid responses from 384 participants across six sites, using a Likert scale to assess factors such as safety, lighting, cleanliness, aesthetics, surface condition, and accessibility; reliability was confirmed with Cronbach's Alpha ($\alpha > 0.70$). Field observations and videographic surveys captured traffic speeds, volumes, and pedestrian flows at the selected sections, while eight key informant interviews with residents, engineers, and safety specialists provided contextual insights.

4.2.2 *Secondary Data*

Secondary data comprised pedestrian crash and fatality records from the Kathmandu Valley Traffic Police Office (2021–2024), along with relevant literature, manuals, and guidelines, including the Nepal Road Standard (2013), Nepal Urban Road Standard (2019), and prior studies such as Patil et al. (2021) and Mukherjee & Mitra (2020).

4.3 Attribute Selection

Drawing from existing literature and national guidelines, a total of 16 sidewalk-specific and 11 crosswalk-specific attributes were identified as critical determinants of pedestrian safety and walkability. The sidewalk attributes were grouped under four categories: facilities and security, aesthetics and surface quality, physical characteristics, and traffic interaction, while crosswalk attributes were classified into two categories, namely geometric and operational characteristics and traffic-related factors. The complete list of attributes and their sources is presented in Tables 2 and 3.

Table 2. List of attributes for crosswalk elements

Crosswalk Elements	Attributes	Source
Crosswalk Characteristics	• Conflicts with traffic • Refuge Island • Signage and road marking • Dropped kerb • Zebra crossing • Lighting at the crossing	Zainol et al, (2014); Sisiopiku and Akin (2003), Majumdar et al. (2021); Galanis and Eliou (2011); Ahmed et al. (2021); NRS (2013); NURS (2019)
Traffic Characteristics	• Traffic speed • Traffic volume • Signal Control • Delay for pedestrians • Pedestrian flow	Mukherjee and Mitra (2020); Fabian et al. (2010); Kadali and Vedagiri (2015); Marisamynathan and Vedagiri (2018); NRS (2013); NURS (2019)

Table 3. List of attributes for sidewalk elements

Sidewalk Elements	**Attributes**	**Source**
Sidewalk facilities and security	• Security from crime • Sidewalk Lighting • Ramps in the sidewalk • Tactile paving • Sidewalk Amenities	Nepal and Lal (2021); Muhammad et al. (2022); Abaya et al. (2011); Rahman et al. (2022); Galanis and Eliou (2011); Zainol et al, (2014); NRS (2013); NURS (2019)
Aesthetics and Footpath Quality	• Aesthetic • Cleanliness • Surface Condition • Raised Curb	Nepal (2021); Majumdar et al. (2021); Abaya et al. (2011); Zainol et al, (2014); NRS (2013); NURS (2019)
Physical Characteristics	• Sidewalk Width • Sidewalk continuity • Physical separation from traffic • Obstruction	Kim et al. (2024); Sisiopiku and Akin (2003); Banerjee et al. (2018); Majumdar et al. (2021); NRS (2013); NURS (2019)

Traffic Characteristics	• Traffic Speed • Traffic Volume • Pedestrian Volume	Mukherjee and Mitra (2020); Banerjee et al. (2018); Fabian et al. (2010); NRS (2013); NURS (2019)

4.4 Analytical Methods

4.4.1 *AHP*

Expert responses were analyzed using AHP through paired comparison questionnaires on sidewalk and crosswalk attributes. The CR was used to validate responses, and 15 of the 25 surveys with CR < 0.10 were retained. Final weights were computed using Super Decision V3.2, providing an objective evaluation of the most influential factors.

4.4.2 *Weighted Sum Method*

SCI and CCI were computed as weighted sums of attribute values using AHP-derived weights:

$$SCI_j = \sum_{a-1}^{n} \quad w_a X_{aij} \tag{1}$$

$$CCI_j = \sum_{b-1}^{m} \quad w_b Y_{bij} \tag{2}$$

Where,

SCI_j, CCI_j: $indices\ for\ the\ j^{th}$ sidewalk/ crosswalk

w_a, w_b : weight of attributes derived from AHP

Xa_{ij}, Yb_{ij}: normalized score of the b^{th} or a^{th} attribute at the j^{th} location

n, m: total number of sidewalk and crosswalk attributes

4.5 Statistical Analysis

User perception data were analyzed using SPSS for descriptive and inferential statistics. Reliability of scales was confirmed with Cronbach's Alpha, and thematic analysis was applied to KII data for qualitative insights

5. Results and Discussion

5.1. Calculation from AHP

The AHP analysis identified signal control (0.50) and zebra crossings (0.47) as the most influential crosswalk attributes, while physical separation from traffic (0.56), sidewalk lighting (0.38), and cleanliness (0.41) were most critical for sidewalks. These results highlight the need for regulated crossings, speed management, and well-maintained pedestrian spaces in KMC. Table 4 presents the relative weights of all attributes.

Table 4. Relative weights of crosswalk and sidewalk attributes

Category	Attributes	Relative weight	Category	Attributes	Relative weight
Crosswalks	Conflicts with traffic	0.19	Sidewalks	Sidewalk amenities	0.19
	Refuge island	0.05		Sidewalk lighting	0.38
	Dropped kerb	0.04		Ramp in sidewalk	0.11
	Lighting at the crossing	0.16		Security from crime	0.25
	Signage & markings	0.09		Tactile paving	0.06
	Zebra crossing	0.47		Aesthetic	0.37
	Delay for pedestrians	0.04		Cleanliness	0.41
	Pedestrian flow	0.07		Raised kerb	0.04
	Signal control	0.5		Surface condition	0.17
	Traffic speed	0.25		Sidewalk continuity	0.24
	Traffic volume	0.14		Obstruction	0.12

	Physical separation from traffic	0.56
	Sidewalk width	0.08
	Pedestrian volume	0.06
	Traffic speed	0.6
	Traffic volume	0.35

5.2. User's Perception

A structured questionnaire survey was administered to pedestrians along the six selected road sections of KMC, yielding 420 valid responses. The survey captured demographic profiles, walking behavior, perceived safety, and user ratings of specific attributes influencing pedestrian safety and walkability. These attributes were evaluated on a five-point Likert scale (1 = Very Poor, 5 = Excellent) and later categorized for condition rating to support the calculation of the SCI and CCI. Table 5 summarizes user demographics, behavior, safety perceptions, and issues, while Tables 6 and 7 present crosswalk and sidewalk attributes with their justifications for inclusion in the CCI and SCI.

Table 5. Summary of user perception survey results

Variable	Key Findings	Sectional Highlights
Gender	Males outnumbered females in all sections.	Highest male share: S2 (81.7%); highest female share: S6 (43.5%).
Age	Majority are in 20–40 years; seniors <5%.	S3 & S4: mostly 30–40 yrs; S2: dominated by 20–30 yrs.
Employment	Predominantly employed, notable student, and self-employed groups.	Students: S1 (27.4%), S5 (18.8%); Self-employed: S6 (30.4%).
Walking frequency	Most walked daily or weekly.	Daily: highest in S2 (60.6%); infrequent: S1 & S5.
Purpose of walking	Shopping, leisure, and access to public transport.	Shopping: S1–S3; Leisure: S5–S6; Transport: S5–S6.
Perceived safety	Varied across sections.	Highest in S6 (71%); lowest in S4 (70.8%); 50% unsafe in S2.
Common issues	Traffic congestion, poor sidewalks, inadequate crossings, and lighting.	Congestion: S3 (54.4%); Poor sidewalks: S2 (49.3%), S4 (41.7%); Inadequate crossings: S1 (42.5%); Lighting: S4 (27.8%), S5 (32.8%).

Table 6. Crosswalk Attributes Rated by Users

Attribute	Description	Justification
Zebra crossing visibility	Clarity and maintenance of markings	Enhances conspicuity and reduces conflicts
Presence of signals	Availability of pedestrian signals	Improves compliance and crossing safety
Waiting time	Average delay experienced at the crossing	Directly affects pedestrian compliance and satisfaction
Crosswalk lighting	Adequacy of lighting at night	Reduces accident risk, increases perceived security
sConflicts with vehicles	Frequency of conflicts with turning/through vehicles	High predictor of pedestrian crashes
Dropped kerbs	Accessibility for wheelchair users, the elderly, and prams	Critical for inclusive mobility
Tactile paving	Presence/quality of tactile surfaces	Assists visually impaired pedestrians

Refuge islands	Median spaces for safe two-stage crossing	Especially useful on wide roads

Table 7. Sidewalk Attributes Rated by Users

Attribute	Description	Justification
Width	Usable walking width of sidewalk	Narrow widths reduce capacity and comfort
Surface quality	Smoothness, absence of cracks/potholes	Poor surfaces discourage use, increase risk
Continuity	Uninterrupted walking path	Discontinuity leads to unsafe detours
Lighting	Adequacy of illumination	Enhances safety and nighttime walkability
Cleanliness	Absence of litter/obstacles	Directly tied to user comfort and hygiene
Trees/greenery	Shading, environmental comfort	Improves aesthetics, reduces heat exposure
Seating/amenities	Benches, bins, shading structures	Encourages longer, safer pedestrian stays
Separation from traffic	Physical buffer from roadway	Reduces exposure to vehicles
Accessibility	Suitability for the elderly/disabled	Ensures equity and inclusiveness

5.3. Traffic and Pedestrian Data

Traffic and pedestrian counts were conducted during three daily peak periods (09:30–10:30, 13:00–14:00, and 16:30–17:30) to capture representative flow conditions across the six study sections. The observed traffic volumes ranged from 4,044 PCU/hr in Section S4 to 6,911 PCU/hr in Section S1, while average vehicular speeds varied between 24.28 km/h (S1) and 35.37 km/h (S5). Correspondingly, pedestrian flows at crosswalks ranged from 308 ped/hr (S3) to 598 ped/hr (S1), and sidewalk pedestrian volumes varied from 881 ped/hr (S3) to 1,707 ped/hr (S1). The detailed figures for each section are summarized in Table 8, which provides a comprehensive overview of traffic volumes, pedestrian flows, and vehicular speeds across the study corridors.

For comparative analysis and integration into the condition indices, these traffic-related parameters were normalized and classified into three risk categories: low, moderate, and high. The thresholds applied are consistent with international safety benchmarks (WHO, 2023; Patil et al., 2021), which highlight the exponential rise in pedestrian crash severity above 30 km/h, as well as with walkability assessments (Nepal & Lal, 2021) that emphasize traffic speed, exposure, and pedestrian demand as key determinants of walkability. This categorization framework ensures methodological robustness and allows for systematic ranking of road sections in terms of both exposure risk (traffic volume), operational safety (speed), and infrastructure demand (pedestrian flow). This categorization framework, presented in Table 9, Categorization of Traffic-Related Parameters for Condition Rating.

Table 8. Summary of the traffic and pedestrian data

Road Sections	Average Traffic Volume (PCU/hr)	Average Traffic Speed (km/hr)	Average Pedestrian Volume (Ped/hr)	
			Crosswalk	Sidewalk
S1	6911	24.28	598	1707
S2	5160	27.9	462	1319
S3	6142	31.3	308	881
S4	4044	25.49	512	1464
S5	6756	35.37	402	1017
S6	5341	26.8	551	1573

Table 9. Categorization of Traffic-Related Parameters for Condition Rating

Parameter	Range	Interpretation
Traffic Speed (km/h)	<25 (Low), 25–35 (Moderate), >35 (High)	Low speeds are safer; above 30 km/h, fatality risk rises sharply
Traffic Volume (PCU/hr)	<4,500 (Low), 4,500–6,000 (Moderate), >6,000 (High)	High volumes increase exposure risk and conflicts
Pedestrian Volume (ped/hr)	<500 (Low), 500–1,000 (Moderate), >1,000 (High)	High volumes highlight demand and the need for infrastructure

5.4. CCI and SCI Calculation

Using normalized attribute values, the explicit formulations applied were developed to combine the weighted contribution of each attribute into a single index score. Normalization ensured that all survey and field data were scaled to a comparable range (0–1), avoiding bias from differing measurement units. This allowed the attributes with higher AHP-derived weights to exert proportionally greater influence on the overall index value. The final equations for CCI and SCI are expressed as follows:

$$SCI_j = (0.19 * X_{amenities}) + (0.38 * X_{lighting}) + (0.11 * X_{ramp}) + (0.25 * X_{security}) + (0.06 * X_{tactile}) + (0.37 * X_{aesthetic}) + (0.41 * X_{cleanliness}) + (0.04 * X_{kerb}) + (0.17 * X_{surface}) + (0.24 * X_{continuity}) + (-0.12 * X_{obstruction}) + (0.56 * X_{separation}) + (0.08 * X_{width}) + (-0.06 * X_{p.volume}) + (-0.60 * X_{speed}) + (-0.35 * X_{t.volume}) \quad (3)$$

$$CCI_j = (-0.19 * Y_{conflict}) + (0.05 * Y_{island}) + (0.04 * Y_{kerb}) + (0.16 * Y_{lighting}) + (0.09 * Y_{signage}) + (0.47 * Y_{zebra\ crossing}) + (-0.04 * Y_{delay}) + (-0.07 * Y_{flow}) + (0.50 * Y_{signal}) + (-0.25 * Y_{speed}) + (-0.14 * Y_{volume}) \quad (4)$$

Both indices range from negative to positive values, where lower or negative scores reflect unsafe and inconvenient pedestrian environments caused by traffic conflicts, poor infrastructure, and inadequate maintenance, while higher scores indicate safer, more functional, and walkable spaces. This approach is consistent with international applications of SCI and CCI, which are widely used to evaluate pedestrian facilities and guide infrastructure priorities (Patil et al., 2021; Mukherjee & Mitra, 2020; Banerjee & Maurya, 2018).

The CCI and SCI values offer a clear numerical representation of crosswalk and sidewalk conditions. Lower scores identify locations in urgent need of intervention, while higher scores suggest lower priority. By normalizing survey and field data, the indices allow consistent ranking of study sections, as shown in Table 10. This systematic, data-driven method helps authorities allocate resources effectively, focusing improvements on the most critical areas to enhance safety and walkability (Patil et al., 2021; Rashidi et al., 2016; Oswald Beiler & Phillips, 2016).

Table 10. CCI and SCI with the ranking of the selected road section

Road section	Crosswalks		Sidewalks	
	CCI	Ranking	SCI	Ranking
S1	0.06	2nd	0.43	3rd
S2	0.11	3rd	0.17	2nd
S3	0.37	4th	0.99	5th
S4	-0.08	1st	-0.04	1st
S5	0.54	5th	0.81	4th
S6	0.62	6th	1.1	6th

5.5. Performance Analysis of Crosswalks and Sidewalks

5.5.1. *Crosswalk Performance*

The calculated CCI values (Table 10) demonstrate varying crosswalk performance across six study sections. The lowest performance was recorded at S4 (CCI = -0.08, Rank 1), indicating severe deficiencies such as high traffic conflicts, lack of signage, and uncontrolled vehicle speeds. Moderate performance was observed at S1 (0.06, Rank 2) and S2 (0.11, Rank 3), where crosswalks suffered from frequent conflicts and insufficient lighting. S3 (0.37, Rank 4) showed improvement, benefiting from better refuge facilities and reduced conflicts. The best performance was seen at S5 (0.54, Rank 5) and S6 (0.62, Rank 6), supported by effective signalization and zebra crossings, though traffic conflicts still pose risks. Overall, the analysis confirms that traffic-related attributes such as speed and volume exert a strong negative influence on crosswalk safety, while signal control and zebra crossings emerge as the most critical determinants of safer conditions. The Nepal-specific practice of implementing signals and zebra crossings together also explains their dominant influence, in contrast to international contexts where these measures are usually independent.

5.5.2. *Sidewalk Performance*

SCI scores revealed substantial variation in pedestrian space quality across the study sections. The lowest performance was found in S4 (SCI = -0.04, Rank 1), marked by discontinuity, obstructions, poor aesthetics, and inadequate amenities. Moderate scores at S1 (0.43, Rank 3) and S2 (0.17, Rank 2) reflected deficits in lighting, security, and sidewalk amenities. S5 (0.81, Rank 4) benefited from wider sidewalks but continued to face challenges related to cleanliness and safety. The highest performance was observed in S3 (0.99, Rank 5) and S6 (1.10, Rank 6), where improved cleanliness, adequate lighting, and physical separation from traffic contributed to safer and more walkable conditions. These results highlight that, similar to crosswalks, traffic speed and volume have the strongest negative effect on sidewalk usability, while factors such as lighting, cleanliness, and separation from traffic are the most influential in creating positive pedestrian environments.

5.6. Improvements for Crosswalks and Sidewalks Based on SCI and CCI Scores

Based on the SCI and CCI scores, targeted improvements are recommended for each road section to enhance pedestrian safety, walkability, and infrastructure quality.

1. S1 (Balaju Chowk to Naya Bazar). The priority should be reducing pedestrian–vehicle conflicts through refuge islands at wide crossings and improving high-visibility signage and road markings. Enhancing sidewalk lighting and providing better security measures will address safety concerns identified by low SCI scores.
2. S2 (Balkhu Chowk to Kuleshwor Ganeshthan Temple). Wider crosswalks and improved dropped kerbs are essential to reduce conflicts and enhance accessibility. Additional lighting, improved aesthetics, and obstruction-free sidewalks will directly improve SCI ratings.
3. S3 (Gaushala Chowk to Old Baneshwor Chowk). Optimized signal control and better lighting at crossings are required to reduce delays and improve safety, consistent with its moderate CCI performance. On sidewalks, ramps for universal access and strategic placement of amenities without causing obstructions are critical. Regular cleaning will maintain high SCI conditions.
4. S4 (Gongabu Chowk to Sarkaridhara Chowk). This section scored lowest in both indices, demanding urgent intervention. High-visibility zebra crossings, reflective markings, improved lighting, and signal optimization should be prioritized to address conflicts and delays. For sidewalks, raised curbs, obstruction removal, and aesthetic upgrades will be essential to raise walkability standards.
5. S5 (Jadibuti Chowk to Ward Office). Installing zebra crossings at critical points and improving signage are needed to support favorable CCI scores. Enhanced lighting, ramp installation, and ensuring sidewalk continuity will improve accessibility and pedestrian comfort.
6. S6 (Narayan Gopal Chowk to T.U. Teaching Hospital). Already performing best in both indices, this section should focus on consolidating gains. Design refinements to further reduce conflicts, along with upgraded lighting, tactile paving, and added security, will ensure inclusivity and sustainability of walkability gains.

6. Conclusion and Recommendation

6.1. Conclusion

This study developed and applied the Sidewalk Condition Index (SCI) and Crosswalk Condition Index (CCI) to assess pedestrian infrastructure in Kathmandu Metropolitan City (KMC). The findings reveal significant deficiencies in sections with high pedestrian crash histories, with S4 performing the worst (CCI = -0.08; SCI = -0.04) due to conflicts, poor signage, and weak infrastructure, while S6 scored highest (CCI = 0.62; SCI = 1.10) with better lighting, signalization, and sidewalk quality. Key attributes such as signal control, zebra crossings, and sidewalk lighting were identified as the strongest determinants of safety and walkability, while traffic speed and volume consistently reduced scores**.**

6.2. Recommendation

The study recommends a priority-based improvement program where low-performing sections, such as S4 and S2, are upgraded first through measures like improved signage, optimized signals, and zebra crossings, while higher-performing sections, like S6, focus on consolidating gains. Policy-level actions include integrating SCI and CCI into walkability maps, enforcing pedestrian right-of-way, and redesigning signal timings at crash-prone locations. For long-term impact, authorities should implement regular maintenance programs, ensure accessibility through universal design, and adopt traffic calming strategies in pedestrian-heavy areas. Future research should extend these methods city-wide, test their applicability in well-designed corridors, and incorporate socioeconomic and behavioral dimensions to capture broader determinants of pedestrian safety and walkability.

7. References

AASHTO. (2004). *Guide for the planning, design, and operation of pedestrian facilities*. American Association of State Highway and Transportation Officials.

Abley, S. (2008). *Walkability research tools – Summary report*. NZ Transport Agency.

Arifin, M., Rasyid, A. R., & Osman, W. W. (2020). Walkability index of real estate housing in Makassar. *IOP Conference Series: Earth and Environmental Science, 419*(1), 012107.

Asadi-Shekari, Z., Moeinaddini, M., & Shah, M. Z. (2014). A pedestrian level of service method for evaluating and promoting walking facilities on campus streets. *Land Use Policy, 38*, 175–193.

Austroads. (2016). *Safe system assessment framework*. Austroads.

Austroads. (2017). *Guide to traffic management part 6: Intersections, interchanges and crossings*. Austroads.

Bahari, N. I., Arshad, A. K., & Yahya, Z. (2013). Assessing the pedestrians' perception of the sidewalk facilities based on pedestrian travel purpose. *Proceedings of the 2013 IEEE 9th International Colloquium on Signal Processing and its Applications*, Kuala Lumpur, Malaysia, 27–32.

BK, A., & Bajracharya, A. R. (2023). Built environment and walkability: Investigating urban design qualities by serial vision method at Itahari Chowk.

Bari, J., Sunny, M. H., Nag, S. K., Tushar, S. H., & Haque, M. T. (2018). Development of sidewalk condition index (SCI) of Dhanmondi R/A, Gulshan & Bashundhara R/A of Dhaka city.

Eghbal, R., Parsafard, M., Medal, H. R., & Li, X. (2016). Optimal traffic calming: A mixed-integer bi-level programming model for locating sidewalks and crosswalks in a multimodal transportation network to maximize pedestrians' safety and network usability. *Transportation Research Part E: Logistics and Transportation Review, 91*, 33-50.

Eluru, N., Bhat, C. R., & Hensher, D. A. (2008). A mixed generalized ordered response model for examining pedestrian and bicyclist injury severity level in traffic crashes. *Accident Analysis & Prevention, 40*(3), 1033–1054.

Gautam, S. (2019). *Assessment of pedestrian safety behavior on selected urban road sections in Kathmandu* (Master's thesis). Nepal Engineering College, Changunarayan, Bhaktapur, Nepal.

Highway Capacity Manual. (2010). *Transportation Research Board of the National Academies*. Washington, D.C.

Hugh, R., Medal, X. L., Parsafard, M., & Rashidi, E. (2015). The mobility and safety of walk-and-ride systems.

Jabbari, M., Fonseca, F., & Ramos, R. (2018). Combining multi-criteria and space syntax analysis to assess a pedestrian network: The case of Oporto. *Journal of Urban Design, 23*(1), 23–41.

Kadali, B. R., & Vedagiri, P. (2016). Review of pedestrian level of service: Perspective in developing countries. *Transportation Research Record, 2581*, 37–47.

Kadali, B. R., & Vedagiri, P. (2015). Evaluation of pedestrian crosswalk level of service (LOS) in perspective of type of land-use. *Transportation Research Part A: Policy and Practice, 73*, 113–124.

Kathmandu Post. (2024, January 10). *Focus on road safety*.

Leather, J., Fabian, H., & Gota, S. (2011). *Walkability and pedestrian facilities in Asian cities: State and issues*. Asian Development Bank.

Mukherjee, D., & Mitra, S. (2020). Modeling risk factors for fatal pedestrian crashes in Kolkata, India. *International Journal of Injury Control and Safety Promotion, 27*(2), 197–214.

Majumdar, B. B., Vendotti, N., Patil, M., & K. A. (2021). A pedestrian satisfaction-based methodology for prioritization of critical sidewalk and crosswalk attributes influencing walkability. *Journal of Urban Planning and Development*.

Mizanur Rahman, M., Shawon, M. T. A., & Sharmin, S. (2020). Walkability and pedestrian settings in Dhanmondi R/A, Dhaka city: Approach of sidewalk condition index (SCI) and perception. *Journal of Transportation Engineering and Traffic Management, 1*(2), 1–16.

Mori, M., & Tsukaguchi, H. (1987). A new method for evaluation of level of service in pedestrian facilities. *Transportation Research Part A: General, 21*(3), 223–234.

Nepal, G., & Lal, A. C. (2021). Designing walkable city through public perspective and walkability assessment: A case of Jhamsikhel neighborhood. *IOE Graduate Conference*.

Patil, M., Majumdar, B. B., & Sahu, P. K. (2021). Evaluating pedestrian crash-prone locations to formulate policy interventions for improved safety and walkability at sidewalks and crosswalks. *Transportation Research Record, 2675*(9), 675-689. https://doi.org/10.1177/03611981211004127 (Original work published 2021).

Piantanakulchai, M., & Saengkhao, N. (2003). Evaluation of alternatives in transportation planning using multi-stakeholders' multi-objectives AHP modeling. *Proceedings of the Eastern Asia Society for Transportation Studies, 4*, 1613–1628.

Qin, X., & Ivan, J. N. (2001). Estimating pedestrian exposure prediction model in rural areas. *Transportation Research Record: Journal of the Transportation Research Board, 1773*, 89–96.

Saaty, T. L. (2004). Decision making—The analytic hierarchy and network processes (AHP/ANP). *Journal of Systems Science and Systems Engineering, 13*(1), 1–35.

Shay, E., Fan, Y., Rodríguez, D. A., & Khattak, A. J. (2006). Drive or walk? Utilitarian trips within a neotraditional neighborhood. *Transportation Research Record: Journal of the Transportation Research Board, 1985*, 154–161.

Shi, G., Yuan, H., Cheng, J., & Huang, X. (2009). Pedestrian safety consideration and improvement. *Proceedings of the International Conference on Transportation Engineering 2009*, Chengdu, China, 899–904.

Sinha, K. C., & Labi, S. (2011). *Transportation decision making: Principles of project evaluation and programming*. John Wiley & Sons.

Sisiopiku, V. P., & Akin, D. (2003). Pedestrian behaviors at and perceptions towards various pedestrian facilities: An examination based on observation and survey data. *Transportation Research Part F: Traffic Psychology and Behaviour, 6*(4), 249–274.

WHO. (2023). *Global status report on road safety: Summary*. Geneva: World Health Organization.

Zahir, S. (2009). Normalization and rank reversals in the additive analytic hierarchy process: A new analysis. *International Journal of Operational Research, 4*, 446-467.

Zainol, R., Ahmad, F., Nordin, N. A., & Aripin, A. W. (2014). Evaluation of users' satisfaction on pedestrian facilities using a pair-wise comparison approach. *IOP Conference Series: Earth and Environmental Science, 18*(1), 012

Journal on Transportation System and Engineering
ISSN: 3059-9865(Print) 3059-9873(Online)
Vol. 1. Issue 2 (December) 2025: 37-49
DOI: https://doi.org/10.3126/jotse.v1i2.87742

Research Article
Received Date: May 29, 2025
Revised Date: October 9, 2025
Accepted Date: November 9, 2025
Published Date: December 21,2025

Evaluating Geogrid-Reinforced Pavements with Field-Validated Soil Models under Vehicle Load Dynamics

Aanchal Tiwari[a,*], Padma Bahadur Shahi[b] Rajan Suwal[c], Ram Chandra Tiwari[d], Prabhat Kumar Jha[e]

[a]Student, M.Sc. in Transportation Engineering, Department of Civil Engineering, Pulchowk Campus, Institute of engineering, Tribhuvan University, Lalitpur, 44700, Nepal
[b,-d]Faculty, Department of Civil Engineering, Pulchowk Campus, Institute of engineering, Tribhuvan University, Lalitpur, 44700, Nepal
[e]Engineer, Ministry of Physical Infrastructure and Transport (MoPIT), Government of Nepal

Abstract

This study investigates the application of geogrid reinforcement to improve the stress-strain behavior of pavement structures, with the goal of mitigating structural deficiencies and surface distresses. A three-dimensional numerical analysis was conducted using Plaxis software, incorporating both field and laboratory data to evaluate the suitability of various soil material models. The analysis focused on the Arughat–Okhale section of the Midhill Highway to determine the most appropriate model among the linear elastic, Mohr-Coulomb, hardening soil, soft soil, and modified Cam-Clay models. Results indicate that the linear elastic model is applicable for certain conditions, while the hardening soil and soft soil models produce outcomes that closely align with field observations. The Mohr-Coulomb, hardening soil, and soft soil models yielded similar results, whereas the modified Cam-Clay model significantly deviated from both the other models and the field measurements. These findings are based on subgrade soil modeling; applying similarly appropriate models to the other pavement layers could yield results that more accurately reflect field conditions.

Keywords: Reinforced Pavement, Soil Models, Vehicle Load Dynamics, Stress-Strain Analysis, Pavement Performance

1. Introduction

The choice of constitutive material models plays a crucial role in accurately simulating geogrid-reinforced pavement behavior under dynamic loading. Over the past decades, researchers have employed a range of models—from simple linear elastic assumptions to advanced plasticity formulations—each attempting to capture the response of flexible pavement systems. The earliest studies, such as Barksdale and Itani (1999), adopted an elastic material model to simulate pavement behavior under cyclic loading. Their work demonstrated the importance of geogrids in enhancing load-bearing capacity and minimizing deformation, setting the foundation for future numerical modeling. Al-Qadi et al. (2007) also used an elastic model to evaluate the performance of geogrid-reinforced pavements under vehicular loads. Their study highlighted the improved load distribution and reduction in surface distresses due to geogrid inclusion.

Liu et al. (2010) moved toward more realistic representations by applying the Mohr–Coulomb model for the base and subgrade layers, while maintaining a linear elastic model for the asphalt. Their findings confirmed geogrid reinforcement's effectiveness in reducing rutting and strain. Kim (2013) applied linear elastic models for asphalt and base layers, with a simplified elastic representation for the geogrid. Despite the simplicity, the study showed positive effects on deformation resistance under dynamic loading.

In 2017, two studies contributed notable insights. Ahmed Alkawaaz et al. (2017) used a 3D finite element model in ABAQUS with elastic material assumptions and validated their findings against lab tests, observing a 7.75% reduction in surface displacement. Patil and Shivananda (2017) employed PLAXIS 2D with linear elastic behavior for asphalt and Mohr–Coulomb plasticity for other layers, concluding that higher geogrid stiffness significantly reduces vertical deformation. Zhou et al. (2018) used elastic models for the asphalt layer and plastic Mohr–

Corresponding Author's Email Address 079mstre001.aanchal@pcampus.edu.np

Coulomb models for base and subgrade. Their hybrid approach revealed substantial reductions in deformation, fatigue damage, and rutting, especially in weak subgrade conditions.

Leonardi and Suraci (2022) adopted the Drucker–Prager plasticity model for unbound granular materials and incorporated a simple creep law for asphalt. This approach enabled realistic predictions of long-term deformation under repeated loads. Banerjee et al. (2022) also used PLAXIS 2D with a fully linear elastic framework to evaluate reinforced pavements. They introduced a Modulus Improvement Factor (MIF) to correlate geogrid stiffness with base layer performance and proposed a design catalogue for various traffic and subgrade conditions.

In 2023, several studies expanded on these approaches. Abdullah (2023) applied the hardening soil model for nonlinear layers like Sabkha and sand subbase, and linear elastic models for the asphalt and geogrid. The simulations were validated using wheel tracking tests and confirmed the efficacy of reinforcement. Chhetri and Deb (2023) built a 3D finite element model using linear elastic assumptions for asphalt and Mohr–Coulomb for granular and subgrade layers. Their study reported up to 49% reduction in vertical compressive strain due to geogrids. Vishwakarma and Karumanchi (2023) used a 2D axisymmetric model, combining linear elastic behavior for asphalt and Mohr–Coulomb elasto-plasticity for base and subgrade layers, showing significant rut depth reductions for low-modulus subgrades when using stiffer geogrids. Finally, Zakarka et al. (2024) advanced model fidelity by calibrating their PLAXIS 3D simulations with laboratory triaxial tests, capturing the mechanical behavior of sand reinforced with geogrids. Their study revealed increased cohesion and affirmed good agreement between numerical and experimental results.

Despite substantial research on geogrid-reinforced pavements, a key gap remains: although various studies have utilized material models such as linear elastic and Mohr–Coulomb, there has been limited systematic evaluation of their effectiveness in replicating real-world pavement behavior. Most existing work lacks direct comparison between model predictions and field-monitored or laboratory-observed responses, particularly concerning subgrade performance under dynamic loading.

This study seeks to fill that gap by focusing on the role of subgrade constitutive models in capturing pavement response under traffic loading. A full-scale geogrid-reinforced pavement section was instrumented with a GeoDynamic data logger system featuring earth pressure cells, strain gauges, and moisture sensors to monitor short- and long-term responses under the passage of a Tata 1613c truck at a controlled speed of 15 km/h. Corresponding numerical simulations were developed in PLAXIS 3D using five distinct subgrade material models—Linear Elastic, Mohr–Coulomb, Hardening Soil, Soft Soil, and Modified Cam-Clay. The Linear Elastic model assumes reversible, small-strain behavior. Mohr–Coulomb adds shear failure but lacks stiffness variation. Hardening Soil includes stress-dependent stiffness and plasticity for realistic settlements. Soft Soil targets compressible clays and organic soils. Modified Cam-Clay models critical-state behavior in normally consolidated clays. Simplicity decreases but accuracy increases from Linear Elastic to Modified Cam-Clay.

By aligning simulated outputs with field-measured stress, strain, and moisture data, this research evaluates the predictive capabilities of each model. The findings aim to inform the selection of subgrade material models in future geogrid-reinforced pavement design, ensuring closer alignment between numerical predictions and real pavement performance.

2. Study Area

The study was conducted along the Arughat–Okhale section of Nepal's Mid-Hill Road Project (Figure 1). Two pavement sections were instrumented: an unreinforced section at CH 1+700 (28°2'22.51"N, 84°48'29.03"E) and a geogrid-reinforced section at CH 1+800 (28°2'20.48"N, 84°48'27.42"E), both referenced from the bridge over the Budhigandaki River, which separates the Dhading and Gorkha districts of Nepal. Sensors including earth pressure cells, strain gauges, and moisture sensors were installed at the mid-depth of the base layer—where the 40/40Q Tensar geogrid was placed—to capture stress, strain, and moisture data under live traffic conditions (Figure 2).

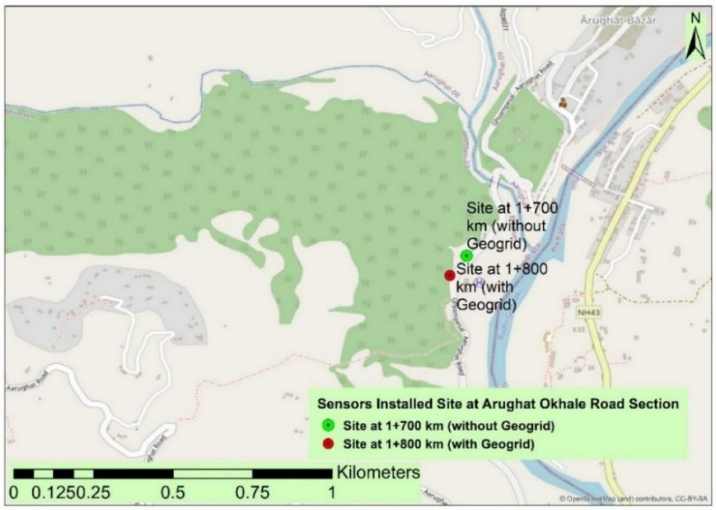

Figure 1. Study area showing test locations

Figure 2. Placement of Geogrid (40/40Q Polypropylene, bi-axial 16kN/m, Tensar Product)

3. Material and Method

This study integrates field data, lab testing, and numerical modeling to assess the performance of geogrid-reinforced pavements under real traffic conditions (Figure 3). A 3D finite element model of the Arughat–Okhale section of Nepal's Mid-Hill Highway was developed using PLAXIS 3D, reflecting the actual pavement geometry (Figure 4). Material properties were obtained through DCPT and laboratory tests (CBR, triaxial, consolidation, permeability, etc.) to define five subgrade models: Linear Elastic, Mohr–Coulomb, Hardening Soil, Soft Soil, and Modified Cam-Clay (Table 1-6).

A bi-axial polypropylene geogrid with stiffness values of 800, 1100, and 1250 kN/m was chosen for its elastic behavior to reinforce the pavement (Table 2). A point load representing the TATA TRUCK 1613C (45/55% front/rear axle distribution) was applied, and harmonic motion was generated based on vehicle speed with appropriate frequency, amplitude, and dynamic time steps. Loading conditions and wheel configurations were based on field observations, and parametric variations in geogrid stiffness and vehicle speed were included to capture realistic traffic behavior.

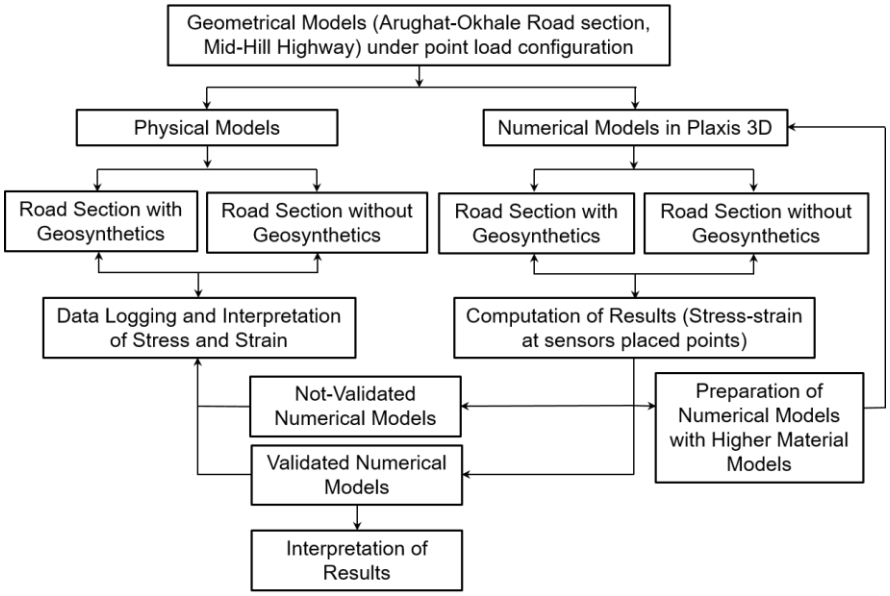

Figure 3. Methodology flow diagram

A GeoDynamic data logger system—equipped with pressure cells, strain gauges, and moisture sensors—monitored stress, strain, and moisture in the field under dynamic loading from a TATA 1613c truck at 15 km/h. Simulated pavement responses were compared against field data to determine which subgrade model most reliably reflects in-service behavior, enabling more reliable model selection for reinforced pavement design.

The numerical simulations are conducted under the same loading and boundary conditions, allowing a direct comparison between modeled outputs and measured field responses. This comparative analysis identifies which subgrade material model best represents the actual performance of geogrid-reinforced pavement, providing practical insights for improving future pavement design and reliability through better model selection.

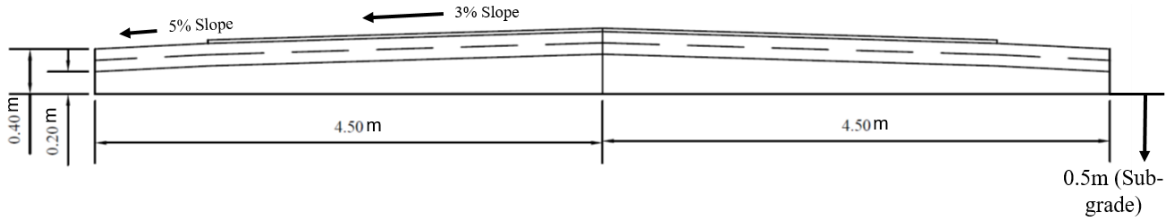

Figure 4. Geometrical model of Arught-Okhale section of MidHill Highway

Table 1. Material models for pavement structure-Linear Elastic (LE)

Item	Description
Identification	Subgrade (CBR: 5%, 5-15% for Parametric Analysis)
Material model	Linear elastic
Drainage type	Undrained-A/Drained
Unsat./Sat.unit weight, γ_{unsat} (kN/m^3)	18/20
Resilient modulus, E (MPa)	E = 10.0 * CBR for CBR ≤ 5 % & E = 17.6 * (CBR)$^{0.64}$ for CBR > 5 % (FPDG, 2014)
Poisson's ratio	0.35
Identification	Granular layer (Subbase CBR: 35%, Base CBR: 85%)
Material model	Linear elastic
Drainage type	Drained
Unsat./Sat. unit weight, γ_{unsat} (kN/m^3)	19/21

Resilient modulus, E (MPa)	$E = 0.2*(h)^{0.45} * MR_{support}$ (FPDG, 2014) Where, h = thickness in mm
Poisson's ratio	0.35
Identification	DBST
Material model	Linear elastic
Drainage type	Non porous
Unsat./Sat. unit weight, γ_{unsat} (kN/m^3)	20/-
Resilient modulus, E (MPa)	2000 (FPDG, 2014)
Poisson's ratio	0.35

Table 2. Geogrid strength properties (Bi-axial)

Item	**Description**
Identification	Geogrid Polypropylene type
Material type	Elastic
Longitudinal (EA1) & Transverse stiffness (EA2) at 2% strain (kN/m)	800 (For Parametric Analysis- 1100, 1250)

Table 3. Material models for Mohr-Coulomb (MC)

Item	**Description**
Identification	Subgrade
Material model	Mohr-Coulomb (MC)
Drainage type	Undrained-A/Drained
Unsat./Sat.unit weight, γ_{unsat} (kN/m^3)	18/20
Initial void Ratio, e_{init}	1.635
Modulus of Elasticity, E (MPa)	E = 10.0 * CBR for CBR ≤ 5 % & $E = 17.6 * (CBR)^{0.64}$ for CBR > 5 % (FPDG, 2014)
Poisson's ratio, υ	0.35
Cohesion (kPa)	9
Friction (Degrees)	28.07
Dilation Angle (Degrees), Ψ	0
Soil Type	Clay
<2µm%	10
Flow Parameter:	
Horizontal Permeability X-dir. Kx m/day	1.4655

Table 4. Material models for Hardening Soil (HS)

Item	**Description**
Identification	Subgrade
Material model	Hardening Soil (HS)
Drainage type	Undrained-A/Drained
Unsat./Sat.unit weight, γ_{unsat} (kN/m^3)	18/20
Initial void Ratio, e_{init}	1.635
Poisson's ratio, υ	0.35
Cohesion (kPa)	9
Friction (Degrees), ϕ	28.07

Dilation Angle (Degrees), Ψ	0
Secant Stiffness in Standard Drained Triaxial test $E50_{ref}$ (kPa)	18.94*e3
Tangent Stiffness for primary Odometer loading $E_{oed\ ref}$ (kPa)	15.15*e3
Loading/reloading Stiffness, E_{ref} (kPa)	$1.05*10^5$
Compression Index, Cc	0.04
Swelling Index, Cs	0.004
OCR	1.0
POP (kN/m2)	0.0
Soil Type	Clay
Horizontal Permeability X-dir. Kx m/day	1.4655

Table 5. Material models for Soft Soil (SS)

Item	**Description**
Identification	Subgrade
Material model	Soft Soil (SS)
Drainage type	Undrained-A/Drained
Unsat./Sat.unit weight, γunsat (kN/m3)	18/20
Poisson's ratio	0.35
Cohesion (kPa)	9
Friction (Degrees)	28.07
Dilation Angle (Degrees)	0
Initial void Ratio, einit	1.635
Soil Type	Clay
Horizontal Permeability X-dir. Kx m/day	1.4655
Consolidation Results:	
Tangent of the critical state, m	1.3
OCR	1.0
POP (kN/m2)	0.0

Table 6. Material models for Modified Cam-Clay (MCC)

Item	**Description**
Identification	Subgrade
Material model	Modified Cam-Clay (MCC)
Drainage type	Undrained-A/Drained
Unsat./Sat.unit weight, γunsat (kN/m3)	18/20
Initial void ratio, e0	1.635
Poisson's ratio	0.35
Cohesion (kPa)	9
Friction (Degrees)	28.07
Dilation Angle (Degrees)	0
Soil Type	Clay
Horizontal Permeability X-dir. Kx m/day	1.4655
Tangent of the critical state, m	1.3
OCR	1.0
POP (kN/m2)	0.0

Figure 5 shows the vehicle load dynamics and load configuration. Figures 6 presents the point/line load and its corresponding mesh schemes for the Tata Truck 1613c in PLAXIS 3D. Point loads simplify tire contact.

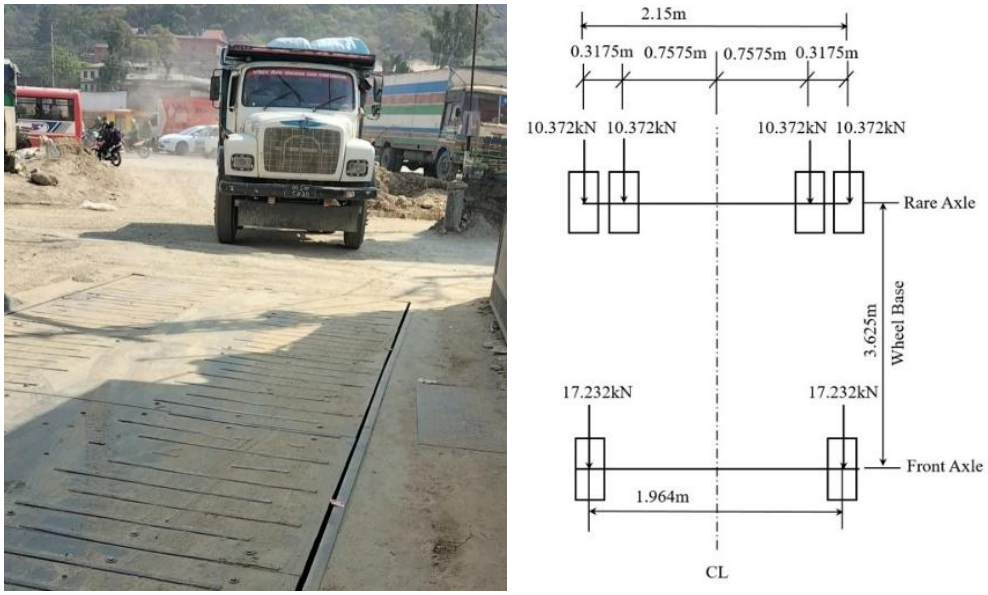

Figure 5. Vehicle load: Left Figure-Empty Truck load; Right Figure-Load configuration

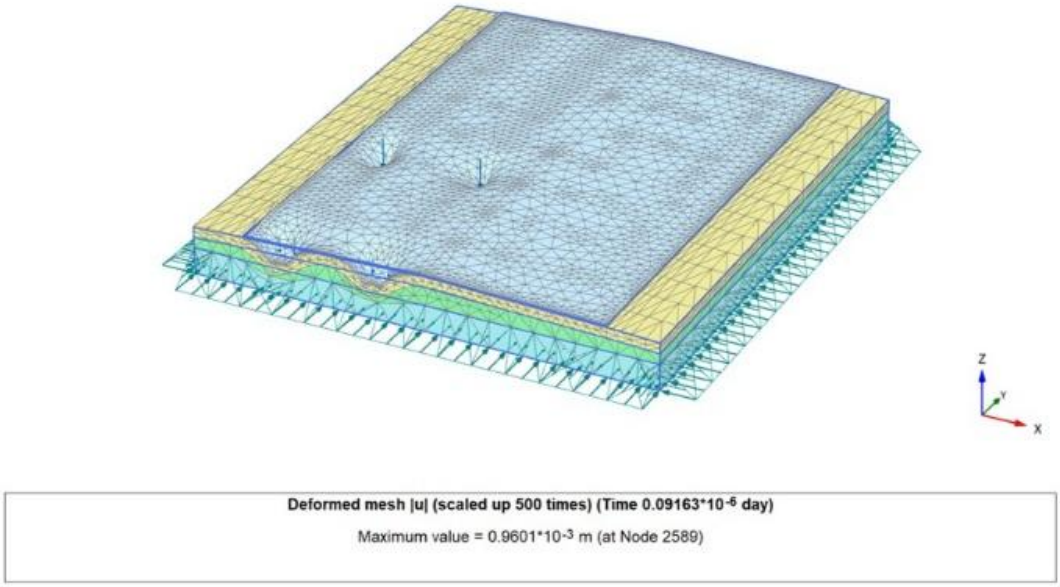

Figure 6. Meshing scheme of 6-wheels Tata Truck 1613c with Point/Line load configuration

The time cycle (Tcycle) equals the wheel perimeter divided by velocity. The motion frequency (f) is its reciprocal, and angular velocity (Ω) equals $2\pi f$. The phase angle (ϕ) is the ratio of wheelbase to curve radius, and the dynamic time step (Δt) is the time cycle divided by the number of time steps (Table 7).

Table 7. Vehicle loading condition.

Vehicle speed (km/hr)	Base frequency (Hz)	Base amplitude (m)	Accelerated amplitude at a=1.0m/sec2	Dynamic Time for time step 100 (Seconds)
15	1.25	0.531	0.584	0.00794
50	4.18	0.538	0.591	0.00171

The staged construction process in PLAXIS 3D was modeled through multiple computation phases, activating soil and structural elements as required. Dynamic analysis was carried out with deformation and mesh parameters adjusted according to geogrid activation. Vehicle movement was simulated along the Y-axis from –0.5 m to 9.5 m at speeds between 15 km/h and 50 km/h, with zero acceleration and results recorded at 100 time steps. The initial phase (K_0 procedure) established in-situ stresses, followed by plastic (static) and dynamic (moving load) phases, where displacements and strains were reset and the mesh updated. Critical nodes were monitored to assess deformation and stress–strain behavior. Static and dynamic boundary conditions assigned in the model are tabulated in Table 8.

Table 8. Static and dynamic boundary conditions assigned in the model

Boundary	BC @ X_{min}	BC @ Y_{min}	BC @ Z_{min}	BC @ X_{max}	BC @ Y_{max}	BC @ Z_{max}
Deformation	Nor. Fixed	Nor. Fixed	Fully Fixed	Nor. Fixed	Nor. Fixed	Free
Dynamic	Viscous	Viscous	None	Viscous	Viscous	None

4. Results and Discussion

4.1 Field validation

The field measurement was conducted at 15 km/hr, which is a suitable speed for capturing responses easily and reliably while observing changes during the data logging process. This measurement was mainly performed for validation purposes. Through parametric analysis, higher speed scenarios such as 50 km/hr could be simulated, representing the design speed of the Mid-Hill Highway. Simulation at this speed helps evaluate the system's response under design conditions and understand its behavior beyond the measured field condition. Data collection at different speeds could also be possible if physical modeling were carried out independently. Figures 7 to 10 illustrate the comparison between numerical simulation and field measurements for geogrid-reinforced pavement under a Tata Truck 1613c moving at 15 km/h. Figures 7 and 9 show simulated principal stress and total displacement across the pavement width, while Figures 8 and 10 present corresponding field data from earth pressure cells and strain gauges. This comparison helps validate the numerical model's ability to capture real pavement behavior under dynamic loading. In Figure 7, the left figure shows a sectional view of the Principal stress 'Sigma 1' along the pavement's symmetric half-width, while the right figure compares the static and dynamic cases. The dynamic case shows higher stress values, with a maximum of -6.095 kN/m² and a minimum of -16.24 kN/m². Figure 8 displays field measurements confirming these results, with fluctuations observed in the pavement width as mentioned in Figure 7.

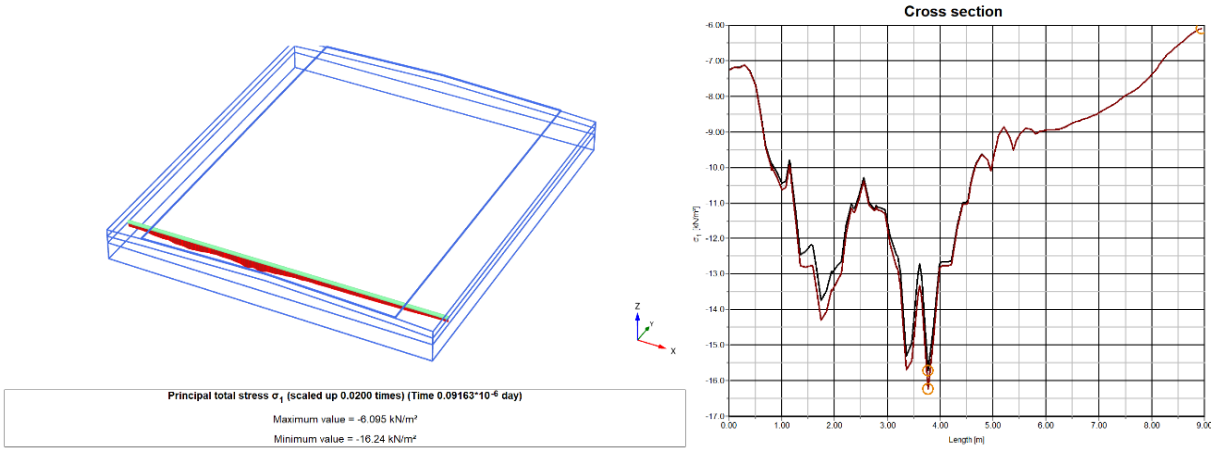

Figure 7. Principal stress (σ_1 in kN/m²) along the symmetric half-width of the pavement (transverse direction) at a constant speed of 15 km/h. Left: Stress distribution at Section 1; Right: Sectional view of stress profile.

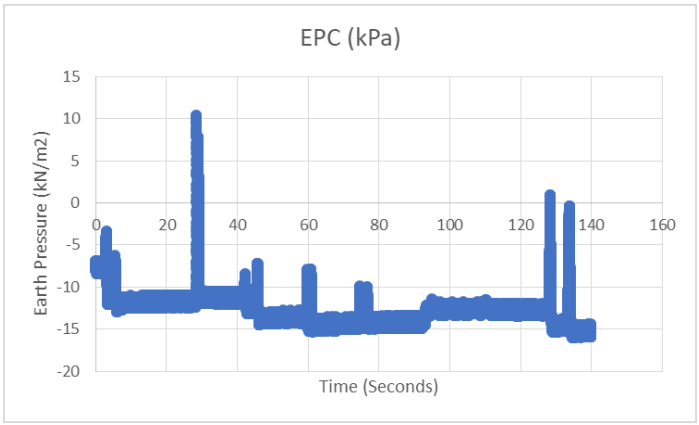

Figure 8. Earth Pressure–Tata Truck 1613c at 15 km/h, Matching Figure 8

Figure 9 shows the computational results for the pavement model with Tata Truck 1613c under a point load, reinforced with geotextile at a speed of 15 km/h. The left figure presents a sectional view-1 of the total displacement 'u' along the symmetric half-width of the pavement, while the right figure compares the static and dynamic cases. The maximum total displacement value obtained is 0.09940×10^{-3} m. Figure 10 shows that field observation confirms the numerical evaluation presented in Figure 9. The deformation pattern indicates that geotextile reinforcement effectively reduces surface displacement and distributes load stresses more uniformly. The close agreement between field and numerical results validates the reliability of the adopted material model and analysis approach.

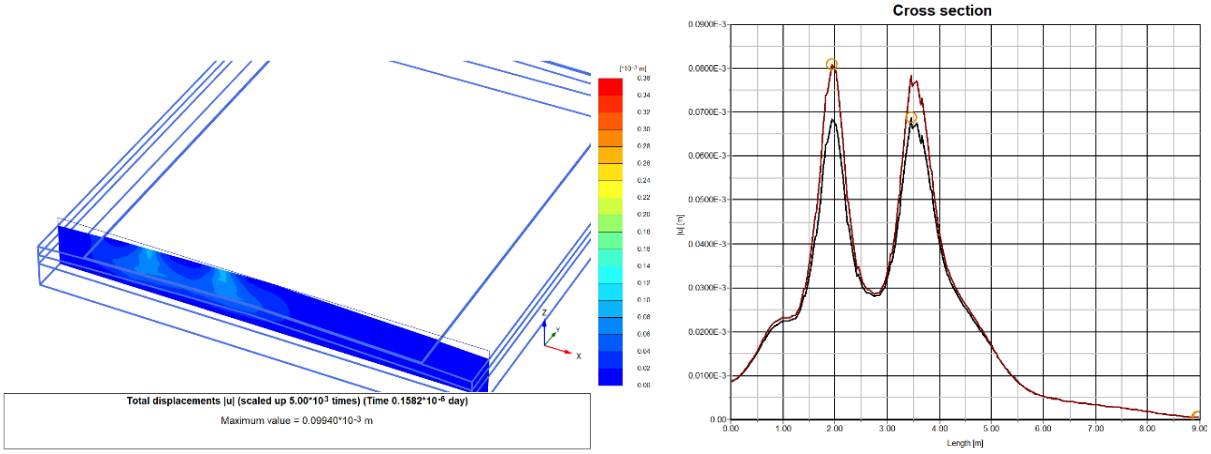

Figure 9. Total displacements (u in m) along the symmetric half-width of the pavement (transverse direction) at a constant speed of 15 km/h. Left: Displacement at Section 1; Right: Sectional view of displacement profile

Figure 11 (Left) shows the stress at the mid-base under a point load from a Tata Truck 1613c at 15 km/h and 1.0 m/s² acceleration, with stress reductions ranging from 6.66% to 40.15% due to geogrid reinforcement. Figure 11 (Right) displays the stress at 50 km/h and 1.0 m/s² acceleration, where geogrid reinforcement results in a reduction of 6.91% to 21.85%.

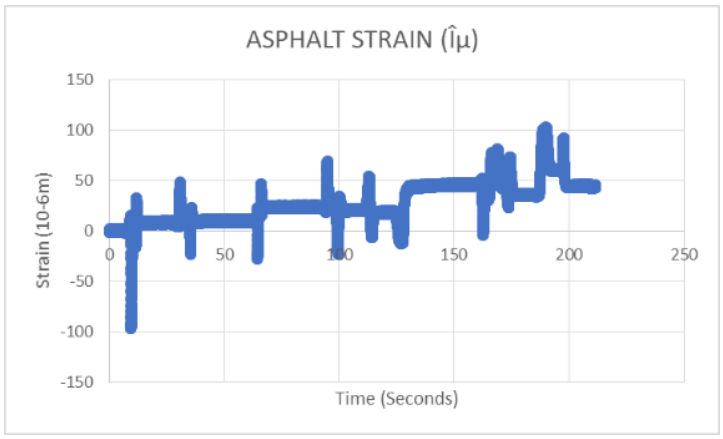

Figure 10. Strain Gauge data–Tata Truck 1613c at 15 km/h, Matching Figure 10

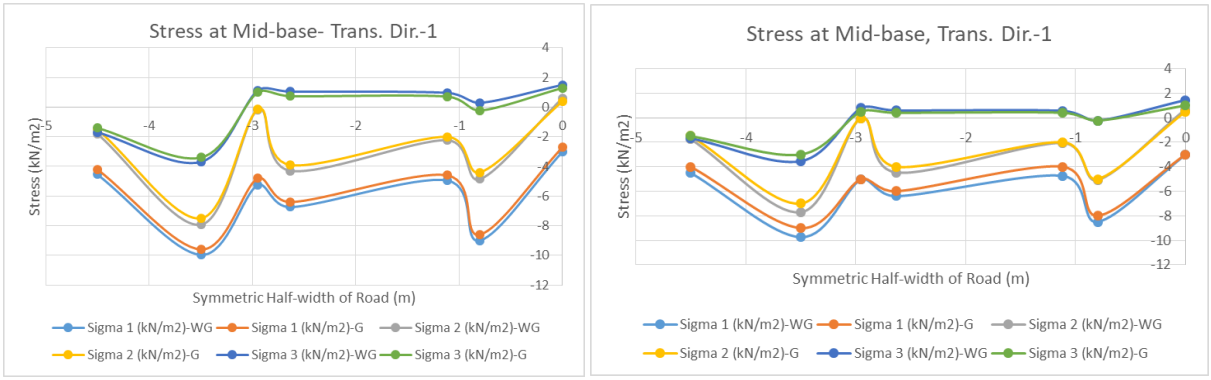

Figure 11. Mid-base stress at 1.0 m/s² acceleration (Tata Truck 1613c), Transverse-1: Left Figure - 15 km/h; Right Figure- 50 km/h, geogrid (G)/without geogrid (WG).

Figures 12 left and right show the variation of principal stress (σ_1) in both transverse and longitudinal directions for cases without and with geogrid reinforcement, respectively. In the absence of geogrid, the stress at higher speeds is observed to be lower. However, in the geogrid-reinforced case, the stress values exhibit both higher and lower extremes. This variation may be attributed to the membrane effect of the geogrid, which influences the stress distribution within the pavement structure.

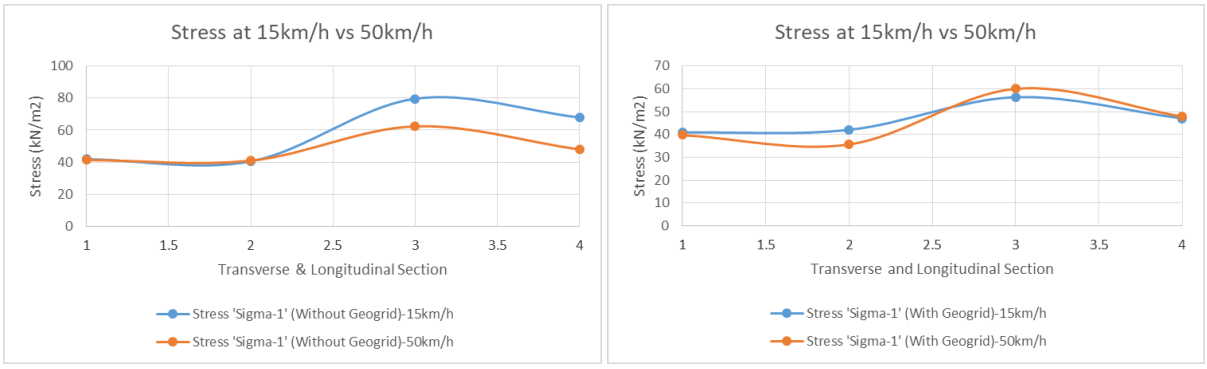

Figure 12. σ_1 Variation (Transverse & Longitudinal): Left Figure-without Geogrid (WG); Right Figure-with Geogrid (G)

4.2 Modeling with Higher Material Models

This modeling is conducted specifically for the subgrade soil layers, while the remaining pavement layers are kept consistent across all cases. Field data were recorded at a speed of 15 km/h for the TATA Truck 1613c, and the analysis further explores potential variations at higher speeds. The Table 9 presents the principal stress (σ_1 in kN/m²) and total displacement (u in meters) obtained from various material models: Linear Elastic, Mohr-Coulomb, Hardening Soil, Soft Soil, and Modified Cam-Clay.

The material models aligned with field measurements were identified using data from the TATA Truck 1613c moving at a constant speed of 15 km/h. Two criteria were evaluated: stress and deformation. Under the stress criterion, all material models—except the modified Cam-Clay model—produced results closely matching field observations. The percentage differences in stress compared to field data are as follows: Linear Elastic – 10%, Mohr-Coulomb – 6.93%, Hardening Soil – 12.3%, Soft Soil – 0.91%, and Cam-Clay – 18.51%. Among these, the Soft Soil model showed the best agreement with field data, although the Linear Elastic, Mohr-Coulomb, and Hardening Soil models are also reasonably applicable. Considering the deformation criterion, the Hardening Soil model shows the closest agreement with field measurements, with a difference of just 1.08%. In comparison, the differences for other models are: Linear Elastic – 27%, Mohr-Coulomb – 43.67%, Soft Soil – 16.27%, and Cam-Clay – 187%. However, all models except the Cam-Clay model are reasonably applicable to field conditions. In summary, the Linear Elastic, Mohr-Coulomb, Hardening Soil, and Soft Soil models can be used with confidence. Among them, the Hardening Soil and Soft Soil models show the best alignment with field data based on both stress and deformation criteria.

Table 9. Material Model(s) aligned with Field Measurements

Field Measurement vs Numerical	Field Measurement	Linear Elastic	Mohr-Coulomb	Hardening Soil	Soft Soil	Modified Cam-Clay
Stress (kN/m2), % difference	30.00	33.00 (10%)	32.08 (6.93%)	33.70 (12.3%)	**29.73 (0.9%)**	24.45 (18.5%)
Displacement (mm), % difference.	1.29	0.93032 (7.88%)	0.7266 (43.67%)	**1.276 (1.08%)**	1.08 (16.27%)	3.705 (187%)

The stress distribution at the mid-base under point loads from the Tata Truck 1613c was analyzed for various road directions (transverse and longitudinal) at a speed of 50 km/h and an acceleration of 1.0 m/s², with and without geogrid reinforcement. Without geogrid, significant stress concentrations were observed, especially in the transverse direction and longitudinal direction-2. When geogrid was applied, stress levels were significantly reduced, particularly in the transverse directions, indicating better load distribution and reduced stress concentrations, enhancing durability under heavy load conditions (Figure 15 and 16). In Figure 13 (left), stress at the mid-base in the transverse direction-1 without geogrid shows significant increases in stress compared to the Linear Elastic (LE) model, with Mohr-Coulomb (MC) at 105.57%, Hardening Soil (HC) at 150.40%, Soft Soil (SS) at 143.46%, and Modified Cam-Clay (MCC) at 268.86%. The HC and SS models show similar stress values, closer to the MC model, while the MCC model deviates significantly. In Figure 13 (right), stress in the longitudinal direction-2 shows similar behavior across all material models, with no significant change in stress percentage, although all models differ from the LE model. In Figure 13, Longitudinal-2 refers to the second wheel position along the wheel path of the TATA truck, taken at 9.5 m. Transverse-2 refers to the rear wheel position along the wheelbase side, taken at 3.5 m, representing the symmetric half of the model according to the vehicle load configuration and dynamics.

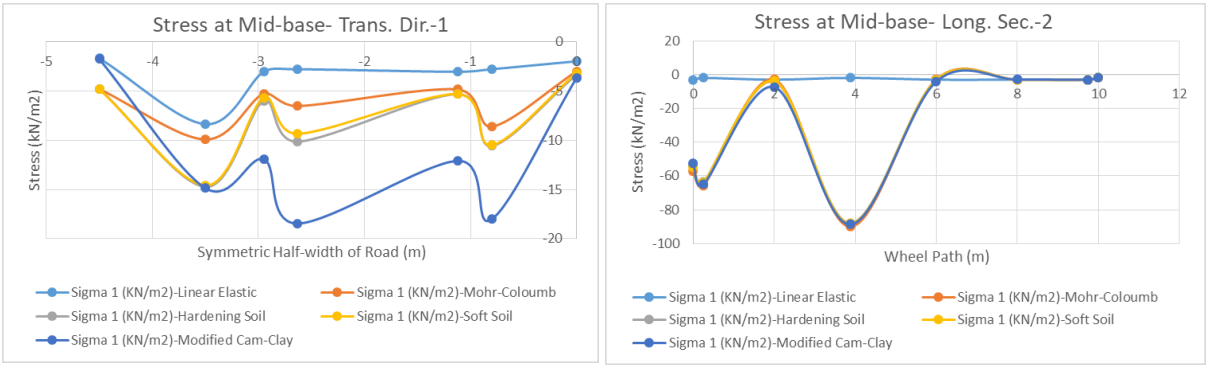

Figure 13. σ_1 stress at Mid–base (Truck, 50 km/h, 1.0 m/s²): Longitudinal–2, without Geogrid; Right–Transverse-2, with Geogrid

Figure 14 (left) illustrates the stress (Sigma 1) at the mid-base under a point load from a Tata Truck 1613c in the transverse direction-2, with geogrid reinforcement, at 50 km/h and 1.0 m/s². Stress reductions compared to the Linear Elastic (LE) model are: Mohr-Coulomb (MC) 0.64%, Hardening Soil (HS) 4.26%, Soft Soil (SS) 1.86%, and Modified Cam-Clay (MCC) 60.19%, with MCC showing the largest deviation. Figure 14 (right) shows stress (Sigma 2) in the longitudinal direction-2, with geogrid reinforcement, where the percentage changes are: MC 2.73%, HS 13.75%, SS 11.04%, and MCC 18.15%. The MC method is closest to the LE model, while HS, SS, and MCC show similar results to each other.

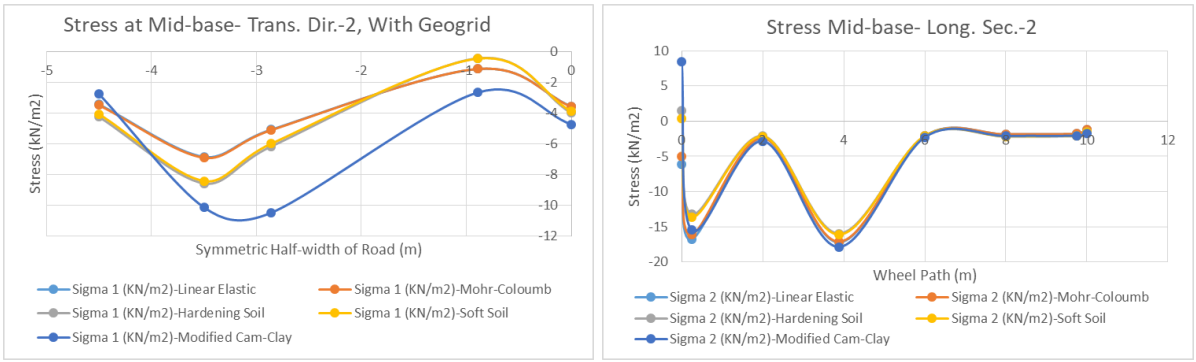

Figure 14. σ_2 Stress at Mid–base (Truck, 50 km/h, 1.0 m/s²): Longitudinal–2, with Geogrid; Transverse–1, without Geogrid

5. Conclusion and Recommendations

This study assessed the effectiveness of geogrid by validating various subgrade material models against field-monitored stress and deformation. Among the five constitutive models tested, significant variation in predictive accuracy was observed. The Soft Soil and Hardening Soil models showed strong alignment with field results, while simpler models like Linear Elastic offered reasonable performance for general use. Key findings are as follows:

- SS model: Best for stress prediction (0.91% deviation); closely matched field data.
- HS model: Most accurate for deformation (1.08% deviation); effectively captured subgrade behavior.
- LE model: Simple and efficient; moderate accuracy (10% stress, 27% deformation deviation).
- MC & MCC models: Moderate to poor alignment; MCC showed the highest deviation and is least suitable.

The study ensures model reliability by aligning numerical results with field measurements and performing parametric analyses across different geogrid stiffnesses and vehicle speeds, effectively capturing real-world traffic behavior and supporting the robustness of the results.

Acknowledgments

We would like to express our gratitude to QRDC, the DOR, and RTU, Pulchowk Campus, for their funding and support in instrumentation. Special thanks to Er. Hemant Tiwari, SOTEN, for his continuous encouragement.

References

Abdullah, G. M. S. (2023). Performance of Enhanced Problematic Soils in Roads Pavement Structure: Numerical Simulation and Laboratory Study. Sustainability, 15(3), 2595. https://doi.org/10.3390/su15032595

Ahmed Alkawaaz, N. G., AL-Badran, Y. M., & Muttashar, Y. H. (2017). Evaluation of Geogrid-Reinforced Flexible Pavement System Based on Soft Subgrade Soils Under Cyclic Loading. Al-Mustansiriyah University.

Al-Qadi, I. L., Ozer, H., & Elseifi, M. A. (2007). Evaluation of geogrid-reinforced pavements. *Journal of Geotechnical and Geoenvironmental Engineering*, 133(12), 1537-1547.

Banerjee, S., Srivastava, M. V. K., Manna, B., & Shahu, J. T. (2022). A Novel Approach to the Design of Geogrid-Reinforced Flexible Pavements. Int. J. of Geosynthetics and Ground Engineering, 8:29. https://doi.org/10.1007/s40891-022-00373-3

Barksdale, R. D., & Itani, R. H. (1999). Design and construction of pavement geosynthetics. *Transportation Research Record*, 1638(1), 37-43.

Chhetri, S., & Deb, P. (2023). Finite Element Analysis of Geogrid-Incorporated Flexible Pavement with Soft Subgrade. Appl. Sci. 2024, 14(13), 5798. https://doi.org/10.3390/app14135798

Federal Highway Administration (FHWA). (2014). Flexible pavement design guide (FPDG).

Kim, Y. (2013). Effectiveness of geogrid reinforcement in flexible pavements under dynamic loading. *Geotextiles and Geomembranes*, 41(2), 77-84.

Leonardi, G., & Suraci, F. (2022). A 3D-FE Model for the Rutting Prediction in Geogrid Reinforced Flexible Pavements. Sustainability, 14(6), 3695. https://doi.org/10.3390/su14063695

Liu, W., Zeng, H., & Chen, G. (2010). Impact of geogrid reinforcement on the performance of flexible pavements. *Geotextiles and Geomembranes*, 28(3), 261-268.

Patil, C. C., & Shivananda, P. (2017). Effect of Axial Stiffness of Geogrid in the Flexible Pavement Deformation through Finite Element Analysis with PLAXIS 2D. JETIR, 4(11), 375–381.

Vishwakarma, P., & Karumanchi, S. R. (2023). Modeling of Semi-Mechanistic Approach for Geo-synthetic Reinforced Flexible Pavement Design. Proceedings of the 9th International Congress on Environmental Geotechnics (9ICEG), Chania, Greece.

Zakarka, M., Skuodis, Š., & Kuhlmann, J. (2024). Geogrid reinforced soil model calibration based on laboratory testing. In Proceedings of the 28th European Young Geotechnical Engineers Conference (EYGEC 2024). Macedonian Association for Geotechnics.

Zhou, Z., Zhang, L., & He, L. (2018). Improvement of pavement performance with geogrid reinforcement: A laboratory and numerical study. *Soil Mechanics and Foundation Engineering*, 55(1), 52-60.

Journal on Transportation System and Engineering
ISSN: 3059-9865(Print) 3059-9873(Online)
Vol. 1. Issue 2 (December) 2025: 50-62
DOI: https://doi.org/10.3126/jotse.v1i2.87743

Research Article
Received Date: May 29, 2025
Revised Date: October 7, 2025
Accepted Date: November 7, 2025
Published Date: December 21, 2025

Exploring the Effectiveness Of Safety Interventions For Reducing Road Crash Occurrence in Different Road Environments

Nitesh Acharya[1], Michael Henry[2]

[1]Department of Roads, Nepal; Email: acharyanites@gmail.com
[2]Shibaura Institute of Technology, Japan; Email: mwhenry@shibaura-it.ac.jp

Abstract:

Despite a recent decline in annual crash fatalities, road safety remains a global issue with significant challenges. Road safety management focuses on analyzing causes and identifying effective ways to mitigate crashes. Among other components of the road environment, safety features and interventions can be improved to enhance safety. This study aims to evaluate the effectiveness of safety interventions in reducing crash occurrence and severity within similar road environments. The condition of the existing safety interventions was assessed along with the types of crashes occurring in certain road environments, and the results showed unique relationships between the same interventions and crash types in different road environments. Such information can be useful for road agencies to plan their safety improvement programs.

Keywords: Road safety management, Safety interventions, Factor analysis on mixed data, Data clustering, Decision tree

1. Introduction:

1.1 Background

Road safety management follows a systematic and planned approach to mitigate road crash occurrence and severity by analyzing the causes and identifying the most effective interventions. Research has shown that the road environment contributes the most to road crash occurrence after human factors (AASHTO, 2010). Analyzing human factors and controlling them is complex since human behavior differs from one person to another, and this makes mitigating crashes through controlling human factors difficult. Hence, it becomes sensible to develop safer or more forgiving roads to overcome human errors and mitigate the occurrence of a large portion of crashes by improving the road environment or driving conditions.

In contrast to the human factors, it is relatively easier to study road environments, as information on the existing or planned roadways is generally always available and can be collected through various measures. The Safe System approach is a modern tool used by safety practitioners in promoting road safety, and one of the pillars considered in this approach for improvement is the road environment or the road itself (PIARC, 2019). Safer road infrastructure has also been listed among the five pillars in the Global Plan for the Decade of Action for Road Safety (2021-2030), which has been proclaimed by the UN General Assembly (WHO, 2023). This highlights the importance and necessity of safer road infrastructure for the mitigation of road crashes.

Corresponding Author's Email Address acharyanites@gmail.com

Road environment features can be broadly divided into road geometry, road type, land use, and existing safety features. Among these, road geometry is assessed and fixed in the design and construction stages through safety audits, and generally remains unchanged over time. Road type and land use, on the other hand, can vary over time due to a variety of external factors. Other road components, including safety features, should be managed to provide the safest driving conditions. In the case of highways in operation, safety audits may be performed to identify deficiencies and potential hazards and, based on the audit results, road safety features are proposed to mitigate the frequency and severity of future crashes (FHWA, 2025). Road safety features, or interventions, are temporary measures designed to enhance safety at a particular road section and to mitigate certain types of crashes and, if found effective, may be used permanently. It is thus much easier to modify safety interventions compared to other road features.

Interventions intended to mitigate road crashes can be of different types. Generally, they can be grouped under five categories: (a) human factors (e.g., enforcement or road user education), (b) road design, infrastructure, and traffic control, (c) legal and institutional framework, (d) post-crash pre-hospital care, and (e) vehicle factors (except car design for occupant protection) and protective devices (Goel, et al., 2024). For simplicity, these safety interventions can be broadly categorized into just two types: road engineering measures and regulatory measures for the enforcement of traffic laws. Road engineering measures focus on enhancing safety by altering the physical condition of existing roads – for example, the construction of sidewalks for pedestrians, roundabouts at junctions, etc. However, the effectiveness of such safety interventions plays a great role, and hence, the interventions must be carefully chosen after a thorough analysis. Different interventions have differing potentials to mitigate certain types of crashes, which is generally expressed using an index called the Crash Modification Factor (CMF) (FHWA, 2025).

Many studies have been conducted globally to assess the CMF and the effectiveness of different safety interventions, with varying results. Most of this research has been conducted in high-income countries (HICs) in Europe and North America, and very few research studies have been found in low- and middle-income countries (LMICs). Goel et al. (2024) prepared an evidence gap map to identify existing evidence from all intervention effectiveness studies and performed a systematic review of road safety interventions. They concluded that limited research was conducted in LMICs, and many interventions that have been found effective in HICs may not be equally effective in LMICs due to distinctly different driving environments and human driving behaviors. A systematic review of literature by Gupta & Bandyopadhyay (2020) conducted in LMICs did not find sufficient evidence that road engineering interventions, when used alone, were effective in reducing road traffic death and injury counts, and their effectiveness when combined with enforcement measures must be assessed. However, with very limited studies on the effectiveness of interventions in LMICs, it is difficult to develop plans for improving road safety with a high degree of confidence.

This gap in the existing literature on the effectiveness of interventions in LMICs motivated the authors to explore whether there exist any relationships between existing safety interventions and road crashes occurring on highways in Nepal. In this study, a novel approach of clustering road segments with similar road geometry and driving environment is considered, with the hypothesis that assessing crashes in similar road environments can provide more realistic scenarios to assess crash frequency and types. It is believed that assessing the crashes occurring on roads with similar road geometry, land use, pavement, and other road environmental features can provide a clearer idea of the factors and patterns of the crashes, along with the crash types and severity. Data clustering is a multivariate data mining technique with the objective of grouping objects based on a set of characteristics or attributes. This technique is generally used in crash analysis as a pre-processing stage to analyze infrastructure and environmental data, the results of which are used to further develop statistical models for assessing the impact of different factors on crash occurrence and severity (Bonera et al., 2022). A systematic review of literature on modeling road crashes showed that cluster analysis, when used together with other machine-learning algorithms for modeling crash frequency and severity, can improve the overall prediction accuracy of the models (Silva et. al., 2020). The same study also showed that decision tree-based

algorithms were among the most common algorithms for analyzing and modeling road crashes and that road-environmental factors are the most commonly used features for modeling road crashes.

1.2 Research objectives

The objective of this study is to analyze crash occurrence in highly similar road environments, which are obtained by cluster analysis. Certain types of crashes may be common for certain road environments, and, hence, analyzing crashes by segregating them based on road environment can provide a better understanding of the causes of crashes. Furthermore, this study aims to evaluate the relationship between safety interventions and road crash types within road sections with highly similar road environments and then examine how this relationship varies between different environments.

2. Methodology:

2.1 Data collection

Data taken on 160 kilometers of the Dhulikhel-Sindhuli-Bardibas highway and 61 kilometers of the Yamdi-Maldhunga section of the Midhill highway were used for the analysis. Homogeneous segments and fixed-length are two common approaches for road segmentation. In mountainous roads, the road features changes within short stretches, resulting in the formation of very small segments, making analysis cumbersome. Hence, fixed-length segmentation was preferred, and the length of 250 meters was adopted, considering it would fairly reflect the actual conditions and characteristics of a mountainous road. Furthermore, the Highway Safety Manual by AASHTO also recommends road segments longer than 160 meters for crash analysis.

Data on road geometry, land use, and existing interventions for each of these segments were collected through the field inspection conducted in August 2022, and additional data were collected from the departmental archive of the Department of Roads, Nepal. The list of the road features considered and their descriptive statistics can be found in Table 1, where it can be seen that the carriageway width of the study highways varies between 4.5 meters and 21.0 meters, with a median width of 5.5 meters. The statistics show that the shoulders are very narrow, and the average longitudinal grade is 3.86%, with a maximum gradient of up to 10%. Similarly, the horizontal curve radius varied between 20.4 meters to 1,025.0 meters, with a median radius of 100 meters. The majority of the segments did not have access roads, but some segments had up to 5 accesses. The average International Roughness Index (IRI), which represents the pavement condition, is 5.77 m/km, which shows the riding quality is not good (Chen et al., 2019). Additionally, Tables 2, 3, and 4 show the descriptive statistics of the categorical features of the road segments. While a majority of the road segments had graveled left shoulders, there were also a substantial number of segments with no left shoulder (31.7%). Similarly, a majority of the road segments had graveled right shoulders, followed by segments with paved right shoulders. Roughly 60% of the road segments did not have ribbon development, whereas 15.4% had full ribbon development, indicating that these segments are passing through an urban area. Among all road segments, only 4.2% were straight segments, while the remaining were curved segments having at least one horizontal curve.

Table 1: Descriptive statistics of the road features (continuous variables)

Variables (unit)	Minimum	Maximum	Range	Median	Mean	S.D. (n-1)
Average Daily Traffic (veh/day)	3,430.00	12,015.00	8,585.00	6,399.00	6,714.42	2,344.68
Carriageway width (meters)	4.52	21.00	16.48	5.50	6.51	3.59
Left shoulder width (meters)	0.00	2.00	2.00	0.50	0.42	0.40
Right shoulder width (meters)	0.00	2.00	2.00	0.50	0.49	0.39
Grade (%)	0.00	10.00	10.00	3.86	3.86	2.22
Curve radius (meters)	20.42	1,025.00	1,004.58	100.00	150.22	147.26

Curve length (meters)	0.00	250.00	250.00	127.76	125.56	57.40
Access presence (number)	0.00	5.00	5.00	0.00	0.25	0.62
International Roughness Index (m/km)	0.00	10.95	10.95	5.15	5.77	1.95

Table 2: Frequency of the shoulder types

Shoulder type	Absent	Composite	Gravel	NA	Paved
Left shoulder type	280.0 (31.7%)	24.0 (2.7%)	403.0 (45.6%)	44.0 (5.0%)	132.0 (14.9%)
Right shoulder type	184.0 (20.8%)	25.0 (2.8%)	408.0 (46.2%)	44.0 (5.0%)	222.0 (25.1%)

Table 3: Frequency of the road segments for different ribbon development levels

Ribbon development	Absent	Full	Partial
Frequency (%)	539.0 (61.0%)	136.0 (15.4%)	208.0 (23.6%)

Table 4: Frequency of straight and curved road segments

Straight?	No	Yes
Frequency (%)	846.0 (95.8%)	37.0 (4.2%)

Three years of crash data (2021 to 2023) were also collected from the respective district traffic offices. The crash data included information on the location, date, and time of the crashes, severity of the crashes, type of crashes, and probable reason for the crashes. A total of 455 crashes occurred on these two highways during the three-year study period. The histogram in Figure 1 shows that 591 (67%) road segments did not record any road crashes in the study period, while 22% had just one recorded crash; however, there exist some sections with multiple crashes. The initial crash data were cleaned by categorizing each crash by type (hit pedestrian, head-on, rear-end, side-swap, right-angle, overturned, run-off, hit fixed object, and others). In the raw crash data, crash outcomes were recorded under four categories: fatal crashes, serious injury crashes, minor injury crashes, and property damage crashes. However, for the analysis, these crash severities were recategorized into two types: fatal and serious injury (FSI) crashes, and non-fatal and serious injury (Non-FSI) crashes. The road segments were given an FSI label if there was at least one fatal or serious injury crash recorded during the study period. Similarly, road segments were labeled as Non-FSI if they had recorded no FSI crashes and at least one crash that resulted in only minor injury or property damage during the study period.

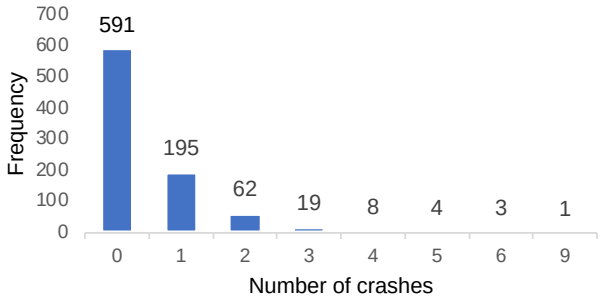

Figure 1: Frequency of road segments with different numbers of road crashes

Data were also collected on the condition of the existing safety measures in the segments of the study highways. Nine safety interventions (crash barriers, center line markings, edge markings, edge delineation, curve delineation, pedestrian crossings, road signage, footpaths, and streetlights) were considered for the analysis, and the condition of these interventions was assessed by experts during the field inspection and was categorized into three levels (good, fair, and poor). This categorization was based on a set of road conditions (criteria), formulated to evaluate road segments on different road interventions. These assessment criteria were developed after a comprehensive review of the literature on road safety audit and inspection. Table 5 provides a summary of the condition of the interventions, and it can be noted that a majority of road segments had edge markings and road signage in good condition, and most of them had edge delineations in fair condition. Additionally, it can be seen that a large share of road segments had crash barriers, centerline markings, curve delineation, zebra crossings, footpaths, and streetlights in poor condition.

Table 5: Frequency of road segments with different safety intervention conditions

Safety interventions	Good	Fair	Poor
Crash barrier	197 (22.3%)	131 (14.8%)	555 (62.9%)
Centerline markings	86 (9.7%)	141 (16.0%)	656 (74.3%)
Edge line markings	416 (47.1%)	309 (35.0%)	158 (17.9%)
Edge delineation	278 (31.5%)	380 (43.0%)	225 (25.5%)
Curve delineation	70 (7.9%)	104 (11.8%)	709 (80.3%)
Zebra crossing	110 (12.5%)	129 (14.6%)	644 (72.9%)
Road signage	391 (44.3%)	331 (37.5%)	161 (18.2%)
Footpath	56 (6.3%)	94 (10.6%)	733 (83.0%)
Street light	58 (6.6%)	123 (13.9%)	702 (79.5%)

2.2 Analytical approach

First, Factor Analysis on Mixed Data (FAMD) was performed, followed by data clustering to identify road segments with highly similar road geometries and land use characteristics. Factor analysis is a feature (dimension) reduction technique used when dealing with many interconnected variables and can help to understand the underlying patterns in the data. FAMD is a technique for factor analysis that deals with mixed data (both continuous and categorical data) (Kassambara, 2017).

It is a matter of huge interest whether the crash types differ in different types of road environments, or remain the same for all road types. In addition, the effectiveness of the interventions may vary from one road environment to another, resulting in different types of crashes. Hence, the importance of such research can never be undermined, and to perform such a study, it is very important that the road segments are clustered so that each individual cluster with specific characteristics can be analyzed. Data clustering is an unsupervised machine learning algorithm that organizes and classifies different objects, data points, or observations into groups or clusters based on similarities or patterns, of which agglomerative hierarchical clustering is one approach to clustering. The road features considered in the clustering included carriageway width, left and right shoulder widths and types, longitudinal gradient, whether the segment is straight or curved, radius of curvature for curved segments, percentage of curved portions in a segment, number of accesses in each segment, level of ribbon development, and pavement roughness. Factor analysis and agglomerative hierarchical clustering were carried out using the open-source software R (R Core Team, 2022) and its libraries “FactoMineR” (Le et al., 2008) and “factoextra” (Kassambara & Mundt, 2020).

Next, the relationship between the condition of existing safety measures and the crash outcomes was analyzed within each cluster. In this analysis, the condition levels of existing safety interventions in the segment were taken as the independent variables, and the crash outcome was taken as the dependent variable. Thus, there exist three possible

crash outcomes for any road segment: no crashes, non-FSI crashes, or FSI crashes. This presents a classification problem, so the resulting datasets were analyzed using decision tree analysis, a supervised machine learning algorithm that builds a set of decisions and their possible consequences. This algorithm is popular among researchers to assess the relationship between the dependent and independent variables, particularly when these variables have a non-linear relationship. Also, their ability to handle mixed types of data is robust. This analytical tool will help to analyze the relationship by generating a tree-like graphical representation of the decision-making stages at different nodes to provide better interpretability and explainability. While often used for prediction, decision tree analysis may also be used for understanding patterns in a dataset, and thus, this analytical approach may be appropriate even for the limited dataset used here. The open-source software R was again used for this analysis, this time utilizing the libraries "rpart" (Therneau & Atkinson, 2013) and "rpart.plot" (Milborrow, 2024)

3. Results and Discussion:

3.1 Clustering of the road segments

Eigenvalues in factor analysis represent the total amount of variance that can be explained by a given principal component while performing FAMD. The idea of Principal Component Analysis (PCA) is to reduce the number of variables (principal components) of a data set, while preserving as much information as possible. Hence, opting for higher variance (more principal components) would be against the objective of PCA analysis, as there would not be a significant reduction in the noise present in the data. On the other hand, selecting very low variance (fewer principal components) would not only result in noise reduction but also lead to a huge loss of information from the data, eventually leading to less accurate analysis. Hence, to find the balance in between, 67% of the total variance was considered sufficient to proceed with the analysis.

The reduced dataset was used to cluster road segments using agglomerative hierarchical clustering, which produced a dendrogram that revealed the similarity of the road segments with respect to their road geometry and land use (Figure 2). Based on the shape of the dendrogram, seven clusters were considered for further analysis.

After clustering, the next step is to characterize the clusters based on the main characteristics of the segments grouped together in each cluster. For this purpose, two metrics are generally used: the Mod/Cla and Cla/Mod. The Mod/Cla explains the percentage of road segments within a cluster with a specific variable category characterizing the similarities within the clusters. Similarly, the Cla/Mod explains the percentage of road segments across the cluster with a specific variable category characterizing the similarities across the clusters. A v.test value greater than 1.96 corresponds to a p-value less than 0.05 and the sign of the v.test indicates whether that category is under or over-expressed, compared to other categories (Husson et al., 2011). In Table 6, only the variables having Mod/Cla greater than 75% have been listed and, using those features, each cluster's characteristics have been defined. It is noted that the number of road segments in the clusters varies from 23 to 285, with three large clusters (Clusters 2, 4, and 5) containing more than 200 segments.

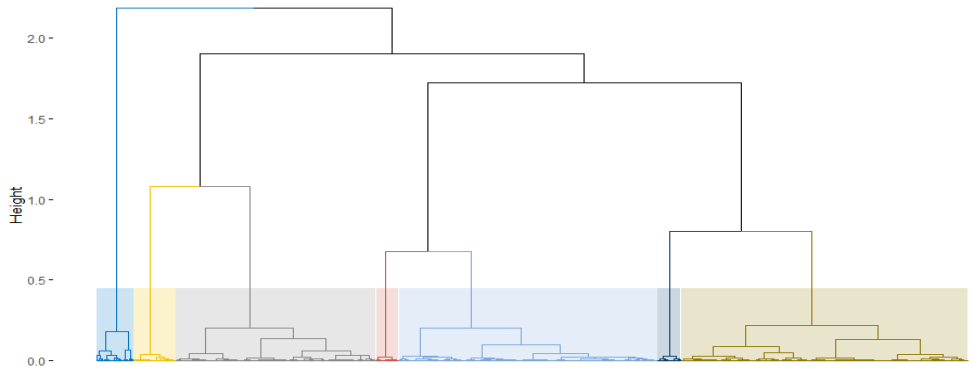

Figure 2: dendrogram showing seven clusters of road segments

Table 6 Cluster statistics and description

Cluster	Variable	Cla/Mod	Mod/Cla	v.test	Cluster description/ Main characteristics
Cluster 1 (n = 24)	RT_shd_type = Composite	96.00	100.00	14.25	Road segments having composite right road shoulder type and no ribbon development
	Ribb_delp = Absent	3.90	87.50	2.80	
Cluster 2 (n = 285)	LT_shd_type = Absent	76.23	86.67	21.80	Road segments are curvy, ribbon development is absent, and there is no shoulder on the left side
	Ribb_delp = Absent	40.26	76.14	6.46	
	Straight_Y_N = No	33.69	100.00	5.08	
Cluster 3 (n = 23)	LT_shd_type = Composite	95.83	100.00	14.01	Road segments having composite left road shoulder type, gravel right shoulder type, and no ribbon development
	RT_shd_type = Gravel	4.90	86.96	4.03	
	Ribb_delp = Absent	3.53	82.61	2.18	
Cluster 4 (n = 269)	LT_shd_type = Gravel	65.26	97.77	22.29	Road segments are curvy, and both left and right shoulders are graveled
	RT_shd_type = Gravel	64.22	97.40	21.84	
	Straight_Y_N = No	31.80	100.00	4.89	
Cluster 5 (n= 202)	RT_shd_type = Absent	75.00	84.65	21.00	Road segments are curvy and do not have right shoulder
	Straight_Y_N = No	23.88	100.00	4.04	
Cluster 6 (n = 43)	RT_shd_type = Absent	18.86	100.00	10.84	Road segments do not have both (left and right) shoulders and have full ribbon development
	LT_shd_type = Absent	13.27	100.00	9.22	
	Ribb_delp = Full	26.9	77.82	7.36	
Cluster 7 (n = 37)	Straight_Y_N = Yes	100.00	100.00	17.19	All the road segments are straight

3.2 Analyzing crashes within clusters

Table 7 provides the details of crashes in each cluster. This includes information on the frequency of different crash types in each cluster, followed by total crashes, average crashes in a segment per ten thousand vehicles, and the standard deviation of the crashes per ten thousand vehicles for each cluster. The average crashes in a segment per ten thousand vehicles was considered an appropriate metric to evaluate and compare crash intensity between the clusters, as it scales according to the cluster size. It was derived by calculating the number of crashes per 10,000 vehicles in each segment and then averaging across all segments in the cluster. From this table, it can be noted that Clusters 1 and 3 – both of which are small clusters – also have very few crashes and relatively lower average crashes per ten thousand vehicles. Cluster 1 (n=24), comprising road segments with either gravel or paved shoulders and without any ribbon development, had the lowest average crashes per ten thousand vehicles (0.39). Conversely, Cluster 6 (n=43), which is characterized by road segments without both left and right shoulders, had the highest average crashes per ten thousand vehicles (1.63). Furthermore, Cluster 7 (n=37), which contains road segments with completely straight stretches, had an average of 0.90 crashes per ten thousand vehicles, which is relatively higher than most of the clusters.

Analyzing the results considering the crash types, it was found that straight road segments (Cluster 7) showed a larger proportion of crashes involving pedestrians and head-on collisions between vehicles. The reason for a larger share of such crashes can be attributed to higher speeds in straight segments. For most clusters, run-off-road crashes and head-on collisions were the predominant crash types. However, Clusters 6 and 7 had a significantly lower proportion of run-off-road crashes. The reason for lower run-off road crashes can be related to either road usage or existing safety

interventions. In other words, if the road segments in these clusters pass through urban areas having high levels of ribbon development, or if they have good crash barriers, then the probability of having run-off road crashes is lower. The cluster characteristics in Table 6 show that Cluster 6 has a high level of ribbon development; hence, the aforementioned hypothesis is correct.

Table 7: Crash statistics in clusters

Crash types	Cluster 1 n= 24		Cluster 2 n= 285		Cluster 3 n= 23		Cluster 4 n= 269		Cluster 5 n= 202		Cluster 6 n= 43		Cluster 7 n= 37	
	Freq	%	Freq	%	Freq	%	Freq	%	Freq	%	Freq	%	Freq	%
Hit pedestrian	0	0.0	6	5.5	1	14.3	22	14.3	6	7.3	19	26.0	8	32.0
Head-on	2	40.0	41	37.6	3	42.9	48	31.2	30	36.6	15	20.5	9	36.0
Rear-end	0	0.0	9	8.3	1	14.3	8	5.2	4	4.9	9	12.3	0	0.0
Right angle	1	20.0	1	0.9	0	0.0	4	2.6	2	2.4	5	6.8	0	0.0
Side swap	0	0.0	0	0.0	0	0.0	2	1.3	1	1.2	0	0.0	0	0.0
Overturned	0	0.0	2	1.8	0	0.0	13	8.4	3	3.7	5	6.8	1	4.0
Run-off	2	40.0	32	29.4	2	28.6	46	29.9	18	22.0	1	1.4	1	4.0
Hit fixed object	0	0.0	8	7.3	0	0.0	7	4.5	6	7.3	12	16.4	4	16.0
Others	0	0.0	10	9.2	0	0.0	4	2.6	12	14.6	7	9.6	2	8.0
Total crashes	5		109		7		154		82		73		25	
Avg. crash pttv*	0.39		0.76		0.54		0.85		0.69		1.63		0.90	
S.D. crash pttv	0.99		1.43		1.33		1.47		1.36		1.77		1.34	

* crash per ten thousand vehicles

3.3 Analyzing the effectiveness of safety interventions using decision trees

In this section, the decision tree algorithms were used for each cluster, and the results were analyzed to study the impacts of the condition of the safety intervention on the crash outcomes (no crash, non-FSI crash, or FSI crash). The decision trees for clusters 2, 4, 5, and 7 are shown in Figures 3, 4, 5, and 6, respectively. The algorithm could not construct the decision trees for clusters 1, 3, and 6 because no relationship between the crash outcomes and the condition of the safety interventions was found for the current datasets.

The decision tree for cluster 2 shows that, in this road environment, FSI crashes are likelier to occur when the curve delineation is in fair condition. On the other hand, the chances of non-FSI crashes are higher when the road segments have good or bad curve delineation, good road signage, and fair zebra crossings. This cluster contains curved road segments, ribbon development is absent, and there is no left shoulder. In such a road segment, curve delineation is essential to warn and guide drivers while maneuvering the curves. The crash statistics in Table 7 show that 29.4% of the crashes occurring in cluster 2 are run-off crashes, which supplements the fact that bad curve delineation can result in FSI crashes, as run-off crashes generally tend to result in FSI crashes.

Cluster 4 comprises curved road segments with both left and right shoulders graveled. The decision tree in Figure 4 shows that, in this road environment, it is more likely that a crash will not occur when the zebra markings are in fair or poor conditions. Likewise, the road segments having good zebra markings, but poor centerline markings and edge delineation may also result in no crash; however, due to a very small sample size, it is difficult to confirm this result with a high confidence level. The conditions for the occurrence of FSI crashes can also be analyzed, but due to the small number of observations leading to FSI crashes, the results cannot be confirmed with a high degree of confidence.

Cluster 5 mostly comprises curved road sections without a right shoulder, and from the decision tree for this cluster (Figure 5), it can be seen that in this road environment, it is more likely that the presence of a crash barrier in fair or good condition will prevent crash occurrence. However, it should be noted that the root node in the decision

tree shows that the majority of the road segments have not observed any sort of crashes, and different safety interventions (in different condition levels) still lead to an outcome of "no crash occurrence."

The decision tree in Figure 6 shows how the centerline marking condition governs the crash outcomes in the case of road segments that are straight (Cluster 7). It can be noted that, in such a road environment, good centerline marking may lead to FSI crashes, whereas fair or poor conditions may result in no crashes. This result is understandable because drivers, while traveling in straight sections with centerline markings, usually feel confident in the width of their driving lane limits and tend to speed. However, when overspeeding, a small distraction or mistake can lead to FSI crashes.

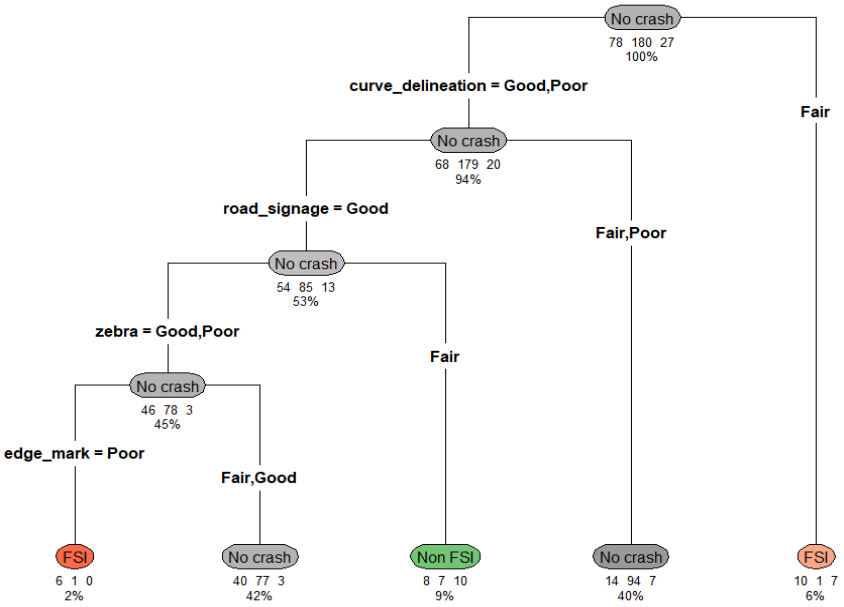

Figure 3: Decision Tree for Cluster 2

To summarize, the decision trees were used to analyze the impact of road safety interventions on crash outcomes in different road environments. Interestingly, it was found that different road environments have different interventions that have a dominant effect on crash outcomes. Even though not all the outcomes of the study are relatable to real-life conditions, the results provide us with insights into how the condition level of the safety interventions can greatly influence the crash outcomes. Such results can be helpful for the decision makers in the regular upgrading of the interventions, as it shows how a level improvement from poor to fair condition, or fair to good condition, can contribute to mitigating the crash severity. Irrespective of the results, the methodology adopted in this study to assess the effectiveness of the safety interventions in mitigating crash occurrence and severity by analyzing different road environments and using machine learning techniques is believed to be a novel approach for road crash studies.

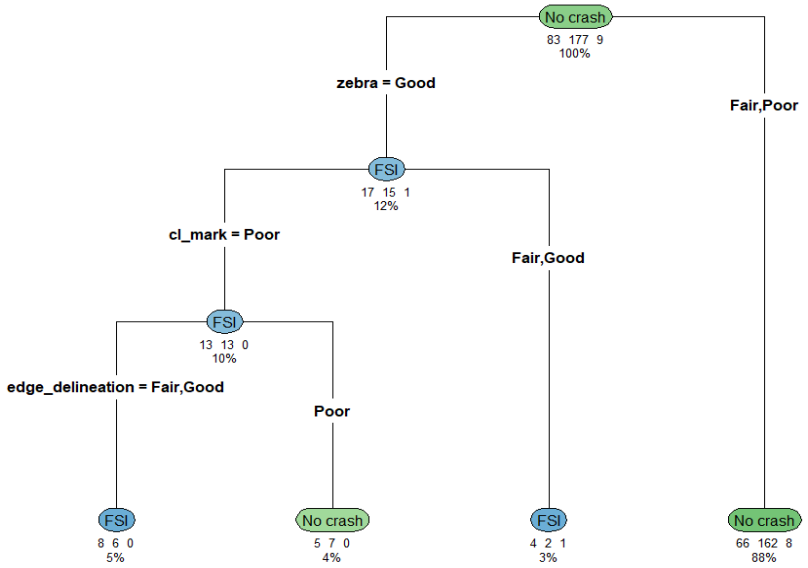

Figure 4: Decision Tree for Cluster 4

It can be noted that some of the results from the study were found counterintuitive. One of the reasons for such results can be related to the downsides of the Decision tree algorithms, which are being susceptible to bias and sensitivity. Hence, a small change in data can result in a different outcome. Hence, the authors believe that the results may differ when analyzed with different machine learning algorithms, for example, Random Forest, which makes the use of an ensemble approach for training the models and predictions, can result in better and realistic results.

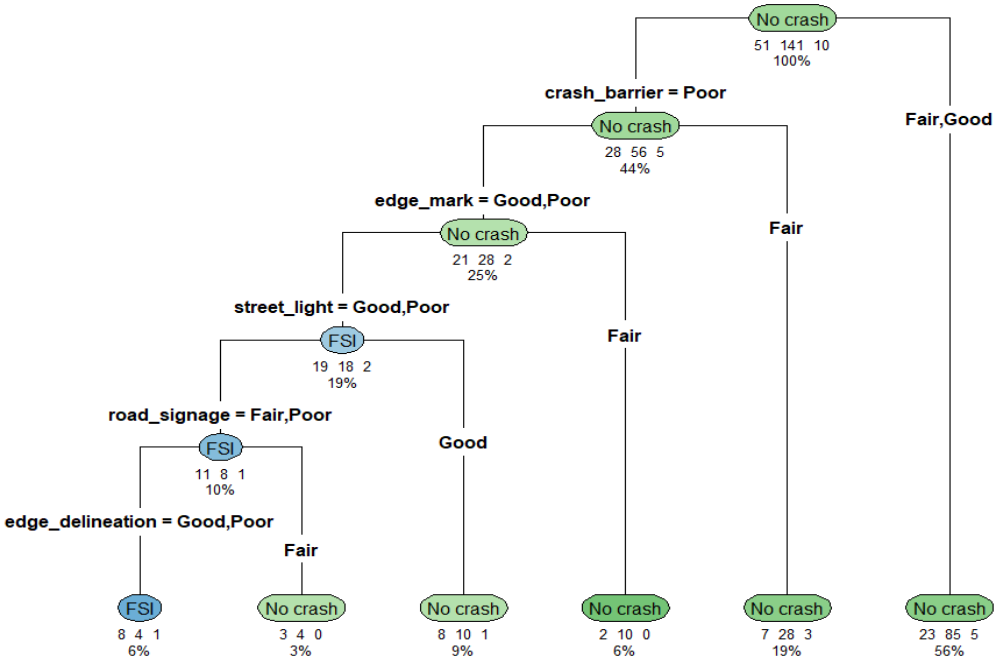

Figure 5: Decision Tree for Cluster 5

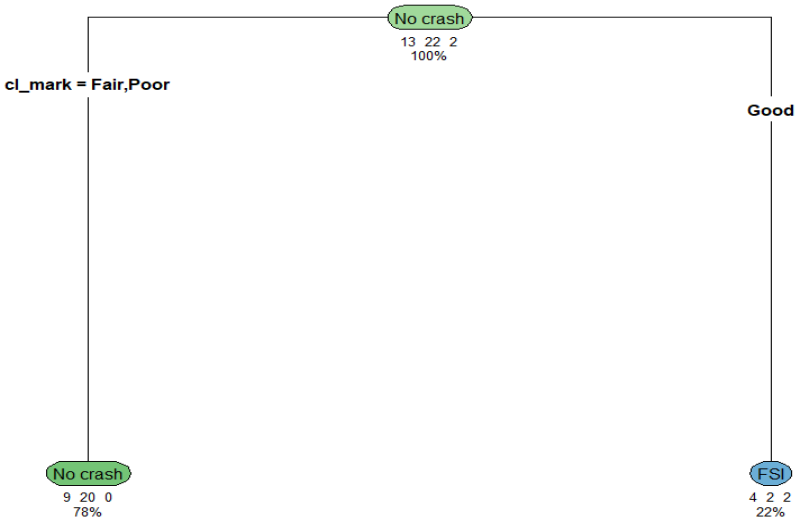

Figure 6: Decision Tree for Cluster 7

4. Conclusion:

The primary objective of this study was to explore road crashes in a group of road segments with highly similar features, hypothesizing that the crash pattern, frequency, and outcomes may be similar for roads with similar environments. Initially, hierarchical clustering was performed on the road geometry features of the road segments after reducing the variance in the features through FAMD. As a result, seven road clusters were identified, and these clusters were further analyzed to assess the crash patterns for each distinct road environment. The study showed that the average number of crashes per ten thousand vehicles is higher when the roads are narrow (in the absence of shoulders) and lower in road segments with graveled or paved shoulders or when the ribbon development level is low. Overall, head-on collisions were the most dominant crashes in the clusters, followed by run-off-road crashes. Pedestrian-related crashes were more common in straight segments, which may be associated with overspeeding. Analyzing the crashes in the clusters only provided information on the frequency and predominant crash types in each road environment type, so further investigation was performed using decision tree analysis to explore the relationship between the conditions of the road safety interventions and the crash outcomes in each cluster.

The results of the decision tree analyses provided insights into how the condition of safety interventions affects crash outcomes. Overall, the condition levels of safety interventions were found to have different relationships with crash outcomes in different road environments. However, some of these relationships went against the conventional belief that better safety intervention conditions make roads safer. These results, therefore, require further investigation before reliable conclusions may be drawn, such as by increasing the size of the dataset or exploring the use of other machine learning algorithms.

This study nonetheless serves as a stepping-stone for future studies to assess the effectiveness of the safety interventions widely used in Nepal. Though these interventions are cheap and common, their effectiveness in reducing crash frequency and severity, and their ability to prevent certain crash types from occurring, have not been assessed properly for the diverse environments along Nepalese roads. The outcomes of this study are therefore of use to road agencies managing highway infrastructure, as they demonstrate how road segments with similar characteristics can be clustered and how the effectiveness of interventions can be assessed considering different road environments. This methodology is believed to be generalizable and may reduce the work effort of road agencies because similar safety interventions can be proposed to segments within a cluster.

Acknowledgements

This research was supported by a scholarship for road asset management from the Japan International Cooperation Agency (JICA).

References

AASHTO (American Association of State Highway and Transportation Officials). (2010). *Highway Safety Manual.* AASHTO.

Bonera, M., Mutti, R., Barabino, B., Guastaroba, G., Mor, A., Archetti, C., . . . Maternini, G. (2022). Identifying clusters and patterns of road crash involving pedestrians and cyclists. A case study on the Province of Brescia (IT). *Transportation Research Procedia 60* (pp. 512-519). Brescia: Elsevier.

Chen, D., Hildreth, J., & Mastin, N. (2019). Determination of IRI Limits and Thresholds for Flexible Pavements. *Journal of Transportation Engineering, Part B: Pavements Vol.145, No.2*.

Federal Highway Administration, U.S. Department of Transportation. (2025, 4 3). *FHWA Highway Safety Programs*. Retrieved from Road Safety Audits (RSA): https://highways.dot.gov/safety/data-analysis-tools/rsa/road-safety-audits-rsa

Federal Highway Administration. (2025, 4 2). *Crash Modification Factors Clearinghouse*. Retrieved from About CMFs: https://cmfclearinghouse.fhwa.dot.gov/about.php

Goel, R., Tiwari, G., Varghese, M., Bhalla, K., Agrawal, G., saini, G., . . . Mohan, D. (2024). *Effectiveness of road safety interventions: An evidence and gap map.* Austin: John Wiley & Sons on behalf of The Campbell Collaboration.

Gupta, M., & Bandyopadhyay, S. (2020). Regulatory and Road Engineering Interventions for Preventing Road Traffic Injuries and Fatalities Among Vulnerable Road Users in Low-and Middle Income Countries: A Systematic Review. *Frontiers in Sustainable Cities*.

Husson, F., Lê, S., & Pagès, J. (2011). *Exploratory Multivariate Analysis by Example Using R.* Boca Raton: Taylor and Francis Group, LLC.

Kassambara, A. (2017). *Practical Guide to Principal Component Methods in R.* STHDA.

Kassambara, A., & Mundt, F. (2020). factoextra: Extract and Visualize the Results of Multivariate Data Analyses.

Le, S., Josse, J., & Husson, F. (2008). FactoMineR: An R Package for Multivariate Analysis. *Journal of Statistical Software 25(1)*, 1-18.

Milborrow, S. (2024). *rpart.plot: Plot rpart Models: An Enhanced Version of plot.rpart. R Package Version 3.1.2*. Retrieved from https://cran.r-project.org/web/packages/rpart.plot/index

PIARC (World Road Association). (2019). *Road Safety Manual- A Guide for Practitioners: The Safe System Approach.* PIARC.

R Core Team. (2022). *R: A Language and Environment for Statistical Computing.* Retrieved from R Foundation for Statistical Computing: https://www.R-project.org/

Silva, P. B., Andrade, M., & Ferreira, S. (2020). Machine learning applied to road safety modeling: A systematic literature review. *Journal of Traffic and Transportation Engineering (English Edition) 2020 7(6)*, 775-790.

Therneau, T., & Atkinson, B. (2013). *Rpart: Recursive Partitioning. R Package Version 4.1-3.* Retrieved from http://CRAN.R-project.org/package=rpart

World Health Organization. (2023, March 6). *Social determinants of health-Safety and Mobility*. Retrieved from Decade of Action for Road Safety 2021-2030: https://www.who.int/teams/social-determinants-of-health/safety-and-mobility/decade-of-action-for-road-safety-2021-2030

Journal on Transportation System and Engineering
ISSN: 3059-9865(Print) 3059-9873(Online)
Vol. 1. Issue 2 (December) 2025: 63-75
DOI: https://doi.org/10.3126/jotse.v1i2.87751

Research Article
Received Date: May 11, 2025
Revised Date: October 10, 2025
Accepted Date: November 15, 2025
Published Date: December 21, 2025

Nepal's National Highway Pavement Optimal Management through Life Cycle Cost Minimization

Manish Man Shakya[a,b*], Kotaro Sasai[c], Felix Obunguta[c], Asanke Adraro Angelo[c], and Kiyoyuki Kaito[d]

[a] *Doctoral Student; Department of Civil Eng., Graduate School of Eng., Osaka University, Suita 2-1, Osaka, Japan*
[b] *Er.; Department of Roads, Ministry of Physical Infrastructure and Transport, Kathmandu, Nepal*
[c] *Specially Appointed Assistant Professor, Department of Civil Eng., Graduate School of Eng., Osaka University, Suita 2-1, Osaka, Japan*
[d] *Prof.; Department of Civil Eng., Division of Global Architecture, Graduate School of Eng., Osaka University, Suita 2-1, Osaka, Japan*

Abstract

Nepal's National Highway (NH) network is vital to meet the country's transportation demands and socio-economic development. However, a big fraction of NH network faces rapid deterioration due to increasing traffic, harsh climatic conditions and inefficient maintenance planning. This study presents a data driven framework for road management planning, utilizing the Markov hazard model for pavement deterioration for two major pavement types – Surface Dressing (SD) and Asphalt Concrete (AC) across two major climatic conditions - Tropical Savannah (Aw) and Temperate Climate with Dry winter (Cw). The framework incorporates Surface Distress Index (SDI), traffic volumes, and life cycle cost analysis (LCCA) to evaluate the long-term effectiveness of various maintenance and upgrading strategies using the Markov model. The result shows that Combined Maintenance (CM) which involves integration of routine and recurrent maintenance activities significantly delay pavement deterioration process, reducing periodic maintenance costs and improving road network performance. Upgrading SD pavement with higher deterioration rates to AC proves highly effective for high traffic roads, improving durability and overall network condition. The study evaluates several maintenance and upgrading strategies, highlighting the balance between LCC and the good to fair road percentage, enabling road agencies to set performance targets within budget constraints. The findings provide valuable information for policymakers and road agencies, emphasizing the importance of proactive, data-driven decision-making in road maintenance planning. Future research could explore indirect benefits, such as vehicle operating cost savings and reduced travel times, to further enhance the decision-making framework.

Keywords: Markov pavement deterioration model; Markov pavement repair model; combined maintenance; life cycle maintenance cost; cost-condition relation.

1. Introduction

Nepal's road network plays a critical role in the country's economic development and daily connectivity. The 16th Five Year Plan of Nepal (2024/25 to 2028/29) has set ambitious targets to be achieved during this period, indicating significant growth over the next five years. This plan also focuses on the importance of developing mechanisms for road maintenance, ensuring organized and systematic maintenance work, mobilizing and managing resources (National Planning Commission, 2024). Despite these attempts in policy-level efforts, a significant portion of the National Highways (NH) faces rapid deterioration due to increasing traffic volumes, diverse climatic conditions, and inefficiencies in maintenance planning. This deterioration lowers road quality, leading to higher maintenance costs and vehicle operating costs (VOC). Present maintenance practices in Nepal are yearly and short term, it lacks a robust, data-driven framework, which supports the decision makers and road agencies to set the acceptable standards of network performance considering the associated cost factor.

* Corresponding Author's *E-mail address:* 28j22803@gmail.com

A key contribution of this study is the integration of Markov hazard model and repair models with climatic and mixed traffic conditions in developing countries to access pavement deterioration considering data base of Nepal's NH. This research evaluates the performance of two major pavement types—Surface Dressing (SD) and Asphalt Concrete (AC)—across two distinct climatic zones: Tropical Savannah (Aw) and Temperate Dry Winter (Cw) which are classified by modifying Köppen - Geiger (KG) climate classification systems to delineate the realistic climatic condition of Nepal. Additionally, the study introduces a cost-condition trade-off framework, which quantifies the relationship between life cycle cost analysis (LCC) and good to fair road percentages (Surface Distress Index (SDI) value ≤ 3). This framework evaluates various maintenance and upgrading strategies over a 24-year horizon, enabling road agencies to make informed decisions based on budget limitations and performance goals. These contributions provide practical tools for data-driven, cost-effective road maintenance planning in resource-constrained settings, with broad applicability to other developing countries facing similar challenges.

2. Literature Review

Referring to AASHTO pavement management guidelines, four types of models are commonly used to predict future pavement conditions: deterministic, probabilistic, Bayesian, and subjective (or expert-based) models (American Association of State Highway and Transportation Officials, 2012). The Markov hazard model, a probabilistic approach, derived from survival analysis principles, which are widely used in infrastructure management, has proven effective in predicting pavement deterioration by considering transition probabilities between condition states (Tsuda et al., 2006). Pavement deterioration process is progressive and depends on several factors such as traffic, environment, construction methods etc. and this probabilistic approach enables infrastructure managers to account for uncertainties in the deterioration process. The deterioration states are categorized into several ranks based on inspection results and their deterioration rates are estimated by the hazard models. The expected deterioration path, which characterizes the average deterioration process, is derived from the Markov transition probabilities. The transitions between condition states are governed by life expectancy computations for the life expectancy in each condition state and the total life expectancy is the sum of life expectancy in each condition state (Tony Lancaster, 1990).

However the Markov pavement repair process is a deterministic, demonstrating its ability to model the transition of pavement condition states after the repair activities (Angelo et al., 2023). In the context of Nepal, the SDI serves as a performance indicator to assess pavement conditions, adapted from the World Bank's recommendations (Department of Roads (DOR) & MRCU, 1995; Ministry of Works and Transport Department of Roads, 1995). The DOR strategy emphasizes on execution of planned maintenance comprising a program of routine, recurrent and periodic maintenance activities for roads that are in a maintainable condition The integrated routine and recurrent maintenance activities is termed as combined maintenance (CM) and the associated cost is the CM cost. (DOR, 2014; Ministry of Works and Transport Department of Roads, 1995).

The life cycle cost of a road infrastructure is defined as the aggregation of initial costs and discounted future costs, such as maintenance cost, user cost, reconstruction, rehabilitation, restoring and resurfacing costs, over the life of the road project. (Federal Highway Administration (FHWA), 2024).

3. Methodology

This study presents a comprehensive, data-driven framework for road maintenance planning. Utilizing Markov hazard (Kobayashi et al., 2012) and Markov repair models (Angelo et al., 2023), the framework is outlined in Figure-1, examines pavement deterioration and evaluates maintenance strategies for two major pavement types: SD and AC. The methodology is divided into four main stages: data collection from road agency, data processing, model description, and analysis of repair strategies. Life cycle cost and predicted road condition is computed for various strategies. The unit cost for combined maintenance (CM), periodic maintenance (PM) and upgrading (U) is acquired from the IARMP 2022-23 national allocation summary. In developing countries like Nepal, roads have been constructed and upgraded by various road agencies and foreign donors, it is very difficult to define the initial construction cost. Instead, in this study LCC excludes the initial construction cost and focuses on the CM cost, PM cost and upgrading cost over the analysis period y.

3.1 Data Collection

The data utilized in this study were collected from periodic inspection reports recorded in the road register of the Highway Management Information System (HMIS) unit at DOR. This dataset includes information on pavement conditions and traffic volumes. DOR considers surface distress of pavement as an indicator to represent the pavement condition. The traffic survey involved traffic counting and analysis from 160 stations which are at

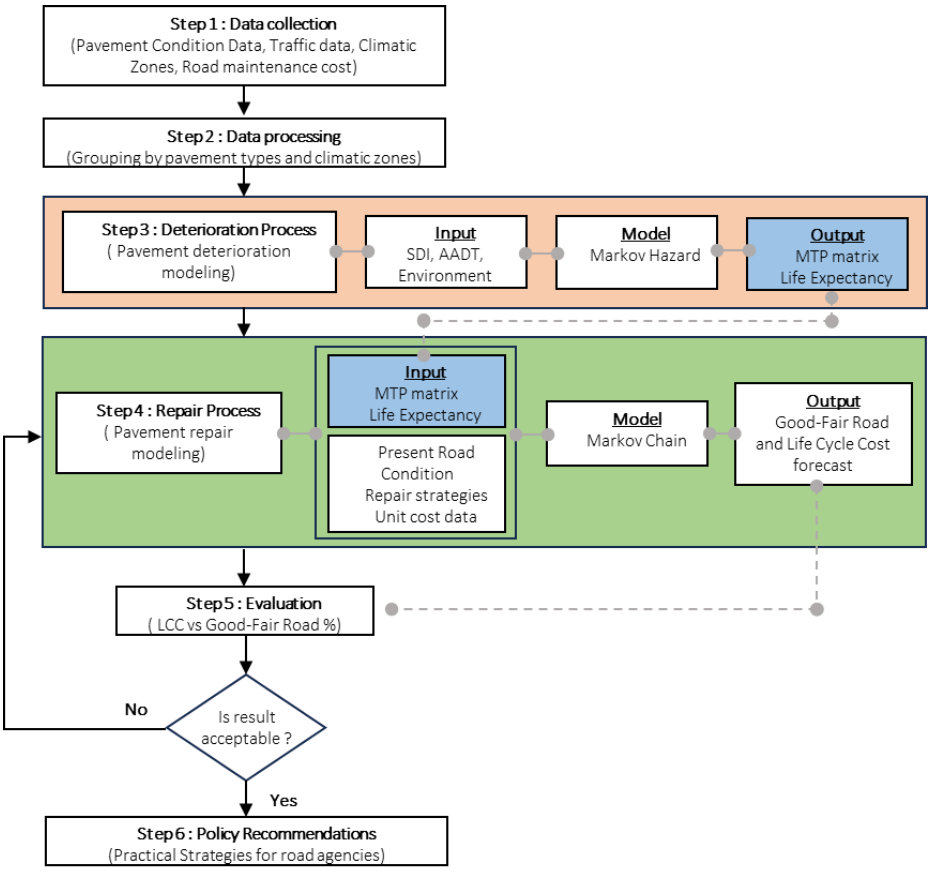

the major nodal locations on the strategic road network of Nepal. The traffic data is represented by the average annual daily traffic (AADT) expressed in Passenger Car Unit (PCU). These are used as an explanatory variable in the hazard model.

Figure 1. Pavement deterioration modelling and maintenance decision making framework.

3.1.1 Pavement Performance Indicator: Surface Distress Index (SDI)

SDI is a measurement of pavement distress which accounts for major defects such as wide cracks, scabbing, rutting, potholes, exposed base, long edge break, corrugations and minor defects such as narrow crack, line crack, bleeding, short edge break etc. Highway engineers and pavement experts conduct visual surveys and record the severity of the distress for each 1 km road section. This data is used to calculate the SDI value for the surveyed road section. In context of Nepal, SDI is expressed in rating scale from 0 to 5. The rating 0 indicates a pavement surface without any defects, whereas a rating of 5 indicates the maximum possible deterioration. This method adopted by DOR is a simplified procedure recommended by the World Bank which has been modified to suit the conditions in Nepal and the need for DOR.

Detail procedure for the determination of SDI value for each road link is described in "Road Pavement Management, MRCU" (Department of Roads (DOR) & MRCU, 1995). To implement the Markov hazard model, the condition ratings presented in Table 1 were used to assess the pavement conditions based on the SDI values. Condition state 1 denotes the best condition, whereas condition state 6 represents the worst pavement condition.

Table 1. Road condition based on SDI

SDI Value	Condition	Incidence of minor defects	Incidence of major defects	Condition State
0	Good	None	None	1
1	Moderate	1 to 200 sq.m. per km.	1 occurrence	2
2	Satisfactory	< 50% of the area	2 to 4 occurrences	3
3	Fair	≥ 50%	< 30% of area	4
4	Poor		30% or potholes and base exposed < 20% of the area	5
5	Bad		Potholes and exposed base = 20% of the area	6

3.2 Data Processing

The national highway network is group into different climatic zones as defined by New Climatic Classification of Nepal, Ramchandra Karki et al. This study identifies the five major types of climatic zones in Nepal by modifying Köppen - Geiger (KG) climate classification systems to delineate the realistic climatic condition of Nepal (Karki et al., 2016). Figure 2 shows the national highway sections under different climatic zones as defined by modified KG climatic classification system.

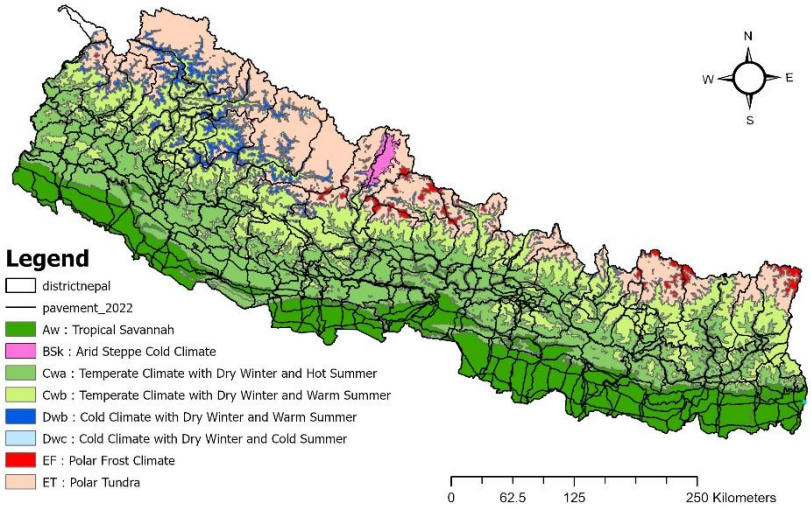

Figure 2. National highway network under different climatic zones.

3.3 Model Description

3.3.1 Markov pavement deterioration model

Markov pavement deterioration hazard model is derived from the survival analysis principle which is widely used for modelling infrastructure deterioration. It is a probabilistic model based on inspection data and taking uncertainty into account to determine the future conditions of the infrastructure. In this model the pavement deterioration process is progressive and depends on several factors such as traffic, environment, construction methods etc. The deterioration process is described by transition probabilities. The deterioration states are categorized into several ranks based on inspection results and their deterioration rates are estimated by the hazard models. For the application of the Markov hazard model, the following assumptions must hold true. Assumptions of the Markov model are : (a) there have been no maintenance and repair activities imposed and no measurement errors during the inspection period and (b) the deterioration process of the road section occurs naturally as its condition state getting worsens over the year (Tsuda et al., 2006).

The Markov transition probability is used to represent the uncertain transition of the condition state during two points in time. If the condition state observed at time $\tau_A = i$, a Markov transition probability, given a condition state $h(\tau_A) = i$ observed at time τ, defines the probability that the condition state at a future time τ_B will change to $h(\tau_B) = j$, that is

$$Prob[h(\tau_B) = j \mid h(\tau_A) = i] = \pi_{ij} \tag{1}$$

The multistage exponential hazard model has been defined as

$$\pi_{ij} = \sum_{k=i}^{j} \prod_{m=i}^{k-1} \frac{\theta_m}{\theta_m - \theta_k} \prod_{m=k}^{j-1} \frac{\theta_m}{\theta_{m+1} - \theta_k} exp(-\theta_k Z) \tag{2}$$

where,

$$\prod_{m=i}^{k-1} \frac{\theta_m}{\theta_m - \theta_k} = 1, at\ (k \le i+1)\ and \prod_{m=k}^{j-1} \frac{\theta_m}{\theta_{m+1} - \theta_k} = 1\ at\ (k \ge j)$$

The hazard rate θ_i ($i = 1, 2, \dots, J-1$) is defined as the function of explanatory variable and the unknown parameter beta ($\boldsymbol{\beta}_i$). The unknown parameter β_i ($i = 1, 2, \dots, J-1$) is determined using the Bayesian estimation method. For detailed explanation of Bayesian method for estimation it is recommended to refer [Han D et al.] (Han et al., 2014). The Markov transition probabilities matrix can be defined by using the transition probabilities between each pair of condition states (i, j) as

$$\prod = \left(\begin{bmatrix} \pi_{11} & \cdots & \pi_{1J} \\ \vdots & \ddots & \vdots \\ 0 & \cdots & \pi_{JJ} \end{bmatrix} \right) \tag{3}$$

where,

$\pi_{ij} \ge 0$

$\pi_{ij} = 0$ (when i > j) since the model does not consider the repair.

$\sum_{\mathrm{j}=1}^{\mathrm{J}} \pi_{ij} = 1$

The final state of deterioration is expressed by condition state J, which remains an absorbing state in the Markov chain if no repair is carried out. In this case $\pi_{JJ} = 1$.

However, in the model, the hazard rate θ_i^k($i = 1, 2, \dots, J-1$) for the inspection sample $k = (1, \dots, K)$ is considered to change in relation to explanatory variables $\mathbf{x^k}$ and the unknown parameter $\beta_i = (\beta_{i,1,} \dots, \beta_{i,M})$ such that :

$$\theta_i^k = exp(\boldsymbol{\beta_{i,1}} + \boldsymbol{\beta_{i,2}} \boldsymbol{x_2^k} + \dots, \boldsymbol{\beta_{i,M}} \boldsymbol{x_M^k}) \tag{4}$$

$$\theta_i^k = f(\boldsymbol{x^k}: \boldsymbol{\beta_i'}) \tag{5}$$

3.3.2 Output of the deterioration prediction model.

Using the periodic inspection data, the model provides two major outputs. First is the Markov Transition Probability (MTP) matrix, which is primary output for forecasting the pavement deterioration process. The MTP matrix $\prod(Z)$ represents the probability of condition transition within a specific time interval Z. Therefore, the MTP matrix $\prod(nZ)$ after n interval can express in terms of the MTP matrix $\prod(Z)$ as:

$$\prod(nZ) = \{\prod(Z)\}^n \tag{6}$$

The second output is the life expectancy (LE) of each condition state which is then defined by means of survival function (Lancaster 1990). The life expectancy of the condition state i of the inspection sample k, LE_i^k can be expressed as :

$$LE_i^k = \int_0^\infty exp(-\theta_i^k y_i^k) dy_i^k = \frac{1}{\theta_i^k} \tag{7}$$

$$LE_i^J = \sum_{i=1}^{J-1} LE_i^k \tag{8}$$

The life expectancy from condition state i to J can be defined by the sum of life expectancies, and the deterioration curve can be attained by their relations. For more details, it is suggested to refer to Tsuda et al., 2006 (Tsuda et al., 2006).

3.3.3 Markov pavement repair model

The Markov pavement repair process is a deterministic process. The Markov repair or maintenance process has the following assumptions: (a) the repair interval and the repair type are decided by the road agency such as DOR. And (b) the repair process improves the condition state from worse to better (Angelo et al., 2023). For formulating the repair process, the transition from condition state i to j after the repair type is defined by r_{ij}.

$$r_{ij} = \begin{cases} 1, for\ \eta(i) = j \\ 0, for\ \eta(i) \neq j \end{cases} \quad (9)$$

In equation 9, $\eta(i)$ denotes the action vector such that $\eta = [\eta(1), \dots, \eta(J)]$. The action vector indicates the change in condition state due to repair action. The repair action $\eta(i)$ stands for the transition from i to state $\eta(i)$. For example if $\eta(i) = j$ indicates the state transition from i to j due to repair action. If the repair is carried out for the road section, the condition state changes to a better condition state, otherwise it remains in its current state. Therefore, the Markov transition probability matrix for repair is expressed as R(η):

$$R(\eta) = \left(\begin{bmatrix} r_{11} & \cdots & r_{1J} \\ \vdots & \ddots & \vdots \\ r_{J1} & \cdots & r_{JJ} \end{bmatrix} \right) \quad (10)$$

If we suppose a road network with pavement condition state vector $S(t_r)$, at inspection time t_r will change its state to $S(\tilde{t}_r)$ after the repair assuming that the repair action is carried out after the inspection.

$$S(\tilde{t}_r) = S(t_r) * R(\eta) \quad (11)$$

The deterioration and repair process are continuous process, the condition state before and after the repair at the n^{th} inspection can be formulated using the initial condition state vector $S(t_0)$, the deterioration transition probability matrix Π and the repair transition probability matrix R(η) as follows:

$$S(\tilde{t}_n) = S(t_0)[\ \Pi . R(\eta)]^{n-1} . \Pi \quad (12)$$

3.3.4 Life Cycle Cost (LCC)

The DOR strategy emphasizes on execution of planned maintenance comprising a program of routine, recurrent and periodic maintenance activities for roads that are in a maintainable condition (DOR, 2014; Ministry of Works and Transport Department of Roads, 1995). The life cycle cost (LCC) of a road infrastructure is defined as the aggregation of initial costs and discounted future costs, such as maintenance cost, user cost, reconstruction, rehabilitation, restoring and resurfacing costs, over the life of the road project (Federal Highway Administration (FHWA), 2024). In context of DOR, the integrated annual cost for routine and recurrent maintenance activities is termed as combined maintenance cost (CM). Thus, LCC is sum of the initial construction cost, CM and periodic maintenance cost (PM) over the analysis period y years as shown in Figure 2. In the context of developing countries like Nepal, roads have been constructed and upgraded over time by various road agencies and foreign donor partners. In this situation, it is very difficult to define the initial construction cost. Focusing on the maintenance cost of the road infrastructure, in this study Life Cycle Cost (LCC) is defined as the sum of CM and PM.

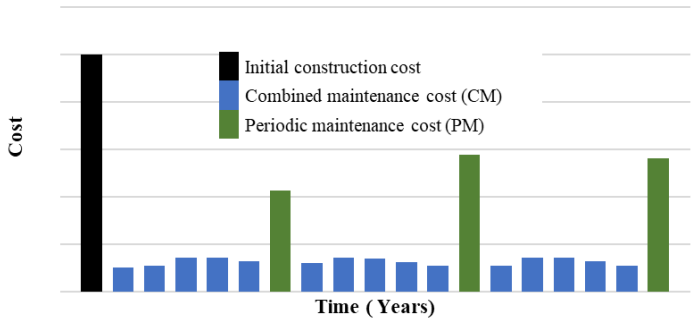

Figure 2. Life cycle cost for road infrastructure.

$$LCC = IC + \sum_{i=1}^{y}[CM_i + PM_i] \quad (13)$$

$$LCC_{Total} = LCC_{SD} + LCC_{AC} \quad (14)$$

3.4 Road maintenance activities

To keep the SRN in a serviceable condition DOR undertakes pavement maintenance activities. These maintenance based on the frequency can be classified into five categories (Department of Roads (DOR), 1994).

i. Routine Maintenance: This category of maintenance is labor intensive and involves activities to keep the road pavement and roadside structures clean and functional. The details of the activities are explained in "Length workers Related Handbook" published by DOR (Department of Roads (DOR), 2006).
ii. Recurrent Maintenance: This category of maintenance is done using hand tools, medium to heavy equipment for repairing potholes, patching, repairing edges and shoulders, crack sealing etc. The interval of recurrent maintenance is 6 months to 2 years. The CM is defined as the integration of routine maintenance and recurrent maintenance activities.
iii. Periodic Maintenance: This category of maintenance refers to the planned cyclic maintenance activity for resealing or resurfacing bituminous surfaced roads at an interval of 6 to 10 years taking account of their present condition, age, geographic location, traffic and their strategic importance. The details procedure for periodic maintenance are explained in " Standard Procedure for Periodic Maintenance Planning" published by DOR (Department of Roads (DOR), 2005).
iv. Emergency Maintenance: This category of maintenance is needed to relate to immediate actions during road closure to keep the traffic movement in SRN. This involves removal of debris and other obstacles; placement of warning signs and diversion works.
v. Preventative Maintenance: This maintenance involves maintenance activities such as slope netting, river training and bank protection works, bioengineering works etc. to preserve the road assets.

4. Empirical Study

For the empirical study the actual pavement inspection data for SRN of Nepal was employed. These road networks have two major types of pavement (a) surface dressing (SD) and (b) Asphalt Concrete (AC). The condition state is defined in Table 1. The data consists of two condition state – the initial condition state corresponds to the road condition from inspection in 2021 and the final condition corresponding to inspection in 2022 for every 1 km road section. The inspection interval is 1 year, and the traffic count is taken as the explanatory variable. The total 4024 data sets are grouped based on the climatic zone as defined by modified Köppen–Geiger climate classification systems. Table 2 shows the inspection data set in different climatic groups.

Table 2. Road section

S.No	Climatic Classification	Inspection data set (Actual)	Inspection data set (Satisfying Markov criteria)
1	Tropical Savannah (Aw)	1701	1669
2	Arid Steppe cold climate (Bsk)	-	-
3	Temperate climate with dry winter and hot summer (Cwa)	1863	1849
4	Temperate climate with dry winter and warm summer (Cwb)	506	506
5	Cold climate with dry winter and warm summer (Dwb)	1	-
6	Cold climate with dry winter and cold summer (Dwc)	-	-
7	Polar Tundra climate (ET)	-	-
8	Polar Frost climate (EF)	-	-

For this study, pavement deterioration was analyzed considering two major pavement types, SD and AC alongside two predominant climatic zones: Tropical Savannah (Aw) and Temperate Climate with Dry winter (Cw).

5. Results and Discussions

5.1.1 Average Markov transition probability matrix

The MTP matrix for each sample is estimated by using the exponential hazard model and the average MTP matric is determined. The MTP matrix for SD and AC pavement is presented in Table 3 and 4.

Table 3. MTP matrix from estimation results – SD

Rating	1	2	3	4	5	6
1	0.29	0.29	0.32	0.08	0.02	0.00
2	-	0.19	0.54	0.20	0.06	0.02
3	-	-	0.51	0.31	0.13	0.06
4	-	-	-	0.41	0.34	0.25
5	-	-	-	-	0.36	0.64
6	-	-	-	-	-	1.00

Table 4. MTP matrix from estimation results – AC

Rating	1	2	3	4	5	6
1	0.43	0.27	0.25	0.04	0.01	0.00
2	-	0.23	0.57	0.16	0.04	0.00
3	-	-	0.61	0.28	0.10	0.02
4	-	-	-	0.51	0.38	0.10
5	-	-	-	-	0.64	0.36
6	-	-	-	-	-	1.00

5.1.2 Life expectancy of pavement under various climatic conditions

The hazard rate for each transition is estimated using equation (5). The expected deterioration path, which characterizes the average deterioration process, is derived from the Markov transition probabilities. Considering that pavement deterioration is a progressive process, transitions between condition states are governed by life expectancy computations using equations (7) and (8) for the life expectancy in each condition state and the total life expectancy respectively. The average deterioration process during the life expectancy rating as shown in Figure 3. The results indicate that SD pavements deteriorate faster than the AC pavement in both Aw and Cw climatic zones.

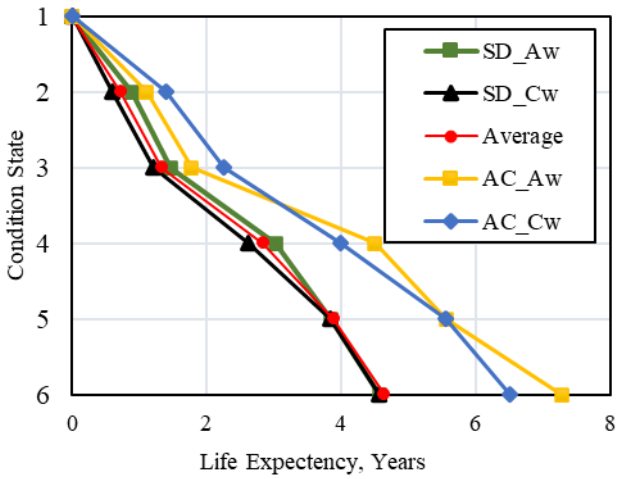

Figure 3. Expected deterioration path of pavement under various climatic conditions

5.1.3 Life expectancy of pavement under various traffic conditions

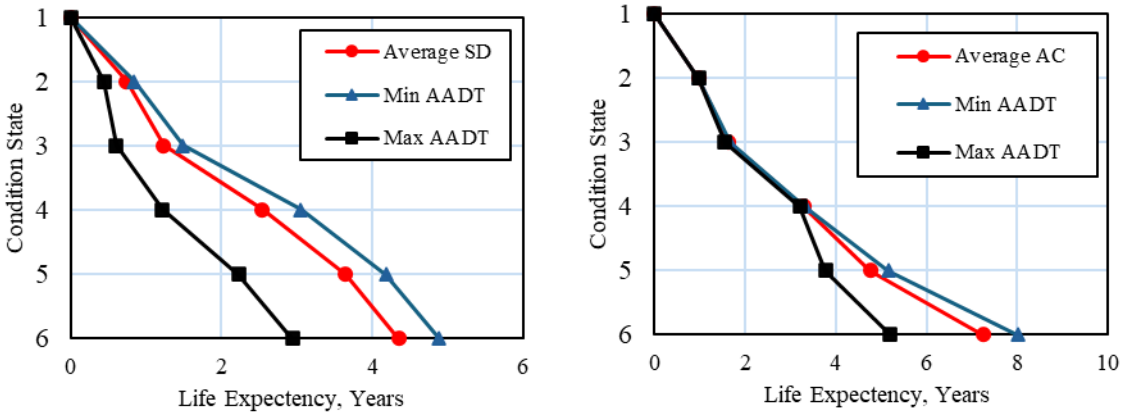

a. b.

Figure 4. Expected deterioration path of pavement under various traffic conditions- a. SD; b. AC

The results of the study for the effect of traffic on SD and AC pavement deterioration are presented in Figure 4. The result indicates that AC pavements demonstrated a higher average life expectancy of 7.25 years, while SD pavements deteriorated more rapidly with an average life expectancy of 4.35 years. The results indicate that traffic has a significant effect on the pavement. With the increase in traffic volume the pavement life is reduced significantly for both SD and AC pavement. The expected deterioration path of SD and AC pavements at minimum and maximum traffic volume is shown in Figure 4 (a) and 4 (b). Figure 4 (a) suggests that the SD pavement with higher traffic volume should be prioritized for upgrading to AC for improving the road condition. Figure 4 (b) indicates that on AC pavements, traffic has deteriorating effect only after it exceeds the fair condition.

5.1.4 Road Condition and associated costs with and without Combined Maintenance

In this study, 100 km of representative NH is considered for simulating the different maintenance strategies. The condition of the road network, represented as the proportion of pavement in each condition state was assessed for SD and AC pavement at the inspection year 2022. The pavement condition state vector for SD and AC pavement was determined as $S\left(t_{0,SD}\right) = (2.3, 3.79, 35.44, 24.74, 12.84, 14.23)$ and $S\left(t_{0,AC}\right) = (0.52, 0.56, 3.29, 1.51, 0.58, 0.20)$ respectively.

The repair actions are described by the repair matrixes. If no maintenance is performed, the road follows a deterioration process as shown in Figure 3 and Figure 4, represented by the identity matrix. Referring to equation (9), the repair action for combined maintenance is defined by $\eta(4) = 2$ indicates the state transition from 4 to 2 due to combined repair action. Based on this, the repair matrix for CM is defined as.

$$R_{CM}(\eta) = \begin{bmatrix} 1 & 0 & 0 & 0 & 0 & 0 \\ 0 & 1 & 0 & 0 & 0 & 0 \\ 0 & 0 & 1 & 0 & 0 & 0 \\ 0 & 1 & 0 & 0 & 0 & 0 \\ 0 & 0 & 0 & 0 & 1 & 0 \\ 0 & 0 & 0 & 0 & 0 & 1 \end{bmatrix} \quad (15)$$

Similarly, when the road pavement is maintainable condition the PM (resealing or overlay) reinstates the pavement to best condition i.e. condition state 1(DOR, 2014; Ministry of Works and Transport Department of Roads, 1995). Therefore, the MTP matrix for repair by PM is defined as:

$$R_{PM}(\eta) = \begin{bmatrix} 1 & 0 & 0 & 0 & 0 & 0 \\ 0 & 1 & 0 & 0 & 0 & 0 \\ 0 & 0 & 1 & 0 & 0 & 0 \\ 0 & 0 & 0 & 1 & 0 & 0 \\ 1 & 0 & 0 & 0 & 0 & 0 \\ 1 & 0 & 0 & 0 & 0 & 0 \end{bmatrix} \quad (16)$$

Combining the two repair strategies PM supplemented by CM, the MTP matrix for repair is defined as:

$$R_{CM+PM}(\eta) = \begin{bmatrix} 1 & 0 & 0 & 0 & 0 & 0 \\ 0 & 1 & 0 & 0 & 0 & 0 \\ 0 & 0 & 1 & 0 & 0 & 0 \\ 0 & 1 & 0 & 0 & 0 & 0 \\ 1 & 0 & 0 & 0 & 0 & 0 \\ 1 & 0 & 0 & 0 & 0 & 0 \end{bmatrix} \quad (17)$$

For applying equation (12) in case of SD pavements, the present pavement condition state vector is given by $S(t_{0,SD})$, the MTP matrix is described in Table 3, and the repair strategies $R(\eta)$ defined in equation (15-17). Similarly, for AC pavement, the present pavement condition state vector is given by $S(t_{0,AC})$, the MTP matrix is described in Table 4, and the repair strategies $R(\eta)$ defined in equation (15-17). The average unit cost for maintenance is acquired from the IARMP 2022-23 national allocation summary. The annual cost for CM and PM of SD and AC pavements are calculated. In Figure 5 the interval period for resealing is assumed to be 6 years and the figure shows the plot of yearly pavement maintenance cost with and without the CM. As shown in Figure 5, yearly CM cost is small compared to the PM cost. By introducing CM every year the PM cost is reduced significantly.

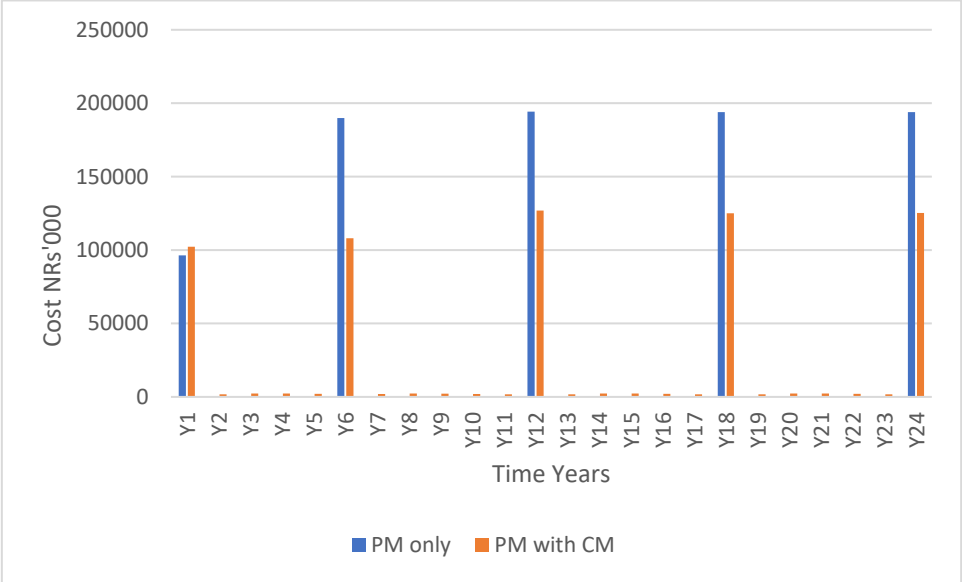

Figure 5. Annual Maintenance Cost for PM only and PM with CM.

Similarly, the associated yearly road maintenance cost for road network (SD pavements at different maintenance interval and AC pavement with 6 year interval) and the road conditions with and without CM are calculated. This yearly road maintenance cost is combined to determine the life cycle cost estimate for 24 years perspective period. Figure 6 illustrates the relationship between the good-fair road condition and the associated cost over different intervals, with and without CM i.e. PM with CM and PM only.

Figure 6 clearly shows that the percentage of good-fair roads increases significantly when combined maintenance is introduced. CM has proved crucial in increasing the service life of the pavement. The red triangles and green dots indicate the serviceable road percentage of road network with PM only and PM with CM respectively. For example, PM at the interval of 5 year, can maintain 22.90% of road network in good-fair condition. For the same interval of PM this percentage is increased to 52.32% when CM is introduced every year. As CM is carried out effectively every year, the service life of road is improved significantly resulting in increased good-fair roads at lower periodic maintenance cost. The red and green lines are the plot of LCC with PM only and PM with CM. This study indicates that at the interval of 5 years the LCC is minimum. The % of good-fair road is increased by 29.42% with reduction of 28.05% LCC. This study suggests that with CM, road conditions are maintained at a much higher percentage with overall lower LCC, suggesting better long-term performance quality.

From Figure 6 it can be inferred that for the study road network with 93.34% SD and 6.66% of AC pavement, the maximum % of serviceable road that can be maintained is 66.54%. This is attained only when the SD pavements

with life expectancy less than the average life expectancy are resealed at the interval of 3 years. This may not be practically feasible with budget and time constraints. The challenge of faster deteriorating pavements can be solved by upgrading the pavement with higher construction standards. In this study the pavements with higher deterioration rates are proposed for upgrading to AC which has comparatively higher life expectancy than SD pavements.

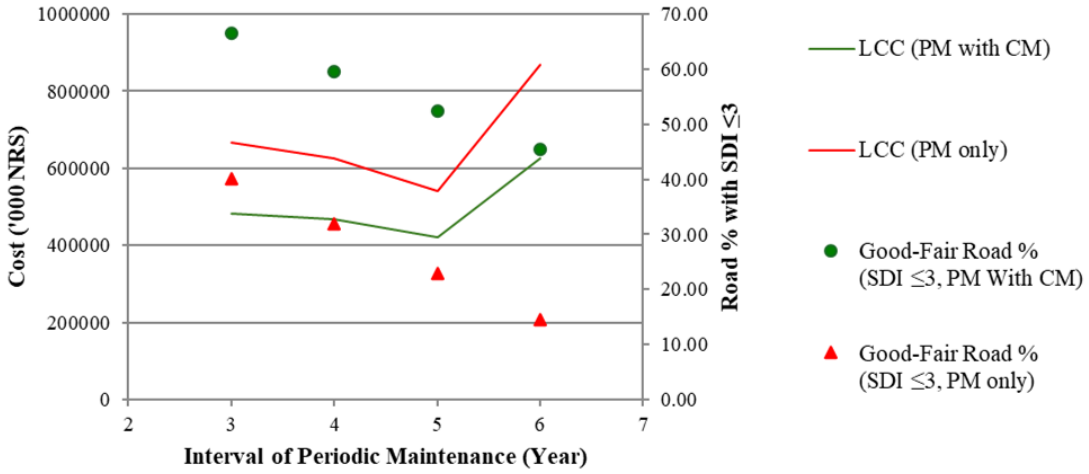

Figure 6. Life Cycle Cost Estimate for maintenance of 100 km road section for 24 years.

As shown in Figure 4 (b) the average life expectancy of AC is 7.25 years. We consider the minimum periodic maintenance interval for AC for this study to be 6 year. The maintenance strategies for upgrading and maintaining SD pavements are summarised in Table 5 .

Table 5. Maintenance Strategies

S.No	Strategy	Description
Strategy 1	U5 C P5	Upgrading 5%, Combined Maintenance and Periodic Maintenance at 5 year interval
Strategy 2	U10 C P5	Upgrading 10%, Combined Maintenance and Periodic Maintenance at 5 year interval
Strategy 3	U15 C P5	Upgrading 15%, Combined Maintenance and Periodic Maintenance at 5 year interval
Strategy 4	U20 C P5	Upgrading 20%, Combined Maintenance and Periodic Maintenance at 5 year interval
Strategy 5	U5 C P4	Upgrading 5%, Combined Maintenance and Periodic Maintenance at 4 year interval
Strategy 6	U10 C P4	Upgrading 10%, Combined Maintenance and Periodic Maintenance at 4 year interval
Strategy 7	U15 C P4	Upgrading 15%, Combined Maintenance and Periodic Maintenance at 4 year interval
Strategy 8	U20 C P4	Upgrading 20%, Combined Maintenance and Periodic Maintenance at 4 year interval
Strategy 9	U5 C P3	Upgrading 5%, Combined Maintenance and Periodic Maintenance at 3 year interval
Strategy 10	U10 C P3	Upgrading 10 %, Combined Maintenance and Periodic Maintenance at 3 year interval
Strategy 11	U15 C P3	Upgrading 15 %, Combined Maintenance and Periodic Maintenance at 3 year interval
Strategy 12	U20 C P3	Upgrading 20 %, Combined Maintenance and Periodic Maintenance at 3 year interval

The yearly maintenance cost for 12 maintenance strategies which upgrade SD pavements with higher deterioration rates to AC, is calculated. The LCC for 24 year perspective period is determined using equation (14). The summary of the results is presented in Figure 7 which shows the relationship between LCC and the good-fair road percentage for the different maintenance strategies

Figure 7 is a plot of cost along the x-axis and road % along the y-axis. In this study the cost is the LCC for maintenance strategy for perspective 24 years and road % is the average good-fair road (SDI $\leq$ 3) percentage. From the results of this study, referring Figure 7 it can be inferred that 52.3 % of good-fair road condition can be achieved at relatively low LCC with strategy 1. Strategies 11 and 12 show the best road conditions but have the higher LCC cost.

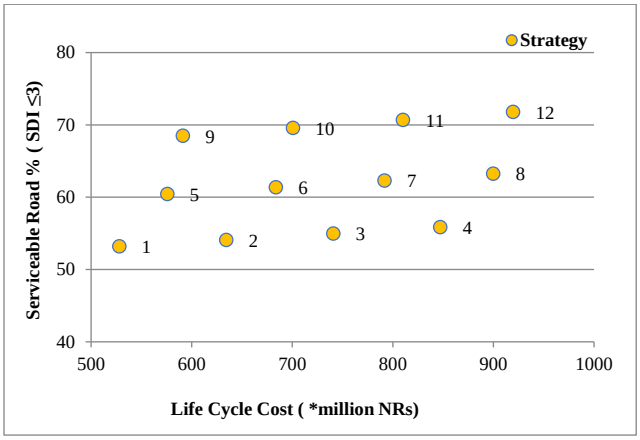

Figure 7. LCC and the serviceable road percentage for the different strategies.

As shown in Figure 7, if a road agency (DOR) sets a minimum acceptance criteria of 60% SRN road network to be in SDI ≤ 3. Based on the data analyzed the following Strategies 5-12 can be chosen. If cost minimization is the primary goal, Strategy 5 would be the most suitable option. However, if the authority is open to a higher investment for significantly better road conditions, Strategy 9 may be preferable, as it offers nearly 8% more roads in good condition for a relatively small additional cost. This extra expenditure can be justified by potential savings in Vehicle Operating Costs (VOC) and travel time due to improved road conditions.

6. Conclusion

This study presents an approach to apply Markov deterioration hazard model to study the deterioration of SD and AC pavement in Tropical Savannah (Aw) and Temperate Climate with Dry Winter (Cw). The study shows that the deterioration process is high with an average life expectancy of 4.22 years. This is similar in both Aw and Cw climate conditions. Similarly, with the increasing traffic volume the life expectancy of SD pavement is significantly reduced which indicates that SD pavements are a cost-effective option, making them suitable for roads with low to medium traffic volumes. On the other hand, AC pavement being superior pavement has higher durability for heavy traffic. Having higher life expectancy, AC can be a better pavement option for upgrading SD pavements with high deterioration rates.

Combined maintenance is a proactive maintenance strategy. The yearly cost is small when compared to periodic resealing cost. The activities during this maintenance process are effective to delay the deterioration process. As shown in Figure 5 and Figure 6, it can be accepted that the combined maintenance is beneficial both in terms of reducing costs and maintaining better pavement performance.

Long term maintenance planning and prioritizing the road sections for upgrading are very important tasks for the road agencies like DOR. The absence of practical guidelines, inadequate maintenance budget and ad hoc practices are valid reasons for poor road network condition of Nepal. A data driven approach can help road agencies make decisions depending on whether the priority is cost savings or maximizing road conditions. This study emphasizes the importance of data-driven decision-making in road maintenance planning. By utilizing cost and road condition data, road agencies can make more improved decisions that are well-supported by road quality outcomes. The results shown in Figure 5 is a clear trade-off between cost and road quality. Better road conditions lead to smoother travel, lower fuel consumption, and fewer vehicle repairs, which could offset the additional cost imposed during upgrading. Additionally, reduced travel times due to better roads could lead to significant economic benefits in terms of increased productivity, faster goods transport, and lower public transportation costs. The findings suggest that adopting a data-driven approach in road maintenance planning can lead to more efficient allocation of resources while ensuring road networks are kept in serviceable condition.

However, this study has some limitations that can be improved in the future studies. The key limitation of this study is the exclusion of the initial construction cost from the LCC analysis. Also, the data set is acquired from two consecutive inspection in 2021 and 2022. Due to the limitation of data in other climatic conditions the study limited to only these two climatic condition Aw and Cw. The traffic growth and the inflation rates are not considered during the perspective period. The direct maintenance cost is only considered for analysis but the indirect benefits,

such as VOC and travel time reductions, to further enhance the decision-making process is not accounted. A separate study on VOC and travel time savings would be necessary to quantify these benefits.

7. References

American Association of State Highway and Transportation Officials. (2012). *Pavement Management Guide*. American Association of State Highway and Transportation Officials, Washington, D.C., USA.

Angelo, A. A., Sasai, K., & Kaito, K. (2023). Safety Integrated Network Level Pavement Maintenance Decision Support Framework as a Practical Solution in Developing Countries: The Case of Addis Ababa, Ethiopia. *Sustainability (Switzerland)*, *15*(11). https://doi.org/10.3390/su15118884

Department of Roads (DOR). (1994). *Definition of Maintenance & Maintenance Activities (Eng)*.

Department of Roads (DOR). (2006). *Lengthworkers_Related_Hand_Book*.

Department of Roads (DOR), M. B. (2005). *Standard Procedure for Periodic Maintenance Planning.* https://www.dor.gov.np/home/publications

Department of Roads (DOR), & MRCU. (1995). *Road Pavement Management Discussion Paper*. https://dor.gov.np/home/publication/general-documents

DOR. (2014). *Departmental policy document strategic road network (SRN) maintenance policy*.

Federal Highway Administration (FHWA). (2024). Life-Cycle Cost Analysis in Pavement Design– Interim Technical Bulletin. Publication No. FHWA-SA-98-079. In *Green Energy and Technology: Vol. Part F2196*. Office of Engineering, Pavement Division. Washington, DC: Federal Highway Administration. https://doi.org/10.1007/978-981-99-9126-6_6

Han, D., Kaito, K., & Kobayashi, K. (2014). Application of Bayesian Estimation Method with Markov Hazard Model to Improve Deterioration Forecasts for Infrastructure Asset Management. *KSCE Journal of Civil Engineering*, *18*(7), 2107–2119. https://doi.org/10.1007/s12205-012-0070-6

Karki, R., Talchabhadel, R., Aalto, J., & Baidya, S. K. (2016). New climatic classification of Nepal. *Theoretical and Applied Climatology*, *125*(3–4), 799–808. https://doi.org/10.1007/s00704-015-1549-0

Kobayashi, K., Kaito, K., & Lethanh, N. (2012). A Bayesian Estimation Method to Improve Deterioration Prediction for Infrastructure System with Markov Chain Model. *International Journal of Architecture, Engineering and Construction*, *1*(1), 1–13. https://doi.org/10.7492/ijaec.2012.001

Ministry of Works and Transport Department of Roads. (1995). *DOR Strategy*.

National Planning Commission. (2024). *16th Five Year Plan of Nepal (2024/25 to 2028/29).*

Tony Lancaster. (1990). *The Econometric Analysis of Transition Data*. Cambridge University Press.

Tsuda, Y., Kaito, K., Aoki, K., & Kobayashi, K. (2006). Estimating Markovian Transition Probabilities for Bridge Deterioration Forecasting. *JSCE*, *23*(2), 241–256.

Journal on Transportation System and Engineering
ISSN: 3059-9865(Print) 3059-9873(Online)
Vol. 1. Issue 2 (December) 2025: 76-83
DOI: https://doi.org/10.3126/jotse.v1i2.87759

Research Article
Received Date: Ma7 29, 2025
Revised Date: October 14, 2025
Accepted Date: November 16, 2025
Published Date: December 21,2025

Rainfall Threshold for Roadside Shallow Landslide in Mid-Himalayan Region of Nepal

Suresh Neupane[1], Netra Prasad Bhandari[2]

School of Science and Engineering, Special Graduate Course on Disaster Mitigation Study, Ehime University, Ehime, Japan.

2 Center for Disaster Management Informatics Research, School of Science and Engineering, Ehime University, Ehime, Japan. Email; - netra.prakash_bhandary.my@ehime-u.ac.jp>

Abstract

Nepal's road transportation infrastructure is primarily dependent on mountain routes, which are severely disrupted by rainfall induced landslides during the monsoon season. An early warning system based on a localized rainfall threshold is essential for disaster risk reduction because slope stabilization is expensive and road protection resources are scarce. This study uses intensity-duration methodologies and statistical analysis of historical rainfall data in the Mid-Himalayan region to ascertain the relationship between the occurrence of landslides and important triggering elements, including rainfall. For the roadside landslide in the Mid-Himalayan region, a local rainfall intensity-duration (I-D) threshold was determined by fitting a power-law equation obtained from 57 landslide events from 2017 to 2024, taking into account lower limitations delineated by quantile regression. The results show that there is a high chance of roadside landslides in the research area starting when there is 1.75 mm of rain per hour for 48 hours. The findings highlight the significance of cumulative antecedent rainfall in landslides and indicate that extended moderate rainfall (>72 hours) considerably adds to slope destabilization. The results show that July and August are the most dangerous months for roadside landslides, with the mid-Himalayan range experiencing the most rainfall and the high Himalayas seeing the least. By integrating this threshold into road infrastructure design and transportation management, authorities may improve disaster preparedness, give timely warnings, and reduce casualties, thereby boosting road network resilience in the mid-Himalaya region.

Keywords: Rainfall threshold; landslide early warning; intensity-duration relationship; climate change

1. Introduction

Among the most destructive geological hazards are landslides, which are especially dangerous in mountainous areas where they can seriously damage transportation networks, infrastructure, and human populations (Chen et al., 2015). Each year, they cause significant economic losses and fatalities, making them the second most consequential geohazard in the world (Azarafza et al., 2018). According to Aziz et al. (2024) and Komadja et al. (2021), landslides often cause extensive environmental damage, traffic disruptions, property loss, and human casualties in areas with delicate geology and heavy rainfall, like the Himalayas. Landslides frequently occur in the tectonically active Himalayan area and are mostly caused by steep slopes, fragile lithological formations, seismic activity, and heavy monsoonal precipitation (Kanungo & Sharma, 2014; Saha & Bera, 2024). More than 90% of rainfall-induced landslides in Nepal, in particular, occur during the monsoon season, which runs from June to September (Harvey et al., 2024). A combination of anthropogenic pressures and natural vulnerabilities increase the frequency and intensity of these catastrophes (Shrestha et al., 2019).

In Nepal's mid-Himalayan area, landslides brought on by rainfall present a serious threat to the road network. Because prolonged or intense rainfall raises pore water pressure and reduces the shear strength of soil materials, these landslides are typically shallow (0.5–2.5 meters deep), with slip surfaces parallel to the slope (Upreti, 1996; Dhital, 2018; Lepore et al., 2013). Several studies have used process-based hydrological models that incorporate soil moisture dynamics (Crozier, 1999) and empirical intensity-duration (I-D) models (e.g., Guzzetti et al., 2007; Caine, 1980) to determine rainfall thresholds for landslide start. I-D models provide useful regional guidance, but they frequently aren't able to capture the intricate subsurface factors that affect slope failure. However, despite its thoroughness,
Corresponding Author's Email Address suresh.n2001@gmail.com

process-based models are less practical for widespread use and necessitate large datasets (Crosta & Frattini, 2017; Aleotti, 2004).

For the purpose of preparing early warning systems and improving catastrophe resilience, precise rainfall threshold estimation is essential, especially for traffic corridors that are vulnerable to slope failures. Different rainfall thresholds for landslide start have been identified by numerous research conducted throughout the Himalayan region. For example, Froehlich et al. (1990) found that shallow landslides might be caused by rainfall of 130–150 mm in a 24-hour period or 180–200 mm over three days in the Darjeeling Himalayas. Kanungo & Sharma (2014) confirmed similar findings in the Uttarakhand region, while Dahal & Hasegawa (2008) postulated an I-D threshold beyond which landslide risk considerably increases in the Nepal Himalaya. These findings highlight the necessity of setting location-specific thresholds that take into consideration regional variations in geology, rainfall patterns, and topography.

The mid-Himalayan region is particularly vulnerable due to its alternating dry and wet phases, with protracted monsoon spells and rare cloudbursts being common triggers for landslides (Harvey et al., 2024; Dahal & Hasegawa, 2008). Climate change is making extreme rainfall events more often, which emphasizes how urgent it is to set localized rainfall thresholds to improve disaster preparedness and infrastructure protection. This area frequently has roadside landslides, which seriously endanger life and property in addition to interfering with mobility. Early warning systems that are both affordable and locally relevant are essential in environments with limited resources.

The empirical relationship between rainfall features and landslide occurrences, specifically the minimal rainfall needed to trigger slope failures, has not been sufficiently characterized for the mid-Himalayan road networks, despite previous efforts. By creating a rainfall intensity-duration (I-D) threshold model based on historical rainfall and landslide data from the mid-Himalayan region and statistically analyzing past precipitation patterns to better understand their impact on landslide initiation and recurrence, this study seeks to close this gap.

2. Study Area

The Kanti Highway (H37), as shown in Figure 1(a), is a strategic road that runs 86 kilometers between Lalitpur Metropolitan City and Hetauda Sub-Metropolitan City. Originally built in 1954 and renamed in 1962 in honor of Queen Kanti, the highway currently serves as the quickest alternate route between Kathmandu and the Nepal-India border. Since its importance for trade and cross-border connectivity grew in the late 1990s, it was formally recognized as a crucial substitute for the Tribhuvan Highway. The 36-kilometer section between Thingan and Tikabhairab is especially vulnerable to shallow landslides brought on by monsoonal rainfall, despite the highway's vital significance. The Upper Siwalik and the Lesser Himalaya are the two main formations that make up the research area's geological framework, as depicted in Figure 1(b). About 4 km of immature, unconsolidated sedimentary rocks, including as mudstone, sandstone, siltstone, and conglomerate, make up the Upper Siwalik zone. These materials are highly weathered and friable, making them particularly vulnerable to erosion and landslide activity. Interbedded boulders and conglomerates, sandstone lenses, and sandy clays in various hues of yellow, brown, and grey are characteristics of the landslide-prone areas of this formation. During times of heavy monsoon rains, these units' mechanical fragility becomes crucial, frequently leading to slope failures.

On the other hand, the Lesser Himalaya, which takes up about 32 km of the highway corridor, is made up of a complicated series of sedimentary and metamorphic rocks that range in age from the Precambrian to the Eocene, including slate, phyllite, schist, quartzite, limestone, and dolomite. Because they are worn and foliated, phyllites are particularly vulnerable to sliding. The potential of instability along this section is further increased by karst-prone limestones and fractured quartzites.

The Lesser Himalayan region is home to three main geological groups:

- The Dadeldhura Group is made up of foliated rocks that allow for planar sliding, including granites, schists, and phyllites.
- The Kathmandu Group is distinguished by structurally distorted elements such as dolomite, quartzite, and limestone that have been considerably weakened by Himalayan tectonic processes.
- The Midland Group is made up of a variety of metamorphic and sedimentary rocks that are frequently broken up by granitic masses.

The Ipa Granite, which is close to Ipa Khola, is of special geological interest because of its coarse-grained texture and xenoliths, which provide even more complexity. This corridor is particularly susceptible to rainfall-induced landslides due to its steep terrain, brittle lithology, and active tectonics, which calls for ongoing monitoring and slope stability evaluation.

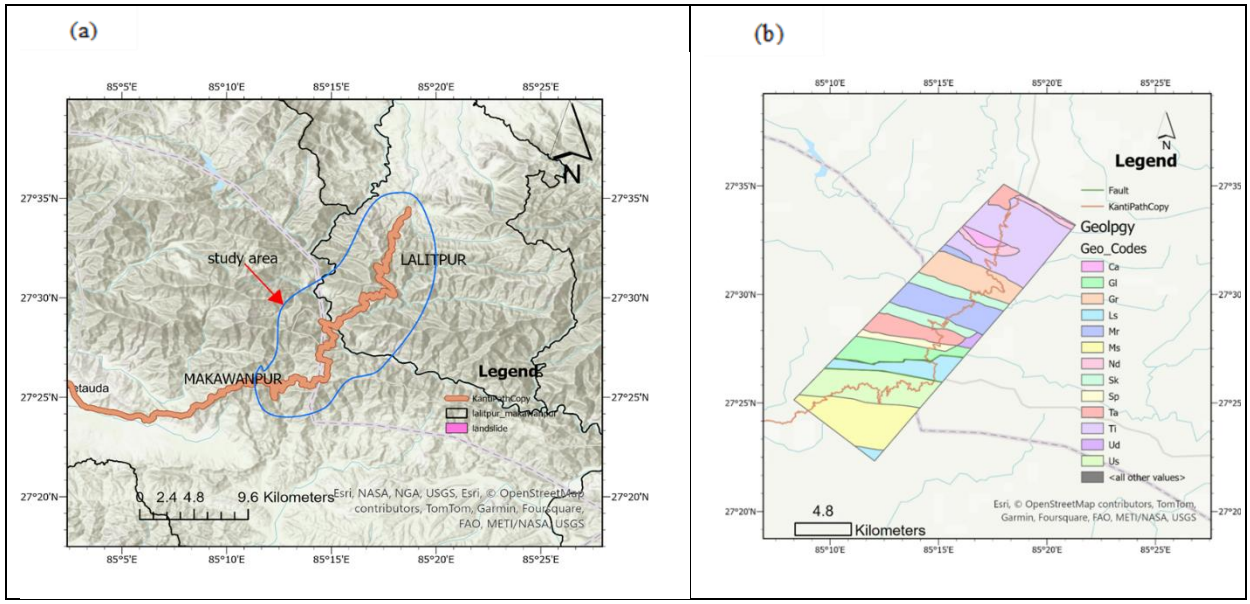

Figure 1: (a) Study area along the Kanti Highway(NH37) showing landslide locations and district boundaries, and (b) Geological map displaying fault and geological formations.

3. Methodology

A comprehensive empirical approach was adopted to establish a localized rainfall threshold for roadside shallow landslides in the mid-Himalayan region. This involves compiling landslide inventory data, analyzing long-term rainfall records, and applying statistical methods to build an empirical intensity–duration (I–D) threshold model.

3.1. Landslide Inventory D

For the years 2017–2024, a comprehensive inventory of 59 rainfall-induced landslides was compiled for the critical 36-km segment of the Kanti National Highway (Thingan–Tikabhairab) in Nepal's Mid-Himalayan region. The database was developed using multiple sources, including daily field reports from the Kanti Highway Project Office, maintenance logs, and personal field records of the first author (who served as Project Manager from 2021 to 2023). Each event was georeferenced and verified through GPS field surveys and cross-checked using Google Earth Pro imagery to ensure spatial accuracy and reliability. Only shallow translational and debris slides that directly affected roadway operations were considered in this analysis.

Among these, two events recorded at Chapagaun station during 2024 showed exceptionally high rainfall intensities (~7.9 mm/hr), corresponding to an extreme rainfall episode. These were statistically identified as outliers and therefore excluded from the regression analysis, though retained in the total landslide inventory count for completeness.

3.2 Rainfall Data Collection and Processing

Rainfall data for this study were obtained from the Department of Hydrology and Meteorology (DHM) of Nepal, which maintains a national network of meteorological stations. Within the study corridor, four nearest stations — Makwanpur Gadi, Lele, Chapagaun, and Khokana — were selected based on spatial proximity and record

completeness. The dataset spans 35 years (1990–2024), with Lele and Khokana stations providing data from 1994 and 1992, respectively.

DHM records daily rainfall at 8:45 AM local time, representing the total precipitation for the preceding 24-hour period. For each documented landslide, event-based rainfall was extracted from the nearest station using spatial correlation in GIS. Since the available DHM dataset consists mainly of daily rainfall totals, a daily-to-hourly conversion was necessary to estimate shorter rainfall durations required for intensity–duration (I–D) analysis.

The empirical relationship developed by Shakya (2002), also adopted by Dahal and Hasegawa (2008), was applied to derive estimated rainfall for any duration (t, in hours) from the 24-hour recorded total (P_{24}, in mm), as shown in Equation (1):

$$\frac{P_t}{P_{24}} = sin\ sin\ \left(\frac{\pi t}{48}\right)^{0.4727} \qquad (1)$$

Where, P_t = estimated rainfall for the duration t (mm),
P_{24} = observed 24-hour total rainfall (mm).
This conversion allowed estimation of rainfall intensity (mm/hr) and duration (hr) for each landslide-triggering event when high-resolution (hourly) data were unavailable.
It is acknowledged that this method may introduce minor bias in intensity estimation because it assumes a uniform rainfall distribution within the 24 hours. However, it remains a practical and widely accepted approach in data-scarce Himalayan environments, enabling consistent comparison of rainfall thresholds across multiple stations and timeframes.

Subsequent statistical analyses were performed using Microsoft Excel and Python, employing descriptive statistics, pivot tables, and analytical libraries to assess spatio-temporal variability, seasonal distribution, and rainfall–landslide relationships within the study area.

3.3 Rainfall Intensity-Duration (I-D) Threshold Method

To define rainfall thresholds for landslide initiation, the intensity–duration (I–D) threshold method was applied—one of the most widely used empirical approaches in landslide hazard assessment (Guzzetti et al., 2007). Earlier studies (Caine, 1980; Chien-Yuan, 2005) relied on manual fitting techniques to determine threshold boundaries. However, recent advancements employ mathematical and statistical models for more objective estimation.

Among these, the quantile regression approach was chosen for its robustness in defining lower threshold boundaries in data-scarce environments. Additional methods referenced include Bayesian inference (Guzzetti et al., 2007) and frequentist analysis (Brunetti et al., 2010).

In this study, the rainfall threshold curve is modeled using a power-law relationship, expressed as:

$$I = \propto D^{-\beta} \qquad (2)$$

where I = rainfall intensity (mm/hr), D = duration (hr). α and β are empirical regression coefficients determined from curve fitting
A rainfall event was classified as landslide-triggering if the daily precipitation equaled or exceeded 2 mm, consistent with threshold standards adopted by ICIMOD and DHM. The rainfall event was considered to continue until the daily total dropped below this threshold. The event window, used to calculate the mean rainfall intensity and duration, varied based on site-specific conditions. To ensure accuracy, the nearest rainfall station to each landslide location was identified using GIS spatial analysis, facilitating precise correlation of meteorological data with recorded slope failure events.

4. **Results and Discussions**

4.1 Analysis of Rainfall Data

Analyzing rainfall patterns is crucial for water resource management, disaster preparedness, and landslide risk assessment in the mid-Himalayan region. The annual and monthly rainfall data from four meteorological stations, Makwanpur Gadi, Lele, Chapagaun, and Khokana were analyzed for the period 1990 to 2024, and the descriptive statistical analysis for annual rainfall was done and summarized in *Table 1*. Among the four stations, Makwanpur Gadi recorded the highest average annual rainfall of 2472.1 mm, with the maximum recorded in 1991 (3746.2 mm) and the minimum in 2010 (1221.4 mm). Lele station had an average annual rainfall of 1688.76 mm, with the highest in 2002 (2349.5 mm) and lowest in 2017 (1038.7 mm). Similarly, Chapagaun station recorded an average of 1304.88 mm, with the highest in 2011 (1758.9 mm) and the lowest in 2015 (771.2 mm). Khokana station showed an average of 1306.31 mm, with the maximum in 2002 (1941.2 mm) and the minimum in 2009 (889.6 mm).

Table 1: Descriptive statics for annual rainfall of the study area

Station	Count	Mean	Percentage of Total Rainfall (PTR)	Minimum (Min)	Maximum (Max)
Makwanpur Gadi	35	2472.11	37.79	1221.40	3746.20
Lele	31	1688.77	22.86	1038.70	2349.50
Chapagaun	35	1304.89	19.95	771.20	1758.90
Khokana	34	1306.31	19.40	889.60	1941.20
Total	135		100.00		

The monthly rainfall distribution for the study area is shown in *Table 2*, displays variations in monthly rainfall from 1990 to 2024 across four stations (Lele, Chapagaun, Khokana, and Makwanpur Gadi). The analysis indicates significant seasonal variation, with the highest rainfall occurring during the monsoon months (June–September) and the lowest rainfall observed in the winter months (November–February). Rainfall is minimal from January to May, with a gradual increase beginning in April. The peak rainfall occurs in July, which coincides with the monsoon season. After September, rainfall starts to decline, reaching its lowest levels in November and December. July experiences the maximum rainfall across all stations. The trends of maximum average monthly rainfall patterns show in decreasing order concerning station from Makwanpur Gadi (702.87 mm), Lele (479.36 mm), Chapagaun (367.71 mm), and Khokana (339.51 mm). Shrestha et al. (2012) studied the climate change and precipitation trend in Nepal and reported that monsoon rainfall has become more erratic, with intense but short-duration rainfall events increasing and observed higher rainfall in mid-Himalayan region. Rainfall shows significant fluctuations from year to year in the study area in 1993,2002,2013,2019 and 2024 the study area experienced higher than average rainfall, which is influenced by monsoon variability. Loo et al.(2015) examines the impact of climate change on monsoon seasonality and rainfall variability in Southeast Asia, highlighting a westward shift of the Indian summer monsoon and since the 1970s, increasing global temperatures have correlated with anomalous precipitation patterns, leading to intensified flooding, infrastructure damage, and food security risks in the region.

Table 2: Descriptive statics for average monthly rainfall data of the study area

Month	Count	Mean	Percentage of Total Rainfall (PTR)	Minimum (Min)	Maximum (Max)
Jan	35	19.40	1.14	0.00	82.51
Feb	35	23.46	1.38	0.00	93.68
Mar	35	30.24	1.78	0.00	84.65
Apr	35	54.53	3.20	0.93	125.55
May	35	125.21	7.35	52.90	241.28
June	35	254.98	14.97	78.68	548.53
Jul	35	474.43	27.85	242.87	950.98
Aug	35	403.60	23.69	264.85	621.53
Sep	35	241.53	14.18	105.95	513.92
Oct	35	61.77	3.63	4.00	219.35
Nov	35	5.04	0.30	0.00	68.80
Dec	35	9.34	0.55	0.00	120.70
Total	420	141.96	100.00	-	-

4.3 Rainfall Intensity – Duration (I-D) Thresholds

This study aims to estimate the rainfall thresholds that trigger roadside landslides in Nepal's Mid-Himalayan region, particularly along the Kanti Highway (H37). The mean rainfall intensity and corresponding duration for each landslide event were calculated using historical data from 2017 to 2024. For each landslide, the event onset was identified based on a daily rainfall of ≥ 2 mm, consistent with DHM and ICIMOD standards. Rainfall data from the nearest rain-gauge station to each landslide site were used to determine both rainfall intensity and duration. The resulting intensity–duration (I–D) values were plotted on a logarithmic scale, where the x-axis represents rainfall duration (hours) and the y-axis represents rainfall intensity (mm/hr). The observed rainfall intensity ranged from 0.5 to 3.8 mm/hr, with durations spanning 47.25 to 308 hours.

To determine the critical threshold boundary above which landslides are likely to occur, a 2nd-percentile quantile regression was applied to the dataset. This regression curve was fitted using a nonlinear power-law model in Python and is expressed as in Equation 3:

$$I = 19.37 * D^{-0.6215} \qquad (3)$$

Where, I= rainfall intensity (mm/hr.), and

D= rainfall duration (hours)

The regression line defines the lower-boundary threshold separating triggering and non-triggering rainfall events. The findings suggest that a rainfall intensity of about 19.37 mm/hr sustained for one hour or 1.75 mm/hr over 48 hours is sufficient to initiate slope failures, while rainfall below 1.10 mm/hr sustained for more than 100 hours can also induce landslides when antecedent moisture is high. Prolonged rainfall exceeding 12 days may trigger failures even under low-intensity conditions (> 0.55 mm/hr).

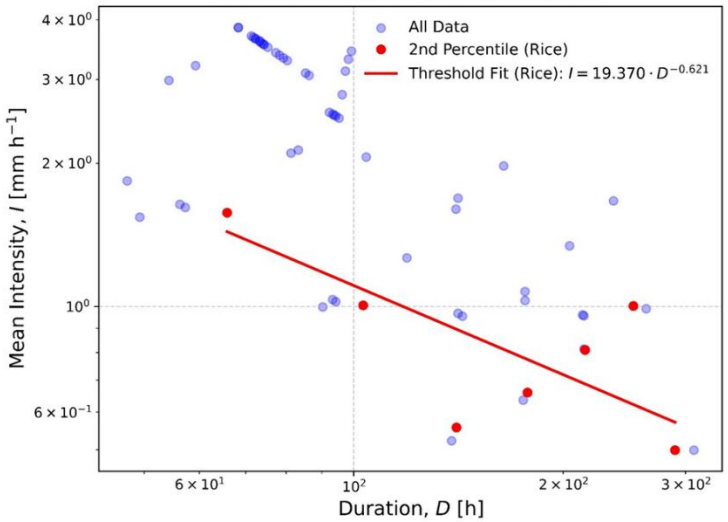

Figure 2: Rainfall intensity-duration scatter plot with 2nd percentile regression threshold curve for roadside landslide in mid-Himalayan region

These results highlight the dual influence of both short-duration, high-intensity and long-duration, low-intensity rainfall on slope instability. The quantile-regression approach applied in this study provides a more objective threshold estimation and reduces uncertainties common in data-scarce regions. The derived threshold ($I = 19.37 \times D^{-0.6215}$) is considerably lower than the regional threshold proposed by Dahal and Hasegawa (2008) for the Nepal Himalaya ($I = 73.90 \times D^{-0.79}$), but higher than the local threshold reported by Saha and Bera (2024) for the Garhwal Himalaya ($I = 1.38 \times D^{-0.126}$). This difference reflects the combined effect of the Mid-Himalayan corridor's more humid climate, moderate slope gradients, and prolonged monsoon episodes compared to the drier Garhwal region and the broader Nepal Himalaya averages.

While the limited number of data points introduces some uncertainty in defining the exact rainfall threshold, this can be minimized by incorporating additional rainfall events (Teja et al., 2019). The study emphasizes the importance of integrating local I–D thresholds with geological and hydrological factors to enhance the accuracy of landslide prediction and risk-assessment strategies for long-duration rainfall events.

4. Conclusion

This study presents an extensive overview of rainfall variability and its impact in inducing roadside landslides along the Kanti Highway (H37) in Nepal's mid-Himalayan region. The study determines a region-specific rainfall intensity–duration (I–D) threshold for shallow landslides by combining long-term rainfall data (1990–2024) from four meteorological stations in the study area with a methodically assembled landslide inventory (2017–2024). The monsoon season, which occurs in July and August, contributes the most rainfall, according to descriptive statistical analysis, which also show significant interannual and seasonal variation. The Makwanpur Gadi station routinely had the highest yearly precipitation of all the stations examined, demonstrating the regional heterogeneity impacted by topography and climate.

The critical conditions for landslide occurrence are effectively characterized by the power-law relationship of the intensity–duration (I–D) threshold established in this study. The findings indicate that a rainfall intensity of 19.37 mm/hr sustained for one hour is sufficient to trigger slope failures. Similarly, prolonged rainfall events, such as 1.75 mm/hr over 48 hours or 0.55 mm/hr over 12 days, are also capable of inducing landslides in the study area. These threshold values highlight the dual influence of both short-duration, high-intensity and long-duration, low-intensity rainfall events on slope instability.

The results highlight the significance of combining I–D thresholds with geological, hydrological, and antecedent soil moisture conditions, even if the work admits several limitations, such as sample size restrictions and the lack of high-resolution hydro-meteorological data. Improving the precision of landslide prediction models requires this kind of integration. Overall, this study supports the use of multi-parameter early warning systems and emphasizes the critical role that localized rainfall thresholds play in determining landslide risk. In Nepal's mountainous areas, these insights are essential for improving the resilience of crucial transportation infrastructure and fortifying readiness for disasters.

5. References

Aleotti, P. (2004). A warning system for rainfall-induced shallow failures. *Engineering Geology*, *73*(3), 247–265. https://doi.org/10.1016/j.enggeo.2004.01.007

Azarafza, M., Ghazifard, A., Akgün, H., & Asghari-Kaljahi, E. (2018). Landslide susceptibility assessment of South Pars Special Zone, southwest Iran. *Environmental Earth Sciences*, *77*(24), 805. https://doi.org/10.1007/s12665-018-7978-1

Aziz, K., Mir, R. A., & Ansari, A. (2024). Precision modeling of slope stability for optimal landslide risk mitigation in Ramban road cut slopes, Jammu and Kashmir (J&K) India. *Modeling Earth Systems and Environment*, *10*(3), 3101–3117. https://doi.org/10.1007/s40808-023-01949-2

Brunetti, S., Rossi, M., Luciani, S. ., Valigi, D., Guzzetti, F., Maria, T., & Peruccacci. (2010). Rainfall thresholds for the possible occurrence of landslides in Italy. *Natural Hazards and Earth System Sciences*, *10*(3), 447–458. https://doi.org/10.5194/nhess-10-447-2010

Caine, N. (1980). The Rainfall Intensity: Duration Control of Shallow Landslides and Debris Flows. *Geografiska Annaler. Series A, Physical Geography*, *62*(1/2), 23. https://doi.org/10.2307/520449

Crosta, G., & Frattini, P. (2017). *Rainfall thresholds for triggering soil slips and debris flow*. *January 2001*.

Crozier, M. (1999). Prediction of rainfall-triggered landslides: a test of the Antecedent Water Status Model. *Earth Surface Processes and Landforms*, *24*(9), 825–833. https://doi.org/10.1002/(sici)1096-9837(199908)24:9<825::aid-esp14>3.0.co;2-m

Dahal, R. K., & Hasegawa, S. (2008). Representative rainfall thresholds for landslides in the Nepal Himalaya. *Geomorphology*, *100*(3–4), 429–443. https://doi.org/10.1016/j.geomorph.2008.01.014

Dhital, M. R. (2018). *Landslides and debris flows of 19-21 July 1993 in the Agra Khola watershed of Central Nepal*. *July 2000*. https://doi.org/10.3126/jngs.v21i0.32143

Guzzetti, F., Peruccacci, S., Rossi, M., & Stark, C. P. (2007). Rainfall thresholds for the initiation of landslides in central and southern Europe. *Meteorology and Atmospheric Physics*, *98*(3–4), 239–267. https://doi.org/10.1007/s00703-007-0262-7

Harvey, E. L., Kincey, M. E., Rosser, N. J., Gadtaula, A., Collins, E., Densmore, A. L., Dunant, A., Oven, K. J., Arrell, K., Basyal, G. K., Dhital, M. R., Robinson, T. R., Van Wyk de Vries, M., Paudyal, S., Pujara, D. S., & Shrestha, R. (2024). Review of landslide inventories for Nepal between 2010 and 2021 reveals data gaps in global landslide hotspot. *Natural Hazards*, *0123456789*. https://doi.org/10.1007/s11069-024-07013-1

Kanungo, D. P., & Sharma, S. (2014). Rainfall thresholds for prediction of shallow landslides around Chamoli-Joshimath region, Garhwal Himalayas, India. *Landslides*, *11*(4), 629–638. https://doi.org/10.1007/s10346-013-0438-9

Komadja, G. C., Pradhan, S. P., Oluwasegun, A. D., Roul, A. R., Stanislas, T. T., Laïbi, R. A., Adebayo, B., & Onwualu, A. P. (2021). Geotechnical and geological investigation of slope stability of a section of road cut

debris-slopes along NH-7, Uttarakhand, India. *Results in Engineering*, *10*(April). https://doi.org/10.1016/j.rineng.2021.100227

Lepore, E., Noto, L., Sivandran, G., Bras, R. L., & Arnone, C. (2013). Physically based modeling of rainfall-triggered landslides: a case study in the Luquillo forest, Puerto Rico. *Hydrology and Earth System Sciences*, *17*(9), 3371–3387. https://doi.org/10.5194/hess-17-3371-2013

Loo, Y. Y., Billa, L., & Singh, A. (2015). Effect of climate change on seasonal monsoon in Asia and its impact on the variability of monsoon rainfall in Southeast Asia. In *Geoscience Frontiers* (Vol. 6, Issue 6, pp. 817–823). https://doi.org/10.1016/j.gsf.2014.02.009

Saha, S., & Bera, B. (2024). Rainfall threshold for prediction of shallow landslides in the Garhwal Himalaya, India. *Geosystems and Geoenvironment*, *3*(3), 100285. https://doi.org/10.1016/j.geogeo.2024.100285

Shrestha, U. B., Shrestha, A. M., Aryal, S., Shrestha, S., Gautam, M. S., & Ojha, H. (2019). Climate change in Nepal: a comprehensive analysis of instrumental data and people's perceptions. *Climatic Change*, *154*(3–4), 315–334. https://doi.org/10.1007/s10584-019-02418-5

Teja, A., Satyam, N., Surya;, & Togaru, D. (2019). Determination of rainfall thresholds for landslide prediction using an algorithm-based approach: Case study in the Darjeeling Himalayas, India. *Geosciences*, *9*(7), 302-NA. https://doi.org/10.3390/geosciences9070302

Upreti, B. N. (1996). Stratigraphy of the western Nepal Lesser Himalaya: A synthesis. *Journal of Nepal Geological Society*, *13*(0 SE-Articles), 11–28. https://doi.org/10.3126/jngs.v13i0.32127

Journal on Transportation System and Engineering
ISSN: 3059-9865(Print) 3059-9873(Online)
Vol. 1. Issue 2 (December) 2025: 84-92
DOI: https://doi.org/10.3126/jotse.v1i2.87760

Research Article
Received Date: May 26, 2025
Revised Date: October 28, 2025
Accepted Date: November 19, 2025
Published Date: December 21,2025

Review of Arbitration Practices in Construction Projects: A Case Study of Highway Projects in Nepal

Chhabi Lal Paudel[1]

[1]*Department of Roads, Ministry of Physical Infrastructure and Transport, Government of Nepal, Kathmandu*

Abstract

Arbitration is a commonly adopted method for resolving disputes in construction contracts. The arbitration process and dispute settlement mechanisms are governed by legal provisions, contractual agreements between the parties, and procedures established by international institutions. However, in Nepal's highway projects, the dispute resolution process has proven to be inefficient, adversely affecting contract management and overall project governance. To address this issue, this research examines existing arbitration practices, claim issues, and decision-making approaches using data and arbitration decisions from highway projects implemented under the Department of Roads. The study analyses 93 ongoing and completed arbitration cases to identify prevailing trends through qualitative and descriptive statistical analysis and investigates five detailed case study projects to explore current practices, issues, contractual and legal grounds for decision-making, and the effectiveness of dispute resolution in highway construction. The case studies are thoroughly reviewed using existing documentation available within the Department of Roads, providing valuable insights for project managers, planners, and contract administrators in identifying key dispute areas and arbitration decision approaches. Furthermore, this research contributes to understanding the trends, issues, and decision patterns in contractual claim resolution. Its findings support improvements in construction contract management by highlighting critical dispute areas that can be mitigated through proactive planning, effective arbitration handling, using standardised forms of contracts and capacity enhancement of stakeholders involved in resolving construction disputes.

Key Words: *Construction Arbitration; Road Projects; Dispute; Contract Management; Dispute Resolution.*

1. Introduction:

Arbitration is a dispute resolution mechanism that addresses conflicts arising between contracting parties. It serves as an alternative to litigation in the construction industry, offering several advantages such as the freedom to select arbitrators, cost-effectiveness, flexibility in handling both legal and technical disputes, confidentiality, and timely resolution of contractual conflicts (Stephenson, 2003). Construction contracts explicitly include arbitration clauses as part of standard contract documents that are widely adopted in civil infrastructure projects worldwide, enabling professionals to manage and resolve contractual disputes efficiently (Beaumont, 2019). The standard contract forms developed by the International Federation of Consulting Engineers (FIDIC) pinpointed the key risk factors that can be settled through the use of standardised mechanisms such as Dispute Avoidance and Adjudication Board (DAAB) and Arbitration (FIDIC, 2017). Those standard forms of contracts are used by public institutions all around the world in executing infrastructure construction projects. The implementation of arbitration is governed by the legal framework of each country and the procedural rules established by international institutions (Voser, 2011; Caron & Caplan, 2013). Although arbitration proceedings may vary across jurisdictions, the core objective remains consistent to resolve contractual disputes effectively and within a reasonable timeframe. Despite existing legal provisions in Nepal's construction sector, arbitration decisions often face limited acceptance from both employers and contractors, frequently escalating to litigation. This situation raises concerns regarding the effectiveness of contract management and the overall efficiency of dispute resolution mechanisms (Mishra & Aithal, 2022). Institutional effectiveness and good governance are critical factors that support foreign direct investment (FDI) in middle- and low-income countries (Walsh & Yu, 2010). Therefore, enhancing institutional capacity and governance in construction contract administration can significantly contribute to improving dispute resolution practices and sustaining FDI inflows in Nepal's infrastructure sector.

Corresponding Author's Email Address chhabipaudel@gmail.com

Furthermore, the decisions made by arbitration, dispute boards, or adjudication panels in the Nepal's highway infrastructure sector during the fiscal year 2022 highlight the current efficiency level of dispute resolution mechanisms. Out of 120 registered disputes, only 41 were resolved through the contractual dispute resolution process facilitated by the Nepal Council of Arbitration (NEPCA) (NEPCA, 2024). However, most arbitration decisions were subsequently referred to the courts, where proceedings often extend from several months to years before reaching a final judgment. An analysis of arbitration case records from the Department of Roads over the past decade revealed that arbitration awards requiring Employers to compensate Contractors amounted to approximately NPR 2,740 million (DoR, 2024). These findings indicate that the existing arbitration practices in highway infrastructure projects are not functioning effectively in resolving disputes between contracting parties. Accordingly, the primary objective of this research is to review the current dispute resolution practices in highway infrastructure implementation management to identify prevailing procedures, issues, legal provisions, and potential improvements for enhancing future decision-making. The contribution of this study lies in identifying weaknesses in the existing system and providing insights into addressing major sources of disputes in future contracts through the adoption of appropriate mitigation measures and improved dispute resolution mechanisms.

2. Data Collection

The road and bridge construction contracts implemented by the Department of Roads (DoR) that were under arbitration or litigation were collected from the Legal and Dispute Management Unit of the DoR. Among the 93 disputes under DoR since from last 10 years; 40 of which had already been decided through arbitration, while the remaining cases were still under process. For the resolved cases, most disputes were subsequently referred to the High Court for further adjudication. Due to confidentiality requirements, the names of the contractors involved have not been disclosed in this research.

Using data from both ongoing and completed arbitration cases related to road and bridge contracts, the study examined trends in arbitration and litigation within DoR projects. Based on this analysis, five representative case study projects were selected and analyzed in detail to identify key arbitration issues, arbitrators' decisions, and the current status of disputes. These case studies encompassed variations in financing arrangements, infrastructure types, bidding methods, arbitration proceedings, contracting approaches, and the frequency of contractors' involvement in arbitration.

The findings from the qualitative and quantitative data analysis and case studies provide valuable insights and a way forward for improving the effectiveness of arbitration in highway construction projects, thereby enhancing overall construction contract management.

3. Methodology

To conduct this research, both ongoing and completed arbitration cases were analyzed using qualitative data analysis approach, quantitative data analysis through descriptive statistics and detailed case studies of selected contracts. Initially, 93 ongoing disputes under the Department of Roads (DoR) were examined through qualitative and statistical analysis to identify issues, decision approach, legal and procedural shortcomings and trends in dispute occurrence across different project environments, including financing arrangements, infrastructure types, contracting methods, company structures, and bidding approaches. Those analyses provided an overview of issues, legal and contractual gaps and the prevailing patterns in dispute resolution within highway construction contracts.

In addition, five arbitration case study projects were selected representing diverse financing arrangements, infrastructure categories, bidding methods, and contracting approaches. These case studies were examined based on arbitration proceeding documents, policy documentation and arbitration awards and court decisions on contractual claims available in the Legal and Dispute Management Unit of the DoR. Each case was thoroughly analyzed qualitatively to understand the nature of disputes, their current status, the basis of claims, and their implications for construction contract management.

4. Results and Discussion

4.1 Results of Quantitative Analysis

Firstly, the results obtained from the descriptive statistical analysis were examined and interpreted. The findings revealed that among the 93 ongoing and completed arbitration cases, 13 contractors were involved in five or more disputes during contract execution (Figure 1). Notably, two of these contractors accounted for approximately 30% of the total arbitration cases in highway projects, while four contractors collectively represented about 45% of all ongoing and completed arbitration matters.

These results indicate that a limited number of construction companies are repeatedly involved in arbitration, suggesting a pattern of recurring contractual disputes. Such information provides valuable insight into the claim and litigation history of contractors, which serves as an important evaluation criterion during the bidding and contractor selection process.

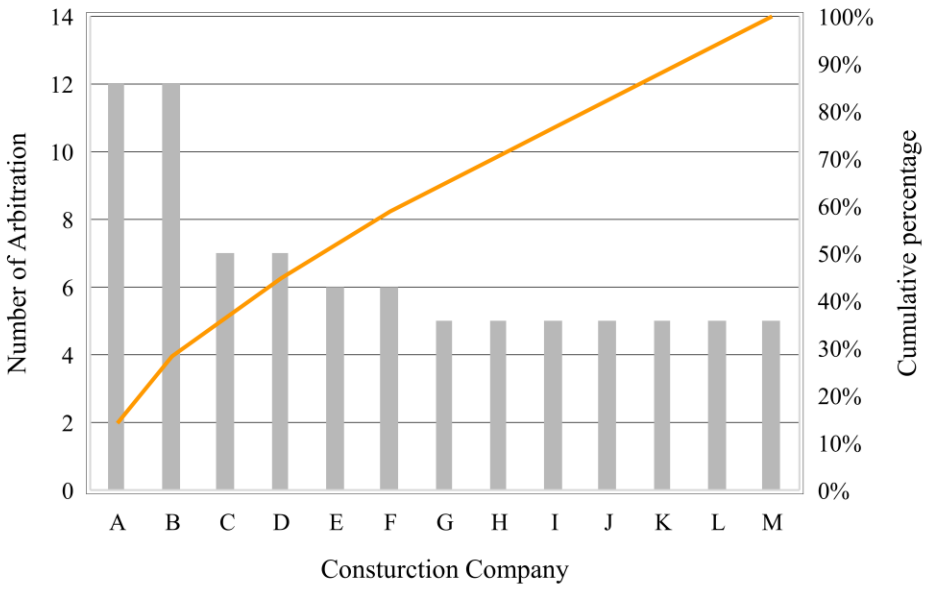

Figure 1. Construction Companies actively involved in Arbitration and litigation in highway projects

Figure 2 illustrates the time delays experienced in projects due to prolonged arbitration decisions and subsequent litigation. In most cases, projects have already exceeded ten years and remain under litigation, despite having been decided through arbitration. This situation raises concerns about the effectiveness of dispute resolution mechanisms, which are intended to provide timely and cost-effective remedies for contractual issues arising during project implementation (Stephenson, 2003). Such inefficiencies not only undermine the performance of institutional mechanisms but also erode credibility in both local and international markets. Consequently, they have a direct and indirect impact on the foreign investment climate within a country's infrastructure construction sector (Wang et. al, 2021). These findings highlight the need for a more efficient contract management environment that enables smooth project execution without hindering the performance of contracting parties or compromising potential project benefits.

Figure 3 illustrates various project management environments within Nepal's highway infrastructure sector, highlighting the occurrence of arbitration cases under specific project conditions. The analysis revealed that road contracts financed by the Government of Nepal (GoN) and executed through joint venture arrangements among contractors experienced a higher frequency of arbitration and litigation. This suggests that GoN-funded projects are

more susceptible to contract management challenges such as delays, site possession and clearance issues, termination disputes, and financial management problems compared to projects financed by foreign development partners.

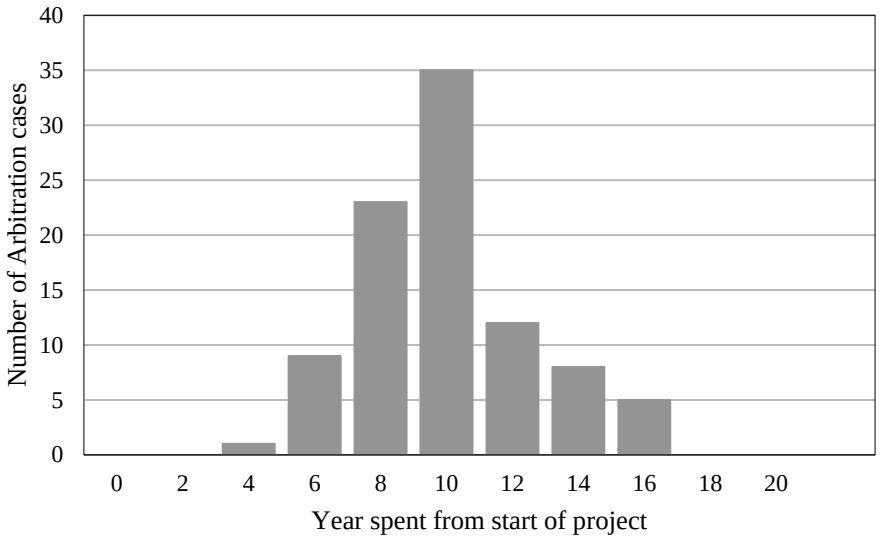

Figure 2. Time spent by contracting parties on Arbitration and litigation

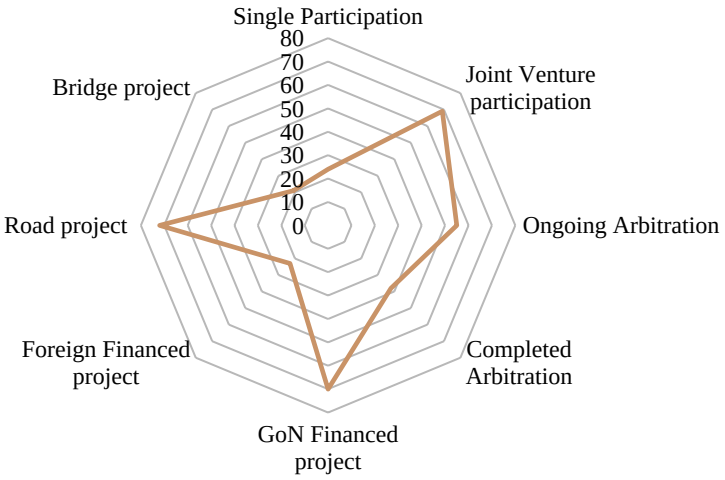

Figure 3. Arbitration and litigation issues in a varying project environment

Similarly, bridge contracts exhibited relatively fewer arbitration and litigation cases among the studied projects. Moreover, contracts involving joint participation of contractors showed a greater tendency toward arbitration than those executed by single contractors. These variations across contract management environments provide insights into the current landscape of contractual disputes, serving as a foundation for further analysis of the underlying causes in

specific project contexts. Accordingly, the subsequent section presents detailed case studies aimed at identifying key dispute issues and proposing improvements for future contract document formulation.

4.2 Results of Qualitative Analysis

The completed arbitration decisions and ongoing cases were qualitatively reviewed with a focus on key aspects such as the nature of disputes, analytical approaches adopted by arbitration panels, relevant contractual provisions, defence documents submitted by Employers and Contractors, court rulings on claims, and the legal references used during arbitration proceedings. Additionally, the qualitative assessment examined how different project management environments characterised by variations in financing mechanisms, contracting methods, infrastructure types, contractor participation, and arbitration procedures addressed contractual disputes.

The content analysis identified the project time extension, termination of contracts, exceptional events and design-related issues as major issues of disputes. Furthermore, the review of arbitration awards, policy documents, and project management contexts highlighted the importance of effective project planning and capacity development for both contracting parties and arbitrators involved in the arbitration and decision-making process. The recurring themes and keywords identified from document reviews further confirmed weaknesses in contract management practices, particularly in the effective settlement of contractual disputes.

4.3 Results of Arbitration Case Studies

The selected arbitration cases representing different project environments were thoroughly examined to identify the key issues underlying each dispute. This analysis was conducted by reviewing the claim documents submitted by the claimants and the corresponding defence documents provided by the respondents. The major disputable issues in each project, along with the remedies determined through arbitration proceedings, were analysed to provide insights into how disputes arise, their resolution status, and potential strategies for improving future dispute management through arbitration. Furthermore, this case study analysis within the highway infrastructure sector contributes to identifying practical mitigation measures aimed at minimising contractual disputes during the early stages of project implementation.

4.3.1 Project 1

The first case involved a bridge construction project financed by the Government of Nepal (GoN) and administered by the Division Road Office. The contract was awarded to a joint venture construction company through a National Competitive Bidding (NCB) process. Arbitration proceedings were conducted under the Nepal Council of Arbitration (NEPCA) rules in accordance with the Arbitration Act of Nepal. The contractor initiated arbitration, raising several issues, including wrongful termination of the contract, encashment of the performance bond, non-payment of the remaining contract amount, compensation for loss of profit, costs associated with idle equipment and manpower, bank commission for security bonds, court proceeding fees, and insurance premiums.

Initially, the contractor issued a notice of termination citing the employer's default, followed by a subsequent termination notice from the employer alleging the contractor's default. The arbitration panel determined that the contractor's termination was valid, concluding that the employer had failed to fulfil its contractual obligations, and accordingly rejected the employer's later termination. The panel further ruled that the employer's termination was unlawful and directed compensation to the contractor, including payment of the outstanding contract amount.

As the arbitration decision was unfavourable to the employer, the employer challenged the award in the High Court, alleging that the arbitrators had exceeded their authority and violated contractual provisions. The High Court, however, upheld the arbitration award and instructed its implementation. Subsequently, the employer appealed to the Supreme Court seeking to overturn the High Court's decision. The project, which commenced in 2018, remains unresolved to date. This case exemplifies the inefficiency of the dispute resolution process and raises serious concerns regarding the performance of contracting parties and the effectiveness of current contract management and dispute settlement practices.

4.3.2 Project 2

The second case involved a road construction project financed by the Government of Nepal (GoN) and administered by the Division Road Office. The overall project environment and arbitration procedures were similar to those in Project 1, with minor differences in the claims presented. In this case, the contractor initiated arbitration, citing non-payment of the final bill, failure to issue the Taking Over Certificate, non-release of the performance bond, compensation for time extension and prolongation costs, and release of retention money with applicable interest. The contractor's claims encompassed both monetary compensation and contractual relief.

Out of the five claims submitted, the arbitration panel accepted three and rejected two. Dissatisfied with the outcome, the Employer appealed to the High Court, arguing that the arbitrators had exceeded their authority and violated the terms of the contract. The project, which commenced in 2013, remains unresolved, reflecting continued inefficiencies in the dispute resolution process within construction contracts.

The issues raised in this case primarily relate to contract management deficiencies that could have been effectively addressed by the employer during project execution to reduce compensation costs. Claims associated with time extension and prolongation could be minimised through proactive planning, timely decision-making, and improved resource management throughout the project lifecycle.

4.3.3 Project 3

The third case study involved a road construction project financed by a foreign development partner and implemented under the Road Improvement and Development Project Office. The contract was awarded to a national–international joint venture through an International Competitive Bidding (ICB) process. Arbitration proceedings were conducted in accordance with the Nepal Council of Arbitration (NEPCA) rules and the Arbitration Act of Nepal.

The contractor raised several dispute issues, including claims for prolongation costs due to contract period extensions, delayed payment interest, compensation for rate revision by the Engineer, compensation for road damage caused by overloaded vehicles during the defect liability period, and payment for additional haulage costs not anticipated during project planning. Compared to the previous two cases, this project presented distinct claims, particularly concerning rate revision compensation and road damage due to heavy vehicle operations.

In this case, the Engineer had revised certain rates to a level below the Engineer's estimate at the time of contract award. The contractor, however, contested this decision and sought payment based on the actual cost conditions prevailing during the variation. Another notable claim involved damage to the constructed road caused by vehicles carrying loads beyond the legal limit, for which the contractor sought compensation.

Upon reviewing all the claims, the arbitration panel ruled in favour of the contractor on all issues except the claim related to road damage caused by overloaded vehicles. Although the project commenced in 2014, the contractual dispute remains unresolved. The employer rejected the arbitration award and referred the matter to the High Court, alleging that the arbitrators had acted beyond their authority, similar to the previous two cases. The High Court upheld the arbitration decision, but the employer again appealed to the Supreme Court, where the case is still pending. This ongoing litigation highlights weaknesses in contract enforcement and demonstrates that the fundamental purpose of arbitration to resolve disputes efficiently within the framework of contractual provisions is not being effectively upheld in international construction contracts in Nepal (Beaumont, 2019).

4.3.4 Project 4

The fourth case study involved a bridge construction project financed by the Government of Nepal (GoN) and administered through a project office established at the construction site. The contract was awarded to a single national contractor through a National Competitive Bidding (NCB) process, and the arbitration proceedings were conducted

under the Nepal Council of Arbitration (NEPCA) rules. The contractor initiated arbitration to seek the settlement of disputes arising during project execution.

The major dispute issues included termination of the contract by the employer, subsequent termination by the contractor, release of the performance bond, payment of outstanding amounts after termination, release of retention money, compensation for idle resources, prolongation costs due to delays, loss of profit resulting from termination, and reimbursement of legal expenses incurred during the dispute process. Most of these issues were consistent with those observed in other case studies, though the sequence of termination differed. Unlike Project 3, where the contractor terminated the contract first, this case involved an initial termination by the employer, followed by the contractor's termination in response. The contractor sought to invalidate the employer's termination and claimed compensation for costs and delays.

Upon review, the arbitration panel accepted all of the contractor's claims except those related to idle charges and administrative costs associated with dispute proceedings. Although the project commenced in 2014, the contractual disputes remain unresolved, as the employer appealed to the High Court seeking to nullify the arbitration award because the decision exceeded the arbitrators' authority and violated contractual provisions. The High Court is currently reviewing the legal validity of the award.

This prolonged dispute, similar to the other cases, underscores the inefficiency of dispute resolution and highlights the challenges in implementing construction contracts within Nepal's highway infrastructure sector. It further emphasises the need to strengthen contract management practices and enhance the institutional capacity of implementing agencies to align with international best practices in contract administration and dispute resolution.

4.3.5 *Project 5*

The final case study involved a road construction project financed by a foreign development agency. The project was administered by a project office with the provision of an international supervision consultant and a dispute board to manage day-to-day contractual issues cost-effectively. The construction contract was awarded through an International Competitive Bidding (ICB) process to a national–international joint venture. Arbitration proceedings were conducted under the UNCITRAL rules.

The disputes in this project were initially reviewed by the dispute board. However, the employer did not accept the board's decision and referred the matter to arbitration for further determination. The contractor's claims primarily concerned the prolongation costs and delayed payments of interim payment certificates. Upon review, the arbitration panel upheld the contractor's claims, concurring with the earlier findings of the dispute board.

The project commenced in 2015 with an original construction period of two years, but was extended by more than three years for completion. Despite physical completion in 2018, the contractual disputes remain unresolved. Although the arbitration award favoured the contractor, the employer appealed the decision to the High Court, asserting that the arbitrators exceeded their authority and violated contractual provisions. Under Nepal's Arbitration Act, judicial review of arbitration decisions is permitted only on limited grounds, such as when arbitrators act beyond their mandate or disregard contractual terms. Nevertheless, the employer's appeal remains under High Court review.

The prolonged dispute has continued to consume significant administrative and financial resources from both parties, demonstrating weaknesses in contract administration and dispute management. Such inefficiencies also increase the cost of dispute resolution and adversely affect the implementation performance of other projects managed by the same institutions. This case, in particular, underscores the shortcomings in administering dispute resolution mechanisms in large-scale international contracts involving foreign contractors, consultants, and full-time dispute boards. It highlights the necessity for a comprehensive review of all types of contracts, whether for roads or bridges, financed by the Government of Nepal or external agencies, and with or without dispute board provisions, to enhance the overall effectiveness of dispute resolution practices.

The review of all five case study projects indicates that key dispute issues are largely similar across projects, including claims related to time extensions, contract termination, idle costs, prolongation costs, and interest. In most cases, arbitration panels ruled in favour of the construction companies, requiring the employer to provide compensation. The panels frequently emphasised employer-related risk events such as delayed site possession, late issuance of design documents, and labour strikes. Some issues, such as adverse weather conditions, earthquakes, and the COVID-19 pandemic, were recognised as beyond the control of either party. Several disputes raised by the employer, however, pertained to resource management and planning deficiencies on the part of the construction companies. Most claims from contractors were associated with project time overruns and their consequential impact on performance. In evaluating these claims, arbitration awards were generally determined based on risk events explicitly stated in the contract agreement. It was observed that arbitration panels did not consistently conduct detailed reviews of contractor work plans, the efficiency of construction companies, or the impact of employer-related disruptions on critical activities (Ndekugri et. al, 2008). These aspects of delay claim analysis were often overlooked in highway project arbitration decisions. This research, therefore, identifies a significant gap in the construction contract dispute resolution practices within Nepal's highway infrastructure sector. Moreover, it underscores the need for arbitration experts handling construction disputes particularly those related to delays to possess in-depth knowledge of construction contract management to ensure more comprehensive and equitable decision-making.

5. Conclusion

In conclusion, the study found that thirteen construction companies were frequently involved in raising contractual claims, with two companies accounting for approximately 30% of all arbitration cases. This research identified the major arbitration issues raised by construction companies in road and bridge projects across different project management environments. On average, projects take more than ten years to resolve contractual disputes. Prolonged dispute resolution not only consumes significant resources but also reduces efficiency in managing new projects due to resource constraints and raises questions about the efficiency of institutions involved in contract management and dispute resolution.

The intended efficiency of arbitration as a dispute resolution mechanism is undermined in practice, with contracting parties taking excessive time to settle disputes. Frequent appeals to the High Court following arbitration decisions indicate a disregard for contractual provisions that are widely recognized in international construction contract management. Such practices raise concerns regarding project governance and negatively affect the country's foreign direct investment climate (Dollar et. al, 2006).

The analysis revealed that joint ventures in Government of Nepal (GoN) financed road contracts experienced a higher number of arbitration cases, reflecting lapses in fulfilling contractual obligations by the employer. Learning from claims raised by contractors is essential to correct these deficiencies. In the projects studied, most claims are still under arbitration or judicial review. Regardless of infrastructure type road or bridge, common issues include site possession delays, late issuance of designs, contract termination, delayed payments, and prolongation costs arising from employer-related risk events.

This comprehensive qualitative and quantitative review of arbitration cases demonstrates that arbitration awards, particularly for time extension claims, are often insufficiently evaluated. Critical analysis of contractors' resource plans and actual resource availability is necessary to ensure claims are assessed accurately. Consequently, this study highlights a future research direction in analysing delay-related claims, which constitute a significant portion of contractual disputes and involve substantial claim and administrative costs.

Overall, this research contributes to construction project management literature by providing new insights into the utilization of arbitration in developing countries like Nepal. It emphasises the need for capacity enhancement among contracting parties to resolve disputes efficiently and evaluates the performance of arbitration in the infrastructure development sector, offering guidance for improving contractual dispute resolution practices through the adoption of existing legal and procedural provisions and international best practices.

6. Recommendations

These research findings explore the nature of disputes in highway construction projects in Nepal and the practices adopted for their resolution through arbitration. Based on the review of arbitration processes, key recommendations for enhancing future dispute resolution in construction contracts include effective project planning with adequate resources, capacity building of contracting parties to better manage delay-related risks, development of robust delay analysis methodologies, and strengthening the competence of arbitrators to ensure fair and independent assessments of construction disputes. Additionally, enhancing institutional capacity through the adoption and proper implementation of standardized contract forms, such as FIDIC standards, is essential to improve dispute resolution mechanisms and attract greater foreign investment in infrastructure development within developing countries.

7. References

Beaumont, B. (2019). *FIDIC Red Book: A Commentary.* London. doi:https://doi.org/10.4324/9781315168494

Caron, D. D., & Caplan, L. M. (2013). *The UNCITRAL arbitration rules: a commentary.* United Kingdom: Oxford University Press.

Dollar, D., Hallward-Driemeier, M., & Mengistae, T. (2006). Investment climate and international integration. *World development, 34*(9), 1498-1516. doi:https://doi.org/10.1016/j.worlddev.2006.05.001

DoR. (2024). *Arbitration Award Payment due under the Department of Roads.* Kathmandu: Department of Roads, Dispute Settlement Unit.

FIDIC. (2017). Standard Contract Agreement forms. *International Federation of Consulting Engineers (FIDIC),* Geneva, Switzerland. http//www.fidic.org.

Mishra, K., & Aithal, P. S. (2022). Effectiveness of arbitration in construction projects. *International Journal of Management, Technology, and Social Sciences (IJMTS)*, 96-111. doi:https://dx.doi.org/10.2139/ssrn.4136673

Ndekugri, I., Braimah, N., & Gameson, R. (2008). Delay analysis within construction contracting organizations. *Journal of construction engineering and management, 134*(9), 692-700. doi:https://doi.org/10.1061/(ASCE)0733-9364(2008)134:9(692)

NEPCA. (2024). *32nd Annual Report of Nepal Council of Arbitration (NEPCA).* Lalitpur: Nepal Council of Arbitration. Retrieved from https://nepca.org.np/wp-content/uploads/2021/12/NEPCA-AGM-32.pdf

Stephenson, D. A. (2003). *Arbitration practice in construction contracts.* London: Routledge. doi:https://doi.org/10.4324/9780203474525

Voser, N. (2011). Overview of the Most Important Changes in the Revised ICC Arbitration Rules. *ASA Bull*, 783.

Walsh, M. J., & Yu, J. (2010). *Determinants of foreign direct investment: A sectoral and institutional approach.* International Monetary Fund.

Wang, Y., Lee, H. W., Tang, W., Whittington, J., & Qiang, M. (2021). Structural equation modeling for the determinants of international infrastructure investment: Evidence from Chinese contractors. *Journal of Management in Engineering*, 04021033. doi:https://doi.org/10.1061/(ASCE)ME.1943-5479.0000933

Journal on Transportation System and Engineering
ISSN: 3059-9865(Print) 3059-9873(Online)
Vol. 1. Issue 2 (December) 2025: 93-100
DOI: https://doi.org/10.3126/jotse.v1i2.87762

Research Article
Received Date: March 21, 2025
Revised Date: September 1, 2025
Accepted Date: November 7, 2025
Published Date: December 21,2025

Road Cut Slope Stability Assessment under Region-Specific Rainfall Scenarios in Middle Hills of Nepal

Tunisha Gyawali[a,b,*], Bhim Kumar Dahal[a]

[a]*Pulchowk Campus, Institute of Engineering, Tribhuvan University, Pulchowk, Lalitpur, 44600*
[b]*Department of Roads, Ministry of Physical Infrastructure and Transport, Government of Nepal, Babarmahal, Kathmandu, 44600*

Abstract

Rainfall-induced landslides, especially in the non-engineered hill roads, have resulted in huge mortality and socio-economic losses in low-income countries like Nepal. In this study, road cut slope stability analysis has been done considering different soil slope scenarios from various road corridors, and incorporating the spatio-temporal distribution of rainfall for site-specific studies in Nepal. The average monsoonal rainfall distribution in the Middle Hills was obtained from satellite GPM IMERG data (2001-2020) to create rainfall regions. We then determined the region-specific rainfall for numerical analysis, and validated them against site slope stability conditions for recent year rainfall from nearby gauged station. Transient seepage analysis was done in Seep/W and Limit Equilibrium Method was employed for slope stability analysis in Slope/W of GeoStudio 2023 using Mohr-Coulomb parameters. Validation for the selected rainfall and soil parameters showed reasonable accuracy to site slope failure conditions and establishes the reliability of the methodology employed for road cut slope stability assessment for regional use. Future scope of this research would be the development of user-friendly versions, with charts and tables for safe cut slope design, and empowerment of field engineers with the knowledge and tools to promote best practices in resilient road construction across vulnerable hilly terrains of Nepal.

Keywords: Cut slope stability; GPM IMERG; Rainfall-induced landslides

1. Introduction

The Nepal Himalayas is highly susceptible to road cut slope failures and landslides due to complex geology, active seismotectonics and intense monsoon (Eslamian et al., 2021). In Nepal, the federal engineers and practitioners generally conduct detailed slope stability analysis in strategic road network and follow the recommendations from Nepal Road Standards 2070 (DOR, 2013), Guide to Road Slope Protection Works, and Roadside Geotechnical Problems: A Practical Guide to Their Solution (DoR-GoN, 2007) for cut slope gradients. However, a majority of the slopes in the Local Road Network are found to be non-engineered and poorly designed with steep cut slopes which have heightened their susceptibility to geohazards.

In low-income countries like Nepal, most of the rural roads are constructed on the basis of "rule-of-thumb" rather than geotechnical investigations due to resource constraints (Robson et al., 2024). This has resulted in haphazard road construction, often without proper drainage, protection, or planning measures in place (Hearn & Shakya, 2017; Paudyal et al., 2023). McAdoo et al. (2018) noted that the non-engineered slopes witness twice as many rainfall-triggered landslides. With the increase in human interventions in the mountainous terrain over the last decade, the incidence of geohazards has increased along road networks (Pradhan, 2021; National Reconstruction Authority and National Disaster Risk Reduction and Management, 2021), claiming numerous lives and disrupting timely emergency access and rescue efforts due to damage in critical infrastructure systems and lifelines.

Around 90% of landslides and debris flow in Nepal occur during the monsoon. In Nepal, the precipitation contribution is approximately 80% of annual precipitation during summer monsoon season (June –September), followed by 12.5% during pre-monsoon (March–May), 4.0% in post-monsoon (October–November), and 3.5% in winter (December–February). Monsoon rains are characterized as high intensity and long-duration rainfall with 2 to 3 day interruptions (Khatun et al., 2023). Studies show that excess precipitation is responsible for triggering floods, avalanches, landslides, and soil erosion in the fragile Himalayan terrain (Aryal et al., 2020; Chalise et al., 2019; Talchabhadel et al., 2019). Dahal & Hasegawa (2008) considered the daily rainfall at failure against cumulative rainfall in the Himalayas and noted that 5 to 90 days of antecedent rainfall lead to landslides triggered by rainfall in general soil slopes.

Corresponding authors Email Address gyawalitunisha1@gmail.com

The infiltrated rainwater influences slope stability by reducing the shear strength as the wetting front advances (B. Jeyanth, 2019; Jiongxin, 1996; Wen et al., 2023). The increase in the pore-water pressure with the rise of groundwater table results in an increase in seepage force, and a subsequent decrease in matric suction in unsaturated soils (Fredlund, D.G., 1993). This is commonly observed in the failed slopes in extended roadways in hilly terrain when water also infiltrates into slide planes of the undercut slope (McAdoo et al., 2018).

Numerous studies have investigated the influence of rainfall infiltration on the stability of unsaturated slopes, and suggest the selection of appropriate rainfall inputs for unsaturated slope design with due consideration to local soil characteristics and climatic conditions. Lu & Godt (2008) emphasized the need of integrating both the unsaturated soil behavior and rainfall patterns into any model attempting to predict rainfall-induced slope failures. Numerical simulations by Tsaparas et al. (2002) on a typical residual soil slope in Singapore assessed the slope's response to rainfall distribution, saturated soil permeability, initial pore-water pressures, and groundwater table depth. Ng & Shi (1998) used Finite Element Method Seep/W to model pore-water pressures and applied the Limit Equilibrium Method to compute the Factor of Safety of the slopes.

Given the significant human and economic losses due to road cut slope failure, a better understanding of the interactions between Nepal's geological characteristics, topography, and rainfall (Sudmeier-rieux et al., 2019), along with user-friendly guidance (Robson et al., 2025) for roadside excavation is essential for constructing safer roads and mitigating geohazards.

In this study, representative sites along National, Feeder, District and Urban roads have been investigated and analyzed to assess the cut slope scenario incorporating physiographic, meteorological and geological conditions for site-specific adaptation in the Middle Hills. This study assesses cut slope stability under region-specific rainfall scenarios in Middle Hills by integrating satellite-based precipitation, field survey data, and geotechnical modeling and validates them against site failure condition for regional use.

2. Methodology

The region of study is the Middle Hills where the highest number of slope failures are recorded. It extends longitudinally from 80˚ 40´ E to 88˚ 12´ E and witnesses high elevation gradient and climate variability in a short stretch.

2.1 Soil parameters

The soils for the slopes chosen for validation were identified based on simplified field tests. On the basis of the USCS classification, the soil material is categorized into six types: Coarse grained soil (GW, SW, GP and SP); Coarse-grained with non-plastic fines (SC, SM-SC, SM and GM), Coarse-grained with plastic fines (GC and SC), Silt (ML and MH), Low plasticity clay (CL) and High Plasticity Clay (CH).

Mohr-Coulomb shear strength parameters like cohesion (c'), friction angle (φ'), and unit weight (γ), as well as seepage parameters like saturated water content (ϑ_s), permeability (k) and suction were investigated from field data and literature (Bureau of Indian Standards, 1997; Minnesota Department of Transportation, 2007; NAVFAC, 1986). The average values of soil parameters for these soils are shown in Table 1. The hydraulic conductivity function, which shows the effect of increase in soil suction on permeability, was modeled via van Genuchten method in GeoStudio 2023.

Table 1. Soil parameters used for validation

Soil	c' (kPa)	φ' (˚)	γ (kN/m^3)	k (mm/hr)	θ_s	Maximum suction (kPa)
Coarse-grained soil (CG)	1	40	20	50	0.33	5
Coarse-grained soil with non-plastic fines (CGNPF)	5	35	20	11.5	0.41	15
Coarse-grained soil with plastic fines (CGPF)	6	33	20	9	0.40	50
Silt	10	27	18.5	0.97	0.37	100
Low Plasticity Clay (CL)	12.5	18	17.5	0.3	0.40	300
High Plasticity Clay (CH)	20	12	19	0.12	0.47	600

2.2 Meteorological studies

The spatio-temporal distribution of precipitation is influenced by the large scale atmospheric and oceanic circulation patterns, steep elevation gradient, orography, and topography (Hamal et al., 2020). Satellite Rainfall Estimates (SRE) obtained from Gridded Satellite based Precipitation Products (SBPPs) offer high spatial and temporal resolutions. They provide spatially continuous rainfall estimate in the regions where low spatial density of gauged stations (Derin et al., 2019) compromise the accuracy and reliability for necessary interpolations in complex terrains. SREs are especially suitable in countries like Nepal with high climatological variability; challenging terrain for routine maintenance and regular monitoring; and limited resources, where data are often laden with gaps, biases and discrepancies (Barros et al., 2000; Duncan & Biggs, 2012; Kansakar et al., 2004).

GPM IMERG has been known to have superior performance in detecting true precipitation, reduced false alarm, overestimation of the heavy precipitation events and an underestimation of precipitation amount during extreme precipitation events which is crucial in the application of SBPPS in flash flood, and landslide prediction. The seasonal variation of precipitation in Nepal is influenced by the summer monsoon rain convection from South East to North West of the country and by the Westerlies in the West during the winter. GPM IMERG also demonstrates a higher ability to capture the seasonal rainfall variability influenced by the complex topography in the mid and high elevation areas of Nepal over the study region with lower RMSE and higher CC values for all seasonal and spatial contexts compared to other satellite products (Sharma et al., 2020).

Rainfall-induced landslides are the most common during the summer monsoon in Nepal. Therefore, the average monsoonal distribution is considered suitable for regional categorization in this study. The NASA's GPM IMERG V07 Late Run algorithm product from 2001 AD to 2020 AD at spatial resolution of approximately 10 kilometers ($0.1° \times 0.1°$) precipitationCal averaged over the twenty year period has been used to obtain the average monsoonal rainfall raster values (Figure 1).

Further, to incorporate the monsoon rainfall in the numerical analysis, for each region, the daily time series data over the 122 days of monsoonal period from June 1 to September 30 was selected from the Department of Hydrology and Meteorology (DHM) station which recorded the highest recorded monsoon rainfall (2003-2023), and validation was done against recent rainfall records from nearby DHM stations. 42 DHM stations were studied, which were selected based on adequacy for rainfall analysis to determine the representative design rainfall for each regional categories, and their proximity to the investigated field sites chosen for validation.

2.3 Numerical Analysis and Validation

Transient Seepage Analysis using Seep/W was done to model the effect of rainfall time series over monsoonal time period on the groundwater table and pore water pressure conditions for cut slope stability. A hydrostatic initial condition was established at the beginning of the transient seepage analysis with a Piezometric surface. The residual water content was taken as 10%. The finite element results of pore water pressure conditions from parent seepage analysis in Seep/W was integrated into the Slope/W of GeoStudio 2023 for static limit equilibrium analysis for tracking the temporal change in Factor of Safety (FoS) to assess the cut slope stability.

The Morgenstern-Price (M-P) method (Morgenstern & Price, 1965) employs the principles of limit state equilibrium to determine the FoS by analyzing potential failure surfaces and assuming that the slope is in a state of impending failure, ie on the verge of sliding. It considers both force and moment equilibrium, and interslice forces for circular slip surface using half-sine function. The critical FoS obtained over the period of 122 days is analyzed and the minimum value observed over that period is considered for determining the stability of the cut slope under extreme recorded region-specific rainfall scenario.

In this study, a representative site is validated and slope behavior is explained in detail. Results of numerical anlaysis of eight other sites of different soil types selected for validation compared with the slope failure condition at site is also presented to inform further advancement in research.

3. Results and Discussions

3.1 Rainfall regions

High, Medium and Low rainfall intensities were obtained from the average monsoonal distribution and the Middle Hills was categorized as Mid Hill – High (>1,200 mm/year); Mid Hill – Medium (1,000-1,200 mm/year); and Mid Hill – Low (800-1,000 mm/year) as shown in Figure 1.

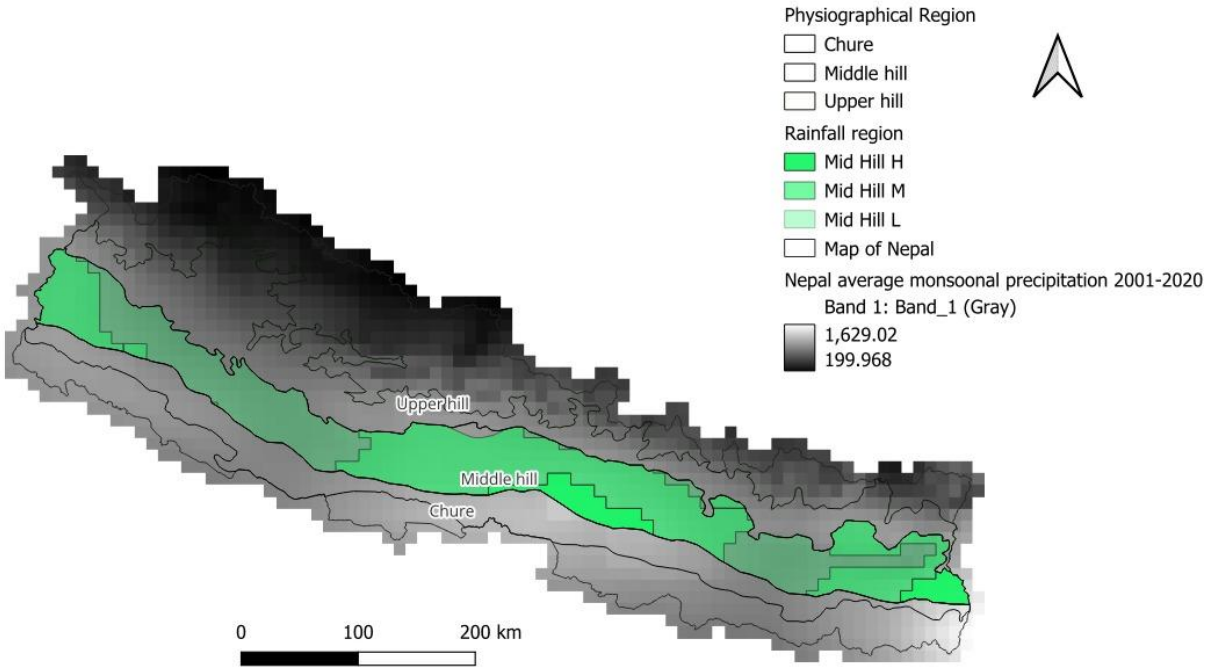

Figure 1. Average monsoonal precipitation (2001-2020) from NASA GPM IMERG is used to obtain regional categories for Middle Hills, namely Mid Hill High (>1,200 mm/year), Mid Hill Medium (1,000-1,200 mm/year) and Mid Hill Low (800-1,000 mm/year). The color band of raster values for average monsoonal precipitation shows that the highest rainfall occurs in the central and eastern region and minimum rainfall in the northern regions.

3.2 Representative Rainfall

Firstly, the average monsoonal rainfall rasters from GPM IMERG recorded the highest precipitation as 1629mm and showed a general underestimation in the magnitude of rainfall for use in the numerical analysis. The complex topography (Cattani et al., 2016), and large scale local climatic variation (Gebregiorgis & Hossain, 2013) is attributed to the uncertainties in the performance of SBPPs. SREs adequately captured the spatio-temporal distribution, however, Sharma et al. (2020) showed severe underestimation in mean annual precipitation, chiefly in the well-known high precipitation areas in central Nepal.

Secondly, an uneven daily precipitation is observed during the rainy season with 10% of the total annual precipitation occurring in a single day while 50% is recorded within 10 days of monsoon period (Alford, 1992). Dahal & Hasegawa (2008) suggest that such an uneven rainfall pattern plays an important role in triggering landslides in Nepal. A study by Pink (2024) showed that the daily satellite rainfall estimate are poorly correlated to gauge daily records and implies higher discrepancy compared to the monthly and annual estimates, especially given the insufficient spatial coverage of the gauge network.

In this context, gauged stations capture the recorded precipitation in a daily time series and enable to investigate the behavior of the soil under antecedent rainfall, varying intensities, as well as the short time gap of zero-rainfall between consecutive high magnitude rainfall. Therefore, an analysis period of 122 days of monsoon, corresponding to June 1 to September 30 from the gauged station was considered to capture the absolute minimum Factor of Safety of the cut slope at varying rainfall intensities and saturation states. The long duration allows the assessment of the stability of cut slopes in unsaturated conditions such that the intermediate instability states are not overlooked. This also serves to analyze the site specific variations depending on geographical location and climate for localized conditions.

Therefore, the regional rainfall for numerical analysis was selected as the time series of the Department of Hydrology and Meteorology station that represented the worst case with the highest monsoonal rainfall in any year (2003-2023 AD) among all the stations in that region (Figure 2); 42 stations were considered for Middle Hills.

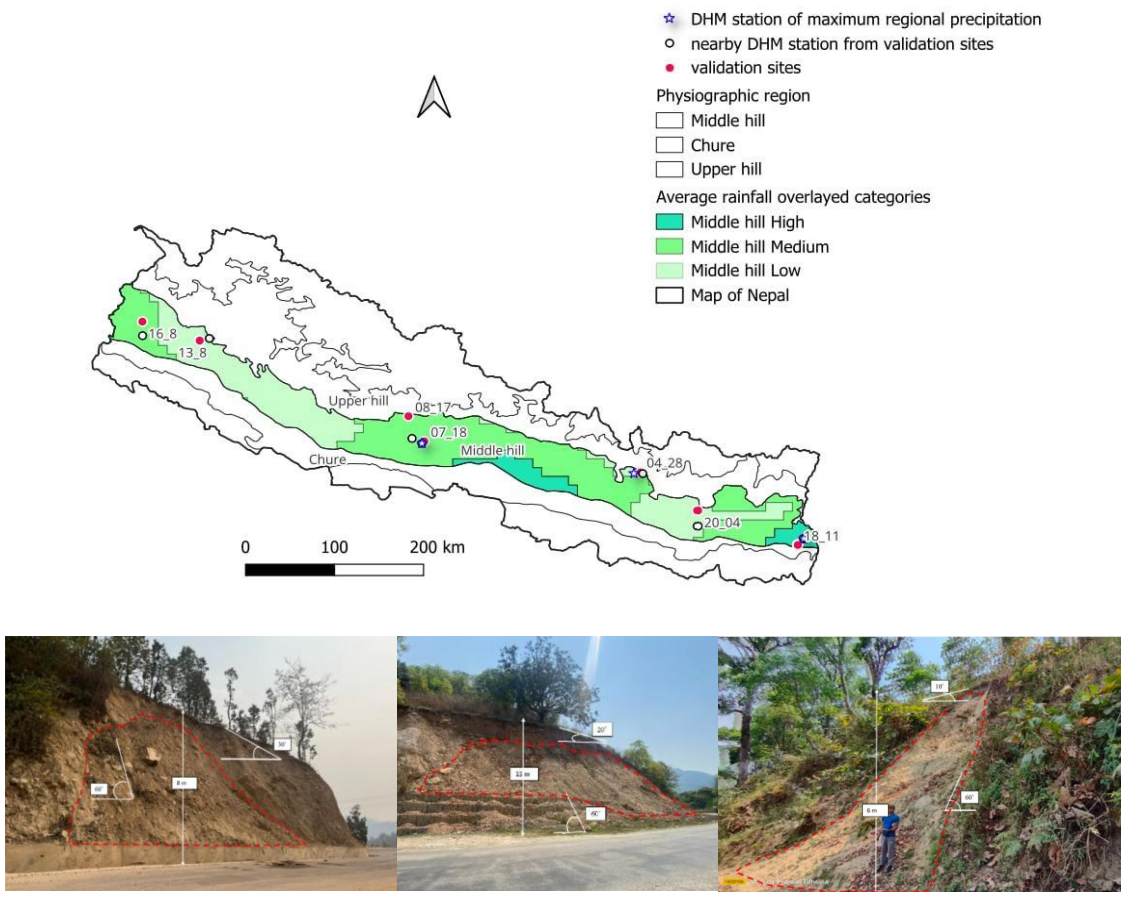

Figure 2. The map shows the Department of Hydrology and Meteorology (DHM) station for Regional Rainfall (station that recorded the maximum rainfall in the regional category) for Middle hill High, Middle hill Medium and Middle hill Low regions. It also shows the nearby DHM stations from the sites used for validation.

3.3 Validation

Validation of sites shown in Figure 2 was done for the regional rainfall and values of soil parameters (Table 1) chosen. The sites for validation are chosen based on material type, status of slope failure and proximity to the available nearby rainfall station for each regional category. Among the nine investigated sites, one is illustrated in detail to assess the road cut slope behavior.

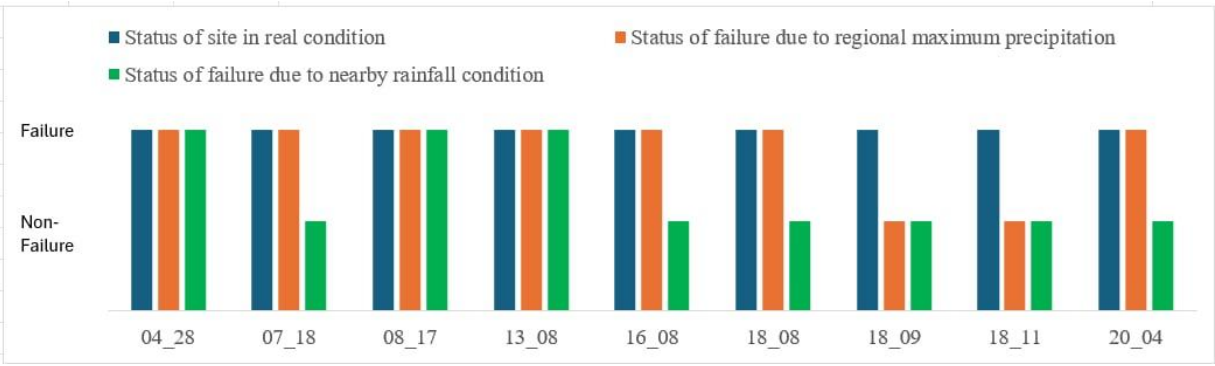

Figure 4 Status of failure from numerical models compared to the real state at site for sites selected for validation in Middle Hills.

Similar analyses for rest of the sites (Gyawali, 2025) showed that 7 out of 9 validated sites analyzed with the regional rainfall failed against 100% of real failure status (Figure 4). It was seen that with 95% confidence in Mc-Nemar's exact test, the true accuracy of the results of slope stability from the validation lies between 93.7% and 45.3% on similar data given the small sample size, which denotes a reasonable accuracy in the selected rainfall and soil parameters for regional generalization, given the high field uncertainties and variability in soil parameter values, as well as contributions from local (de)stabilizing factors. This establishes the reliability of the methodology employed and further informs the soil behavior dynamic under varying rainfall scenarios for accurate slope assessment.

4. Conclusions and Recommendations

Nepal suffers from rainfall-induced road cut slope failures in the fragile mountainous terrain which has resulted in huge socio-economic losses and mortality. The integration of the satellite-based average monsoonal rainfall distribution (GPM IMERG) and the regional maximum monsoonal rainfall event (2003-2023) from the gauged data offers a robust framework for numerical modeling and simulating site-specific scenario to assess cut slope stability across Middle Hills of Nepal. A detailed validation of low plasticity clay road cut slope has been illustrated and the validation results for the rest of the eight cut slopes is presented. The results confirm the reliability of the selected soil parameters and regional maximum rainfall, as well as the use of 122-day monsoon window for dynamic tracking of Factor of Safety to capture critical instability thresholds, offering actionable insights for slope design under varying rainfall intensities.

This study informs further research in the development of Region-Specific Design Charts and Tables with recommendations for safe slope angles for different soil types, cut height and slope geometry that are tailored for quick reference by field engineers and local contractors; extension to the Upper Hills and Chure; and validation through pilot studies in high-risk areas. The sample size of the validation sites could be extended to incorporate the diversity across varied terrain. We also suggest complementing this with training to the local engineers and practitioners on soil identification, choosing the regional zone of the site, and using design charts effectively as a series of diagrams and questions for confidence in local use.

By bridging satellite climatology, geotechnical modeling, and field validation, this approach lays the groundwork for a new generation of resilient road infrastructure in Middle Hills of Nepal, one that is both technically sound and locally grounded.

5. Acknowledgement

This research is funded by the EPSRC Impact Acceleration Account [EP/X525546/1] and supported by Institute of Hazard, Risk and Resilience, Durham University, UK. The authors would like to thank Prof. David Toll, Dr. Ellen B. Robson, and Prajwal Timsina for their guidance and support, as well as Prof. Alex Densmore and Prof. Nick Rosser (Durham University) for the use of their monthly averaged GPM IMERG dataset. The data can be made available upon request.

6. References

Alford, D. (1992). Streamflow and sediment transport from mountain watersheds of the Chao Phraya Basin, northern Thailand: a reconnaissance study. *Mountain Research & Development*, *12*(3), 257–268. https://doi.org/10.2307/3673669

Aryal, D., Wang, L., Adhikari, T. R., Zhou, J., Li, X., Shrestha, M., Wang, Y., & Chen, D. (2020). A model-based flood hazard mapping on the southern slope of Himalaya. *Water (Switzerland)*, *12*(2). https://doi.org/10.3390/w12020540

B. Jeyanth. (2019). Effect of Moisture Content on Shear Strength of the Stabilized Soil. *International Journal of Engineering Research And*, *V8*(12). https://doi.org/10.17577/ijertv8is120111

Barros, A. P., Joshi, M., Putkonen, J., & Burbank, D. W. (2000). A study of 1999 monsoon rainfall in a mountainous region in central Nepal using TRMM products and rain gauge observations. *Geophysical Research Letters*, *27*(22), 3683–3686. https://doi.org/10.1029/2000GL011827

Bureau of Indian Standards. (1997). *Indian Standard: retaining wall for hill area-guidelines*. *14458*(May).

Cattani, E., Merino, A., & Levizzani, V. (2016). Evaluation of monthly satellite-derived precipitation products over East Africa. *Journal of Hydrometeorology*, *17*(10), 2555–2573. https://doi.org/10.1175/JHM-D-15-0042.1

Chalise, D., Kumar, L., & Kristiansen, P. (2019). Land degradation by soil erosion in Nepal: A review. *Soil Systems*, *3*(1), 1–18. https://doi.org/10.3390/soilsystems3010012

Derin, Y., Anagnostou, E., Berne, A., Borga, M., Boudevillain, B., Buytaert, W., Chang, C. H., Chen, H., Delrieu, G., Hsu, Y. C., Lavado-Casimiro, W., Manz, B., Moges, S., Nikolopoulos, E. I., Sahlu, D., Salerno, F., Rodríguez-Sánchez, J. P., Vergara, H. J., & Yilmaz, K. K. (2019). Evaluation of GPM-era Global Satellite Precipitation Products over Multiple Complex Terrain Regions. *Remote Sensing*, *11*(24). https://doi.org/10.3390/rs11242936

Delwyn G. Fredlund, H. R. (1993). *Soil Mechanics for Unsaturated Soils*.

Derin, Y., Anagnostou, E., Berne, A., Borga, M., Boudevillain, B., Buytaert, W., Chang, C. H., Chen, H., Delrieu, G., Hsu, Y. C., Lavado-Casimiro, W., Manz, B., Moges, S., Nikolopoulos, E. I., Sahlu, D., Salerno, F., Rodríguez-Sánchez, J. P., Vergara, H. J., & Yilmaz, K. K. (2019). Evaluation of GPM-era Global Satellite Precipitation Products over Multiple Complex Terrain Regions. *Remote Sensing*, *11*(24). https://doi.org/10.3390/rs11242936

DoR-GoN. (2007). Roadside Geotechnical Problems: A Practical Guide to their Solution. *Kathmandu:Department of Road, Government of Nepal.*, *June*. https://dor.gov.np/uploads/publication/publication_1472971151.pdf%0Ahttps://dor.gov.np/uploads/publication/publication_1472792371.pdf

DOR. (2013). Nepal Road Standard 2070. *Department of Roads*, 55.

Duncan, J. M. A., & Biggs, E. M. (2012). Assessing the accuracy and applied use of satellite-derived precipitation estimates over Nepal. *Applied Geography*, *34*, 626–638. https://doi.org/10.1016/j.apgeog.2012.04.001

Eslamian, S., Eslamian, F., Frameworks, N., & Resilience, B. (2021). Handbook of Disaster Risk Reduction for Resilience. In *Handbook of Disaster Risk Reduction for Resilience*. https://doi.org/10.1007/978-3-030-61278-8

Fattah, M. Y., Ahmed, M. D., & Mohammed, H. A. (2013). Determination of the Shear Strength , Permeability and Soil Water Characteristic Curve of Unsaturated Soils from Iraq. *Journal of Eearth and Geotechnical Engineering*, *3*(1), 97–118.

Gebregiorgis, A., & Hossain, F. (2013). Performance evaluation of merged satellite rainfall products based on spatial and seasonal signatures of hydrologic predictability. *Atmospheric Research*, *132–133*, 223–238. https://doi.org/10.1016/j.atmosres.2013.05.003

Gyawali, T. (2025). *Region-Specific Safe Cut slopes for Resilient Roads in Middle Hills of Nepal: Integrating Topography and Spatio-temporal distribution of Rainfall* (Master's thesis). Tribhuvan University.

Hamal, K., Sharma, S., Baniya, B., Khadka, N., & Zhou, X. (2020). Inter-Annual Variability of Winter Precipitation Over Nepal Coupled With Ocean-Atmospheric Patterns During 1987–2015. *Frontiers in Earth Science*, *8*(May). https://doi.org/10.3389/feart.2020.00161

Hearn, G. J., & Shakya, N. M. (2017). Engineering challenges for sustainable road access in the himalayas. *Quarterly Journal of Engineering Geology and Hydrogeology*, *50*(1), 69–80. https://doi.org/10.1144/qjegh2016-109

Jiongxin, X. (1996). Benggang erosion: The influencing factors. *Catena*, *27*(3–4), 249–263. https://doi.org/10.1016/0341-8162(96)00014-8

Kansakar, S. R., Hannah, D. M., Gerrard, J., & Rees, G. (2004). Spatial pattern in the precipitation regime in Nepal. *International Journal of Climatology*, *24*(13), 1645–1659. https://doi.org/10.1002/joc.1098

Khatun, M., Hossain, A. T. M. S., & Sayem, H. M. (2023). Climate Variability & Establishment of Rainfall Threshold Line for Landslide Hazards in Rangamati, Bangladesh. *Open Journal of Geology*, *13*(09), 959–979. https://doi.org/10.4236/ojg.2023.139041

Lu, N., & Godt, J. (2008). Infinite slope stability under steady unsaturated seepage conditions. *Water Resources Research*, *44*(11). https://doi.org/10.1029/2008WR006976

McAdoo, B. G., Quak, M., Gnyawali, K. R., Adhikari, B. R., Devkota, S., Lal Rajbhandari, P., & Sudmeier-Rieux, K. (2018). Roads and landslides in Nepal: How development affects environmental risk. *Natural Hazards and Earth System Sciences*, *18*(12), 3203–3210. https://doi.org/10.5194/nhess-18-3203-2018

Minnesota Department of Transportation. (2007). *MnDOT pavement design manual*.

Morgenstern, N. R., & Price, V. E. (1965). The Analysis of the Stability of General Slip Surfaces. *Https://Doi.Org/10.1680/Geot.1965.15.1.79*, *15*(1), 79–93. https://doi.org/10.1680/GEOT.1965.15.1.79

National Reconstruction Authority and National Disaster Risk Reduction and Management. (2021). *Manual for Hands-on Training to Engineers on Slope Stabilization Techniques.*

NAVFAC. (1986). *Design Manual-7.02 Foundations and Earth Structures*.

Ng, C. W. W., & Shi, Q. (1998). Influence of rainfall intensity and duration on slope stability in unsaturated soils. *Quarterly Journal of Engineering Geology*, *31*(2), 105–113. https://doi.org/10.1144/GSL.QJEG.1998.031.P2.04

Paudyal, P., Dahal, P., Bhandari, P., & Dahal, B. K. (2023). Sustainable rural infrastructure: guidelines for roadside slope excavation. *Geoenvironmental Disasters*, *10*(1). https://doi.org/10.1186/s40677-023-00240-x

Pink, I. T. (2024). *Predicting the impact of climatic and geomorphic changes on ood hazards in Central Himalayan Rivers . An environmental modelling framework to predict potential ood hazards in the Karnali River in* (Vol. 0). Durham E-Theses.

Robson, E. B., Dahal, B. K., & Toll, D. G. (2025). A participatory approach to determine the use of road cut slope design guidelines in Nepal to lessen landslides. *Natural Hazards and Earth System Sciences*, *25*(3), 949–973. https://doi.org/10.5194/nhess-25-949-2025

Samprada Pradhan. (2021). *Impacts of road construction on landsliding in Nepal*. http://dx.doi.org/10.1007/s11069-006-9100-%0Ahttp://etheses.dur.ac.uk

Sharma, S., Khadka, N., Hamal, K., Shrestha, D., Talchabhadel, R., & Chen, Y. (2020). How Accurately Can Satellite Products (TMPA and IMERG) Detect Precipitation Patterns, Extremities, and Drought Across the Nepalese Himalaya? *Earth and Space Science*, *7*(8). https://doi.org/10.1029/2020EA001315

Sudmeier-rieux, K., Mcadoo, B. G., Devkota, S., Chandra, P., Rajbhandari, L., & Howell, J. (2019). Mountain roads in Nepal at a new crossroads. *Natural Hazards and Earth System Sciences*, *19*, 655–660.

Talchabhadel, R., Karki, R., Yadav, M., Maharjan, M., Aryal, A., & Thapa, B. R. (2019). Spatial distribution of soil moisture index across Nepal: a step towards sharing climatic information for agricultural sector. *Theoretical and Applied Climatology*, *137*(3–4), 3089–3102. https://doi.org/10.1007/s00704-019-02801-3

Tsaparas, I., Rahardjo, H., Toll, D. G., & Leong, E. C. (2002). Controlling parameters for rainfall-induced landslides. *Computers and Geotechnics*, *29*(1), 1–27. https://doi.org/10.1016/S0266-352X(01)00019-2

Wen, Y., Jiang, H., Kasielke, T., Zepp, H., Yang, Y., Wu, W., & Zhang, B. (2023). Prewinter soil water regime affects the post-winter cracking position on gully sidewall and slumping soil dynamics in Northeast China. *Geoderma*, *435*(May), 116508. https://doi.org/10.1016/j.geoderma.2023.116508

Journal on Transportation System and Engineering
ISSN: 3059-9865(Print) 3059-9873(Online)
Vol. 1. Issue 2 (December) 2025: 100-112
DOI:https://doi.org/10.3126/jotse.v1i2.87763

Research Article
Received Date: March 30, 2025
Revised Date: October 3, 2025
Accepted Date: November 9, 2025
Published Date: December 21,2025

Road Traffic Crash Cost Human Capital Approach: A Case Study of Kailali District

Maheshwari Dhami[a] , Pradeep Kumar Shrestha[b], Hemant Tiwari[c]

Pulchowk Campus, Institute of Engineering,Tibhuwan University,Nepal
[c]General Secretary, Society of Transport Engineers Nepal, Kathmandu,Nepal

Abstract

Road traffic crashes continue to impose substantial economic and social burdens, particularly in developing countries such as Nepal, where resources for road safety are limited. This study employs the Human Capital Approach to estimate the costs of road traffic crashes in Kailali District for the fiscal years 2022–23 and 2023–24. The costs associated with crashes were categorized into six main components: lost productivity, quality of life losses, medical expenses, property damage, damage-only crashes, and administrative costs. Using secondary data obtained from traffic police records, hospitals, insurance companies, and other relevant sources, the study found that the average age of fatality was 38 years in 2022–23 and 37 years in 2023–24. Between 2022–23 and 2023–24, the total economic cost of road crashes rose by 38.93%, reflecting a growing financial and social burden. Among the cost components, lost productivity remained the largest contributor, followed by quality of life losses. Although medical expenses, property damage, administrative costs, and damage-only crashes accounted for smaller proportions of the total cost, they showed a noticeable upward trend. These findings highlight the pressing need for comprehensive and effective road safety measures in Kailali District to mitigate both the human and economic impacts of traffic crashes.

Keywords: Crash Cost; developing country; Fatalities; Human Capital Approach; Road traffic crashes.

1. Introduction

Traffic crashes are a pressing global concern, imposing significant economic and social burdens. Each year, most countries lose more than 3% of their GDP due to road traffic crashes, with the main contributors being medical expenses, lost productivity from injuries and fatalities, and damage to vehicles and infrastructure (WHO, 2018). The impact is particularly severe in low- and middle-income countries, which, despite possessing only 60% of the world's motor vehicles, account for 92% of all road traffic fatalities. This imbalance exacerbates economic hardship, especially for low-income families who are often ill-prepared to cover sudden medical bills or funeral expenses (World Bank, 2024).

The Human Capital Approach (HCA), which takes into account both direct costs (such as medical bills, property damage, and administrative fees) and indirect costs (such as lost productivity, pain, and suffering), is frequently used to estimate the costs of traffic crashes. According to studies, crashes in underdeveloped countries may go unreported, which could result in an underestimating of their actual economic impact (Mofadal and Kanitpong, 2016).

The working-age population (18–59 years old) is disproportionately affected by fatal traffic crashes, which has long-term financial consequences for both households and entire countries. Families may become exhaust and their dependent ratios may rise as a result of losing their principal provider, thereby taxing social welfare systems (World Bank, 2024).

Road traffic crashes in Nepal have been increasing steadily over the past decade, posing serious economic and social challenges. According to national data, the number of crashes rose from 8,484 in FY 2012/13 to 24,537 in FY 2021/22, while fatalities increased from 1,816 to 2,883 during the same period. These figures reflect a worrying upward trend, highlighting the growing burden of road crash on individuals, families, and society. Although Nepal has formulated a National Road Safety Action Plan (2021–2030) and set clear targets to reduce fatalities, implementation has been limited, with less than half of the planned interventions under the "safer roads and

Corresponding author's email address: mdhami.2050@gmail.com

mobility" pillar completed. The causes of crashes are multifaceted, involving human error, vehicle issues, and road and environmental conditions. While only a small proportion of crashes are directly due to roadway factors, the inclusion of roadside conditions raises this contribution to nearly one-third, emphasizing the critical role of road design and maintenance in preventing crashes (Tiwari, H. and Luitel, S., 2023).

Within this national context, Sudurpashchim Province emerges as one of the least prioritized regions for road safety initiatives. Limited infrastructure, and low public awareness contribute to a higher risk of crashes. These challenges underscore the urgent need for targeted measures to improve road conditions and promote road safety education.

Karnali Province, characterized by mountainous terrain and challenging road conditions, faces a similarly critical situation. Between 2018 and 2024, the province recorded over 3,000 vehicle crashes, resulting in nearly 800 fatalities and more than 6,000 injuries. The combination of difficult terrain, adverse weather, and insufficient road safety measures makes travel in Karnali particularly hazardous. Efforts are ongoing to improve infrastructure and implement road safety programs, but the region continues to demand focused attention to reduce the human and economic costs of traffic crashes (Khadka, R., Tiwari, B., Acharya, U.P., BC, U.B., Adhikari, R. and Thapa, K., 2024).

At the district level, Kailali mirrors this broader pattern, with traffic crashes causing substantial economic and social impacts. A comprehensive assessment of costs including lost productivity, quality of life losses, medical expenses, property damage, damage-only crashes, and administrative costs is vital for grasping the local consequences of road crashes and for designing interventions that are both targeted and effective.

1. Research Objective

The primary objective of this research is to estimates the total economic burden due to road traffic crashes in the Kailali District, applying the Human Capital Approach.

2. Literature Review

A study by (Azmi, A.A., Ram, S. 2024) reviewed various methods for calculating the costs of road crashes, including the Human Capital Approach (HCA), the Willingness-to-Pay method and others. The researchers found that the HCA is particularly well-suited for developing countries, as it captures key factors like lost productivity and medical expenses while remaining practical even when detailed economic data is scarce. Based on these findings, the study recommends using the HCA to estimate road crash costs. (Chin, H. C., Hague, M. M., and Jean, Y. H., 2006) attempt to update the cost estimates of road traffic crashes studied by the Asian Development Bank (ADB) that has shown the annual cost of road traffic crashes in 2001 was US$699.36 million which was 0.5% of the annual GDP. More precise methods of computing the human cost, lost output and property damage are adopted which grew in an annual cost of US$610.3 million or 0.338% of the annual GDP in 2003. A more conservative estimate of U$878,000 for fatal crash is also obtained, compared to the earlier figure of US$1.4 million. This study has shown that it is necessary to update the annual traffic crash costs regularly, as the figures vary with the number of crash which change with time.

(Samikshya Rizal, Hemant Tiwari, 2023) This paper study estimate the total road crash cost of Kathmandu Valley, which shares 7.8 % to 9.2% of fatalities and 52.5% to 60.5% of crashes of Nepal; based on the crash database for the fiscal year 2007 to 2020. The detailed road crash database was collected from Traffic police. The primary data regarding vehicle damage cost and medical cost was obtained from purposive convenient sampling, whereas insurance data was collected from sampled companies. Human Capital Approach was used for calculation of crash costing. The average age of fatalities was found to be 34 years, which is an economically active age group. The total cost of road crashes in Kathmandu Valley for the fiscal year 2020 was calculated a NRs. 1827.67 million. Among various components of crash cost, the total cost of lost output share 46.28 %, Vehicle damage cost shares 36.27 %, Medical cost shares 2.16 %, Administrative cost shares 6.01 % and Quality of life shares 9.25 % respectively.

3. Methodology

The research was conducted as shown in Figure 1 The research begins with literature review of past study on crash cost component followed by selection of study area.

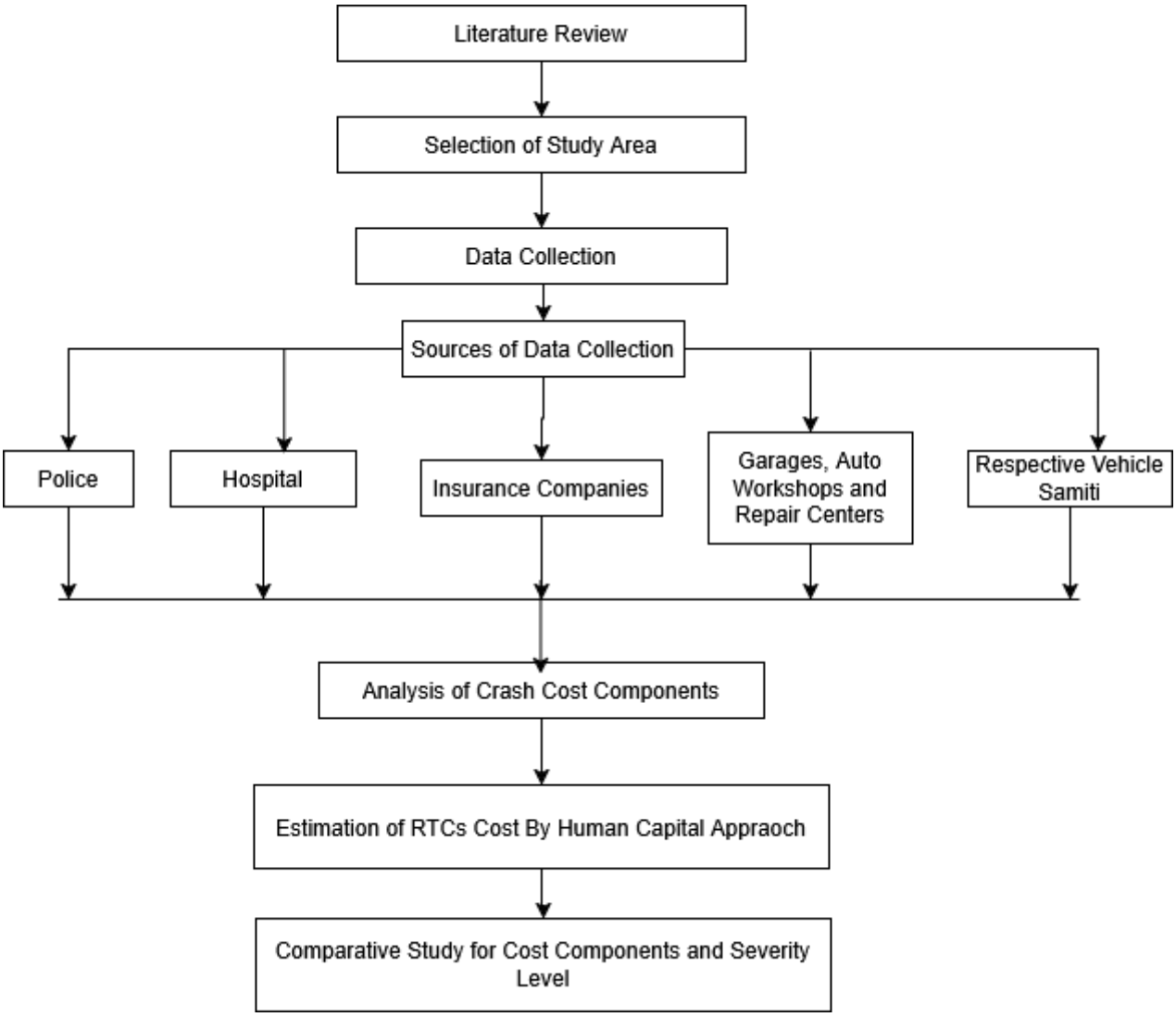

Figure 1: Flow Chart of Methodology

The crash data of FY2022-2023 to 2023-2024 were collected from the District Traffic Police, kailali. The number of crashes and their severity level were necessary data for the calculation of total crash cost. Collected crash data were shorted as per number of crashes, severity of the crash, type of vehicle involved, and age of victims. The data collection includes the data from secondary source: Police, Hospitals, Insurance company, Auto Workshop and respective vehicle operator committee. Questionnaire survey was done while collecting data from vehicle operator committee and Auto workshop for damage only crash. The age of person involved in fatal crash was calculated from police data and wage rate from Kailali district rate to calculate loss output, for medical cost data were obtained from the record maintained by hospital in software. Vehicle damage cost data are obtained from three non- life insurance company. The purposive convenient sampling technique was adopted. Three non-life insurance company were chosen for this study. The claim amount for vehicle damage of different types of vehicles was collected for the year FY 2022/2023 and FY2023/2024 from those three insurance companies. And the number of

damage only crash was obtained by questionnaire with Traffic police regarding the number of vehicles with damage only crash and most common type of damage and from Auto Repair Center the question regarding number and type of vehicle that visit to repair center involving in damage only crash, time taken to repair the vehicle and average cost of vehicle. The quality of life cost was calculated using Net output method and administrative cost was calculated as percentage basis suggested by Sillock and TRL.

The calculation of road crash cost using Human Capital Approach include estimation of loss of productivity, quality of life cost, medical cost, property damage cost, damage only crash cost and administrative cost as explained in following section.

3.1 Loss of Productivity

The economic loss resulting from a person's inability to work due to injury or fatality caused by a crash. It includes lost wages as explained in (Adam I.A. Mofadal, 2016) -

Fatality loss of output= [No. fatalities] * [foregoing income per year using i=0nW1+rn where, (1) W = average year per capita GDP, r = discount/interest rate, n = average number of years of lost productivity per crash fatality

Major Injury loss of output= [No. of serious injuries] * [No. of days in hospital +No. of follow up days] * [average wage per day]

Minor Injury loss of output= [No. 0f minor injuries]*[No. of days in hospital] +No. of follow up days] * [average wage per day]

Lost output of care taker= [No. of injuries by severity] * [No. of day to take care] *[average wage per day] *No. of career to injury =1:1

3.2 Quality of Life cost

The economic valuation of the loss of well-being and life satisfaction due to a fatal crash. It represents the non-economic burden on the victim's family and society, including emotional distress, grief, and the irreversible loss of life. Quality of life cost is equal to difference in amount he/she can earn if alive and amount he/she consumes during life time. The amount that would have been earned is represented by the lost productivity of fatalities. The amount consumed was obtained from the Nepal Living Standards Survey from 1995 to 2023 conducted by National Statistical data. According to national statistical data, the average annual nominal consumption per capita was estimated at NRs. 156,330. This value was calculated as the mean consumption of the top 20% richest households and the bottom 20% poorest households.

3.3 Medical costs

For calculating medical cost firstly administrative department of each hospital was visited and emergency register of the patient were obtained. The RTC cases were filtered out and the date of crash, age and gender with date of admission of patient was verified. The matched detail of patient, along with IPD number were noted and made available to IT section. Using that IPD number, the details about patient, regarding date of admission, date of discharge, Emergency cost, Medicine cost and total cost excluding the emergency and medical cost were obtained. Data was obtained from all selected hospital. Data was collected for out patients only.

The expenses incurred for the treatment of crash victims, including emergency care, hospitalization, medication, and follow-up treatments. The medical cost is calculated for injury crash only and the cost is categorized as emergency cost, medicine cost and total cost excluding EC and MC and calculated as mentioned below (database of hospital):-

Major and Minor Injury Emergency cost (EC) per fatal crash =Total Emergency cost from software maintained by hospital divided by numbers of major and minor injury for fatal crash.

Major and Minor Injury Medicine cost (MC) per fatal crash = Total Medicine cost from software maintained

by hospital divided by numbers of major and minor injury for fatal crash.

Major and Minor Injury total cost excluding EC and MC per fatal crash = Total cost exclusive of EC and MC from software maintained by hospital divided by numbers of major and minor injury for fatal crash.

Major and Minor Injury Emergency cost (EC) per Injury crash =Total Emergency cost from software maintained by hospital divided by numbers of major and minor injury for injury crash.

Major and Minor Injury Medicine cost (MC) per Injury crash =Total Medical cost from software maintained by hospital divided by numbers of major and minor injury for injury crash.

Major and Minor Injury total cost excluding EC and MC per Injury crash =Total Emergency cost from software maintained by hospital divided by numbers of major and minor injury for injury crash.

3.4 Property Damage Costs

The financial loss due to damage to vehicles. This includes repair or replacement costs for vehicles, and revenue lost due to vehicle being out of work. It was calculated as explained below:

Vehicle Damage cost = [No. of total vehicles damaged] * [average vehicle damage *costs].*

*Vehicle Detention cost = Total numbers of vehicle repaired * Average vehicles repaired period *average revenue generated per day.*

3.5 Damage only crash cost

The cost associated with crashes that result in property damage but do not involve injuries or fatalities. The above crash cost component contribute to the total cost resulting from causality crashes. However, there are also a significant number of road-crashes which do not involve any causalities but vehicle damage or damage only road traffic crash. The cost for those vehicles having the minor type of damage which generally involved in road traffic crash but not reported were obtained from the inquiry with the Traffic Police according to which generally 40% total crash were damage only crash. Then the weighted average unit cost for the vehicles involved in damage only road traffic crash was determined with the percentage of involvement of vehicle in a road traffic crash was calculated. Finally, the total cost of damage only road traffic cost was calculated as the product of the number of vehicles involved in damage only crashes with the weighted average unit cost of vehicles.

3.6 Administrative cost

Police, court, and insurance costs are all included in administrative costs. First, the total resource cost was determined as recommended by the Transport Research Laboratory due to the challenge of measuring the administrative cost. The total resources cost was calculated by adding the costs of lost productivity, medical cost and property damage cost. For fatal crashes, the administrative cost was calculated to be 0.2% of the total resource cost. According to Silcock and Transport Research Laboratory (2003), the administration cost for major injury was calculated to be 4% of the total resource cost, whereas the administrative cost for minor crashes was calculated to be 14% of the total resource cost and 10% of damage-only crashes.

Total Cost of Road Crash=Total Causality Cost+ Total Damage Only Cost

4. Result and Discussion

4.1 Human Cost

4.1.1 Lost productivity

The average age of fatality was 38 and 37 years for respective fiscal year. The retirement age is 58 years. And the year lost for respective fiscal year was obtained by subtracting fatality age from retirement age which was found to be 20 and 21 years respectively.

The average rate was NRs. 1016 per day and NRs. 1065 per day for FY 2022-23 and FY 2023-24 respectively. The yearly wage rate per fatality was found to be NRs. 370,680 and NRs. 388563 respectively. As per 2017 RTI costing study in Nepal the total length of hospitalization was 7 days and follow-up days were 20. So, the total lost days for major injury was 27 days and 3 days for minor injury (Tiwari, H., Adhikari, A., & Bhatt, M. (2023)].

Table 1 Average lost output per Road Traffic Crashes

Lost output	Time	Cost/unit	Cost
Fatality			
F/Y 2022/23	20 years	NRs. 3,70,680 discounted @ 3%/yr.	NRs. 58,85,464
F/Y 2023/24	21 years	NRs. 3,88,563 discounted @ 3%/yr.	NRs. 63,78,264
Major			
F/Y 2022/23	27 days	NRs. 1016/day x 27	NRs.27,432
F/Y 2023/24	27 days	NRs. 1065/day x 27	NRs.28,755
Minor			
F/Y 2022/23	3 days	NRs. 1016/day x 3	NRs.3,048
F/Y 2023/24	3 days	NRs. 1065/day x 3	NRs.3,195

The average lost output per fatality, major injury and minor injury was found to be NRs.58,85,464, NRs. 27,432 and NRs. 3,048 respectively for FY 2022-23. For FY 2023-24 average lost output per fatality, major injury and minor injury was found to be NRs.63,78,264, NRs. 28,755 and NRs. 3,195 respectively.

Table 2 Total Cost of Lost Output of Road Traffic Crashes

Casualty	**Fatal Crash**					
	Cost per casualty (NRs.)		**No of casualty involved**		**Cost (NRs.)**	
F/Y	2022/23	2023/24	2022/23	2023/24	2022/23	2023/24
Fatality	5885464	6378264	1	1.02	5885464	6474905
Major	27432	28755	0.42	0.47	11472	13506
Minor	3048	3195	0.87	0.52	2660	1646
Care taker lost cost						
Major	27432	28755	0.42	0.47	11472	13506
Minor	3048	3195	0.87	0.52	2660	1646
Cost of lost output per fatal crash					5913728	6505209
Total cost of lost output for fatal crashes			55	66	325255027	429343787
Casualty	**Injury Crash**					
	Cost per casualty (NRs.)		**No of casualty involved**		**Cost (NRs.)**	
	2022/23	2023/24	2022/23	2023/24	2022/23	2023/24
Fatality	-	-	-	-	-	-
Major	27432	28755	1.32	1.14	36119	32666
Minor	3048	3195	0.78	0.69	2388	2198
Care taker lost cost						

Major	27432	28755	1.32	1.14	36119	32666
Minor	3048	3195	0.78	0.69	2388	2198
Cost of lost output per injury crash					77013	69728
Total cost of lost output for injury crashes			60	125	4620768	8715960
Total cost of lost output of RTC					329875795	438059747

The number of causality involved as fatality, major and minor injury was found to be 1, 0.42, 0.87 respectively per fatal crash for FY 2022-23 and for FY 2023-24 it was found to be 1.02, 0.47, 0.52 respectively. And per injury crash the number of causality involved as major and minor injury was found to be 1.32 and 0.78 respectively for FY 2022-23 and for FY 2023-24 it was found to be 1.14 and 0.69 respectively. The total cost of lost output was calculated as NRs. 329,875,795 and NRs. 438,059,747 for FY 2022-23 and FY 2023-24 respectively.

5.1.2 Quality of life costs

The amount earned is equal to lost productivity of fatalities and amount consumed was obtained from the study survey of Nepal living life standard from 1995 to 2023 conducted by National Statistical data found to be Nrs.156330 per year. Therefore, the cost of quality of life was found as NRs.151,721,047 and NRs.207366302 respectively for FY 2022-23 and FY2023-24.

5.1.3 Medical costs

The medical costs associated with road traffic crashes (RTC) in Kailali District for the fiscal years 2022–23 and 2023–24, broken down by crash type (fatal and injury) and severity (major and minor). For fatal crashes, the medical costs per casualty are highest for major injuries, with emergency costs (EC), medicine costs (MC), and other medical expenses totaling 177,405 NRs per casualty in 2022–23 and 181,590 NRs in 2023–24. Minor casualties in fatal crashes incur lower costs, with total costs per casualty around 26,727 NRs in 2022–23 and 27,850 NRs in 2023–24. The total medical cost of fatal crashes increased from approximately 4.26 million NRs in 2022–23 to 5.25 million NRs in 2023–24.

For injury crashes, major casualties also have the highest cost per casualty, averaging over 177,405 NRs in 2022–23 and 181,590 NRs in 2023–24, while minor casualties have significantly lower costs. The total medical cost of injury crashes rose sharply from around 12.2 million NRs in 2022–23 to 22.5 million NRs in 2023–24, reflecting both an increase in the number of casualties and higher treatment costs. Overall, the total medical cost of all road traffic crashes increased from about 20.63 million NRs in 2022–23 to 34.79 million NRs in 2023–24, indicating a substantial rise in the economic burden of traffic-related injuries and fatalities over the two-year period.

5.2 Property Damage Costs

5.2.1 Vehicle Damage Costs

The vehicle damage cost data has been analyze based on data obtained from insurance data and workshop data. From the insurance records, the amount paid for damage due to crash was obtained for each category of vehicles and same was also obtained from Workshop. The overall mean value was calculated. Thus, the overall mean value cost of Commercial vehicles, Private cars, and Motorcycles for FY2022-23 was NRs. 1,95,970, NRs. 2,16,500 and NRs. 71,261 respectively and similarly the overall mean value cost of Commercial vehicles, Private cars, and Motorcycles for FY2023-24 was NRs. 229,632, NRs.181,392 and NRs. 1,55,830 respectively.

Table 3 Average vehicle damage cost

Source	**Average Cost (NRs.)**					
	Commercial		**Private Car**		**Motorcycle**	
	22/23	**23/24**	**22/23**	**23/24**	**22/23**	**23/24**
Sagarmatha Insurance	134,623	272,419	168,139	165,330	168,879	364,781

NLG Insurance	201,189	279,575	197,528	370,400	26,827	111,250
IGI PRUDENTIAL INSURANCE LIMITED	166,150	219,571	198,833	71,200	38,750	90,000
Auto Repair Workshop	281,917	146,961	301,498	118,636	50,587	57,289
Overall average	195,970	229,632	216,500	181,392	71,261	155,830

Table 4 Net vehicle damage cost

Vehicle Type	F/Y	Repair Cost (NRs.)	Duty (25%) and Vat (13%) on spare parts (NRs.)	Estimated Salvage Value (NRs.)	Survey Fee (NRs.)	Net Vehicle Damage Cost (NRs.)
Commercial	22-23	195,970	49,646	19,597	12,000	138,727
	23-24	229,632	58,173	22,963	12,000	160,495
Private Car	22-23	216,500	54,847	21,650	10,000	150,003
	23-24	181,392	45,953	18,139	10,000	127,300
Motorcycle	22-23	71,261	18,053	7,126	9000	55,082
	23-24	155,830	39,477	15,583	9000	109,770

The net vehicle damage cost was calculated adding a survey fee to calculated overall mean value with deduction of salvage value and duties and a value-added tax of the spare parts. In this study, the cost of spare parts was assumed as 2/3 of the cost of repair with including 25% duty and 13% VAT as per 2007 RTC cost study. The salvage value was taken as 10% as per inquiry with insurance companies and also surveyor fee was obtained by consulting with insurance companies. Therefore, net vehicle damage cost for FY2022-23 for commercial vehicles, private cars and motorcycles was calculated as NRs. 138,727, NRs. 150,003 and NRs. 55,082 respectively and NRs. 160,495, NRs. 127,300 and NRs. 109,770 respectively for FY2023-24.

The vehicle damage cost per fatal crash was calculated as NRs.129,190 and NRs.191,007 per injury crash for FY2022-23 and for FY2023-24 vehicle damage cost per fatal crash was calculated as NRs.144,569 and NRs.196,132 per injury crash. Similarly, the total vehicle damage cost for fatal crashes was calculated as NRs.7,105,445 and NRs.9,541,566 for respective year. Also total vehicle damage cost for injury crashes was calculated as NRs.11,460,395 and NRs. 24,516,525 for respective year. The total vehicle damage cost of RTC was calculated as NRs.18,565,840 and NRs.34,058,091 for particular FY respectively.

Table 5 Total vehicle damage cost

	Fatal Crash						**Injury Crash**					
Vehicle damage cost	Average Repair cost (NRs.)		Number of vehicles involved		Cost (NRs.)		Average Repair cost		Number of vehicles involved		Cost (NRs.)	
	22-23	23-24	22-23	23-24	22-23	23-24	22-23	23-24	22-23	23-24	22-23	23-24
	114,604	132,522	1.13	1.09	129,190	144,569	114,604	132,522	1.67	1.48	191007	196,132

Total number of fatal crashes	55	66		Total number of injury crashes	60	125
Total vehicle damage cost for fatal crashes		7,105,445	9,541,566	Total vehicle damage cost for injury crashes	11460395	24,516,525
Total vehicle damage cost of RTC					**18,565,840**	**34,058,091**

5.2.2 Vehicle Detention Costs

The average vehicle detention cost per fatal crash was NRs.84,930 and NRs.46,165 respectively and per injury crash was NRs.103,393 and NRs.117,335 for respective fiscal year. For FY2022-23 the total vehicle detention cost for fatal and injury crash was NRs.4,671,162 and NRs.3,046,871 respectively. and FY2023-24 the total vehicle detention cost for fatal and injury crash was NRs.6,203,599 and NRs.14,666,912 respectively Therefore, total cost of vehicle detention was calculated as NRs.10,874,761 and NRs.17,713,782 for FY2022-23 and FY2023-24 respectively.

5.3 Damage only Crash Costs

The total numbers of damage only crash was obtained as 85 and 125 respectively for FY 2022-23 and FY 2023-24. The average repair cost for damage only crash was calculated as NRs. 20,361 and NRs. 34,000 respectively. The number of vehicle involvement per damage only crash was obtained as 1.67 and 1.49 for respective FY which was determined by dividing the value of the difference between the total number of vehicle involvement and number of vehicles involved in fatal crash with the value of the difference between total road crash and fatal road crash. The cost per damage only crash of vehicles was NRs. 33,935 and NRs.50,726 respectively for FY2022-23 and FY2023-24. And the total damage only crash cost of the vehicle was calculated as NRs.2,884,491 and NRs. 6,340,726 for respective fiscal year.

5.4 Administrative Costs

The administrative cost per fatal crash was NRs.15,844 and NRs.18,664 for respective fiscal year and administrative cost per injury crash was NRs. 112,668 and NRs.109,593 for respective year. The administrative cost for damage only crash per crash was NRs.3,394 and NRs.5,073 for respective year. The total administrative cost for fatal crash was Nrs.871,433 and Nrs.1,231,828 for respective fiscal year and for injury crash it was NRs.6,760,076 and NRs.13,699,125 respectively for respective fiscal year. Therefore, the total administrative cost was NRs. 7,631,509 and NRs. 14,930,953 respectively for respective year.

5.5 Total Crash Costs

The total cost of casualty crashes in Kailali District for the year 2022-2023 and 2023-2024 was NRs.524,187,855 and NRs.753,262,918 respectively.

Table 6 Total crash cost and component contribution

Cost Component	**Total Cost (NRs.)**		**Percentage**	
	F/Y: 2022-23	**F/Y: 2023-24**	**F/Y: 2022-23**	**F/Y: 2023-24**
Lost Output	329,875,795	438,059,747	60.84%	58.15%
Quality of life	151,721,047	207,366,302	27.98%	27.53%
Medical Cost	20,634,412	34,793,316	3.81%	4.62%

Property damage cost	29,440,601	51,771,874	5.43%	6.87%
Damage Only Crash	2,884,491	6,340,726	0.53%	0.84%
Administrative cost	7,631,509	14,930,953	1.41%	1.98%
Total	542,187,855	753,262,918	100%	100%

The largest contribution to costs is lost output, which accounted for 60.84% in 2022–2023 and 58.15% in 2023–2024. As the quality of life lost cost was calculated using net output method it results as the second highest contributor making up 27.98% in FY2022–23 and 27.53% in FY2023–24.

In FY 2023–2024, the percentage of medical expenses increased from 3.81% in FY 2022–2023 to 4.62%. This rise implies that increasingly severe injuries requiring continuous care are placing a greater burden on the healthcare system. The cost of property damage increased significantly from 5.43% in FY 2022–2023 to 6.87% in FY 2023–2024.

Similarly administrative cost and damage only crash contribute 1.41% and 0.53% respectively for FY2022–23 and 1.98% and 0.84% respectively for FY2023–24.

5. Conclusion

Road traffic crash costing provides the basis for the allocation of sufficient financial resources to decision maker and to those concerned with road safety. Human capital approach method was used for calculating the total road crash cost.

Traffic crash costs in Kailali District was found to be increased by 38.93% from NPR 542.19 million during FY 2022–2023 to NPR 753.26 million during FY 2023–2024. The highest cost component of the road crash cost was lost productivity.

The analysis reveals that traffic crashes place a substantial financial burden on society, arising not only from serious injuries and fatalities but also from minor crashes and the administrative costs associated with them. Although damage-only and administrative expenses account for a smaller share of the total cost, their rising trend suggests that even minor crashes are becoming increasingly costly. These findings underscore the importance of implementing comprehensive strategies aimed at reducing both the frequency and severity of traffic crashes, thereby lessening their overall economic impact.

7. Recommendation and future study

The achieved results and findings of the total road traffic crash cost study in Kailali district using HC crash costing valuation method highlighted the following recommendation as below:

- It would be better to consider the costs from government and private hospitals separately rather than using just an average rate. Doing this would give a clearer and more accurate picture of crash costs.
- There are some crash cost components such as loss due to non- vehicle damage cost, long term disability cost and travel delay cost for road users, which have not been included in this study due to lack of data. These three cost component would be part future crash costing studies in Kailali District.

8. References

Adam I. A. Mofadal*, K. K. (2016). Analysis of road traffic accident costs in Sudan using the Human Capital Method. Open journal of civil engineering, 203-216.

Administration, O. D. (1995), Costing road accident in developing countries. United Kingdom.

Atreya, A., Shrestha, D. B., Budhathoki, P., & Nepal, S. (2021). Epidemiology of road traffic accidents in Nepal from 2009/10 to 2019/20: a 10 year study.

Banstola, A., Kigozi, J., Barton, P., & Mytton, J. (2020). Economic burden of road traffic injuries in Nepal. International journal of environmental research and public health, 17(12), 4571.

Bishwokarma, S., Adhikari, C., Khatri, D., Gauchan, B., Sapkota, V. P., & Ranabhat, C. L. (2022). Multiple Burdens of Road Traffic Crashes in Pokhara, Nepal: A Patient Approach. medRxiv, 2022-05.

Carozzi S, Elorza ME, Moscoso NS, Ripari NV. Methodologies for estimating the indirect costs of traffic accidents. Revista Médica del Instituto Mexicano del Seguro Social. 2017 Aug 15;55(4):441-51.

Central Bureau of Statistics (CBS). Nepal Living Standards Survey 2023 Report. Government of Nepal, 2023.

Chin, H. C., Haque, M.M. and Jean,Y.H (2006). An estimate of road accident costs in Singapore. (pp. 28-35). International conference on road safety in developing countries.

Dhakal, K. P. (2018). Road traffic accidents in Kathmandu valley. Journal of Health Promotion, 6, 37-44.

FAHAD ALRUKAIBI, '. A. (2015). Methodology for calculation of the traffic accidents costs.

Huang, L., Adhikary, K. P., Choulagai, B. P., Wang, N., Poudyal, A. K., & Onta, S. R. (2016). Road traffic accident and its characteristics in kathmandu valley. Journal of the Nepal Medical Association, 55(203).

Joshi, S.K. and Shrestha, S., 2009. Economic and social burden due to injuries and violence in Nepal: a cross-sectional study. Kathmandu University medical journal, 7(4), pp.344-350.

Karkee, R., & Lee, A. H. (2016). Epidemiology of road traffic injuries in Nepal, 2001–2013: systematic review and secondary data analysis. BMJ open, 6(4), e010757.

Kuikel J, Aryal B, Bogati T, Sedain B. Road traffic deaths and injuries in Kathmandu. Journal of Health Promotion. 2022 Dec 31;10(1):73-88.

Maen Ghadi, A. T. (2017). Study of Economic Cost of road accident in Jordan. Periodica Poltechnica Transportation Engineering.

Mohammad Reza Ahaid, H. R. (2015). Estimating the cost of road traffic accident in Iran suing Human Capital Method. International journal of transportation Engineering, 2(3).

Nepal Law Commission (1993) Civil Service Act,Chapter 6 Retirement, Gratuity and Pension. Available at: https://www.lawcommission.gov.np/en/archives/20280# (Accessed: 4 April 2021).

Pachaivannan Partheeban, E. A. (2008). Road accident cost prediction model using systems dynamics approach. Transport, 59-60.

Parkinson, F., Kent, S. J. W., Aldous, C., Oosthuizen, G., & Clarke, D. (2014). The hospital cost of road traffic accidents at a South African regional trauma centre: a micro-costing study. Injury, 45(1), 342-345.

Poudel-Tandukar, K., Nakahara, S., Poudel, K. C., Ichikawa, M., & Wakai, S. (2004). Traffic fatalities in Nepal. JAMA, 291(21), 2542-2542.

Risbey, T., de Silva, H., & Tong, A. (2007). Road crash cost estimation: A proposal incorporating a decade of conceptual and empirical developments. Canberra, Australia: Bureau of Transport and Regional Economics.

Samikshya Rizal, H. T. (2023). Analysis of Road Traffic Crash Cost in Kathmandu valley. 2nd International conference on integrated Transport for Sustainable Mobility.

Silcock R. Guidelines for estimating the cost of road crashes in developing countries. London: Department for International Development. 2003 May.

Silcock, R. (2003). Guidelines for estimating the cost of road crashes in developing countries.

Sumayya Naznin P H, S. A. (2023). Human capital Approach for road accident in an Indian city. European Transport/ Irasporti Europei.

Ting Lian, B. P. (2024). Communications in transportation research. Communication in transportation research.

Wijnen, W., & Stipdonk, H. (2016). Social costs of road crashes: An international analysis. Accident Analysis & Prevention, 94, 97-106.

Journal on Transportation System and Engineering
ISSN: 3059-9865(Print) 3059-9873(Online)
Vol. 1. Issue 2 (December) 2025: 128-136
DOI: https://doi.org/10.3126/jotse.v1i2.87766

Research Article
Received Date: May 20, 2025
Revised Date: October 10, 2025
Accepted Date: November 2, 2025

The Push-Pull Effects of Expressways: The Case of TPLEX for Baguio City, Philippines

Daniel L. Mabazza[a], Glenn Simon Latonero[b]

[a]*Department of Geography, College of Social Sciences and Philosophy, University of the Philippines, Diliman,* Quezon City, 1101, *Philippines*
[b]*National Center for Transportation Studies, University of the Philippines, Diliman,* Quezon City, 1101, Philippines

Abstract

This study investigates the impact of the Tarlac-Pangasinan-La Union Expressway (TPLEX) on the tourism industry of Baguio City, Philippines. By analyzing historical trends in tourist arrivals and expressway development, the study establishes a strong correlation between increased accessibility and heightened visitor influx. Findings indicate that expressway openings reduced travel time and stimulated continuous tourism growth, even beyond traditional peak seasons. These results confirm the role of expressways in overcoming the friction of distance and illustrate their push-pull effects on urban mobility. The study highlights the need for integrated planning to mitigate potential congestion and suggests further research on employment shifts and regional migration patterns.

Keywords: Expressways; Tourism; Friction of Distance; Time-Space Convergence

1. Introduction

There is a huge literature that discusses the effects of expressways in overcoming the friction of distance. This has been repeatedly demonstrated in many case studies. One of which is the situation for places that are considered tourist destinations that are experiencing huge numbers of tourist arrivals to a point where there is a growing concern among local residents due to congestion not only during vacation period but also during weekends on a regular period or season. There is a growing belief that this was attributed to the opening of the expressways that made travel between the origin and destination cities shorter. This is the subject of this paper using the case study of the TPLEX opening that made the difference to travelling between the Metropolitan Manila and Baguio City. This paper will investigate if there is indeed a correlation between the opening of the expressway, particularly the TPLEX, in the increase in the tourist arrivals in the tourist destination city (see Figure 1).

Baguio City, Philippines, often called the "Summer Capital of the Philippines," is a premier tourist destination known for its cool climate, scenic mountain landscapes, and vibrant cultural heritage. Nestled in the Cordillera Central Mountain range at approximately 1,540 meters above sea level, the city offers breathtaking views of pine-covered hills, lush gardens, and picturesque valleys.

Tourists flock to Baguio for its refreshing weather, especially during the summer months when temperatures in the lowlands soar. Baguio is also a cultural hub, home to the indigenous Cordilleran communities, whose traditions are reflected in local crafts, festivals, and cuisine. The annual Panagbenga Festival, or Flower Festival, is a major draw, featuring grand parades and street dances celebrating the city's floral abundance.

1.1 Transportation Context of Baguio City

Baguio City, located approximately 246 km north of Metro Manila, has traditionally relied on a national public road named MacArthur Highway for connectivity. Before the TPLEX development, travel between Manila and Baguio took around 6–8 hours via congested roads. The majority of visitors originated from Metro Manila and neighboring regions such as Central Luzon (north of Metro Manila) and CALABARZON (south of Metro Manila), often using intercity bus services and private vehicles. These regions including Metro Manila is the concentration of people in the country where the spread effects of development and urbanization from the capital region spillover. These transportation modes faced capacity constraints and frequent delays, especially during peak seasons (vacation and long weekends due to holidays). With the introduction of Subic-Clark-Tarlac Expressway (SCTEX) and eventually TPLEX, expressway infrastructure enabled smoother and faster access. However, a formal study

Corresponding author's email address dlmabazza@up.edu.ph

on modal share changes is lacking. Preliminary government reports suggest that more than 70% of tourists still rely on road-based modes, with a gradual shift toward private car use due to travel time reductions and toll efficiency.

2. Scope and Objectives

This study seeks to investigate the multifaceted relationship between expressway infrastructure and regional tourism development, with a particular focus on the Tarlac-Pangasinan-La Union Expressway (TPLEX) and its influence on Baguio City. Specifically, it aims to examine the correlation between the construction and operationalization of TPLEX and the observed increase in tourist arrivals in the city. The research also assesses how enhanced accessibility and reduced travel time have reshaped tourism dynamics across the region, potentially redistributing visitor flows and altering travel behavior. Furthermore, the study explores the "push-pull" mechanisms by which expressways affect urban mobility and destination attractiveness, offering insights into how transport infrastructure can simultaneously facilitate outbound movement and stimulate inbound tourism demand.

3. Review of Relevant Literature

The development of expressways plays a critical role in shaping economic activity, tourism, and population movement in different regions. Several studies have examined the correlation between expressways and destination attractiveness, focusing on economic impacts, accessibility improvements, and demographic shifts.

Expressways are widely recognized as economic catalysts, enhancing regional accessibility and promoting investment opportunities. A study by Komori et al. (1998) applied Benefit Incidence Analysis to assess how improved transport networks influence local economies, showing that regions connected by expressways experience higher economic growth due to reduced logistics costs and increased business activities. The presence of expressways enables agglomeration effects, wherein businesses and industries cluster around key transport corridors, further stimulating economic development.

Figure 1 Map of Major Expressways in Luzon: TPLEX, SCTEX, NLEX, and SLEX

The impact of expressways on tourism is another widely studied area. Several researchers emphasize that expressway connectivity reduces travel time and costs, thereby making destinations more attractive to tourists. This

is particularly relevant for regions relying on domestic visitors, as seamless transportation networks encourage short-term travel and weekend tourism. The study by Mabazza and Tamura (2010) on toll-free expressways in Japan observed that making expressways free resulted in a higher influx of travelers, boosting local tourism-related businesses such as hospitality, food services, and leisure activities.

Figure 2 Map of the Tarlac-Pangasinan-La Union Expressway (TPLEX) with Sections and Interchanges

The expansion of expressways significantly influences population mobility and settlement patterns. The study by Allen and Sangler (1981) introduced a self-organization model to explain how expressways shape urban migration. Their model suggests that improved transport infrastructure contributes to a "push-pull effect", where people move toward urban centers due to better job opportunities, amenities, and reduced commuting costs.

4. Limitations of the Study

This study was limited by the availability and completeness of data. Tourist arrival figures were only available on an annual basis, which constrained the analysis of monthly or seasonal variations. The AADT (Annual Average Daily Traffic) data for TPLEX were not fully obtained due to limited time for data collection and coordination with concerned agencies. As a result, the study relied on partial data from selected exits and years (2020–2024), restricting the depth of correlation analysis between vehicle flow and tourist arrivals.

Additionally, the study used secondary data without accounting for other influencing factors such as fuel prices, toll rate changes, local events, and post-pandemic recovery effects. The absence of detailed travel mode and demographic data also limited behavioral insights. Future research should secure more comprehensive datasets and longer observation periods to strengthen the analysis and validate the expressway's long-term impact on regional tourism

5. Methodology

5.1 Research Design

This study employs a quantitative research approach to examine the correlation between expressway development and tourist arrivals in Baguio City. A longitudinal study design is used to analyze historical trends in tourism data and expressway developments over time. The research will utilize statistical modeling and time-series

analysis to assess the relationship between expressway expansion, accessibility improvements, traffic volume, and changes in tourist volume.

5.1.1 Data Collection

Two primary datasets will be analyzed:

1. Tourist Arrival Data – This dataset serves as the dependent variable, reflecting the number of visitors to Baguio City.
2. Expressway Data – This includes information on expressway openings, expansions, travel time reductions, toll policies, and traffic volume data to capture usage intensity and access levels. These variables will serve as independent factors in analyzing their effect on tourism dynamics.

a. Dependent Variable: Baguio City Tourist Arrivals

- Source: City Government of Baguio
- Data Type: Monthly or annual tourist arrivals
- Coverage Period: At least 10 years (to capture trends before and after major expressway developments)
- Variables Collected: Total tourist arrivals, Domestic vs. international visitors, Seasonal variations (e.g., peak and off-peak seasons)

b. Independent Variables: Expressway Infrastructure Data

- Source: Toll Regulatory Board (TRB), Expressway Operators (e.g., Private Infrastructure Development Corporation or PIDC)
- Key Expressways Considered: Tarlac–Pangasinan–La Union Expressway (TPLEX) – Primary route to Baguio
- Variables Collected: Expressway opening and expansion timelines (e.g., interchange openings), Travel time reductions from Manila to Baguio, Toll policy (toll rates or toll-free periods), Traffic volume data (e.g., Annual Average Daily Traffic per segment) – to represent actual expressway utilization, particularly during peak tourist seasons

5.2 Operationalizing the Push-Pull Framework

The concept of 'push-pull' effects in transport and tourism studies refers to two complementary forces: 'push' factors, which compel people to leave their place of origin (e.g., congestion, stress, climate), and 'pull' factors that attract them to a specific destination (e.g., cooler weather, festivals, scenic landscapes). In this study, we used the correlation between tourist arrivals and vehicle throughput at TPLEX exits, particularly Rosario, to validate this framework. Expressways reduce travel time (push from city), while Baguio's climate and culture attract (pull to periphery). The strong statistical relationship between traffic and tourism demonstrates how these effects operationalize through infrastructure.

This study confirms that expressway infrastructure such as TPLEX significantly contributes to the tourism growth of Baguio City. Findings revealed a strong correlation between Annual Average Daily Traffic at TPLEX exits—especially Rosario—and increased tourist arrivals. The expressway's travel time reductions and direct access to highland roads have operationalized the push-pull framework, where urban residents are 'pushed' from congested centers and 'pulled' toward accessible, appealing destinations. These findings are consistent with the self-organization and time-space convergence models described in prior transport studies (Allen & Sangler, 1981; Yamaguchi et al., 1990). Future studies should examine regional employment shifts and migration to deepen our understanding of expressway-induced mobility changes.

6. Results and Discussion

The series of opening the expressways initially by the addition of SCTEX (Subic Clark Tarlac Expressway) in 2008 decreased the friction of distance (or the time cost) between the Manila and Baguio corridor since the segment provided an alternative route for faster travel. The staggered opening of TPLEX (Tarlac Pangasinan La Union Expressway) in November 2013 until the Rosales interchange that moved closer the alternative route to the destination. This resulted in the continuous increase in the tourist arrival until the year 2018 when it peaked at 1,760,729 tourist arrivals (see Figure 2) along with the opening of the Binalonan interchange in the year 2016 and the Pozorrubio interchange in the year 2017 (see Figure 3). This confirms the positive correlation between the additional openings of the interchanges that are closer to the destination and the increase in the number of tourist arrivals in the destination. There was a slight decrease in the year 2019 that is a little more than the year 2017 level

for unverifiable reasons and a drop in the year 2020 when the pandemic started in spite of the opening of the Rosario interchange (the latest and the closest to the destination) that opened on 15 July 2020.

The concluding period of the pandemic in the year 2022 resulted in the dramatic increase and steep slope between 2021 and 2022 tourist arrival which reached the level slightly lower than the pre-pandemic year of 2015. The year 2023 reached the level that is slightly higher than the year 2016 and the last year 2024 reached the level that is higher than the years 2017 and 2018 levels. Upon observation, there is a tendency that it is reaching the peak year of 2019 if all other factors remain constant (see figures 2 and 3).

Figure 3 Baguio City Tourist Arrival (2011-2024)

Table 1 presents the Annual Average Daily Traffic (AADT) counts for northbound traffic at selected exits along the Tarlac–Pangasinan–La Union Expressway (TPLEX) from 2020 to 2024. The data reflects a clear upward trend in vehicle volume across the Rosario, Pozorrubio, Binalonan, and Sison exits, key interchanges for motorists en route to Baguio City via Marcos Highway and Kennon Road.

The Rosario Exit, being the last exit of TPLEX and the nearest to Baguio, recorded a dramatic increase in AADT from 250,617 in 2020 to nearly 2 million in 2024. This suggests that Rosario has become the dominant egress point for tourists and private vehicles heading to Baguio, likely due to its direct access to both Marcos Highway and Kennon Road, the two primary mountain roads leading to the city. Notably, Rosario Exit's AADT surged by over 680% in just four years, a strong indicator of post-pandemic travel recovery and growing road dependence for leisure trips to the highlands.

Similarly, traffic volumes at Binalonan Exit increased significantly from 183,005 in 2020 to 412,429 in 2024, while Pozorrubio Exit, though experiencing a dip in 2021, recovered steadily, reaching 169,036 in 2024. The upward trend at these exits reflects their strategic role as alternate approaches to the city, especially during times when Rosario becomes congested.

The Sison Exit, while still posting the lowest traffic figures among the four, displayed notable growth from 17,178 in 2020 to 148,549 in 2024, suggesting that even peripheral exits are seeing increased use. This uptick may be attributed not only to local tourism and alternate route diversions but also to the presence of popular stopover establishments in the Sison area that cater to both buses and private vehicles. These rest areas and roadside eateries serve as key breakpoints for meals, refreshments, and refueling before travelers continue their ascent to Baguio via Marcos Highway or Kennon Road. As such, Sison functions as a strategic pause point, enhancing the overall travel experience and encouraging continued usage of this exit despite it being slightly more distant from the city proper.

Table 1 TPLEX Annual Average Daily Traffic (AADT) Northbound

Toll Plaza	2020	2021	2022	2023	2024
	Northbound	Northbound	Northbound	Northbound	Northbound
Rosario Exit	250,617	798,669	1,544,612	1,878,848	1,962,804
Sison Exit	17,178	101,382	184,122	166,041	148,549
Pozzorubio Exit	531,349	113,875	141,851	161,544	169,036
Binalonan Exit	183,005	209,778	362,647	405,261	412,429

6.1 Correlation Between Vehicle Volume and Tourist Arrivals

Figure 3 illustrates the correlation between northbound vehicle volume at the Rosario Exit of TPLEX and annual tourist arrivals in Baguio City over the 5-year period from 2020 to 2024. A clear positive relationship is observed between the two variables, indicating that increases in vehicle throughput through the Rosario Exit are strongly associated with higher tourist inflows into the city.

Notably, the trend line (dotted) demonstrates a strong linear correlation, with the slope suggesting that Baguio's tourist arrivals tend to rise proportionally with the volume of vehicles entering through the Rosario Exit—recognized as the closest expressway access point to the city. This reflects how improvements in regional accessibility translate into greater tourism activity, particularly post-2020 when mobility restrictions began to ease.

The significant jump in both traffic and tourist numbers between 2021 and 2022 supports the hypothesis that expressway use is a key predictor of tourism demand. The dip in tourist arrivals in 2021 despite high traffic suggests the presence of pandemic-related travel hesitations, but the sharp rise afterward reinforces the pent-up demand for leisure travel once conditions normalized.

This correlation further validates the push-pull effects framework, where the reduction in travel time and road friction (enabled by the expressway system) "pulls" visitors to upland destinations like Baguio, especially on weekends and holidays. The Rosario Exit thus acts not only as a physical gateway but as a quantifiable mobility indicator directly tied to tourism flows.

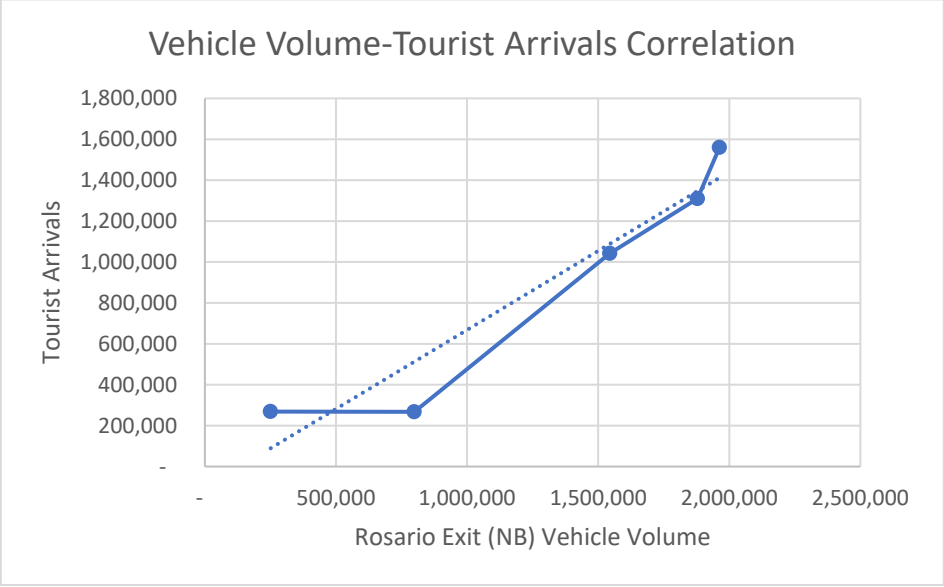

Figure 4 Vehicle Volume – Tourist Arrivals Correlation (Rosario Exit (NB)

Figure 4 illustrates the correlation between tourist arrivals in Baguio City and the northbound traffic volumes at four key TPLEX exits: Sison, Pozorrubio, Binalonan, and Rosario—from 2020 to 2024. The tourist arrivals line (yellow) is plotted against the traffic volume data for each exit to examine how closely each location aligns with visitor influx trends.

A clear pattern emerges showing that exits closest to Baguio, especially Rosario Exit, have the strongest positive correlation with rising tourist arrivals. The Rosario Exit, located at the northern terminus of TPLEX and directly feeding into Marcos Highway and Kennon Road, shows a steep upward trend aligned with Baguio's increasing tourist arrivals. This correlation affirms its role as the primary gateway to the city for private vehicles and tour

buses. The area around Rosario also features several bus stopovers, rest areas, and food establishments, making it an ideal final stop before the ascent to Baguio. These amenities likely encourage higher usage, especially for long-distance travelers.

The Binalonan Exit, also used as an alternative access point via local roads, shows moderate correlation and consistent growth in traffic volume. This supports its function as a secondary route for both regional traffic and leisure travelers, especially during congestion on Marcos Highway.

The Pozorrubio Exit, despite a strong start in 2020, exhibits a weaker and even declining correlation with tourist arrivals in the latter years. This might reflect shifting traveler preferences toward exits closer to Baguio or the opening of newer interchanges. Additionally, Pozorrubio's connectivity to the mountain roads may not be as direct or time-efficient compared to Rosario.

Sison Exit, while posting the lowest traffic volume, has shown a steady increase in use and maintains a gentle upward trend. The presence of bus and private car stopovers in the Sison area may partly explain this growth, as it serves as a rest-and-refresh point for motorists before heading to Baguio's upland terrain.

Overall, the figure confirms that proximity to Baguio and the presence of rest facilities are key factors influencing expressway exit choice. The closer the exit is to Baguio City, the more strongly its vehicle volume correlates with tourist influx—underscoring the importance of last-mile infrastructure and traveler convenience in shaping mobility behavior.

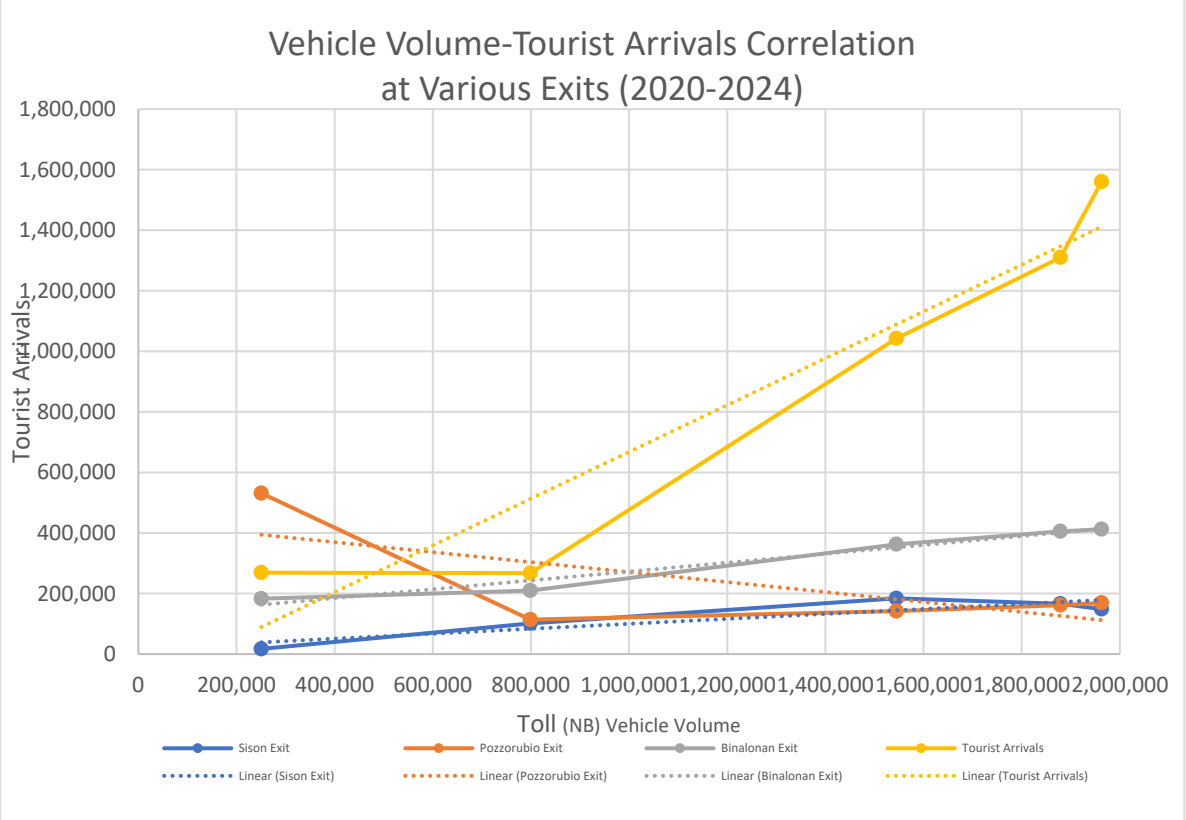

Figure 5 Vehicle Volume-Tourist Arrivals Correlation at Various Exits (2020-2024)

6.2 Travel Time

The completion of the Tarlac–Pangasinan–La Union Expressway (TPLEX) brought a substantial reduction in travel time between Metro Manila and Baguio City. Prior to TPLEX, motorists relied on the MacArthur Highway, a national road prone to congestion and frequent slowdowns due to urban settlements and mixed traffic conditions.

6.2.1 Travel Time Comparisons

Pre-TPLEX (via MacArthur Highway): Estimated travel time from Manila to Rosario, La Union (the terminus of TPLEX and gateway to Baguio) ranged between 5 to 6 hours, or longer during peak seasons.

Post-TPLEX (via Expressway): Travel time was projected to decrease to approximately 3.5 to 4 hours with the completion of the TPLEX segments, particularly between Tarlac City and Rosario.

According to the DPWH Feasibility Study conducted prior to project implementation: *"The construction of the TPLEX will reduce travel time from Tarlac City to Rosario, La Union from 3.5 hours to about 1 hour. This 2.5-hour reduction is expected to improve connectivity, reduce vehicle operating costs, and increase access to tourism and commercial centers in Northern Luzon."— DPWH Feasibility Study for the Tarlac-Pangasinan-La Union Expressway Project, 2007*

This projection emphasized the critical role of travel time savings in improving economic efficiency, encouraging tourism, and facilitating interregional movement. The study further justified user willingness to pay toll fees in exchange for faster, more reliable travel.

5.2.2 Value of Time: Users Substituting Money for Time

The expressway's success also reinforces a key behavioral insight in transport economics: travelers are willing to substitute money for time savings. By choosing TPLEX over free but slower alternatives like MacArthur Highway, motorists—especially tourists—demonstrate a clear preference for faster and safer routes. This is particularly relevant in leisure travel, where the value of time is often heightened by the limited duration of holidays or weekends.

The same feasibility study also indicated that:*"The value of time savings was a major component in the cost-benefit analysis, and was used to justify the investment through reduced travel time for private vehicles, buses, and freight carriers."*

Pre-construction feasibility studies for TPLEX projected strong time-saving and economic development benefits, especially for the northern Luzon corridor. These studies estimated:

- Increased vehicle throughput (over 20,000 vehicles/day),
- Greater efficiency in logistics and tourism travel,
- Enhanced regional competitiveness for provinces along the route.

7. Conclusion

The result of the correlation between the openings of the expressways along with the staggered openings that comes closer to the destination, and the increase in the number of tourist arrivals in next years illustrated the push from the populous national capital region where administrative, business and commerce, and employment are concentrated to the pleasure periphery that pulls them in this tourist destination. It further validates the observation and impression among the locals of the destination that the expressways made it easier for the tourists to move to this popular destination that high tourist arrivals are not only felt during holidays, and long breaks but also during weekends during ordinary weeks. It fortifies the concept of Time-Space Convergence was achieved in overcoming the friction of distance. Hence the push and pull effects were operationalized by the expressway openings.

The inclusion of employment, population changes, and gravity models that illustrate regional movement should be included in the improvement of this paper.

8. References

Allen, P. M., & Sangler, M. (1981). Urban evaluation, self-organization, and decision-making. Environment and Planning A, 13, 167–183.

Department of Public Works and Highways (DPWH), Feasibility Study for the Tarlac-Pangasinan-La Union Expressway Project, 2007

Komori, U., Ueda, K., et al. (1998). Benefit incidence analysis of the improvement of transport network with increasing returns. Infrastructure Planning (JSCE), 15(1), 205–215.

Mabazza, D., & Tamura, T. (2010). Effects of Toll-Free Expressways on Population Movement in Hokkaido, Japan.

Philippine Daily Inquirer, New route to speed up travel to north. Retrieved from https://newsinfo.inquirer.net/594260/new-route-to-speed-up-travel-to-north

Port Calls, TPLEX final section now open, cuts by half travel time between Baguio and Manila. Retrieved from https://portcalls.com/tplex-final-section-now-open-cuts-by-half-travel-time-between-baguio-and-manila/

Port Calls. TPLEX final section now open, cuts by half travel time between Baguio and Manila. Retrieved from https://portcalls.com/tplex-final-section-now-open-cuts-by-half-travel-time-between-baguio-and-manila

Sasaki, T., et al. (2001). Study in a straw effects of highway construction: A case study of Yubari-Shimizu highway. Infrastructure Planning Review, 18(1), 155–161

Yamaguchi, K., et al. (1990). A study on self-organization model of regional population distribution: The case of Hokkaido. Journal of Pavement Engineering, JCSE, 46, 475–480.

Journal on Transportation System and Engineering
ISSN: 3059-9865(Print) 3059-9873(Online)
Vol. 1. Issue 2 (December) 2025: 112-127
DOI: https://doi.org/10.3126/jotse.v1i2.87765

Research Article
Received Date: March 30, 2025
Revised Date: October 28, 2025
Accepted Date: November 27, 2025

Transit-Oriented Development Indicators for Suburban Railway Stations in Thailand: A Context-Specific Fuzzy Delphi Approach

Chaiwat Sangsrichan[a], Patcharida Sungtrisearn[a], Preda Pichayapan[b,*]

[a]*Doctor of Philosophy Program in Civil Engineering, Faculty of Engineering, Chiang Mai University, Chiang Mai, Thailand*
[b]*Department of Civil Engineering, Faculty of Engineering, Chiang Mai University, Chiang Mai, Thailand*

Abstract

This study identifies suitable indicators for Transit-Oriented Development (TOD) in suburban areas of Thailand using the Fuzzy Delphi Method to gather expert consensus. While TOD has been extensively studied in urban cores, suburban regions with distinct characteristics, including lower densities, tropical climates, and prevalent informal transportation, have received limited attention. The research examined 48 indicators from international literature across three components: Transit System Indicators, Oriented System Indicators, and Development System Indicators. Through two rounds of expert consultation with ten professionals, 44 indicators were accepted, while four were rejected as being contextually inappropriate. Train service frequency (0.950), pedestrian walkway width (0.940), and mixed land use (0.940) emerged as the highest priorities. Rejected indicators included station retail outlets (0.710), pedestrian pathway gradient (0.670), high-rise building areas (0.670), and government service centers (0.677), revealing fundamental differences between suburban and urban TOD contexts. Three key themes emerged: climate-responsive infrastructure is essential in tropical environments, informal transportation modes require integration rather than elimination, and suburban development should pursue moderate-density horizontal mixed-use patterns rather than high-density urban forms. These findings provide practical guidance for evaluating and planning TOD around Thailand's expanding suburban railway network, supporting effective resource allocation and implementation strategies aligned with suburban realities while advancing sustainable mobility objectives.

Keywords: Transit-Oriented Development Indicators; Transit-Oriented Development; Fuzzy Delphi Method; Suburban; Railway Station

1. Introduction

Transit-Oriented Development (TOD) has emerged as a crucial concept in urban planning and the development of public transportation systems, emphasizing the creation of dense communities, mixed land-use patterns, and pedestrian-friendly environments (Ibraeva, A., et al., 2012; Vale, 2015). This approach has gained widespread recognition as a key strategy for reducing private vehicle dependency and promoting sustainable mobility (Loo, B. P. Y., & du Verle, F., 2016). However, while most TOD studies and applications focus on urban core areas, suburban regions with their distinct characteristics and challenges have received relatively little attention (Pengjun, Z., & Shengxiao, L., 2018).

Thailand is currently experiencing rapid urbanization and suburban expansion, particularly in peripheral metropolitan areas. This growth presents significant challenges in transportation planning and land-use management, characterized by low population density, high private vehicle dependency, and land-use patterns that differ substantially from those in urban cores (Kamruzzaman et al., 2014; Singh et al., 2014). The Thai government has invested substantially in expanding the regional railway network, with four major corridors spanning over 2,680 kilometers and serving 92 stations connecting suburban areas to urban centers. Research by Bolleter, J., & Ramalho, C.E. (2020) indicates that implementing Transit-Oriented Development (TOD) in suburban areas is more complex than in urban cores, requiring consideration of distinct accessibility factors and diverse transit connectivity needs.

The fundamental challenge in Thai suburban TOD implementation lies in the direct application of urban-centric principles without considering context-specific factors. Unlike dense urban cores, where TOD principles have proven effective, suburban areas in Thailand face different realities that significantly impact TOD feasibility and design. Additionally, the prevalence of informal transportation modes, particularly motorcycle taxis, which provide flexible first- and last-mile connectivity, necessitates station area designs that accommodate these services rather than exclude them.

* Corresponding author. *E-mail address:* preda.p@cmu.ac.th

The cultural preferences for low-rise residential developments, fresh markets, and community-based activity spaces further distinguish Thai suburban contexts from Western models typically featured in TOD literature.

The absence of appropriate indicators hinders urban planners' and policymakers' ability to accurately evaluate Transit-Oriented Development (TOD) projects in suburban contexts, potentially leading to suboptimal development strategies (Schlossberg, M., et al., 2004). Developing suitable indicators for suburban TOD assessment is crucial, as indicators designed for urban cores may not fully capture the specific context and challenges of suburban areas. Previous studies have identified numerous indicators for evaluating TOD potential (Vale, 2015; Singh et al., 2014; Kamruzzaman et al., 2014), yet most originate from research conducted in urban core areas of developed countries with temperate climates and formal transportation systems. The direct application of these indicators to Thai suburban contexts may lead to misguided planning priorities, such as emphasizing high-density vertical development when moderate-density horizontal integration may be more culturally appropriate and economically viable.

To address these challenges, this study applies the Fuzzy Delphi Method, which has proven effective in urban planning and transportation research (Abdullah, R., et al., 2024). This approach combines expert knowledge with fuzzy logic to manage uncertainty and subjectivity in expert opinions. Rather than comprehensively examining all possible TOD factors, this research focuses on identifying which indicators, derived from international literature, are most relevant and applicable to the Thai suburban context. The study examines three critical components: transit systems, accessibility and connectivity, and spatial development, providing a comprehensive framework for evaluating TOD potential in suburban contexts while specifically addressing Thai challenges, including climatic impacts on walkability, integration of informal transport modes as intermodal transfer facilitators, and appropriate development densities that respect local cultural and market conditions.

The specific research objectives are: (1) to systematically compile TOD indicators from international literature relevant to suburban contexts; (2) to evaluate these indicators through structured expert consensus using the Fuzzy Delphi Method, determining which are most applicable given Thailand's specific challenges; (3) to develop a validated set of indicators specifically suited for assessing and planning TOD in Thai suburban railway station areas; and (4) to provide practical guidance for policymakers and planners in prioritizing interventions around suburban transit stations. By focusing on actionable, context-specific indicators rather than attempting comprehensive coverage of all TOD factors, this research aims to produce findings that can directly inform planning practice and support the development of more sustainable and livable suburban communities around Thailand's expanding railway network.

2. Literature Review

2.1 Transit-Oriented Development in Suburban Contexts

Transit-Oriented Development (TOD) represents a planning approach that integrates land use and transportation to create compact, walkable, mixed-use communities centered around high-quality transit systems. While extensively studied in urban core areas, suburban TOD presents distinct challenges requiring specialized consideration. Pengjun, Z., & Shengxiao, L. (2018) examined suburbanization and lifestyle mobility in Beijing's metro station areas, revealing that suburban passengers exhibit different travel patterns and activity choices compared to urban residents, with greater dependence on private vehicles for non-commute trips. This finding underscores the need for context-specific TOD strategies that acknowledge suburban realities.

Bolleter, J., & Ramalho, C.E. (2020) identified fundamental differences between urban and suburban TOD implementation, noting that suburban areas require greater attention to first-and last-mile connectivity, parking provision, and integration with existing low-density development patterns. Ahmad, M. S., & Suratman, R. (2020) conducted a critical review of suburban transit-oriented development, emphasizing that suburban TOD must balance transit accessibility with automobile accommodation during transitional periods, rather than immediately restricting car use, as in urban contexts.

2.2 Climate and Cultural Considerations in TOD

The influence of climate on TOD success remains underexplored in existing literature, which predominantly focuses on temperate regions. In tropical and subtropical contexts, high temperatures and humidity significantly impact pedestrian behavior and walking distances. Yang, W., Li, T., & Cao, X. (2024) studied TOD circles in the Tokyo metropolitan area, noting variations in sustainability performance from urban to suburban areas, partly attributable to environmental comfort factors affecting active transportation modes.

Cultural preferences and community characteristics also shape TOD viability. Ahmad, S., Rashid, M. F., & Suratman, R. (2022) assessed TOD readiness in Perak's suburban areas in Malaysia, finding that local community acceptance and cultural appropriateness of development densities were critical factors often overlooked in Western-derived TOD frameworks. This research highlighted the importance of considering traditional market spaces, religious facilities, and community gathering areas in suburban TOD planning.

2.3 Informal Transportation Integration

Developing countries often feature informal transportation modes that provide essential mobility services, particularly for first- and last-mile connectivity. Chatman, D. G. (2013) questioned whether TOD necessarily requires rail access, demonstrating that factors beyond rail transit, including bus services and informal transport, significantly contribute to TOD success. Gao, W., Yao, E., Zhang, Y., & Liu, S. (2024). Improved catchment area identification for suburban railway stations by incorporating whole-journey-based mode choices, recognizing that passengers often combine formal transit with motorcycle taxis, shared rides, and other informal modes.

The integration of informal transportation modes as legitimate components of the transit ecosystem, rather than obstacles to be eliminated, represents a crucial shift in suburban TOD thinking for developing countries. This approach acknowledges that motorcycle taxis, songthaews, and similar services offer flexible and affordable connectivity that formal systems struggle to replicate in lower-density suburban contexts.

2.4 TOD Indicators and Evaluation Frameworks

Comprehensive frameworks for evaluating TOD potential have been developed across various contexts. Vale, D.S. (2015) combined the node-place model with pedestrian shed ratio to evaluate station areas in Lisbon, creating a methodology that assesses both transit service quality and urban development characteristics. Singh, Y.J., Fard, P., & Zuidgeest, M. (2014) developed a spatial multi-criteria assessment approach for Arnhem and Nijmegen, incorporating accessibility, density, diversity, and design factors.

More recent research has refined TOD indicators for specific contexts. Li, Z., et al. (2019) analyzed variations, typology, and optimization of TOD among metro stations in Shanghai, identifying distinct suburban TOD patterns requiring different planning strategies than urban stations. Chen, X., et al. (2024) addressed integrated TOD with suburban rail network design for maximizing profits, demonstrating the economic viability considerations essential for suburban contexts. Xia, Z., et al. (2024) conducted a comprehensive literature review from 2000 to 2023, identifying built environment indicators that influence TOD performance, noting gaps in understanding suburban-specific factors.

2.5 Research Gaps and Study Rationale

Despite extensive TOD research, significant gaps remain regarding suburban contexts in developing tropical countries. Existing frameworks predominantly derive from urban core areas in developed temperate regions, potentially overlooking critical factors such as: (1) climatic impacts on walkability and necessary supporting infrastructure (covered walkways, rest areas) in hot, humid environments; (2) integration strategies for informal transportation modes as legitimate components of suburban transit ecosystems; (3) culturally appropriate development densities and land-use mixes that respect local preferences while supporting transit viability; and (4) context-specific station area amenities that reflect suburban travel patterns where stations serve primarily as transit points rather than destinations.

This study addresses these gaps by systematically evaluating which TOD indicators from international literature are most applicable to Thai suburban railway contexts, explicitly considering climatic, cultural, and transportation system characteristics unique to the region.

3. Research Methodology

3.1 Research Design and Expert Selection

This study applies the Fuzzy Delphi Method through a structured research process designed to identify context-appropriate TOD indicators for suburban railway stations in Thailand. The Fuzzy Delphi Method was selected for its effectiveness in managing uncertainty and subjectivity in expert opinions while building consensus on complex planning issues (Abdullah, R., et al., 2024).

The expert panel comprised 10 professionals with extensive experience in transit-oriented development, urban planning, and transportation engineering in Thailand. Expert selection followed purposive sampling criteria to ensure diverse perspectives and comprehensive expertise: (1) Academic experts: Four professors and associate professors from leading Thai universities specializing in transportation planning and urban development, with an average of 18 years of experience and publications in peer-reviewed international journals on TOD topics; (2) Government planners: Three senior planners from the Department of Public Works and Town & Country Planning and the Office of Transport and Traffic Policy and Planning, with direct involvement in railway station area planning projects and an average of 15 years of professional experience; (3) Practicing consultants: Three transportation and urban planning consultants who have conducted TOD feasibility studies and master planning projects for Thai railway stations, with an average of 12 years of consulting experience.

This expert composition ensures balanced perspectives incorporating theoretical knowledge, policy implementation experience, and practical market realities. The panel size of 10 experts aligns with recommendations by Habibi, A., et al. (2015) for Fuzzy Delphi applications, providing sufficient diversity while maintaining manageability for iterative consultation rounds.

3.2 Seven-Step Research Process

3.2.1 Study Area Delineation

This research focuses on evaluating Transit-Oriented Development (TOD) indicators for suburban railway stations along Thailand's regional railway network. The study area encompasses four main corridors: (1) Northern Line from Ban Phachi Junction to Chiang Mai Station (661 kilometers, 29 stations); (2) Northeastern Line from Ban Phachi Junction to Nong Khai Station (531 kilometers, 20 stations), with a branch to Ubon Ratchathani Station (309 kilometers, five stations); (3) Eastern Line from Chachoengsao Junction to Aranyaprathet Station (194 kilometers, five stations), with a branch to Ban Chang Station (125 kilometers, eight stations); and (4) Southern & Western Line from Ban Pong to Hat Yai Junction (860 kilometers, 25 stations).

The entire network comprises 92 stations and 2,680 kilometers of railway infrastructure. Station selection used a comprehensive assessment framework prioritizing: transportation significance (high-speed rail, light rail, provincial stations); economic positioning (special economic zones); appropriate land use within 500 meters (favoring urban zones over environmental conservation areas); population density thresholds; and excluding standalone bus terminals due to limited TOD potential. This selection ensures focus on stations with genuine suburban TOD development opportunities.

3.2.2 Indicator Data Collection

A comprehensive literature review identified 48 TOD indicators from 14 relevant studies published between 2012 and 2024, systematically documenting their frequency of appearance across the literature (Table 1). The researchers developed an evaluation framework categorizing these indicators into three primary components aligned with TOD theory and practice:

- Transit System Indicators (TS): 16 indicators covering service operations (train service frequency, multimodal transit connectivity, service hours), infrastructure facilities (park-and-ride capacity, kiss-and-ride areas, transit interchange facilities), and station amenities (basic amenities, retail outlets, wayfinding systems, accessibility features, security systems).
- Oriented System Indicators (OS): 15 indicators focusing on pedestrian infrastructure (walkway width, covered walkways, street crossings, continuous walkways, surface quality, universal design, gradient), access environment (route lighting, rest points, directional signage, route safety), and non-motorized transport (cycling networks, bicycle parking, shared pedestrian-cycling paths, walking distance to key points).
- Development System Indicators (DS): 17 indicators addressing land use and development (mixed land use, residential density, commercial distribution, high-rise building areas, vacant land development, land value, local employment), community facilities and services (educational facilities, healthcare facilities, religious facilities, recreational areas, community centers, government service centers, community market areas), and infrastructure and environment (public green space, basic infrastructure, environmental management).

Each indicator includes explicit measurement methodologies to ensure practical applicability and consistent evaluation across different station contexts.

3.2.3 Expert Data Collection

Data collection was conducted through a systematic two-round consultation process. In the first round, experts received a comprehensive questionnaire package including: (1) research objectives and methodology explanation; (2) definitions and measurement methods for all 48 indicators; (3) study area context describing Thai suburban characteristics; and (4) evaluation forms using a 7-point Likert scale ranging from "Extremely Important" (7) to "Extremely Unimportant" (1).

Experts assessed each indicator's importance for evaluating TOD potential in Thai suburban railway station areas, considering factors including: climatic appropriateness for hot, humid tropical conditions; compatibility with informal transportation modes prevalent in Thai suburbs; cultural appropriateness for Thai community preferences and lifestyles; practical measurability and data availability; and relevance to suburban rather than urban core contexts.

Experts also provided qualitative feedback explaining their ratings and suggesting modifications to indicator definitions or measurement approaches. The first-round questionnaire required approximately 90 minutes to complete. Following the initial analysis, indicators that did not meet the acceptance threshold (crisp value < 0.75) were revised based on expert feedback and re-evaluated in a second round with refined definitions and measurement criteria. The second-round questionnaire focused solely on previously rejected indicators, requiring approximately 30 minutes to complete.

3.2.4 Conversion of Variables into Fuzzy Numbers

The conversion of linguistic variables into triangular fuzzy numbers followed the methodology proposed by Habibi et al. (2015). Each expert's importance rating on the 7-point Likert scale was converted to a triangular fuzzy number (l, m, u), where l represents the lower bound (minimum acceptable value), m represents the most probable value (mode), and u represents the upper bound (maximum possible value).

The conversion scale used was: Extremely Important (7) = (0.9, 1.0, 1.0); Very Important (6) = (0.75, 0.9, 1.0); Important (5) = (0.5, 0.75, 0.9); Moderately Important (4) = (0.3, 0.5, 0.75); Unimportant (3) = (0.1, 0.3, 0.5); Very Unimportant (2) = (0, 0.1, 0.3); Extremely Unimportant (1) = (0, 0, 0.1).

This approach offers greater flexibility than crisp values in handling the inherent ambiguity and uncertainty in expert opinion expression, particularly for complex, multidimensional concepts such as TOD appropriateness.

3.2.5 Aggregation of Fuzzy Evaluation Values

The aggregation of fuzzy evaluations across experts was conducted using fuzzy arithmetic operations. For each indicator, the ten experts' triangular fuzzy numbers were combined using the fuzzy averaging method. The aggregated triangular fuzzy number for indicator i was calculated as:

$$\tilde{A}_i = (\tilde{l}_i, \tilde{m}_i, \tilde{u}_i) \quad (1)$$

where:

$$\tilde{l}_i = (l_{1i} + l_{2i} + \ldots + l_{10i}) / 10 \quad (2)$$

$$\tilde{m}_i = (m_{1i} + m_{2i} + \ldots + m_{10i}) / 10 \quad (3)$$

$$\tilde{u}_i = (u_{1i} + u_{2i} + \ldots + u_{10i}) / 10 \quad (4)$$

This method enables the synthesis of diverse expert opinions while preserving the uncertainty information embedded in the fuzzy representations (Abdullah & Othman, 2023).

3.2.6 Defuzzification

The conversion of aggregated fuzzy values back to crisp values employed the arithmetic mean method, as described by Wu and Fang (2011). For each indicator's aggregated triangular fuzzy number ($\tilde{l}$, $\tilde{m}$, $\tilde{u}$), the defuzzified crisp value was calculated as:

$$\text{Crisp Value} = (\tilde{l} + \tilde{m} + \tilde{u}) / 3 \quad (5)$$

This simple yet effective defuzzification method provides an intuitive interpretation of the fuzzy evaluation results, offering a clear understanding of the underlying data. Indicators with crisp values of≥ 0.75 were accepted as appropriate for evaluating Thai suburban TOD, representing a 75% consensus threshold commonly used in Delphi studies.

3.2.7 Expert Consensus Analysis and Indicator Finalization

The analysis of expert opinion consistency employed a consensus acceptance criterion of at least 75% agreement (crisp value ≥ 0.75), following the approaches of Murray and Hammons (1995) and Chu and Hwang (2008). After the first evaluation round, results were compiled and indicators were classified as either "Accepted" (crisp value ≥ 0.75) or "Requiring Review" (crisp value < 0.75).

For indicators requiring review, the research team analyzed qualitative expert feedback to identify specific concerns, then revised indicator definitions, measurement approaches, or contextual explanations to address these concerns. The revised indicators were presented to the same expert panel in a second round, along with clarifications addressing the concerns raised in the first round. This iterative process continued until consensus was achieved or it was determined that an indicator was genuinely inappropriate for the Thai suburban context despite attempts at refinement.

The final indicator set represents those achieving expert consensus as relevant, measurable, and appropriate for evaluating TOD potential around suburban railway stations in Thailand, considering the unique climatic, cultural, and transportation system characteristics of the context.

4. Analysis Results

4.1 Overview of Expert Evaluation Process

The evaluation of Transit-Oriented Development (TOD) indicators for Thai suburban railway stations was conducted through a systematic two-round expert consultation process involving ten experts with extensive experience in transportation planning, urban development, and TOD implementation in Thailand. The initial assessment of 48 indicators revealed varying levels of consensus, with 42 indicators achieving acceptance in the first round and six requiring refinement and re-evaluation. This section presents the comprehensive findings from both evaluation rounds, analyzing the indicators that achieved consensus as well as those that were ultimately rejected due to contextual inappropriateness for Thai suburban railway contexts.

4.2 First Round Evaluation Results

The first round of expert evaluation assessed all 48 indicators across three main components: Transit System Indicators (TS), Oriented System Indicators (OS), and Development System Indicators (DS). Each expert's linguistic assessment on the 7-point Likert scale was systematically converted into triangular fuzzy numbers, aggregated across all ten experts, and defuzzified to produce crisp values representing overall expert consensus.

The first-round results revealed that 42 out of 48 indicators (87.5%) achieved the acceptance threshold of a crisp value ≥ 0.75, indicating a strong overall consensus on the relevance of most international TOD indicators to the Thai suburban context. However, six indicators failed to meet this threshold, categorized into borderline indicators (0.70 < crisp value < 0.75) and low-consensus indicators (crisp value ≤ 0.70), requiring further examination and potential revision.

4.2.1 High-Consensus Indicators

Several indicators emerged with firm expert consensus, achieving crisp values exceeding 0.90 and demonstrating their critical importance for Thai suburban TOD evaluation:

- Train Service Frequency (TSO1: 0.950) received the highest rating among all indicators. Experts emphasized that frequent and reliable service is even more critical in suburban areas than in urban cores, as it helps compete with the convenience of private vehicles. One expert noted: "Without frequent service, suburban residents will not change their car-dependent behavior. Service frequency is the foundation of suburban TOD." The high consensus reflects recognition that lower suburban densities make service frequency the primary determinant of transit competitiveness against automobile travel.
- The pedestrian walkway width (OSP1: 0.940) achieved near-unanimous support, with experts emphasizing its particular importance in hot climates. Expert feedback revealed specific concerns about Thai suburban

conditions: "In Thailand's heat, people need wider walkways to avoid crowding in shaded areas. Narrow walkways force people into direct sunlight, significantly reducing walking willingness." Experts recommended minimum effective widths of 2.5-3.0 meters for main access routes to stations, substantially wider than typical suburban sidewalks, to accommodate comfortable pedestrian flow while allowing people to seek shaded portions of the walkway.

- Mixed Land Use (DSL1: 0.940) received strong consensus, with experts noting that suburban areas must develop mixed-use patterns to reduce travel distances and support transit viability. One urban planning expert commented, "Suburban areas often have single-use zoning that forces car dependency. Mixed land use within walking distance of stations is essential for TOD success, even more critical than in urban areas where destinations are already closer together." The high rating reflects understanding that land-use integration is foundational to reducing automobile dependency in suburban contexts.
- Additional high-performing indicators included Connecting Transit Services (TSO2: 0.910), emphasizing bus-rail connectivity and informal transport integration; Park & Ride Facilities (TSF1: 0.910), supporting mode shift during transitional periods; Cycling Network (OSN1: 0.910), recognizing potential for electric bicycles and properly shaded routes despite hot climate; Security Systems (TSA5: 0.910), addressing safety concerns in lower-density suburban environments; Community Market Areas (DSC7: 0.910), reflecting importance of traditional Thai fresh markets; and Local Employment (DSL7: 0.908), supporting two-way transit flows and service cost-effectiveness.

4.2.2 Indicators Requiring Review

Six indicators failed to achieve the acceptance threshold in the first round, revealing important contextual differences between Thai suburban areas and the international urban contexts from which these indicators originated:

Borderline Indicators ($0.70 < \text{crisp value} < 0.75$):

- Station Signage and Symbols (TSA3: 0.727) - Initial expert assessments were mixed, with some considering comprehensive wayfinding systems important for all contexts. In contrast, others argued that suburban stations' smaller scale and simpler layouts reduce this need compared to those in complex urban areas. The indicator proceeded to a second round with clarified definitions emphasizing basic rather than elaborate signage systems.
- Covered Walkways (OSP2: 0.717) - Despite Thailand's hot climate, this indicator received surprisingly moderate ratings. Qualitative feedback revealed that experts distinguished between "covered walkways" (fully enclosed or tunnel-like structures) and "shaded walkways" (those with a tree canopy or a simple roof structure). Several experts expressed concern that the indicator might be misinterpreted as requiring expensive enclosed corridors, which are inappropriate for suburban contexts. The indicator was revised to clarify that simple roof structures or tree canopies providing shade and rain protection would suffice.

Low-Consensus Indicators ($\text{crisp value} \leq 0.70$):

- Number of Retail Outlets in Stations (TSA2: 0.633) - This indicator received notably low ratings with substantial disagreement among experts. Government planners and consultants consistently rated it low, explaining that suburban passengers primarily use stations as transit points rather than destinations for shopping or dining. One consultant elaborated: "In Bangkok's urban metro stations, retail outlets attract customers and generate revenue. In suburban railway stations, passengers arrive shortly before trains and leave immediately after arrival. Retail outlets would not be viable commercially and do not serve suburban passenger needs."
- Pedestrian Pathway Gradient (OSP7: 0.633) - Low ratings reflected experts' observations that most Thai suburban areas are characterized by relatively flat terrain, making slope considerations less critical than in mountainous or hilly contexts. Several experts noted that this indicator may be relevant for specific locations, such as Chiang Mai's foothill areas, but has limited applicability to Thailand's Central Plains, Northeastern Plateau, and coastal areas, where most suburban development occurs.
- High-Rise Building Areas (DSL4: 0.633) - This indicator generated substantial discussion and disagreement among experts. Urban planners initially rated it moderately high, viewing high-rise development as a means to achieve transit-supportive densities. In contrast, government planners and consultants rated it very low,

citing market realities and cultural preferences. One consultant explained: "The Thai real estate market shows limited demand for high-rise residential buildings in suburban locations. Families prefer landed housing or low-rise condominiums. Emphasizing high-rises would not reflect market realities or cultural preferences and would likely result in unsuccessful developments."

- Government Service Centers (DSC6: 0.617) - Experts generally agreed that lower population densities in suburban areas do not justify or require concentrated government service provision near every station. Several noted that digital government services are increasingly reducing the need for physical service centers, particularly in suburban areas where residents have better internet access than those in remote rural areas. One expert commented: "Major government offices might locate near some important suburban stations, but this should not be a general TOD evaluation criterion for all stations."

4.3 Second Round Evaluation Results

Following a comprehensive analysis of the first-round results and expert feedback, the research team revised the definitions and measurement approaches for the six indicators that required review. The revised indicators were presented to the same expert panel in a second consultation round, with clarifications specifically addressing concerns identified in the qualitative feedback.

4.3.1 Successfully Revised Indicators

Two indicators achieved acceptance in the second round after definitional revision and clarification:

- Station Signage and Symbols (TSA3: 0.727 → 0.863) - The revised definition clarified that this indicator focuses on basic wayfinding elements (platform signs, exit indicators, route maps, universal symbols) rather than elaborate digital signage systems or complex wayfinding networks. Experts responded positively to this practical interpretation, with one noting: "Basic signage is important even in small stations, especially for elderly passengers and tourists unfamiliar with the area. We do not need sophisticated electronic systems, but clear, simple signs with universal symbols are essential for station functionality." The crisp value increased substantially from 0.727 to 0.863, well exceeding the acceptance threshold and confirming the importance of basic wayfinding infrastructure.
- Covered Walkways (OSP2: 0.717 → 0.787) - The revised definition explicitly distinguished between "covered walkways" (continuous weather protection along primary routes to stations, including simple roof structures, tree canopy, or arcade-style coverings) and "fully enclosed walkways" (expensive climate-controlled corridors). This clarification emphasized that in Thai suburban contexts, practical weather protection through affordable structures would suffice rather than costly enclosed facilities. Several experts commented that this interpretation made the indicator both more appropriate for suburban contexts and more financially achievable. The crisp value increased from 0.717 to 0.787, achieving acceptance and confirming the critical importance of climate-responsive pedestrian infrastructure.

4.3.2 Persistently Rejected Indicators

Four indicators remained below the acceptance threshold even after revision and re-evaluation, indicating genuine contextual inappropriateness for Thai suburban railway stations rather than merely unclear definitions:

- Number of Retail Outlets in Stations (TSA2: 0.710) - Despite attempts to revise the indicator to focus on minimal convenience retail (small convenience stores, coffee vendors) rather than extensive shopping facilities, expert consensus remained that retail provision within suburban stations is not a priority evaluation criterion. The second-round crisp value of 0.710 improved slightly from 0.633 but still fell short of the 0.75 acceptance threshold. Expert feedback emphasized: "In suburban areas, passengers primarily use stations as transit points rather than spending extended time within the station. Commercial activities should focus on the surrounding area, not inside the station building. Limited retail might include ticket vendors and perhaps one small convenience store, but this should not be an evaluation priority." This finding contrasts sharply with urban TOD literature, where station retail is often considered important for activation, revenue generation, and creating vibrant station environments.

- Pedestrian Pathway Gradient (OSP7: 0.670) - The second-round evaluation attempted to reframe this indicator as applicable to areas with any topographic variation, not just mountainous terrain, but expert ratings remained consistently low. The crisp value of 0.670 showed minimal improvement from the first round's 0.633, confirming limited relevance. Expert consensus indicated: "Most suburban areas being considered for TOD in Thailand are on level terrain. Resources should focus on other pedestrian infrastructure priorities like width, surface quality, shade provision, and lighting rather than gradient management." Several experts noted that for the few suburban stations in areas with topographic variation, the gradient would be addressed through standard engineering practices rather than requiring a specific TOD evaluation.
- High-Rise Building Areas (DSL4: 0.670) - This indicator generated the most extensive discussion in both evaluation rounds. The revised definition attempted to frame high-rise development as one option among several density strategies rather than a requirement, but expert consensus remained negative. The second-round crisp value of 0.670 showed minimal change from 0.633, confirming persistent rejection. Expert feedback revealed fundamental disagreement with emphasizing high-rise development in suburban contexts: "Suburban areas should maintain moderate density and building heights appropriate to their context. The Thai real estate market shows limited demand for high-rise residential buildings in suburban locations, and cultural preferences favor landed housing or medium-rise condominiums." Another expert elaborated: "TOD should increase density, yes, but through medium-rise buildings (4-8 floors), efficient land use, and horizontal mixed-use development, not through high-rises. That urban model does not fit suburban market conditions or community preferences." This rejection underscores the importance of context-appropriate density strategies that consider local market conditions and cultural preferences.
- Government Service Centers (DSC6: 0.677) - The second-round revision attempted to reframe this indicator as "access to government services" (including either physical centers or digital service points), but expert ratings remained consistently low. The crisp value of 0.677 showed minimal improvement from the first round's 0.617, remaining substantially below the acceptance threshold. Expert feedback emphasized: "Due to lower population density in suburban areas, a high concentration of government service centers near every station is neither necessary nor economically justifiable. Major government offices might be located near some important suburban stations serving as regional centers, but this should not be a general TOD evaluation criterion applied to all suburban stations." This finding reflects the distinct service provision patterns appropriate for lower-density suburban contexts, where regional centers serve multiple communities rather than every station requiring comprehensive government services.

4.4 Final Accepted Indicator Framework

The two-round evaluation process resulted in 44 accepted indicators out of 48 initially proposed (91.7% acceptance rate), demonstrating a strong overall consensus while identifying four indicators that were genuinely inappropriate for the Thai suburban railway context. Table 2 presents the complete results showing crisp values and acceptance decisions for all indicators across both evaluation rounds.

Table 1. Transit-Oriented Development Indicators

		Transit System Indicators (TS)			
	Service Operations		**Infrastructure Facilities**		**Station Amenities**
TSO1	Train service frequency	TSF1	Park & Ride facilities	TSA1	Basic amenities
TSO2	Connecting transit services	TSF2	Kiss & Ride Areas	TSA2	Station retail outlets
TSO3	Multimodal transport integration	TSF3	Vehicle/motorcycle parking	TSA3	Station signage and symbols
TSO4	Ticketing system	TSF4	Transit connection points	TSA4	Ramps and elevators
TSO5	Service information system	TSF5	Information service points	TSA5	Security systems
TSO6	Service hours				
		Oriented System Indicators (OS)			
	Pedestrian Infrastructure		Access Environment		Non-Motorized Transport
OSP1	Pedestrian walkway width	OSE1	Route lighting	OSN1	Cycling network
OSP2	Covered walkways	OSE2	Rest points along routes	OSN2	Bicycle parking

	Pedestrian Infrastructure		Access Environment		Non-Motorized Transport
OSP3	Street crossings	OSE3	Directional signage	OSN3	Shared pedestrian-cycling paths
OSP4	Continuous walkways	OSE4	Route safety	OSN4	Walking Distance to key points
OSP5	Walking surface quality				
OSP6	Universal design implementation				
OSP7	Walkway gradient				

Development System Indicators (DS)

	Land Use and Development		**Community Facilities/Services**		**Infrastructure and Environment**
DSL1	Mixed land use	DSC1	Educational facilities	DSE1	Public green space
DSL2	Residential density	DSC2	Healthcare facilities	DSE2	Basic infrastructure
DSL3	Commercial distribution	DSC3	Religious facilities	DSE3	Environmental management
DSL4	High-rise building areas	DSC4	Recreational areas		
DSL5	Vacant land development	DSC5	Community centers		
DSL6	Land value	DSC6	Government service centers		
DSL7	Local employment	DSC7	Community market areas		

Table 2. Results of Expert Consensus Evaluation

Transit System Indicators (TS)

	Service Operations				**Infrastructure Facilities**				**Station Amenities**			
Code	Opinion's mean	Crisp value	Result	Code	Opinion's mean	Crisp value	Result	Code	Opinion's mean	Crisp value	Result
TSO1	(0.87,0.98,1.00)	0.950	Accepted	TSF1	(0.80,0.93,1.00)	0.910	Accepted	TSA1	(0.65,0.84,0.96)	0.817	Accepted
TSO2	(0.80,0.93,1.00)	0.910	Accepted	TSF2	(0.70,0.87,0.98)	0.850	Accepted	TSA2**	(0.42,0.65,0.83)	0.633	Rejected
TSO3	(0.77,0.91,1.00)	0.893	Accepted	TSF3	(0.65,0.84,0.96)	0.817	Accepted		(0.51,0.73,0.89)	0.710	Rejected
TSO4	(0.68,0.86,0.97)	0.837	Accepted	TSF4	(0.68,0.86,0.97)	0.837	Accepted	TSA3*	(0.53,0.75,0.90)	0.727	Rejected
TSO5	(0.68,0.86,0.97)	0.837	Accepted	TSF5	(0.65,0.84,0.96)	0.817	Accepted		(0.72,0.89,0.98)	0.863	Accepted
TSO6	(0.65,0.84,0.96)	0.817	Accepted					TSA4	(0.78,0.91,1.00)	0.897	Accepted
								TSA5	(0.80,0.93,1.00)	0.910	Accepted

Oriented System Indicators (OS)

	Pedestrian Infrastructure				**Access Environment**				**Non-Motorized Transport**			
Code	Opinion's mean	Crisp value	Result	Code	Opinion's mean	Crisp value	Result	Code	Opinion's mean	Crisp value	Result
OSP1	(0.85,0.97,1.00)	0.940	Accepted	OSE1	(0.70,0.87,0.98)	0.850	Accepted	OSN1	(0.80,0.93,1.00)	0.910	Accepted
OSP2*	(0.50,0.75,0.90)	0.717	Rejected	OSE2	(0.65,0.84,0.96)	0.817	Accepted	OSN2	(0.78,0.91,1.00)	0.897	Accepted
	(0.60,0.82,0.94)	0.787	Accepted	OSE3	(0.68,0.86,0.97)	0.837	Accepted	OSN3	(0.65,0.84,0.96)	0.817	Accepted
OSP3	(0.70,0.87,0.98)	0.850	Accepted	OSE4	(0.65,0.84,0.96)	0.817	Accepted	OSN4	(0.68,0.86,0.97)	0.837	Accepted
OSP4	(0.65,0.84,0.96)	0.817	Accepted								
OSP5	(0.78,0.91,1.00)	0.897	Accepted								
OSP6	(0.65,0.84,0.96)	0.817	Accepted								
OSP7**	(0.42,0.65,0.83)	0.633	Rejected								
	(0.46,0.69,0.86)	0.670	Rejected								

Development System Indicators (DS)

	Land Use and Development				**Community Facilities/Services**				**Infrastructure and Environment**			
Code	Opinion's mean	Crisp value	Result	Code	Opinion's mean	Crisp value	Result	Code	Opinion's mean	Crisp value	Result
DSL1	(0.85,0.97,1.00)	0.940	Accepted	DSC1	(0.78,0.91,1.00)	0.897	Accepted	DSE1	(0.78,0.91,1.00)	0.897	Accepted
DSL2	(0.78,0.91,1.00)	0.897	Accepted	DSC2	(0.70,0.87,0.98)	0.850	Accepted	DSE2	(0.65,0.84,0.96)	0.817	Accepted
DSL3	(0.70,0.87,0.98)	0.850	Accepted	DSC3	(0.65,0.84,0.96)	0.817	Accepted	DSE3	(0.68,0.86,0.97)	0.837	Accepted
DSL4**	(0.42,0.65,0.83)	0.633	Rejected	DSC4	(0.68,0.86,0.97)	0.837	Accepted				
	(0.46,0.69,0.86)	0.670	Rejected	DSC5	(0.65,0.84,0.96)	0.817	Accepted				
DSL5	(0.68,0.86,0.97)	0.837	Accepted	DSC6**	(0.40,0.63,0.82)	0.617	Rejected				

	Land Use and Development				Community Facilities/Services			Infrastructure and Environment
DSL6	(0.65,0.84,0.96)	0.817	Accepted		(0.47,0.69,0.87)	0.677	Rejected	
DSL7	(0.80,0.93,1.00)	0.908	Accepted	DSC7	(0.80,0.93,1.00)	0.910	Accepted	

Note: Result: Accepted if Crisp value ≥ 0.75, Rejected if Crisp value < 0.75

* Indicators not meeting criteria in the first round but accepted in the second round

** Indicators not meeting criteria in both first and second rounds Table 3 summarizes the progression of accepted indicators through both evaluation rounds, showing improvements in Transit System Indicators (TSA) and Oriented System Indicators (OSP) categories following second-round revisions, while confirming persistent rejection of contextually inappropriate indicators.

Table 3. Summary of Consensus-Based Accepted Indicators

Round	Result	Transit System Indicators (TS)			Oriented System Indicators (OS)			Development System Indicators (DS)			Total
		TSO	TSF	TSA	OSP	OSE	OSN	DSL	DSC	DSE	
1	Accepted	6	5	3	5	4	4	6	6	3	42
	Rejected			(2)	(2)			(1)	(1)		(6)
2	Accepted	6	5	4	6	4	4	6	6	3	44
	Rejected			(1)	(1)			(1)	(1)		(4)

4.5 Thematic Analysis of Findings

The evaluation results reveal three significant themes regarding TOD indicator appropriateness in Thai suburban railway contexts, with important implications for planning practice and policy development:

4.5.1 Climate-Responsive Infrastructure is Critical, Not Optional

Indicators related to climate protection achieved strong acceptance, with pedestrian walkway width (0.940), covered walkways (0.787 after revision), route lighting (0.850), and rest points along routes (0.817) all exceeding the acceptance threshold. Expert feedback consistently emphasized that Thailand's hot, humid climate fundamentally shapes pedestrian behavior and infrastructure requirements in ways not adequately addressed in international TOD literature focused on temperate climates.

One expert articulated this point emphatically: "We cannot simply copy TOD principles from temperate countries. In Thailand, the 400-800 meter walking catchment commonly cited in TOD literature must include substantial shade and rest opportunities, or people will not walk regardless of land-use mix or density. Climate response is not optional—it determines whether pedestrian access is viable at all." Another expert provided specific guidance: "In Thailand's heat, acceptable walking distance to stations is substantially reduced compared to temperate climates unless we provide continuous shade through tree canopy, covered walkways, or building arcades. A 500-meter walk in full sun feels like 1,000 meters and will deter all but the most determined transit users."

This finding has significant practical implications for Thai suburban TOD projects. First, substantial resources must be allocated to climate-responsive pedestrian infrastructure, potentially increasing development costs compared to temperate-region TOD but making the crucial difference between success and failure in attracting pedestrian access. Second, the conventional TOD walking catchment of 400-800 meters may need to be reduced in Thai suburban contexts unless extensive climate protection infrastructure is provided. Third, the sequencing of TOD development should prioritize climate-responsive pedestrian infrastructure as foundational, before pursuing other TOD objectives, such as density increases or land-use mixing.

4.5.2 Informal Transport Integration is Essential, Not Problematic

Indicators supporting multimodal integration achieved strong consensus, with multimodal transport integration (0.893), transit connection points (0.837), and connecting transit services (0.910) all receiving high ratings. Expert feedback revealed a perspective on informal transportation that differs substantially from conventional TOD literature, which often views informal modes as problems to be eliminated or merely tolerated during transitional periods.

Thai experts, instead, view informal transportation—particularly motorcycle taxis, informal van services, and songthaews—as permanent and valuable components of the suburban transit ecosystem, requiring purposeful integration into station area design. One consultant explained: "We need designated waiting areas for motorcycle

taxis with shade and seating, clear zones for informal vans to load passengers, and integration with songthaew routes. These services extend station catchment areas far beyond walking distance and provide flexible connectivity that formal bus systems cannot match in low-density suburbs where destinations are dispersed and travel patterns are irregular."

A government planner elaborated on this integration approach: "Rather than viewing motorcycle taxis as competing with formal transit, we should recognize them as essential first-and-last-mile connectors. Stations should include dedicated motorcycle taxi waiting areas with comfortable facilities, clear numbering systems for passenger-driver matching, and potentially even formal licensing or registration systems to improve safety and service quality. Similarly, informal van services provide flexible connections to employment centers and residential areas not served by fixed-route buses."

This finding challenges conventional TOD frameworks and suggests that successful Thai suburban TOD requires reconceptualizing the transit ecosystem to include both formal and informal modes as complementary rather than competitive. Practical implications include: designating specific spaces for informal transport operations within station area plans; providing amenities (shade structures, seating, lighting) for informal transport operators and waiting passengers; potentially establishing formal coordination mechanisms between railway operations and informal transport services; and recognizing informal transport in ridership forecasting and catchment area analysis rather than assuming all station access occurs through walking, cycling, or formal connecting transit.

4.5.3 Suburban Development Patterns Should Differ from Urban TOD

The rejection of high-rise building areas (DSL4: 0.670) despite two rounds of evaluation, combined with limited enthusiasm for extensive station retail (TSA2: 0.710), reflects expert consensus that suburban TOD should not attempt to replicate urban TOD physical forms or intensities. This finding has profound implications for how TOD is conceptualized and implemented in suburban contexts.

Accepted indicators support an alternative suburban TOD model emphasizing moderate-density, horizontally mixed-use development: mixed land use (0.940), residential density (0.897), commercial distribution (0.850), and local employment (0.908) all received strong support, suggesting suburban TOD should focus on bringing diverse uses closer together at moderate densities rather than pursuing high-density vertical development.

One consultant summarized this perspective: "Successful suburban TOD in Thailand will look different from Bangkok's urban BTS stations surrounded by high-rise condominiums and shopping complexes. We need 4-8 story mixed-use buildings, not 40-story towers. We need fresh markets and local shops mixed with townhouses and low-rise apartments, not mega-retail complexes and luxury high-rises. The goal is the same—reduce car dependency and support transit ridership—but the physical form must fit suburban contexts, market conditions, and cultural preferences."

An urban planning expert elaborated on density strategies: "The emphasis should be on efficient use of land near stations through horizontal integration—mixing housing, shops, services, and offices in medium-rise buildings along station access corridors—rather than vertical integration in isolated towers. This approach matches Thai suburban real estate demand, provides gradual density transitions from stations to surrounding neighborhoods, and can be implemented incrementally as market conditions support development."

This finding suggests several practical implications for suburban TOD planning: First, zoning and planning guidelines should permit and encourage 4-8 story mixed-use development along station access corridors rather than requiring or emphasizing high-rise development. Second, density targets for suburban TOD should be calibrated to local market conditions and cultural preferences, potentially in the range of 50-100 dwelling units per hectare rather than the 100+ units standard in urban TOD guidelines. Third, station area master plans should emphasize horizontal land-use mixing and incremental infill development rather than comprehensive redevelopment centered on landmark high-rise projects. Fourth, public investment should prioritize enabling infrastructure (such as streets, sidewalks, and utilities) that facilitates small-scale, market-responsive development, rather than large-scale, government-coordinated projects.

4.6 Implications for Thai Suburban TOD Practice

The accepted indicator framework provides practical guidance for evaluating and planning TOD around Thailand's suburban railway stations. The 44 accepted indicators span transit service provision, pedestrian and cycling infrastructure, multimodal connectivity, land-use integration, community facilities, and environmental quality—offering a comprehensive yet context-appropriate evaluation tool.

The four rejected indicators highlight critical differences between Thai suburban contexts and the international urban settings from which much TOD literature originates. Thai suburban TOD should not prioritize extensive station retail, slope management in predominantly flat terrain, high-rise development, or concentrated government services—instead focusing resources on climate-responsive pedestrian infrastructure, informal transport integration, and moderate-density mixed-use development aligned with market demand and cultural preferences.

This context-specific framework enables more effective resource allocation, focusing limited public and private investment on interventions most likely to support transit ridership and sustainable development outcomes in Thai suburban contexts. The framework also provides a foundation for future research examining relationships between these indicators and TOD outcomes, potentially enabling predictive models for evaluating proposed suburban station locations or development scenarios.

5. Conclusions

The application of the Fuzzy Delphi Method to evaluate Transit-Oriented Development (TOD) indicators for Thai suburban railway stations has yielded significant findings that contribute to both theoretical understanding and practical implementation of suburban TOD in developing tropical countries. Through systematic consultation with ten experts across two evaluation rounds, this study successfully identified 44 context-appropriate indicators from an initial set of 48 derived from the international literature, achieving a 91.7% acceptance rate while revealing four indicators that were genuinely inappropriate for Thai suburban contexts. The highest-ranking indicators—train service frequency (TSO1: 0.950), pedestrian walkway width (OSP1: 0.940), and mixed land use (DSL1: 0.940)—demonstrate that fundamental factors in transit service provision, climate-responsive pedestrian infrastructure, and integrated land-use planning remain crucial for suburban TOD success. Conversely, the persistent rejection of indicators, including the number of retail outlets in stations (TSA2: 0.710), pedestrian pathway gradient (OSP7: 0.670), high-rise building areas (DSL4: 0.670), and government service centers (DSC6: 0.677), reveals important contextual differences between Thai suburban areas and the international urban settings from which most TOD frameworks originate.

The findings reveal three critical themes distinguishing Thai suburban TOD from conventional urban-centric frameworks. First, climate-responsive infrastructure emerges as essential rather than optional, with experts emphasizing that Thailand's hot, humid climate fundamentally shapes pedestrian behavior and infrastructure requirements in ways inadequately addressed in temperate-region TOD literature. The strong consensus on covered walkways, adequate walkway widths, rest points, and lighting reflects recognition that, without substantial climate protection, even well-designed mixed-use, transit-oriented developments will fail to attract pedestrian access regardless of proximity or land-use diversity. Second, informal transportation modes—particularly motorcycle taxis, van services, and songthaews—should be recognized as legitimate and essential components of the suburban transit ecosystem, requiring purposeful integration rather than elimination. This perspective challenges conventional TOD frameworks that often view informal modes negatively, suggesting instead that in lower-density suburban contexts, these services provide flexible connectivity that formal systems struggle to replicate cost-effectively. Third, suburban development patterns should differ from urban TOD, with expert rejection of high-rise emphasis reflecting consensus that moderate-density, horizontally mixed-use development (4-8 stories) better aligns with Thai suburban market conditions, cultural preferences, and incremental development capacities than attempts to replicate high-density urban forms.

These findings have important practical implications for multiple stakeholder groups. Government planners and policymakers can use the validated framework to more accurately assess TOD potential around existing and planned stations, prioritizing public investment in service frequency, climate-responsive pedestrian infrastructure, and zoning frameworks that encourage moderate-density mixed-use development rather than requiring high-rise projects. Transit operators should recognize service frequency as foundational to suburban ridership while actively coordinating with informal transport providers as partners rather than competitors. Property developers receive clear guidance that successful suburban station-area projects will emphasize moderate-density mixed-use buildings integrated into complete neighborhoods rather than isolated high-rise developments. Local communities can engage in TOD planning processes with confidence that appropriate suburban TOD will enhance rather than disrupt community character through moderate development intensities, preservation of community spaces such as fresh markets and religious facilities, and gradual density transitions.

While this study makes important contributions, several limitations should be acknowledged. The expert panel, though diverse, comprised only ten individuals, and the study focused on indicator identification rather than weighting or empirical validation of relationships between indicators and actual TOD outcomes. Future research should develop indicator weighting methodologies and composite indices, conduct empirical validation studies examining which indicators most strongly predict successful suburban TOD, explore detailed design guidelines

for climate-responsive infrastructure, investigate models for informal transport integration, and undertake longitudinal studies tracking station areas over time as TOD interventions are implemented. Comparative international research examining suburban TOD in other tropical developing countries could identify common challenges and successful strategies with potential applicability across contexts.

In conclusion, this research demonstrates that successful suburban TOD in Thailand requires context-specific approaches that acknowledge climatic realities, integrate informal transportation, and pursue culturally appropriate development forms rather than attempting to replicate urban TOD models. The validated framework of 44 indicators provides a practical evaluation tool for Thailand's expanding suburban railway network, supporting more effective resource allocation, policy development, and implementation strategies. By recognizing that suburban TOD is not simply scaled-down urban TOD but a distinct approach requiring different strategies, Thailand can develop more sustainable, livable suburban communities around railway investments, reducing automobile dependency while respecting suburban character and community preferences. As Thailand continues railway network expansion into suburban areas, applying these context-sensitive insights can support improved TOD outcomes, contributing to broader goals of sustainable urban development, reduced greenhouse gas emissions, and enhanced quality of life for suburban residents. The framework developed through this research offers both a validated assessment tool and a strategic roadmap for prioritizing interventions, ultimately enabling more successful Transit-Oriented Development implementation in Thai suburban contexts and potentially informing similar efforts in other developing tropical countries facing comparable challenges.

6. References

Abdullah, N., & Othman, N. (2023). Applying the Fuzzy Delphi Method to the Content Validity of the Female Leadership Personality Instrument. Thailand Statistician, 21(2), 337–350. retrieved from https://ph02.tci-thaijo.org/index.php/thaistat/article/view/249005

Abdullah, R., Xavier, B. D., Namgung, H., Varghese, V., & Fujiwara, A. (2024). Managing transit-oriented development: A comparative analysis of expert groups and multi-criteria decision making methods. Sustainable Cities and Society, 115, 105871. https://doi.org/10.1016/j.scs.2024.105871

Ahmad, M. S., & Suratman, R. (2020). Critical review on suburban transit orientation development. Planning Malaysia: Journal of the Malaysian Institute of Planners, 18(4), 365-374.

Ahmad, S., Rashid, M. F., & Suratman, R. (2022). Readiness of Transit-Oriented Development (TOD) Concept Implementation in Perak's Suburban Areas. Planning Malaysia Journal, 20(1). https://doi.org/10.21837/pm.v20i20.1086

Bolleter, J., Ramalho, C.E. (2020). Transit-Oriented Development (TOD) and Its Problems. In: Greenspace-Oriented Development. SpringerBriefs in Geography. Springer, Cham. https://doi.org/10.1007/978-3-030-29601-8_2

Chatman, D. G. (2013). Does TOD Need the T? On the Importance of Factors Other Than Rail Access. Journal of the American Planning Association, 79(1), 17–31. https://doi.org/10.1080/01944363.2013.791008

Chen, X., Dong, C., Tao, S., Peng, Q., & Liu, J. (2024). Integrated Transit-Oriented Development (TOD) with suburban rail network design problem for maximizing profits. Transportation Letters, 16(10), 1318–1337. https://doi.org/10.1080/19427867.2024.2304999

Chu, H. C., & Hwang, G. J. (2008). A Delphi-based approach to developing expert systems with the cooperation of multiple experts. Expert Systems with Applications, 34(4), 2826-2840. https://doi.org/10.1016/j.eswa.2007.05.034

Dow, Kyle (2024). Complete Communities in the Suburbs: Evaluating Transit-Oriented Development Potential North of Toronto. Toronto Metropolitan University. Thesis. https://doi.org/10.32920/25167491.v1

Gao, W., Yao, E., Zhang, Y., & Liu, S. (2024). Improving the catchment area identification for suburban railway stations by incorporating whole-journey-based mode choices and unevenly distributed population. Cities, 155, 105487. https://doi.org/10.1016/j.cities.2024.105487

Habibi, A., Firouzi, F. F., & Sarafrazi, A. (2015). Fuzzy Delphi Technique for Forecasting and Screening Items. Asian Journal of Research in Business Economics and Management, 5(2), 130-143. https://doi.org/10.5958/2249-7307.2015.00036.5

Ibraeva, A., Correia, G. H. A., Silva, C., & Antunes, A. P. (2020). Transit-oriented development: A review of research achievements and challenges. Transportation Research Part A: Policy and Practice, 132, 110-130. https://doi.org/10.1016/j.tra.2019.10.018

Ivan, I., Boruta, T., & Horák, J. (2012). Evaluation of railway surrounding areas: the case of Ostrava city. WIT Transactions on The Built Environment, 128, 141-152. https://doi.org/10.2495/UT120131

Kamruzzaman, M., Baker, D., & Turrell, G. (2014). Advance transit oriented development typology: Case study in Brisbane, Australia. Journal of Transport Geography, 34, 54-70. https://doi.org/10.1016/j.jtrangeo.2013.11.002

Li, Z., Han, Z., Xin, J., Luo, X., Su, S., & Weng, M. (2019). Transit oriented development among metro station areas in Shanghai, China: Variations, typology, optimization and implications for land use planning. Land Use Policy, 82, 269-282. https://doi.org/10.1016/j.landusepol.2018.12.003

Loo, B. P. Y., & du Verle, F. (2016). Transit-oriented development in future cities: towards a two-level sustainable mobility strategy. International Journal of Urban Sciences, 21(sup1), 54–67. https://doi.org/10.1080/12265934.2016.1235488

Lyu, G., Bertolini, L., & Pfeffer, K. (2016). Developing a TOD typology for Beijing metro station areas. Journal of Transport Geography, 55, 40-50. https://doi.org/10.1016/j.jtrangeo.2016.07.002

Murray, J. W., & Hammons, J. O. (1995). Delphi: A versatile methodology for conducting qualitative research. Review of Higher Education, 18(4), 423-436.

Pengjun, Z., & Shengxiao, L. (2018). Suburbanization, land use of TOD and lifestyle mobility in the suburbs: An examination of passengers' choice to live, shop and entertain in the metro station areas of Beijing. Journal of Transport and Land Use, 11(1), 195–215. https://www.jstor.org/stable/26622399

Schlossberg, M., Brown, N., Bossard, E. G., & Roemer, D. (2004). Using spatial indicators for pre- and post-development analysis of TOD areas: A case study of Portland and the Silicon Valley (MTI Report 03-03). Mineta Transportation Institute, San Jose State University. https://transweb.sjsu.edu/sites/default/files/SchlossbergBook.pdf

Singh, Y.J., Fard, P., & Zuidgeest, M. (2014). Measuring transit oriented development: a spatial multi criteria assessment approach for the City Region Arnhem and Nijmegen. Journal of Transport Geography, 35, 130-143. https://doi.org/10.1016/j.jtrangeo.2014.01.014

Vale, D.S. (2015). Transit-oriented development, integration of land use and transport, and pedestrian accessibility: Combining node-place model with pedestrian shed ratio to evaluate and classify station areas in Lisbon. Journal of Transport Geography, 45, 70-80. https://doi.org/10.1016/j.jtrangeo.2015.04.009

Wu, C., & Fang, W. (2011). Combining the Fuzzy Analytic Hierarchy Process and the fuzzy Delphi method for developing critical competences of electronic commerce professional managers. Quality and Quantity, 45(4), 751-768. https://doi.org/10.1007/s11135-010-9425-6

Xia, Z., Feng, W., Cao, H., & Zhang, Y. (2024). Understanding the Influence of Built Environment Indicators on Transit-Oriented Development Performance According to the Literature from 2000 to 2023. Sustainability, 16(21), 9165. https://doi.org/10.3390/su16219165

Yang, W., Li, T., & Cao, X. (2024). Are different TOD circles oriented towards sustainability amidst urban shrinkage? Evidence from urban areas to suburbs in the Tokyo metropolitan area. Journal of Environmental Management, 372, 123274. https://doi.org/10.1016/j.jenvman.2024.123274